*Year :* 2022

# Drivers and consequences of amoxicillin resistance in the opportunistic human pathogen Streptococcus pneumoniae

Gibson Paddy Susanne

Gibson Paddy Susanne, 2022, Drivers and consequences of amoxicillin resistance in the opportunistic human pathogen Streptococcus pneumoniae

Originally published at : Thesis, University of Lausanne

Posted at the University of Lausanne Open Archive http://serval.unil.ch
Document URN : urn:nbn:ch:serval-BIB_D428B0D381965

UNIL | Université de Lausanne
Faculté de biologie et de médecine

**Department of Fundamental Microbiology**

# Drivers and consequences of amoxicillin resistance in the opportunistic human pathogen *Streptococcus pneumoniae*

**Thèse de doctorat ès sciences de la vie (PhD)**

présentée à la

Faculté de biologie et de médecine
de l'Université de Lausanne

par

**Paddy Susanne GIBSON**

Biologiste diplômé ou Master de l'Université de Canterbury

**Jury**

Prof. Bengt Kayser, Président

Prof. Jan-Willem Veening, Directeur de thèse

Prof. Willem Van Schaik, Expert

Prof. Markus Hilty, Expert

Lausanne

(2022)

UNIL | Université de Lausanne
Faculté de biologie et de médecine

**Department of Fundamental Microbiology**

# Drivers and consequences of amoxicillin resistance in the opportunistic human pathogen *Streptococcus pneumoniae*

**Thèse de doctorat ès sciences de la vie (PhD)**

présentée à la

Faculté de biologie et de médecine
de l'Université de Lausanne

par

**Paddy Susanne GIBSON**

Biologiste diplômé ou Master de l'Université de Canterbury

**Jury**

Prof. Bengt Kayser, Président

Prof. Jan-Willem Veening, Directeur de thèse

Prof. Willem Van Schaik, Expert

Prof. Markus Hilty, Expert

Lausanne

(2022)

UNIL | Université de Lausanne
Faculté de biologie
et de médecine

**Ecole Doctorale**
**Doctorat ès sciences de la vie**

# Imprimatur

Vu le rapport présenté par le jury d'examen, composé de

| | | | | |
|---|---|---|---|---|
| **Président·e** | Monsieur | Prof. | Bengt | **Kayser** |
| **Directeur·trice de thèse** | Monsieur | Prof. | Jan-Willem | **Veening** |
| **Expert·e·s** | Monsieur | Prof. | Willem | **van Schaik** |
| | Monsieur | Prof. | Markus | **Hilty** |

le Conseil de Faculté autorise l'impression de la thèse de

**Paddy Susanne Gibson**

Master Of Science, University of Canterbury, Nouvelle-Zélande

intitulée

**Drivers and consequences of amoxicillin resistance in the opportunistic human pathogen *Streptococccus pneumoniae***

Lausanne, le 1 juillet 2022

pour le Doyen
de la Faculté de biologie et de médecine

Prof. Bengt Kayser

# Academic Summary

*Streptococcus pneumoniae* (the pneumococcus) is a Gram-positive, ovococcoid-shaped, commensal member of the human nasopharyngeal microflora. Colonization is normally asymptomatic, however movement to other regions results in rapid inflammation, and the pneumococcus is a leading cause of community-acquired pneumonia and otitis media. In addition, it can cross epithelial barriers to cause invasive diseases, such as sepsis and meningitis. The World Health Organization has listed *S. pneumoniae* as a top 12 priority pathogen due the high burden of disease, and rapid dissemination of antibiotic resistance.

The frontline antibiotic amoxicillin (AMX) is most often prescribed for the treatment of upper respiratory tract infections, such as those caused by the pneumococcus, and is one of the most highly sold antibiotics worldwide. It belongs to the β-lactam family and inhibits cell wall synthesis by irreversibly binding in the active transpeptidase site of penicillin binding proteins (PBPs). This blocks peptidoglycan cross-linking, stalling cell wall synthesis, and triggering the activity of pneumococcal autolysin LytA, resulting in cell lysis. In this species, β-lactam resistance is mediated by large-scale modifications to the transpeptidase domain of the PBPs, reducing the antibiotic binding affinity. *S. pneumoniae* is naturally competent, capable of up taking exogenous DNA from the environment and recombining it into its genome. This has enabled the accumulation of significant variation at these loci, and its rapid spread in response to clinical intervention.

For AMX, resistance has been associated with modifications to at least three of its six PBPs, as well as several non-PBP determinants. In the second chapter of this thesis, we explored the evolution of AMX resistance in susceptible laboratory strains, through sequential rounds of transformation with genomic DNA from an AMX resistant clinical isolate. Using whole genome sequencing, we identified multiple recombination events occurring around the chromosome during each round of transformation. We observed examples of non-contiguous recombination and showed that these complex events could arise either from non-contiguous integration of a single donor molecule, or from the uptake of multiple donor DNA fragments. We confirmed the four main determinants of AMX resistance to be *pbp2x*, *pbp2b*, *pbp1a*, and *murM*, and demonstrated the optimal order of mutant allele uptake for resistance evolution without major fitness defects.

Following PBP inhibition by a β-lactam antibiotic, LytA begins to hydrolyze the PG amide bonds, separating glycan strand and peptide. Substrate access is mediated by the choline binding domain which anchors the lysin to wall teichoic acid phosphorylcholine residues. Despite its importance, to both virulence and β-lactam treatment response, how LytA is transported outside of the cell and how the timing of this is so tightly regulated remains a mystery. In chapter 3, we used AMX-induced lysis in combination with genome-wide CRISPRi-seq screening to identify BeaU, a previously uncharacterized membrane protein. *S. pneumoniae* mutated for *beaU* experience earlier late stationary phase autolysis and increased susceptibility to β-lactam treatment. We show that these phenotypes are LytA-dependent, and that this association likely involves a role for BeaU in cell wall structure that indirectly affects the activity of LytA.

An important component of a cell's response to antibiotic treatment, is its ability to sense stress, and alter gene expression accordingly. Two-component system CiaRH, is part of the pneumococcal general cell wall stress response. The histidine kinase CiaH responds to a stress signal by phosphorylating response regulator CiaR. In chapter 4, we examine the role of hyperactive CiaH mutations in decreased AMX susceptibility. Using low-level antibiotic selection, we show for the first time that AMX can also select for point mutations in *ciaH* and confirm that the resulting substitutions increase expression from a CiaR-dependent promoter.

To summarize, AMX treatment has wide ranging effects on pneumococcal cells, beyond PBP inhibition. Exploring these effects enabled us to gain insight into different aspects of pneumococcal molecular biology, providing fundamental information for novel drug development and implementation of antibiotic stewardship programs.

# Résumé académique

*Streptococcus pneumoniae* (le pneumocoque) est une bactérie à Gram positive de forme ovale, commensale de la microflore nasopharyngée humaine. La colonisation est normalement asymptomatique, mais le déplacement vers d'autres régions entraîne une inflammation rapide. Par conséquent, le pneumocoque est une cause majeure de pneumonie et d'otite communautaires. En outre, il peut traverser les barrières épithéliales pour provoquer des maladies invasives, telles que la septicémie et la méningite. L'Organisation mondiale de la santé a classé *S. pneumoniae* parmi les 12 agents pathogènes prioritaires en raison de la charge de morbidité élevée et de la diffusion rapide de la résistance aux antibiotiques.

L'amoxicilline (AMX), antibiotique de première ligne, est le plus souvent prescrite pour le traitement des infections des voies respiratoires supérieures, telles que celles causées par le pneumocoque. C'est l'un des antibiotiques les plus vendus dans le monde. Elle appartient à la famille des β -lactamines et inhibe la synthèse de la paroi cellulaire en se fixant de manière irréversible sur le site actif de la transpeptidase des protéines de liaison de la pénicilline (PBP). Cela bloque la réticulation du peptidoglycane, bloquant la synthèse de la paroi cellulaire et déclenchant l'activité de l'autolysine LytA du pneumocoque, entraînant ainsi la lyse des cellules. Chez cette espèce, la résistance aux β-lactamines est due à des modifications à grande échelle du domaine transpeptidase des PBP, ce qui réduit l'affinité de liaison des antibiotiques. *S. pneumoniae* est naturellement compétent, capable de prendre de l'ADN exogène dans l'environnement et de le recombiner dans son génome. Cela a permis l'accumulation d'une variation importante au niveau de ces loci, et sa propagation rapide en réponse à une intervention clinique.

Pour l'AMX, la résistance a été associée à des modifications d'au moins trois de ses six PBPs, ainsi qu'à plusieurs éléments qui ne sont pas des PBP. Dans le deuxième chapitre de cette thèse, nous avons exploré l'évolution de la résistance à l'AMX dans des souches de laboratoire sensibles, par des cycles séquentiels de transformation avec l'ADN génomique d'un isolat clinique résistant à l'AMX. En séquençant l'entier du génome, nous avons identifié de multiples événements de recombinaison se produisant sur le chromosome pendant chaque cycle de transformation. Nous avons observé des exemples de recombinaison non contiguë

et montré que ces événements complexes pouvaient provenir soit de l'intégration non contiguë d'une seule molécule donneuse, soit de l'absorption de multiples fragments d'ADN donneur. Nous avons confirmé que les quatre principaux déterminants de la résistance à l'AMX sont *pbp2x*, *pbp2b*, *pbp1a* et *murM* et nous avons démontré l'ordre optimal d'absorption des allèles mutants pour une évolution de la résistance sans défaut majeur de fitness.

Après l'inhibition d'un PBP par un antibiotique de type β-lactam, LytA commence à hydrolyser les liaisons amides du peptidoglycane, séparant le glycane et le peptide. L'accès au substrat est assuré par le domaine de liaison à la choline qui ancre la lysine aux résidus phosphorylcholine de l'acide teichoïque de la paroi. Malgré son importance, à la fois pour la virulence et pour la réponse au traitement parβ-lactam, la façon dont LytA est transportée à l'extérieur de la cellule et comment ce transport est si étroitement régulé reste un mystère. Dans le chapitre 3, nous avons utilisé la lyse induite par AMX en combinaison avec un criblage CRISPRi-seq à l'échelle du génome pour identifier BeaU, une protéine membranaire jusqu'alors non caractérisée. Les *S. pneumoniae* mutés pour *beaU* présentent une autolyse plus précoce en fin de phase stationnaire et une sensibilité accrue au traitement par β-lactamines. Nous montrons que ces phénotypes sont dépendants de LytA, et que cette association implique probablement un rôle de BeaU dans la structure de la paroi cellulaire qui affecte indirectement l'activité de LytA.

Un élément important de la réponse d'une cellule à un traitement antibiotique est sa capacité à détecter le stress et à modifier l'expression génétique en conséquence. Le système à deux composants CiaRH, fait partie de la réponse au stress de la paroi cellulaire générale du pneumocoque. L'histidine kinase CiaH répond à un signal de stress en phosphorylant le régulateur de réponse CiaR. Dans le chapitre 4, nous examinons le rôle des mutations CiaH hyperactives dans la diminution de la sensibilité à l'AMX. En utilisant une sélection antibiotique de faible concentration, nous montrons pour la première fois que l'AMX peut également sélectionner des mutations ponctuelles de *CiaH* et confirmons que les substitutions résultantes augmentent l'expression à partir d'un promoteur dépendant de CiaR.

En résumé, le traitement par l'AMX a des effets très variés sur les cellules pneumococciques, au-delà de l'inhibition des PBPs. L'étude de ces effets nous a permis de mieux comprendre

différents aspects de la biologie moléculaire du pneumocoque, fournissant des informations fondamentales pour le développement de nouveaux médicaments et la mise en œuvre de programmes thérapeutiques appropriés.

# Non-academic Summary

*Streptococcus pneumoniae* (the pneumococcus) is a rugby ball-shaped bacterial species that is a natural colonizer of the human nasopharynx. However, given the opportunity, it can move to the lungs or the middle ear, resulting in pneumonia or otitis media. In more severe cases, bacteria spread into the bloodstream, resulting in invasive infections such as sepsis or meningitis. The World Health Organization has listed *S. pneumoniae* as a top 12 priority pathogen due the high number of infections worldwide, and the increasing risk of antibiotic resistance.

Infections caused by the pneumococcus are commonly treated with broad-spectrum β-lactam antibiotics such as amoxicillin, commonly marketed under the name Augmentin. It inhibits bacterial growth by binding to the penicillin binding proteins (PBPs), blocking the essential cross-linking step of cell wall synthesis. The cell wall is an essential structure for a bacterial cell, helping it to withstand osmotic pressure. Its synthesis is a tightly choreographed sequence of events, with many proteins acting in concert at just the right time to construct the perfect structure. Blocking one of these steps throws out the entire balance, stalling synthesis, which then activates the activity of lysin LytA. LytA begins to break the wall even further, eventually resulting in cell lysis.

*S. pneumoniae* develops resistance to β-lactam antibiotics through extensive modifications to the active sites of the target enzymes. For AMX, resistance has been associated with modifications to at least three of its six PBPs, as well as several non-PBP determinants. These mutations are acquired through natural transformation, where the pneumococcus takes up DNA from its environment and recombines it into its chromosome. In Chapter 2 of this thesis, we explored the development of AMX resistance in pneumococcus, by transforming fully susceptible strains with DNA from a resistant isolate. Using whole genome sequencing, we could follow recombination events through each round of transformation, allowing us to correlate specific loci to resistance level. In this way, we determined the essential components of AMX resistance to be *pbp2x*, *pbp2b*, *murM*, and *pbp1a*, acquired in that order.

Following PBP inhibition by a β-lactam antibiotic, LytA begins to break down the cell wall further. In Chapter 3, we used AMX-induced lysis in combination with genome-wide synthetic lethal screening to identify BeaU, a previously uncharacterized membrane protein. *S.*

*pneumoniae* mutated for *beaU* lyse earlier in stationary phase and show increased susceptibility to β-lactam antibiotics. We demonstrate that these phenotypes are LytA-dependent, and that this association likely involves a role for BeaU in construction of the final cell wall structure that indirectly affects the activity of LytA.

The ability of a cell to sense stress, and to respond appropriately, is critical for mitigating the impacts of antibiotic treatment. The pneumococcus encodes a specific system for the detection of cell wall stress, called CiaRH. In this system, the histidine kinase CiaH responds to a stress signal by activating the response regulator CiaR. CiaR then modifies the expression of a set of genes. In Chapter 4, we examined the role of hyperactive CiaH mutations in decreased AMX susceptibility. Using low-level antibiotic selection, we show for the first time that AMX can also select for point mutations in *ciaH* and confirm that the resulting substitutions increase CiaR-dependent gene expression. Using CRISPRi repression, we identified at least four members of the regulon which may be involved in altering the cell to better tolerate AMX-induced cell wall stress.

In this this thesis we explore how pneumococcal cells respond to AMX treatment, both through investigating the mechanism and evolution of resistance, and through identifying novel proteins, or novel roles for known proteins in the response to cell wall synthesis inhibition. Understanding cellular response to specific drug treatments is critical for the development of appropriate stewardship programs, in order to conserve current antibiotics for future use.

# Résumé non académique

*Streptococcus pneumoniae* (alias pneumocoque) est une espèce bactérienne en forme de ballon de rugby qui colonise de manière naturelle le nasopharynx humain. Dans certains conditions, elle peut néanmoins migrer vers les poumons ou l'oreille moyenne, causant une pneumonie ou une otite moyenne. Dans les cas les plus graves, la bactérie se propage dans la circulation sanguine, entraînant des infections invasives telles que la septicémie ou la méningite. L'Organisation Mondiale de la Santé a classé *S. pneumoniae* parmi les 12 agents pathogènes prioritaires en raison du nombre élevé d'infections dans le monde et du risque croissant de résistance aux antibiotiques.

Les infections causées par le pneumocoque sont généralement traitées par des antibiotiques β -lactames à large spectre tels que l'amoxicilline (AMX), couramment commercialisée sous le nom d'Augmentin. L'AMX inhibe la croissance bactérienne en se liant aux protéines cibles de la pénicilline (PBP), bloquant ainsi l'étape essentielle de réticulation de la synthèse de la paroi cellulaire. La paroi cellulaire est une structure essentielle de la cellule bactérienne qui l'aide à contrecarrer la pression osmotique et empêcher l'explosion de la cellule. Sa synthèse suit une séquence d'événements étroitement orchestrés. Elle implique de nombreuses protéines agissant de concert à des moments précis pour construire une structure compacte et robuste. Le blocage de l'une de ces étapes déséquilibre le processus entier. Ce bloquaga de la synthèse pariétale résulte alors en lactivition de la lysine LytA qui amplifie le phénomène en dégradant la paroi, ce qui entraîne finalement la lyse de la cellule.

*S. pneumoniae* développe une résistance aux antibiotiques β -lactames par des modifications importantes des sites actifs des enzymes cibles. Pour l'AMX, la résistance est associée à des modifications ponctuelles d'au moins trois de ses six PBP, ainsi que de plusieurs déterminants non PBP. Ces mutations sont acquises par transformation naturelle, phénomène lors duquel le pneumocoque internalise de l'ADN présent dans son environnement et l'intègre à son génome. Dans le chapitre 2 de cette thèse, nous avons exploré l'aquisition de la résistance à l'AMX chez le pneumocoque, en transformant des souches sensibles avec de l'ADN d'un isolat bactérien résistant. En séquençant leur génome, nous avons pu suivre les événements successifs de recombinaison à chaque étape de transformation. Ceci nous a permis de corréler des loci spécifiques associés à la résistance. De cette manière, nous avons déterminé

que les gènes essentiellement impliqués dans la résistance à l'AMX étaient *pbp2x*, *pbp2b*, *murM* et *pbp1a*, acquis dans cet ordre.

Dans le chapitre 3, nous avons utilisé la lyse induite par l'AMX en combinaison avec un criblage létal synthétique à l'échelle du génome pour identifier BeaU, une protéine membranaire non caractérisée jusqu'à présent. Les souches de *S. pneumoniae* mutées pour *beaU* lysent précocement en phase stationnaire et présentent une sensibilité accrue aux antibiotiques β-lactames. Nous démontrons que ces phénotypes sont dépendants de LytA. Cette association implique probablement un rôle de BeaU dans la construction de la structure finale de la paroi cellulaire, ce qui affecterait l'activité de LytA de manière indirecte.

La capacité d'une cellule à détecter un stress et d'y répondre de manière appropriée est essentielle pour minimiser les effets d'un traitement antibiotique. Le pneumocoque possède un système spécifique pour la détection de stress associés à la paroi cellulaire, à savoir CiaRH. Dans ce système, l'histidine kinase CiaH répond à un signal de stress en activant le régulateur de réponse CiaR. CiaR modifie alors l'expression d'un ensemble de gènes. Dans le chapitre 4, nous avons examiné le rôle de mutations hyperactives de CiaH dans la diminution de la sensibilité à l'AMX. En utilisant de faibles concentrations d'antibiotique (doses sublétals), nous montrons pour la première fois que l'AMX peut également sélectionner des mutations ponctuelles dans le gène *ciaH* et confirmons que les substitutions qui en résultent augmentent l'expression des gènes dépendants de CiaR. En utilisant le système de répression CRISPRi, nous avons identifié au moins quatre membres du régulon qui peuvent être impliqués dans la modification de la paroi cellulaire pour mieux tolérer le stress induit par l'AMX.

Dans cette thèse, nous explorons la manière dont les pneumocoques répondent aux traitements à l'AMX, à la fois en étudiant le mécanisme et l'acquisition de la résistance, mais aussi en identifiant de nouvelles protéines impliquées dans la réponse à l'inhibition de la synthèse de la paroi cellulaire. La compréhension de la réponse cellulaire à des traitements médicamenteux spécifiques est essentielle pour le développement de programmes thérapeutiques appropriés, afin de conserver l'efficacité de ces antibiotiques et permettre leur utilisation dans le futur.

# Acknowledgements

There are so many people without whom I could not have completed this thesis that I cannot even begin to thank them all. But here I go, willing to try in any case. After all, what else does one learn during a PhD?

I would first like to acknowledge **Jan-Willem**. Without your support, mentorship, feedback, and brainstorming prowess, this thesis would not exist and I would not be the scientist I grew to be over the last five years. You have carefully cultivated such a special environment in the Veening Lab, one of scholarship and excellence, yet also one of friendliness, mutual support, and collaboration. It has been an absolute privilege to be a part of your team, and I cannot thank you enough for the opportunity to be here.

When I first started in the Veening lab I was inexperienced and completely lost. Luckily there were some incredible PostDocs and experienced PhDs who were able to get me up to speed. You introduced me to the world of pneumococcal biology and microscopy, and I would have wasted much more time (and broken more expensive things) without you. Thank you to **Arnau** who introduced me to the lab and was my antibiotic resistance buddy. To **Lance** for always being ready with a joke, for proofreading all my professional emails, and letting me borrow your sweet, sweet cat for 6 weeks through lockdown. Huge thank you to our lab mum **Xue**, for always checking in, as well as sharing your excellent science and sense of humour. To **Clement**, without whom the lab would be significantly less energetic, thank you for all your help with microscopy and protein biology. Sorry you had to answer the same questions every year. To **Renske**, thank you for your feedback, creativity, inspiration, and kind heart. I look forward to catching up about cool science and crochet patterns very soon. To **Jun** for always always being available with a helping hand, **Stefano** for teaching us the ways of the world, and **Monica** for your technical support and cool vibe. To lab big sister and my loyal bench neighbour **Anne-Stephanie.** Thank you for the technical and personal advice, gossip, crepe recipes, and cat pictures. Give Oligo and Merlin a kiss from me. To **Liselot**, our favourite TikTok star, thank you for the advice, help, and dance lessons. I'm not sure they helped but at least we had fun trying.

The lab changed a lot in the last two years, but our newer members quickly became essential parts of the team. A huge shout out to **Vik**, **Axel**, **Maria**, and **Jesus**. Our time together has been short but sweet, and I already can't imagine the lab without any of you. **Jessica**, thanks

for the writing cookies and all the cell wall questions, I'm looking forward to seeing what you come up with. Honorable mention to **Johann** for having the best jokes of the whole group, and always complimenting my schematics. Never change. **Amelieke**, you started supporting me in my pneumococcal antibiotic resistance foray before you even officially joined the lab. Thank you for sharing feedback, ideas, and clinical knowledge, and for always being up for an adventure. To **Bevika**, our fresh wee bébé, thanks for all the giggles, adventures, and for understanding my accent. You are going to do great, and don't forget you can always reach out for help if you need it.

Over the years I have supervised several students, all of whom contributed hugely to this project, and had to put up with my novice (although hopefully improved) supervision skills. My first student **Alice** introduced me to Swiss life and encouraged my French language development. Without your tutoring I would have made many more inappropriate errors in my quest to become a conversationalist in French. Your future students will be lucky to have you. To **Evan**, thank you for all your amazing work on the recombination project, I don't think I could have finished it without your help. Your advice for the Swiss Riviera was noted. To **Sylvia**, you were a delight to teach, and I'm so happy I could introduce you to the molecular biology side of microbiology. We can chat about the *lac* operon any time. To **Auriane**, you did wonderful work during your year here, and I wish you all the best for your PhD. It was lovely to finally have a piece of Oceania in the lab. To **Nina**, you were more of a collaborator than a student, but I'll put you here because our little AMX resistance team was the best. You kept me sane during one of the most difficult years, and a took on more than you should have in order to do so. Thank you for your help and support, and I look forward to seeing where your talent and ambition take you.

No PhD experience is complete without the lab PhD crew. To **Dimitra**, I can't believe I had to move to Switzerland and start a PhD just to find my soul sister. Together we brought the best drama, the best adventures, and the best sass to every occasion. Thanks for the nose piercing, and let's keep booking impulse flights together forever. To **Julien**, my work wife, eternal tea buddy, and colour selector, thank you for the chats, R help, and brainstorming sessions. I still believe you made BactExtract just for me, so thanks for that too. To **Afonso**, thank you for never saying no to whatever mountain adventure I suggested. Your skiing has come such a long way over the years, and I'm looking forward to freezing through another camping trip

soon. To **Vincent**, you saved my statistical analysis from myself at least weekly, and somehow always knew when I was upset. Unfortunately, that meant I cried on you a lot, and I am sorry for that, but thanks for the support anyway.

I was very fortunate to be located within an incredible department during my time at UNIL. From numerous BBQs to mimosa-drenched weekend trips, we really did it all. To **Rita**, you are the kindest, most empathetic, and sassy person that I know. You're an amazing scientist, and I can't wait to see you knock it out of the park in a few months. To **Silvia** and **Ania**, it wouldn't have been the same without your senses of humour and willingness to pop prosecco anywhere. To **Diogo** and **Konstantin**, who supported me in a brief foray into football, I appreciate the effort. To the Lunch Club, **Andrew**, **Sudip**, and **Vish**, it's been a pleasure seeing you at 12 every day and I'll miss our food and science chats. To the DMF, we are very privileged to work such in a diverse and welcoming department, and it's impossible to mention everyone who contributed to this experience. Thank you for making this such a great place to work. Thank you for the weeks where we had aperos every day. And thank you for last minute beer/crafts/BBQ suggestions. Honorable mentions to **German**, **Lucie**, **Bjorn**, **Ljiljana**, **Florian**, **Vladimir**, **Aline**, **Nadine**, **Nassime**, **Nassife**, and **Janette**.

I can't talk about the DMF without mentioning the Gruber Lab. It's a pleasure to be your only honorary lab member. Thank you for the ski retreats, BBQs, and all my random protein stuff. To **Taschi**, I literally could not have done this without you to solve my problems. I still don't know if I'm supposed to put the acid or the base first though. To **Flo**, it's been a good run. Thanks for teaching me to pour my own acrylamide gels, model proteins, and to just be generally sensible. To **Roberto**, you left too soon, and we miss seeing your smile in the corridors. To **Hammam** habibi, thank you for always being yourself, for dragging me out of my comfort zone, and always being the life of the party. You're doing so well, and I'm really proud of you. To **Ophélie**, you're a gem and they are lucky to have you. Never lose the sass.

To **Sarah** and **Emily**, thank you for listening to my problems and always giving such good advice. I miss you, and I look forward to catching up on everything we missed these last few years (yes, I do mean repeating the bachelorette and housewarming parties).

**Paolo**, you arrived pretty late in the piece, but you've earned a spot on this page. Thank you for being so proud of me and so supportive, and making sure I remembered to eat and had clean clothes to wear during these last months. Thank you for discussing science with me over breakfast and for always telling me my figures are pretty. I can't wait to see where we end up together. Ti amo.

Lastly and most importantly, to my family. To my baby brother **Sam**, thanks for being the best, and always showing your most authentic self. To **Jin** and **Stephen**, thank you for always making the effort to call or email, I appreciate all your support.

**Mum** and **Dad**, you pushed and supported me for my entire academic career and I wouldn't be here without you. You told me to go to university and study what I love, so I did, although I'm not sure that you expected me to be here eleven years later, still studying what I love. I miss you, and I cannot wait to celebrate this achievement together.

# Table of Contents

# Chapter 1

## In Review: The molecular biology of amoxicillin resistance evolution in *Streptococcus pneumoniae*

Paddy S. Gibson, Jan-Willem Veening

Department of Fundamental Microbiology, Faculty of Biology and Medicine, University of Lausanne, Biophore Building, CH-1015 Lausanne, Switzerland

This chapter was written by PG with feedback from JWV

## Abstract

*Streptococcus pneumoniae* is the most common cause of community-acquired pneumonia, and one of the main pathogens responsible for otitis media infections in children. Amoxicillin is a broad-spectrum β-lactam, used heavily for the treatment of bacterial respiratory tract infections. Here, we discuss the pneumococcal response to amoxicillin, including the mode of action, the effects on autolysin regulation, and the evolution of resistance through natural transformation.

## Introduction

Amoxicillin (AMX) is the frontline antibiotic for the treatment of bacterial respiratory tract infections such as otitis media and pneumonia. The Gram-positive opportunistic pathogen *Streptococcus pneumoniae* (the pneumococcus) is an important commensal member of the human nasopharyngeal microflora. While colonisation is usually asymptomatic (Nunes et al., 2005), local spread or invasion of other regions results in rapid inflammation (Shak et al., 2013). It remains the leading cause of community-acquired pneumonia worldwide and one of the most common causes of otitis media in children (Ho and Ip, 2019). In addition, the pneumococcus is capable of crossing epithelial barriers to cause severe invasive disease (IPD), such as sepsis and meningitis, and is responsible for 1.5 million deaths annually (O'Brien et al., 2009; Troeger et al., 2018; Weiser et al., 2018). Antibiotic resistance is evolving rapidly and the high burden of pneumococcal disease, despite vaccine introduction, led to the WHO listing *S. pneumoniae* as a top 12 priority pathogen in 2017 (Weiser et al., 2018). It is of particular concern in regions with limited access to healthcare and vaccination, with the incidence of invasive pneumococcal disease (IPD) in children < 5 years old 2-3 times higher in African nations than reported in Western Europe (Tam et al., 2017).

Vaccines are based on capsular polysaccharide (CPS), of which more than 100 serotypes have been described to date (Ganaie et al., 2021, 2020). Due to the large diversity, and since only a confined group of serotypes caused the majority invasive disease, the pneumococcal conjugate vaccines were designed to target only a small number of clinically relevant serotypes (Weiser et al., 2018). However, the pneumococcus is naturally competent, able to respond to environmental conditions to uptake extracellular DNA and recombine it into its genome, resulting in remarkable genomic plasticity (Salvadori et al., 2019). The result is frequent and large-scale recombination events, enabling an everchanging landscape of vaccine-escape and antibiotic resistant variants (Croucher et al., 2011; Wyres et al., 2013).

Amoxicillin (AMX) is one of the most active penicillin-derived β-lactams towards *S. pneumoniae*, including isolates with reduced susceptibility towards penicillin (PEN) (Andes and Craig, 1998; Davies et al., 1999). In addition, the high absorption rate of AMX into the bloodstream reduces side effects and increases serum concentrations, making it desirable as an oral treatment. It is primarily used for the treatment of respiratory tract infections, some urinary tract infections, and in the prevention of endocarditis prior to dental treatments

(Wright, 1999). The current clinical breakpoints for oral AMX treatment recommended by EUCAST are minimum inhibitory concentration (MIC) < 0.5 μg/mL to be considered fully susceptible and ≥ 1 μg/mL for resistance (The European Committee on Antimicrobial Susceptibility Testing, V12.0, 2022).

AMX resistant *S. pneumoniae* isolates first appeared in the United States, France, and Spain in the mid-90s (Doern et al., 1996; Doit et al., 1999; Pérez-Trallero et al., 2001). Strains with AMX MICs greater than 16 μg/mL were isolated in Romania between 2005 and 2006 (Soriano et al., 2008), and are currently on the rise in Spain, a phenomenon which correlates with increased usage of oral AMX/clavulanic acid (Càmara et al., 2018). β-lactamase enzymes have never been isolated from *S. pneumoniae* (Zapun et al., 2008). Instead, resistance in this species is mediated by large-scale modifications to the penicillin binding proteins (PBP), although mutations in non-PBP genes have also been implicated (Grebe et al., 1997; Guenzi et al., 1994; Smith and Klugman, 2001). While highly conserved in PEN sensitive strains, PBPs of resistant isolates are highly variable, with up to 10% of amino acid changes (Hakenbeck et al., 2012). Other resistance determinants such as MurM, CiaRH, and PgdA have also been described (Filipe et al., 2002; Guenzi et al., 1994; Tait-Kamradt et al., 2009).

AMX usage and consequent resistance evolution did not occur in a time when pneumococcal β-lactam resistance was unheard of. Low-affinity PBPs had been circulating for more than 20 years, since the first PEN resistant strain was identified in 1967 (Hansman and Bullen, 1967), and AMX resistance likely evolved in PEN resistant clones (Pérez-Trallero et al., 2007, 2003; Stanhope et al., 2007). In order to the understand the origin and specific quirks of AMX resistance, we must first delve into the general mechanisms of β-lactam resistance in the pneumococcus.

In this introductory chapter, we discuss the evolution of β-lactam and AMX resistance through rampant horizontal gene transfer between *S. pneumoniae* and commensal Streptococcal species. We examine the fundamental process of cell wall synthesis and its inhibition by β-lactam antibiotics, as well as the downstream effects of this obstruction, including autolysis. We then summarise the current knowledge of β-lactam resistance determinants in the pneumococcus and discuss how these changed in response to the shift towards broad clinical usage of AMX.

## Natural competence and amoxicillin resistance evolution in the pneumococcus

The first AMX resistant strains isolated between 1994 and 1995 had comparable minimum inhibitory concentrations (MICs) to PEN (Doern et al., 1996). Isolates with higher MICs for AMX than for PEN began to be isolated in France in 1997 (Doit et al., 1999), while two large cohort studies across Spain between the years of 1998-1999 and 2001-2002 found that 5% of isolates were AMX resistant, a figure which increased to 20% when only PEN resistant isolates were taken into account (Pérez-Trallero et al., 2005, 2001). A more in depth study of 165 pneumococcal strains isolated from 17 Spanish hospitals between 1998 and 1999 found that 9.8% were AMX non-susceptible (Pérez-Trallero et al., 2007, 2003). Among the AMX resistant isolates collected during this time, approximately 78% of them belonged to five clonal complexes notorious for PEN resistance: Spain$^{23F}$-1, Spain$^{6B}$-2, Spain$^{9V}$-3, Poland$^{23F}$-16, and an England$^{14}$-9 (Pérez-Trallero et al., 2007; Stanhope et al., 2007). However, these studies all occurred in the pre-vaccine era, and although the sequence types associated with these clones are still common culprits in AMX resistant infections, they are often found with different serotypes due to prevalent capsule switching (Càmara et al., 2018; González-Díaz et al., 2020). AMX non-susceptible clones have also been associated with increased rates of cephalosporin and clindamycin resistance (Pérez-Trallero et al., 2007).

*S. pneumoniae* is naturally competent, and resistant variants primarily arise through homologous recombination among strains, or from closely related species that occupy the upper respiratory tract niche (Croucher et al., 2012). Indeed, among AMX resistant pneumococcal isolates, the relative horizontal transfer frequency of *pbp2x* and *pbp2b* was found to be high (10.2 and 7.8% respectively), indicating that movement of *pbp* alleles with low AMX affinity between pneumococcal strains has contributed to the dissemination of resistance (Stanhope et al., 2007). Evidence of *pbp* allele transfer among *Streptococcus mitis*, *Streptococcus oralis*, and *S. pneumoniae* has been found in clinical isolates (Chi et al., 2007; Dowson et al., 1993; Kalizang'oma et al., 2021; Potgieter and Chalkley, 1995; Sibold et al., 1994), while similar allele alterations have also been identified in *Streptococcus gordonii* (Haenni and Moreillon, 2006). In addition, low-affinity HMW *pbp* alleles from *S. mitis* were able to be transformed and selected for with β-lactam antibiotics in *S. pneumoniae* under laboratory conditions (Hakenbeck et al., 1998b). Large variation in *pbp* alleles among β-lactam susceptible commensal isolates, along with the identification of regions homologous to low-

affinity mosaic *pbp* fragments in β-lactam resistant S*. pneumoniae*, led to the hypothesis that *pbp*-mediated resistance evolved through the accumulation of point mutations in commensal Streptococcal species. These species then became donors of low-affinity *pbp* alleles for lateral gene transfer into, and among, pneumococcal isolates, enabling rapid dissemination of *pbp*-mediated resistance. The current model is a global gene pool of highly variable alleles, shared among commensal and pathogenic Streptococcal species (Dowson et al., 1997; Hakenbeck et al., 2012; Jensen et al., 2015; Reichmann et al., 1997).

Genetic variation is accessible in this way because both natural competence and homologous recombination are powerful tools, and *S. pneumoniae* utilises them both to the best of its ability. Competence is controlled by a quorum sensing pathway, where the competence stimulating peptide (CSP) interacts with the ComDE two-component system (Straume et al., 2015). Phosphorylated ComE activates transcription of the alternative sigma factor *comX*, resulting in a signalling cascade to rapidly transcribe and translate all proteins necessary for exogenous DNA uptake, including a type IV-like pilus (Laurenceau et al., 2013; Martin et al., 2013; Slager et al., 2019; Ween et al., 1999) (Chapter 2, Fig 1). In addition, genes implicated in fratricide, such as *cbpD*, *lytA*, *cibA*, and *cibB*, are also upregulated (Håvarstein et al., 2006). This phenomenon involves the killing of non-competent cells by competent cells, and is thought to increase gene exchange under natural conditions, by freeing up more extracellular DNA (Claverys and Håvarstein, 2007). Competent cells protect themselves by simultaneously producing an immunity protein, ComM (Håvarstein et al., 2006). Competence is an energetically expensive process that is tightly regulated, with the transcriptional cascade switched off within 20 minutes of CSP induction (Alloing et al., 1998; Martin et al., 2013; Mirouze et al., 2013; Piotrowski et al., 2009; Weng et al., 2013). Upon cytoplasmic entry, ssDNA is bound by RecA and DprA, thought to initiate the homology search, while extra ssDNA molecules form eclipse complexes with SsbB (Attaiech et al., 2011; Bergé et al., 2003; Lisboa et al., 2014; Morrison et al., 2007; Quevillon-Cheruel et al., 2012). Once RecA-mediated crossover has begun the homology required for initiation decreases, allowing some mismatches to occur, a requirement for the recombination of highly variable *pbp* loci (Danilowicz et al., 2015).

While RecA, DprA, and SsbB are all essential to avoid ssDNA degradation by endogenous nucleases, the accumulation of ssDNA-SsbB eclipse complexes in the cytoplasm also serves as

a reservoir for repeated rounds of homology searching and recombination within one competence window, increasing the likelihood of successful DNA integration (Attaiech et al., 2011). This allows for the occurrence of significant horizontal gene transfer events, in spite of the energy cost and time restrictions. Regions of recombination up to 50 Kb in length have been described in clinically relevant pneumococcal isolates such as PMEN-1 (Croucher et al., 2011; Wyres et al., 2013, 2012), and during the polyclonal infection of a paediatric patient more than 7% of the pneumococcal genome was found to have been exchanged within three months (Hiller et al., 2010). In addition, cell-to-cell contact, for example in biofilms on nasopharyngeal mucosal membranes, has been found to facilitate longer DNA fragment transfer (Cowley et al., 2018), and a single transformation event can simultaneously change the capsular serotype and resistance profile as the *cps* locus located close to both *pbp2x* and *pbp1a* (Trzciński et al., 2004). There is also evidence to support co-transfer of distantly located *pbp* loci (Gibson et al., 2021; Hakenbeck et al., 1998b; Reichmann et al., 1997), indicating a role for epistatic interactions between resistance determinants (Arnold et al., 2018; Dewé et al., 2019; Skwark et al., 2017).

The mechanistic of recombination can itself contribute to an already significant pool of genetic variation. While recombination events can be long contiguous stretches of easily identifiable sequence transfer, non-contiguous events also readily occur, both in the natural ecological niche and in the laboratory (Croucher et al., 2012; Gibson et al., 2021; Mell et al., 2011). In this case, identified regions of recombination appear fragmented, interrupted by stretches of recipient genome but with donor-identified sequences located more closely together than would be expected for unlinked recombination events occurring randomly in the genome (Croucher et al., 2012). It is not yet known whether these events occur from fragmented donor DNA, or from a single donor molecule. In theory, sequestered cytoplasmic ssDNA-SsbB eclipse complexes could increase the likelihood of proximal integration of fragmented donor DNA. However, it has also been hypothesised that multiple points of contact with the recipient chromosome initiated by a single ssDNA-RecA presynaptic filament could result in the formation of several displacement-loops (D-loops) located close together (Bell and Kowalczykowski, 2016; Forget and Kowalczykowski, 2012; Gibson et al., 2021; Hsieh et al., 1992; Yang et al., 2020). This would correlate with observations where recombination event density was independent of the concentration of transforming DNA, something that

would not be expected under a multi-fragment hypothesis (Croucher et al., 2012). If or how these events contribute to the evolution of β-lactam resistance is not known, but transformation of PCR fragments into the *pbp2x* locus with AMX selection resulted in as many as four blocks of donor mutations in the region (Gibson et al 2021) (Chapter 2). This could suggest a beneficial role of non-contiguous recombination at the population level, providing increased allelic variation in the relentless search for low affinity, yet more fit, *pbp* alleles.

## β-lactam treatment and the cell wall

Cell wall synthesis is essential for cell viability, making this pathway an attractive target for antibiotic development (Sham et al., 2012). In the pneumococcus, the cell wall is composed of roughly equal quantities of both peptidoglycan (PG) and teichoic acids (TA), both of which play a role in the cellular response to β-lactam antibiotic treatment (Fig. 1).

PG precursor formation begins with formation of the pentapeptides, by the consecutive addition of amino acids to UDP-MurNAc (synthesised from UDP-GlcNAc by MurA and MurB), which are then modified in two membrane-bound steps by MraY and MurG, resulting in lipid II (Hakenbeck and Chhatwal, 2007). Lipid II precursors are then flipped and exposed on the outside of the membrane, possibly by YtgP (Ruiz, 2009; Sham et al., 2014). In addition to linear lipid II, branched muropeptides are produced by the enzymes MurM and MurN, which add L-Ser-L-Ala or L-Ala-L-Ala to the stem peptide lysine. Incorporation of lipid II into the PG occurs in two steps performed by penicillin binding proteins (PBPs) (Scheffers and Pinho, 2005). Transglycosylation, in which precursors are assembled into peptidoglycan chains, is followed by transpeptidation, where cross-links between neighbouring peptides are formed. Of the six PBPs encoded by *S. pneumoniae*, only Pbp2x and Pbp2b are essential under normal growth conditions. They are high molecular weight (HMW) class B PBPs and possess a single transpeptidase (TP) domain each, while Pbp2x additionally has two PASTA domains at the C-terminus important for its septal localisation (Morlot et al., 2003; Peters et al., 2014; Schweizer et al., 2014). Septal and longitudinal PG synthesis are maintained in a delicate balance and inhibition of the two essential PBPs is tolerated to different extents (Philippe et al., 2015). Pbp2x is the main PBP required for septal PG synthesis and cells depleted for Pbp2x show an elongated phenotype, while Pbp2B is mainly involved in peripheral PG synthesis and

depletion leads to short cells (Berg et al., 2013). Pbp1a, Pbp1b, and Pbp2a, HMW class A PBPs, have both TP and transglycosidase (TG) domains. They are not essential in normal growth conditions, although a double deletion of *pbp1a* and *pbp2a* is synthetic lethal, suggesting some functional redundancy (Hoskins et al., 1999). Pbp3 is a low-molecular weight (LMW) D,D-carboxypeptidase which regulates PG synthesis by cleaving the fifth amino acid from pentapeptides already integrated in the PG matrix, reducing the available substrates for incorporation of new lipid II monomers (Morlot et al., 2004). Pbp3 is not essential in *S. pneumoniae*, although mutating the protein results in spherical cells with multiple septa and reduced cell separation (Schuster et al., 1990). This phenotype was also associated with changes in the localization of cell-division proteins, including the high-molecular weight PBPs, indicating the importance of PG maturation by Pbp3 in the coordination of cell division (Morlot et al., 2004). In addition to the PBPs, essential members of the shape, elongation, division and sporulation (SEDS) protein family, RodA and FtsW, were also recently shown to polymerise peptidoglycan (Emami et al., 2017; Taguchi et al., 2019).

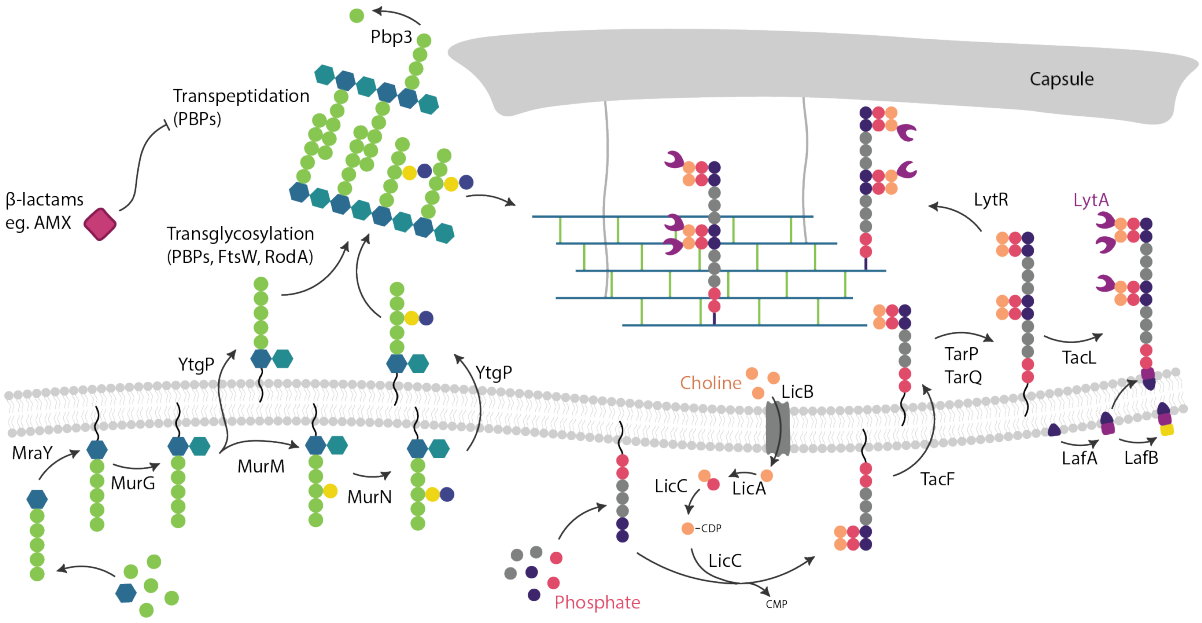


**Figure 1: Overview of cell wall synthesis in the pneumococcus.** Pentapeptides are synthesized in the cytoplasm by MurA-F, then modified in two membrane-bound steps by MraY and MurG. Lipid II is then either transferred over the membrane by predicted flippase YtgP, or additional branched amino acids are added by MurM and MurN before flipping. Precursors are then added to the PG matrix via PBP, RodA, and FtsW-mediated transglycosylation. Transpeptidation is thought to be largely catalyzed by Pbp2b and Pbp2x. Pbp3 contributes to PG maturation by cleaving the terminal alanine from Lipid II, blocking further crosslinking. TA precursors are also synthesized in the cytoplasm, with Lic proteins involved in the addition of choline then flipped over the

membrane by TacF. TarP and TarQ then build up the repeating units extracellularly. Although traditionally this was believed to occur inside the cell, it is currently under debate. Multimers are then either attached to a glycolipid anchor by TacL, or anchored to the PG matrix presumably by LytR, competing for anchor points with capsule tethers. Glycolipid anchors are thought to consist of glucosyl-diacylglycerol (Glc-DAG), produced by LafA. However the pneumococcus has a second glycolipid GalGlc-DAG produced by LafB. LytA attaches to phosphorylcholine residues on TA at certain stages of growth. Inspired by Denapaite et al (2012), Vollmer et al. (2019), and Domenech et al. (2018).

β-lactam antibiotics mimic the D-ala-D-ala moiety of the muropeptides which is recognized by the PBPs for transpeptidation, allowing an interaction with the active-site serines of TP and D,D-carboxypeptidase domains (Waxman and Strominger, 1983). The resulting acylation reaction cracks open the high energy β-lactam ring to form a covalent penicilloyl-enzyme complex. Reversing this reaction is slow, and the antibiotic blocks the active site for an extended period (Hakenbeck et al., 2012). Inhibition of transpeptidation is the critical step that stops cell wall synthesis, although almost all β-lactams also exhibit potent inhibition of Pbp3 via the D,D-carboxypeptidase domain (Kocaoglu et al., 2015). Blocking transpeptidation has negative downstream effects, inducing nascent PG turnover and depleting the intracellular stock of cell wall building blocks. Cell shape is dependent on tight control of and association between transpeptidation and tranglycosylation, thus TP domain inhibition results in a high concentration of unlinked glycan strands without the structural support of crosslinking, contributing to bacterial inhibition (Cho et al., 2014).

## B-lactam treatment triggers autolysis

β-lactams are considered bacteriolytic antibiotics, meaning that treatment often results in explosive cell lysis (Chapter 2, Fig 3). For a long time, lysis was attributed to a weakened cell wall in the presence of overwhelming osmotic pressure. However, this changed upon the observation that mutants defective in autolysis also do not lyse in the presence of PEN, unless purified autolysin is added to the culture (Tomasz and Waks, 1975). The major pneumococcal autolysin LytA is responsible for the characteristic stationary phase autolysis in liquid media (Avery and Cullen, 1923; Garcia et al., 1985; Howard and Gooder, 1974; Tomasz, 1968). It is an *N*-acetylmuramoyl L-alanine amidase with a choline binding domain (CBD). Choline binding proteins bind to the phosphorylcholine residues that decorate TAs in the pneumococcal cell

wall (Briese and Hakenbeck, 1985) (Fig. 1). TA precursors are assembled in the cytoplasm, then flipped outside the cell by TacF. Wall TAs (WTA) are covalently linked to the PG structure, whereas lipid TAs (LTA) are anchored in the plasma membrane. It is believed that LytA must be bound to choline on the WTAs in order for its substrate to be accessible to the active site of the amidase domain (Flores-Kim et al., 2019; Mellroth et al., 2012). Choline is essential for LytA-dependent lysis to occur, but too much choline in the media leads to inhibition of LytA activity (Giudicelli and Tomasz, 1984; Holtje and Tomasz, 1975; Tomasz, 1968). LytA deletion mutants show attenuated virulence in murine infection models (Berry et al., 1989; Berry and Paton, 2000; Canvin et al., 1995; Hirst et al., 2008). LytA is cytoplasmic during exponential growth, yet how it gets outside the cell to access WTA and its PG substrate upon entrance to stationary phase or β-lactam treatment is not known. It is constitutively expressed through all growth phases, indicating strict regulation at the protein level (Olivares et al., 2011).

It has been hypothesised that the unlinking of transpeptidation and tranglycosylation activities combined with the loss of cell wall synthesis quality checking capabilities of other proteins during β-lactam treatment is involved in the misactivation of autolytic hydrolases (Cho et al., 2014). β-lactam tolerance through defective lysis is rarely caused by mutations in *lytA*, but rather through changes to autolysin regulatory elements (Liu and Tomasz, 1985; Moreillon et al., 1988; Moscoso et al., 2010; Olivares et al., 2011). PEN resistance and defective lysis are two separate genotypes that could be unlinked through genetic crosses, although 70% of PEN resistant pneumococcal isolates at the time displayed defective lysis (Moreillon et al., 1988). In some cases, autolysin was still present in lower concentrations than in a wild-type strain, and tolerant isolates were still susceptible to lysis via other induction routes (Liu and Tomasz, 1985). We screened for mutants with altered lysis following AMX treatment and revealed a novel membrane protein of the pneumococcus which increases lysis when deleted. This phenotype was shown to be LytA-dependent, and increased lysis was observed both in late stationary phase and in the presence of AMX. The protein is hypothesised to indirectly regulate the activity of LytA, although the molecular mechanism through which this occurs is not yet clear (Chapter 3). Understanding the regulation of autolysis provides information not just for the fundamental molecular biology of cell wall synthesis but is critical to fully understand the effects that heavily utilised antibiotics such as AMX have on the species they are used to target.

## Pbp2x, Pbp2b, Pbp1a and MurM implicated in amoxicillin resistance

In *S. pneumoniae*, low-affinity variants of Pbp1a, Pbp2x, and Pbp2b are considered the main resistance determinants for β-lactam antibiotics, although variable alleles of all five high molecular weight PBPs have been isolated (du Plessis et al., 2000; Hakenbeck et al., 1998a). Substitutions must alter the active site in a way that reduces affinity for the β-lactam molecule but does not impact the essential enzymatic function. There are different mechanisms by which this can occur, for example the Q552E mutation in Pbp2x introduces a net negative charge near the entrance of the active site and is often associated with a closed configuration, whereas mutations S398L and N514H are linked to an open configuration and have been linked to AMX resistant isolates (Pernot et al., 2004; Stanhope et al., 2008). However, no mutation or block of mutations in any one *pbp*, when transferred to a susceptible strain, has been sufficient to confer resistance (Hakenbeck et al., 1998a; Kosowska et al., 2004) and multiple residue sites in all three of Pbp1a, 2x, and 2b have been found to be under positive selection in AMX resistant isolates (Stanhope et al., 2008).

The strength of the TP active site interaction depends on both antibiotic and PBP chemistry, such that the exact mechanism of PG crosslinking inhibition depends on the β-lactam in question (Hakenbeck et al., 2012; Kocaoglu et al., 2015). Large-scale modifications to the PBPs alter the structure of enzymatic active sites and reduce β-lactam binding affinity, however the extent of the resistance phenotype can look very different depending on the antibiotic (Grebe et al., 1997; Guenzi et al., 1994; Smith and Klugman, 2001). For example, selection on cefotaxime results in substitutions in Pbp2x, while alterations to Pbp2b allow for reduced susceptibility to piperacillin (PIP) (Grebe and Hakenbeck, 1996). The Pbp2x mutations did not provide cross-resistance to PIP, and vice versa (Grebe and Hakenbeck, 1996; Krauß et al., 1996), and the Pbp2x T550A substitution found in cefotaxime (CTX) resistant mutants increased susceptibility to AMX (Sifaoui et al., 1996). As an alternative example, PIP is thought to target Pbp2x, blocking septal PG cross-linking as demonstrated by lemon-shaped cells upon antibiotic treatment (Kocaoglu et al., 2015; Philippe et al., 2015). However, passaging in PIP under laboratory conditions repeatedly results in *pbp2b* mutations (Grebe and Hakenbeck, 1996), a phenomenon also observed for AMX (Chapter 4).

Catalytic motifs within the TP domains of PBPs are often hotspots for mutations which reduce the stability of the β-lactam-PBP interaction. The active-site serines of Pbp2x include S337, S395, and S571 which have been shown to stabilize CTX embedded in the active site (Gordon et al., 2000), and respective neighbouring sites 338, 394, and 572 were found to be under positive selection in the context of AMX resistance (Stanhope et al., 2008). Substitutions from T338 to A, S, or G have been heavily implicated in β-lactam resistance (Cafini et al., 2006; Dessen et al., 2001; Gordon et al., 2000; Mouz et al., 1999, 1998; Nagai et al., 2002), while S571 has a critical interaction with T338 and Y586, which is often specifically altered in low-affinity Pbp2x variants (Dessen et al., 2001). Outside of the TP domain, relatively few substitutions have been linked to resistance (although many studies only report the sequence of TP domains), and were not found to be essential for AMX resistance (Gibson et al., 2021)(Chapter 2). Within Pbp2b the T446A substitution has been selected for in laboratory experiments with both PIP and AMX (Grebe and Hakenbeck, 1996) (Chapter 4), as well as found in collections of PEN and AMX resistant clinical isolates (Cafini et al., 2006; Nichol et al., 2002). A set of 10 mutations at the C-terminal of the Pbp2b TP domain has also been associated with AMX resistance, and is thought be important for high-level resistance (discussed below) (Cafini et al., 2006; Stanhope et al., 2008).

Both Pbp2x and Pbp2b are enzymes that perform an essential function in the cell, and the active site modification found in pneumococcal isolates are severe. Deleterious effects of these alterations have been observed (Albarracín Orio et al., 2011; Garcia-Bustos and Tomasz, 1990), but presumably are compensated for in some way, to allow these strains to survive competition in the absence of antibiotic treatment. Despite being non-essential, mutations in Pbp1a are consistently linked to β-lactam resistance phenotypes in clinical isolates. In *pbp* transformation experiments, it has been observed that transferring only mosaic *pbp2x* causes a growth defect which can be restored upon addition of the matching *pbp1a* (Zerfaß et al., 2009). Low-affinity Pbp1a variants usually have a narrower active-site, which is linked to the T371A substitution next to the active-site serine and the TSQF(574–577)NTGY substitution in a loop close to the active site cleft (Job et al., 2008). In *S. gordonii*, deletion of Pbp1a drastically increased the rounds of selection necessary for evolution of resistance to PEN, although removing it from an already evolved strain had minimal effects on the minimum inhibitory concentration (MIC) (Haenni and Moreillon, 2006). In addition, uptake of low-affinity *pbp2x*

and *pbp1a* alleles were sufficient to correct the cell division defects and overall fitness costs of the low-affinity *pbp2b* allele (Albarracín Orio et al., 2011).

Fitness compensation through modifications to the aminoacyl-tRNA ligase MurM has also been reported in resistant isolates (Filipe et al., 2002; Filipe and Tomasz, 2000; Garcia-Bustos and Tomasz, 1990; Smith and Klugman, 2001). Along with low-affinity Pbp2x, Pbp2b, and Pbp1a, mutant MurM was found to be essential for AMX resistance in a serotype 11A clinical isolate (Gibson et al., 2021)(Chapter 2). Although the protein is non-essential under normal conditions, deletion resulted in almost complete loss of PEN resistance, even in the presence of low-affinity PBPs (Filipe and Tomasz, 2000). MurM variants in highly PEN and CTX resistant isolates have been associated with increased proportions of branched muropeptides in the cell wall (Garcia-Bustos and Tomasz, 1990; Smith and Klugman, 2001). The importance of branched muropeptides to β-lactam resistance is not well understood, although it has been hypothesised that the different lipid II shape either fits the low-affinity variant active sites better, thus reducing the effect on TP activity, or is a stronger competitor against β-lactams for PBP binding (Hakenbeck et al., 2012). It has also been shown that the order of allele uptake is important for optimal AMX resistance evolution, likely due to fitness compensation effects (du Plessis et al., 2002; Gibson et al., 2021) (Chapter 2).

## Penicillin vs Amoxicillin: A changing selective landscape

AMX began to be recommended for clinical use as rates of PEN resistance in *S. pneumoniae* increased. It was initially found that most PEN resistance isolates could still be treated with AMX, with AMX MICs lower than those for PEN (Nagai et al., 2002; Pankuch et al., 1995). Importantly, this observation implies that resistant mutations acquired under PEN selective pressure do not necessarily confer the same reduction in PBP affinity for AMX. Interestingly, there is evidence suggesting that early AMX resistant lineages were very closely related to PEN resistant lineages of the same serotypes already circulating in the population (Doit et al., 1999; Stanhope et al., 2007). Several studies comparing *pbp* allele sequences or restriction fragment length polymorphism patterning within PEN resistant strains either resistant or susceptible to AMX found large variation within *pbp2x* and *pbp1a* (Chesnel et al., 2005; Doit et al., 1999; du Plessis et al., 2002; Kosowska et al., 2004; Sanbongi et al., 2004). The only PBP

substitutions shared among AMX resistant isolates were in Pbp2b, specifically those located towards the C-terminal end of the TP domain (amino acids 590-641). Up to 10 substitutions have been identified in this region, with AMX MIC increasing with the number of alterations (Kosowska et al., 2004). Interestingly, this block of mutations could not be transformed into a susceptible lab strain unless low-affinity alleles of other *pbp* genes were already present in the genome (Cafini et al., 2006; Gibson et al., 2021; Hakenbeck et al., 1998b) (Chapter 2), potentially explaining the greater ease with which PEN resistant clones acquired AMX resistance (Doit et al., 1999).

## No one right way: Variable mechanisms for amoxicillin resistance

Although Pbp2x, Pbp2b, Pbp1a, and MurM are heavily associated with AMX resistance, their relative importance in the phenotype and the potential involvement of other genomic factors differ according to the genomic context. For example, strains carrying the same PBP TP domain and *murM* alleles had different AMX MICs, and transforming these alleles into a susceptible lab strain conferred only intermediate AMX resistance (Chesnel et al., 2005; Soriano et al., 2008). In another study, transfer of alleles of *pbp2x*, *pbp2b*, *pbp1a*, and *murM* were sufficient for the full resistance phenotype (Gibson et al., 2021), while in alternative AMX resistant clinical isolates the TP domain of *pbp1a* was not mutated but novel substitutions in *pbp2x* were identified (Soriano et al., 2008). A link between C-terminal Pbp2x substitutions and modified PgdA (PG N-acetylglucosamine deacetylase) has also been associated with high-level PEN and AMX resistance (Tait-Kamradt et al., 2009), and the two-component system CiaRH (Guenzi et al., 1994) (Chapter 4) as well as CpoA have been implicated in general β-lactam resistance (Grebe et al., 1997; Hakenbeck et al., 2012).

Perhaps most interestingly, *murM* from a serotype 23F isolate was unable to confer comparable resistance to the donor when transformed to susceptible lab strain R6 carrying *pbp2x*, *pbp2b*, and *pbp1a* alleles from the same donor. However, the same *murM* allele could confer further resistance to R6 in the presence of *pbp* alleles from different multidrug resistant clinical isolates (du Plessis et al., 2002). This draws attention to the complex relationships between MurM and other non-PBP resistance determinants, and the PBPs themselves. Different substitutions in the PBPs appear to affect the proteins and their

functions in different ways, requiring the concurrent evolution of diverse mechanisms for fitness compensation in order to maximise resistance phenotypes.

Another significant observation is the correlation of certain *murM* alleles with specific *pbp2b* mutations in AMX resistant clinical isolates (Cafini et al., 2006; Càmara et al., 2018). One hypothesis is that the altered muropeptide shape in murM mutants is a better competitor for the modified PBP active sites (Hakenbeck et al., 2012). Interestingly, Pbp2b-depleted cells have been shown to incorporate more branched muropeptides into the cell wall. Deleting *murM* introduces synthetic lethality with *pbp2b*, where decreasing the amounts of Pbp2b protein becomes toxic in a dose dependent manner. This is not the case for Pbp2x, indicating a dependence on branched muropeptides for peripheral cell wall synthesis but not for septal PG synthesis. The authors hypothesised that as branched muropeptides are longer and more flexible, their inclusion in glycan strands may strengthen the PG structure when cross-linking activity is reduced, and that the Pbp2b specificity was due to mid-synthesis turgor pressure experienced at the periphery but not the septum (Berg et al., 2013). These findings provide an interesting alternative hypothesis to the role of alternative *murM* alleles in AMX and indeed β-lactam resistance, and imply a tight link in the roles of Pbp2b and MurM in the phenomenon.

## Cell wall stress response via two-component system CiaRH

While serial passaging experiments to select for mutants with reduced susceptibility to β-lactam antibiotics such as PIP and CTX provided valuable information regarding antibiotic targets and key PBP affinities for resistance, these experiments are challenging to perform for AMX. Previous studies have shown no or very minor decreases in susceptibility, with no more than a 2-fold increase in MIC (Sifaoui et al., 1996). Maintaining selection for 24 passages did result in a 10-fold increase in MIC, but at 0.125 g/mL was still significantly below the clinical breakpoint for intermediate resistance (Davies et al., 1999), and starting with PEN resistant clinical isolates did not result in MIC increases at all (Pankuch et al., 1998). However, selecting for mutants that grew after population exposure to AMX identified the two-component signal transduction system (TCS) CiaRH as a potential low-level resistance determinant (Chapter 4).

Substitutions in the histidine kinase CiaH were first identified in strains serially passaged in CTX and PIP, usually clustered proximal to the conserved histidine residue (H226) (Guenzi et al., 1994), while more distally locating substitutions have been identified in clinical isolates (Muller et al., 2011) (Chapter 4). In addition, differential expression of the *ciaRH* operon was reported when pneumococcal cells were under vancomycin stress (Haas et al., 2005). The response regulator CiaR regulates transcription from 21 operons when phosphorylated, including genes involved in choline uptake and metabolism, teichoic acid synthesis, and competence (Halfmann et al., 2011; Slager et al., 2019). In theory, CiaR is phosphorylated and thus activated by CiaH, however the reverse reaction is reported to occur for this TCS in certain conditions such as C + Y growth media, making it difficult to extrapolate the effects of mutations in a natural setting (Muller et al., 2011). In laboratory conditions, the same *ciaH* mutations conferring increased CTX resistance also reduce both natural competence and autolysis (Mascher et al., 2003). CiaRH is a general response to cell wall stress, rather than specific to AMX. However, the signal to which CiaH responds by phosphorylating (or dephosphorylating) CiaR is not known, and exactly which member(s) of its 21 operon regulon is responsible for the changes in β-lactam susceptibility remains elusive.

## Thesis outline

Since the frontline antibiotic AMX began to be used heavily for the treatment of upper respiratory tract infections, including those caused by the human pathogen *S. pneumoniae*, resistant strains have been isolated. How resistance to this drug is mediated, and how resistance differs from that for other β-lactam antibiotics is not well understood. In this thesis we applied three different approaches to study the effects of AMX on the pneumococcal cell. We first used sequential transformations of genomic DNA from a clinically resistant isolate to confer AMX resistance to two different fully susceptible commonly used strains (serotype 2 D39V and serotype 4 TIGR4). By applying next generation sequencing we were able to track the development of resistance through generations, and confirm the necessary resistance determinants required for this mechanism of AMX resistance. We also observed non-contiguous recombination and propose a model for how these complex events occur (Chapter 2). We then used CRISPRi-seq to search for unknown genes which might regulate autolysis in the presence of an AMX-induced bottleneck. We identified the hypothetical protein BeaU,

and propose a model for its indirect involvement in the regulation of LytA-dependent autolysis (Chapter 3). Finally, we selected for single mutants with reduced AMX susceptibility, and identified the known β-lactam resistance determinant CiaRH. We attempted to uncover the mechanism by which CiaRH enables pneumococcal cells to respond to cell wall stress (Chapter 4).

## References


Albarracín Orio AG, Piñas GE, Cortes PR, Cian MB, Echenique J. 2011. Compensatory evolution of pbp mutations restores the fitness cost imposed by β-lactam resistance in *Streptococcus pneumoniae*. *PLoS Pathogens* **7**:e1002000. doi:10.1371/journal.ppat.1002000

Alloing G, Martin B, Granadel C, Claverys JP. 1998. Development of competence in *Streptococcus pneumoniae*: Pheromone autoinduction and control of quorum sensing by the oligopeptide permease. *Molecular Microbiology* **29**:75–83. doi:10.1046/J.1365-2958.1998.00904.X

Andes D, Craig WA. 1998. In vivo activities of amoxicillin and amoxicillin-clavulanate against *Streptococcus pneumoniae*: application to breakpoint determinations. *Antimicrob Agents Chemother* **42**:2375–9. doi:10.1128/AAC.42.9.2375

Arnold BJ, Gutmann MU, Grad YH, Sheppard SK, Corander J, Lipsitch M, Hanage WP. 2018. Weak epistasis may drive adaptation in recombining bacteria. *Genetics* **208**:1247–1260. doi:10.1534/genetics.117.300662

Attaiech L, Olivier A, Mortier-Barrière I, Soulet AL, Granadel C, Martin B, Polard P, Claverys JP. 2011. Role of the single-stranded DNA-binding protein SsbB in pneumococcal transformation: Maintenance of a reservoir for genetic plasticity. *PLoS Genetics* **7**:e1002156. doi:10.1371/journal.pgen.1002156

Avery OT, Cullen GE. 1923. Studies on the enzymes of pneumococcus: IV. Bacteriolytic enzyme. *Journal of Experimental Medicine* **38**:199–206. doi:10.1084/jem.38.2.199

Bell JC, Kowalczykowski SC. 2016. RecA: Regulation and Mechanism of a Molecular Search Engine. *Trends in Biochemical Sciences*. doi:10.1016/j.tibs.2016.04.002

Berg KH, Stamsås GA, Straume D, Håvarstein LS. 2013. Effects of low PBP2b levels on cell morphology and peptidoglycan composition in *Streptococcus pneumoniae* R6. *Journal of Bacteriology* **195**:4342–4354. doi:10.1128/JB.00184-13

Bergé M, Mortier-Barrière I, Martin B, Claverys JP. 2003. Transformation of *Streptococcus pneumoniae* relies on DprA- and RecA-dependent protection of incoming DNA single strands. *Molecular Microbiology* **50**:527–536. doi:10.1046/j.1365-2958.2003.03702.x

Berry AM, Lock RA, Hansman D, Paton JC. 1989. Contribution of autolysin to virulence of *Streptococcus pneumoniae*. *Infection and Immunity* **57**:2324–2330. doi:10.1128/iai.57.8.2324-2330.1989

Berry AM, Paton JC. 2000. Additive attenuation of virulence of *Streptococcus pneumoniae* by mutation of the genes encoding pneumolysin and other putative pneumococcal

virulence proteins. *Infection and Immunity* **68**:133–140. doi:10.1128/IAI.68.1.133-140.2000

Briese T, Hakenbeck R. 1985. Interaction of the pneumococcal amidase with lipoteichoic acid and choline. *European Journal of Biochemistry* **146**:417–427. doi:10.1111/j.1432-1033.1985.tb08668.x

Cafini F, del Campo R, Alou L, Sevillano D, Morosini MI, Baquero F, Prieto J, García E, Casal J, Fenoll A, de la Campa AG, Bouza E, Baquero F, Soriano F, Pallarés R, Liñares J, Garau J, Lacasa JM, Latorre C, Pérez-Trallero E, García de Lomas J, Fleites A. 2006. Alterations of the penicillin-binding proteins and murM alleles of clinical *Streptococcus pneumoniae* isolates with high-level resistance to amoxicillin in Spain. *Journal of Antimicrobial Chemotherapy* **57**:224–229. doi:10.1093/jac/dki442

Càmara J, Cubero M, Martín-Galiano AJ, García E, Grau I, Nielsen JB, Worning P, Tubau F, Pallarés R, Domínguez MÁ, Kilian M, Liñares J, Westh H, Ardanuy C. 2018. Evolution of the β-lactam-resistant *Streptococcus pneumoniae* PMEN3 clone over a 30 year period in Barcelona, Spain. *Journal of Antimicrobial Chemotherapy* **73**:2941–2951. doi:10.1093/jac/dky305

Canvin JR, Marvin AP, Sivakumaran M, Paton JC, Boulnois GJ, Andrew PW, Mitchell TJ. 1995. The Role of Pneumolysin and Autolysin in the Pathology of Pneumonia and Septicemia in Mice Infected with a Type 2 Pneumococcus. *Journal of Infectious Diseases* **172**:119–123. doi:10.1093/infdis/172.1.119

Chesnel L, Carapito R, Croizé J, Dideberg O, Vernet T, Zapun A. 2005. Identical penicillin-binding domains in penicillin-binding proteins of *Streptococcus pneumoniae* clinical isolates with different levels of beta-lactam resistance. *Antimicrob Agents Chemother* **49**:2895–2902. doi:10.1128/AAC.49.7.2895

Chi F, Nolte O, Bergmann C, Ip M, Hakenbeck R. 2007. Crossing the barrier: Evolution and spread of a major class of mosaic pbp2x in *Streptococcus pneumoniae*, *S. mitis* and *S. oralis. International Journal of Medical Microbiology* **297**:503–512. doi:10.1016/j.ijmm.2007.02.009

Cho H, Uehara T, Bernhardt TG. 2014. Beta-Lactam Antibiotics Induce a Lethal Malfunctioning of the Bacterial Cell Wall Synthesis Machinery. *Cell* **159**:1300–1311.

Claverys JP, Håvarstein LS. 2007. Cannibalism and fratricide: Mechanisms and raisons d'être. *Nature Reviews Microbiology*. doi:10.1038/nrmicro1613

Cowley LA, Petersen FC, Junges R, Jimson D. Jimenez M, Morrison DA, Hanage WP. 2018. Evolution via recombination: Cell-to-cell contact facilitates larger recombination events in *Streptococcus pneumoniae*. *PLOS Genetics* **14**:e1007410. doi:10.1371/journal.pgen.1007410

Croucher NJ, Harris SR, Barquist L, Parkhill J, Bentley SD. 2012. A high-resolution view of genome-wide pneumococcal transformation. *PLoS Pathogens* **8**:e1002745. doi:10.1371/journal.ppat.1002745

Croucher NJ, Harris SR, Fraser C, Quail MA, Burton J, van der Linden M, McGee L, von Gottberg A, Song JH, Ko KS, Pichon B, Baker S, Parry CM, Lambertsen LM, Shahinas D, Pillai DR, Mitchell TJ, Dougan G, Tomasz A, Klugman KP, Parkhill J, Hanage WP, Bentley SD. 2011. Rapid pneumococcal evolution in response to clinical interventions. *Science (1979)* **331**:430–434. doi:10.1126/SCIENCE.1198545

Danilowicz C, Yang D, Kelley C, Prévost C, Prévost P, Prentiss M. 2015. The poor homology stringency in the heteroduplex allows strand exchange to incorporate desirable mismatches without sacrificing recognition in vivo. *Nucleic Acids Research* **43**:6473–6485. doi:10.1093/nar/gkv610

Davies TA, Pankuch GA, Dewasse BE, Jacobs MR, Appelbaum PC. 1999. In Vitro Development of Resistance to Five Quinolones and Amoxicillin-Clavulanate in *Streptococcus pneumoniae* **43**. doi:10.1128/AAC.43.5.1177

Denapaite, D., Brückner, R., Hakenbeck, R., & Vollmer, W. 2012. Biosynthesis of teichoic acids in *Streptococcus pneumoniae* and closely related species: lessons from genomes. *Microbial drug resistance*, 18(3), 344-358. doi:10.1089/mdr.2012.0026

Dessen A, Mouz N, Gordon E, Hopkins J, Dideberg O. 2001. Crystal structure of PBP2x from a highly penicillin-resistant *Streptococcus pneumoniae* clinical isolate: A mosaic framework containing 83 mutations. *Journal of Biological Chemistry* **276**:45106–45112. doi:10.1074/jbc.M107608200

Dewé TCM, D'aeth JC, Croucher NJ. 2019. Genomic epidemiology of penicillin-non-susceptible *Streptococcus pneumoniae*. *Microbial Genomics* **5**. doi:10.1099/MGEN.0.000305

Doern G v, Brueggemann A, Holley HP, Rauch AM. 1996. Antimicrobial resistance of *Streptococcus pneumoniae* recovered from outpatients in the United States during the winter months of 1994 to 1995: results of a 30-center national surveillance study. *Antimicrob Agents Chemother* **40**:1208–13. doi:10.1128/AAC.40.5.1208

Doit C, Loukil C, Fitoussi F, Geslin P, Bingen E. 1999. Emergence in France of Multiple Clones of Clinical *Streptococcus pneumoniae* Isolates with High-Level Resistance to Amoxicillin. *Antimicrobial Agents and Chemotherapy* **43**:1480–1483. doi:10.1128/AAC.43.6.1480

Domenech, A., Slager, J., & Veening, J. W. 2018. Antibiotic-induced cell chaining triggers pneumococcal competence by reshaping quorum sensing to autocrine-like signaling. *Cell reports*, 25(9), 2390-2400. doi:10.1016/j.celrep.2018.11.007

Dowson CG, Barcus V, King S, Pickerill P, Whatmore A, Yeo M. 1997. Horizontal gene transfer and the evolution of resistance and virulence determinants in Streptococcus. *Journal of Applied Microbiology Symposium Supplement* **83**:42–51. doi:10.1046/j.1365-2672.83.s1.5.x

Dowson CG, Coffey TJ, Kell C, Whiley RA. 1993. Evolution of penicillin resistance in *Streptococcus pneumoniae*; the role of *Streptococcus mitis* in the formation of a low affinity PBP2B in *S. pneumoniae*. *Molecular Microbiology* **9**:635–643. doi:10.1111/j.1365-2958.1993.tb01723.x

du Plessis M, Bingen E, Klugman KP, Plessis M du, Bingen E, Klugman KP, du Plessis M, Bingen E, Klugman KP. 2002. Analysis of Penicillin-Binding Protein Genes of Clinical Isolates of *Streptococcus pneumoniae* with Reduced Susceptibility to Amoxicillin. *Antimicrobial Agents and Chemotherapy* **46**:2349–2357. doi:10.1128/AAC.46.8.2349

du Plessis M, Smith AM, Klugman KP. 2000. Analysis of penicillin-binding protein 1b and 2a genes from *Streptococcus pneumoniae*. *Microbial Drug Resistance* **6**:127–131. doi:10.1089/107662900419438

Emami K, Guyet A, Kawai Y, Devi J, Wu LJ, Allenby N, Daniel RA, Errington J. 2017. RodA as the missing glycosyltransferase in *Bacillus subtilis* and antibiotic discovery for the peptidoglycan polymerase pathway. *Nature Microbiology 2017 2:3* **2**:1–9. doi:10.1038/nmicrobiol.2016.253

Filipe SR, Severina E, Tomasz A. 2002. The murMN operon: A functional link between antibiotic resistance and antibiotic tolerance in *Streptococcus pneumoniae*. *Proceedings of the National Academy of Sciences* **99**:1550–1555. doi:10.1073/PNAS.032671699

Filipe SR, Tomasz A. 2000. Inhibition of the expression of penicillin resistance in *Streptococcus pneumoniae* by inactivation of cell wall muropeptide branching genes. *Proceedings of the National Academy of Sciences* **97**:4891–4896. doi:https://doi.org/10.1073/pnas.080067697

Flores-Kim J, Dobihal GS, Fenton A, Rudner DZ, Bernhardt TG. 2019. A switch in surface polymer biogenesis triggers growth-phase-dependent and antibiotic-induced bacteriolysis. *Elife* **8**. doi:10.7554/eLife.44912

Forget AL, Kowalczykowski SC. 2012. Single-molecule imaging of DNA pairing by RecA reveals a three-dimensional homology search. *Nature 2012 482:7385* **482**:423–427. doi:10.1038/nature10782

Ganaie F, Maruhn K, Li C, Porambo RJ, Elverdal PL, Abeygunwardana C, van der Linden M, Duus J, Sheppard CL, Nahm MH. 2021. Structural, Genetic, and Serological Elucidation of *Streptococcus pneumoniae* Serogroup 24 Serotypes: Discovery of a New Serotype,

24C, with a Variable Capsule Structure. *J Clin Microbiol* **59**:e0054021. doi:10.1128/JCM.00540-21

Ganaie F, Saad JS, McGee L, van Tonder AJ, Bentley SD, Lo SW, Gladstone RA, Turner P, Keenan JD, Breiman RF, Nahm MH. 2020. A new pneumococcal capsule type, 10D, is the 100th serotype and has a large cps fragment from an oral streptococcus. *mBio* **11**. doi:10.1128/mBio.00937-20

Garcia E, Gareia -Luis, Garcia P. 1985. Cloning and expression of the pneumococcal autolysin gene in Escherichia coil **201**:225–230.

Garcia-Bustos J, Tomasz A. 1990. A biological price of antibiotic resistance: major changes in the peptidoglycan structure of penicillin-resistant pneumococci. *Proc Natl Acad Sci U S A* **87**:5415–9. doi:10.1073/pnas.87.14.5415

Gibson PS, Bexkens E, Zuber S, Cowley L, Veening J-W. 2021. The acquisition of clinically relevant amoxicillin resistance in *Streptococcus pneumoniae* requires ordered horizontal gene transfer of four loci. *bioRxiv* 2021.12.17.473165. doi:10.1101/2021.12.17.473165

Giudicelli S, Tomasz A. 1984. Attachment of pneumococcal autolysin to wall teichoic acids, an essential step in enzymatic wall degradation. *Journal of Bacteriology* **158**:1188–1190. doi:10.1128/jb.158.3.1188-1190.1984

González-Díaz A, Machado MP, Càmara J, Yuste J, Varon E, Domenech M, del Grosso M, Marimón JM, Cercenado E, Larrosa N, Quesada MD, Fontanals D, El-Mniai A, Cubero M, Carriço JA, Martí S, Ramirez M, Ardanuy C. 2020. Two multi-fragment recombination events resulted in the β-lactam-resistant serotype 11A-ST6521 related to Spain 9V-ST156 pneumococcal clone spreading in south-western Europe, 2008 to 2016. *Eurosurveillance* **25**:1900457. doi:10.2807/1560-7917.ES.2020.25.16.1900457

Gordon E, Mouz N, Duée E, Dideberg O. 2000. The crystal structure of the penicillin-binding protein 2x from *Streptococcus pneumoniae* and its acyl-enzyme form: Implication in drug resistance. *Journal of Molecular Biology* **299**:477–485. doi:10.1006/jmbi.2000.3740

Grebe T, Hakenbeck R. 1996. Penicillin-Binding Proteins 2b and 2x of *Streptococcus pneumoniae* Are Primary Resistance Determinants for Different Classes of β-Lactam Antibiotics. *ANTIMICROBIAL AGENTS AND CHEMOTHERAPY* **40**:829–834.

Grebe T, Paik J, Hakenbeck R. 1997. A novel resistance mechanism against β-lactams in *Streptococcus pneumoniae* involves CpoA, a putative glycosyltransferase. *Journal of Bacteriology* **179**:3342–3349. doi:10.1128/jb.179.10.3342-3349.1997

Guenzi E, Gasc A-M, Sicard MA, Hakenbeck R. 1994. A two-component signal-transducing system is involved in competence and penicillin susceptibility in laboratory mutants of *Streptococcus pneumoniae*. *Molecular Microbiology* **12**:505–515. doi:10.1111/j.1365-2958.1994.tb01038.x

Haas W, Kaushal D, Sublett J, Obert C, Tuomanen EI. 2005. Vancomycin stress response in a sensitive and a tolerant strain of *Streptococcus pneumoniae*. *J Bacteriol* **187**:8205–10. doi:10.1128/JB.187.23.8205-8210.2005

Haenni M, Moreillon P. 2006. Mutations in Penicillin-Binding Protein (PBP) genes and in non-PBP genes during selection of penicillin-resistant *Streptococcus gordonii*. *Antimicrobial Agents and Chemotherapy* **50**:4053–4061. doi:10.1128/AAC.00676-06

Hakenbeck R, Brückner R, Denapaite D, Maurer P. 2012. Molecular mechanisms of β-lactam resistance in *Streptococcus pneumoniae*. *Future Microbiology*. doi:10.2217/fmb.12.2

Hakenbeck R, Chhatwal S, editors. 2007. Molecular Biology of Streptococci. Horizon Scientific Press, 2007.

Hakenbeck R, Nig AK, Kern I, Van Der Linden M, Keck W, Billot-Klein D, Legrand R, Schoot B, Gutmann L. 1998a. Acquisition of Five High-M r Penicillin-Binding Protein Variants during Transfer of High-Level β-Lactam Resistance from *Streptococcus mitis* to *Streptococcus pneumoniae*. *Journal of Bacteriology* **180**:1831–1840.

Hakenbeck R, Nig AK, Kern I, van der Linden M, Keck W, Billot-Klein D, Legrand R, Schoot B, Gutmann L, König A, Kern I, van der Linden M, Keck W, Billot-Klein D, Legrand R, Schoot B, Gutmann L. 1998b. Acquisition of Five High-M r Penicillin-Binding Protein Variants during Transfer of High-Level beta-Lactam Resistance from *Streptococcus mitis* to *Streptococcus pneumoniae*. *Journal of Bacteriology* **180**:1831–1840.

Halfmann A, Schnorpfeil A, Müller M, Marx P, Günzler U, Hakenbeck R, Brückner R. 2011. Activity of the two-component regulatory system CiaRH in *Streptococcus pneumoniae* R6. *J Mol Microbiol Biotechnol* **20**:96–104. doi:10.1159/000324893

Hansman D, Bullen MM. 1967. A resistant pneumococcus. *Lancet* **2**:264–265.

Håvarstein LS, Martin B, Johnsborg O, Granadel C, Claverys JP. 2006. New insights into the pneumococcal fratricide: Relationship to clumping and identification of a novel immunity factor. *Molecular Microbiology* **59**:1297–1037. doi:10.1111/j.1365-2958.2005.05021.x

Hiller NL, Ahmed A, Powell E, Martin DP, Eutsey R, Earl J, Janto B, Boissy RJ, Hogg J, Barbadora K, Sampath R, Lonergan S, Post JC, Hu FZ, Ehrlich GD. 2010. Generation of Genic Diversity among *Streptococcus pneumoniae* Strains via Horizontal Gene Transfer

during a Chronic Polyclonal Pediatric Infection. *PLOS Pathogens* **6**:e1001108. doi:10.1371/JOURNAL.PPAT.1001108

Hirst RA, Gosai B, Rutman A, Guerin CJ, Nicotera P, Andrew PW, O'Callaghan C. 2008. *Streptococcus pneumoniae* deficient in pneumolysin or autolysin has reduced virulence in meningitis. *Journal of Infectious Diseases* **197**:744–751. doi:10.1086/527322

Ho J, Ip M. 2019. Antibiotic-Resistant Community-Acquired Bacterial Pneumonia. *Infectious Disease Clinics of North America*. doi:10.1016/j.idc.2019.07.002

Holtje J v., Tomasz A. 1975. Lipoteichoic acid: a specific inhibitor of autolysin activity in pneumococcus. *Proc Natl Acad Sci U S A* **72**:1690–1694. doi:10.1073/pnas.72.5.1690

Hoskins J, Matsushima P, Mullen DL, Tang J, Zhao G, Meier TI, Nicas TI, Jaskunas SR. 1999. Gene disruption studies of penicillin-binding proteins 1a, 1b, and 2a in *Streptococcus pneumoniae*. *J Bacteriol* **181**:6552–5.

Howard L v., Gooder H. 1974. Specificity of the autolysin of Streptococcus (Diplococcus) pneumoniae. *Journal of Bacteriology* **117**:796–804. doi:10.1128/jb.117.2.796-804.1974

Hsieh P, Camerini-Otero CS, Camerini-Otero RD. 1992. The synapsis event in the homologous pairing of DNAs: RecA recognizes and pairs less than one helical repeat of DNA. *Proc Natl Acad Sci U S A* **89**:6492–6496. doi:10.1073/pnas.89.14.6492

Jensen A, Valdórsson O, Frimodt-Møller N, Hollingshead S, Kilian M. 2015. Commensal streptococci serve as a reservoir for β-lactam resistance genes in *Streptococcus pneumoniae*. *Antimicrob Agents Chemother* **59**:3529–40. doi:10.1128/AAC.00429-15

Job V, Carapito R, Vernet T, Dessen A, Zapun A. 2008. Common alterations in PBP1a from resistant *Streptococcus pneumoniae* decrease its reactivity toward β-lactams: Structural insights. *Journal of Biological Chemistry* **283**:4886–4894. doi:10.1074/jbc.M706181200

Kalizang'oma A, Chaguza C, Gori A, Davison C, Beleza S, Antonio M, Beall B, Goldblatt D, Kwambana-Adams B, Bentley SD, Heyderman RS. 2021. *Streptococcus pneumoniae* serotypes that frequently colonise the human nasopharynx are common recipients of penicillin-binding protein gene fragments from *Streptococcus mitis*. *Microbial Genomics* **7**:000622. doi:10.1099/mgen.0.000622

Kocaoglu O, Tsui H-CCT, Winkler ME, Carlson EE. 2015. Profiling of β-lactam selectivity for penicillin-binding proteins in *Streptococcus pneumoniae* D39. *Antimicrobial Agents and Chemotherapy* **59**:3548–3555. doi:10.1128/AAC.05142-14

Kosowska K, Jacobs MR, Bajaksouzian S, Koeth L, Appelbaum PC. 2004. Alterations of Penicillin-Binding Proteins 1A, 2X, and 2B in *Streptococcus pneumoniae* Isolates for

Which Amoxicillin MICs Are Higher than Penicillin MICs **48**. doi:10.1128/AAC.48.10.4020-4022.2004

Krauß J, van der Linden M, Grebe T, Hakenbeck R. 1996. Penicillin-Binding Proteins 2x and 2b as Primary PBP Targets in *Streptococcus pneumoniae*. *Microbial Drug Resistance* **2**:183–186. doi:10.1089/mdr.1996.2.183

Laurenceau R, Péhau-Arnaudet G, Baconnais S, Gault J, Malosse C, Dujeancourt A, Campo N, Chamot-Rooke J, le Cam E, Claverys JP, Fronzes R. 2013. A Type IV Pilus Mediates DNA Binding during Natural Transformation in *Streptococcus pneumoniae*. *PLoS Pathogens* **9**:e1003473. doi:10.1371/journal.ppat.1003473

Lisboa J, Andreani J, Sanchez D, Boudes M, Collinet B, Liger D, Tilbeurgh H van, Guérois R, Quevillon-Cheruel S. 2014. Molecular determinants of the DprA-RecA interaction for nucleation on ssDNA. *Nucleic Acids Research* **42**:7395–7408. doi:10.1093/nar/gku349

Liu HH, Tomasz A. 1985. Penicillin Tolerance in Multiply Drug-Resistant Natural Isolates of *Streptococcus pneumoniae*. *The Journal of Infectious Diseases* **152**:365–372. doi:10.1093/INFDIS/152.2.365

Martin B, Soulet AL, Mirouze N, Prudhomme M, Mortier-Barrière I, Granadel C, Noirot-Gros MF, Noirot P, Polard P, Claverys JP. 2013. ComE/ComE∼P interplay dictates activation or extinction status of pneumococcal X-state (competence). *Molecular Microbiology* **87**:394–411. doi:10.1111/mmi.12104

Mascher T, Zähner D, Merai M, Balmelle N, de Saizieu AB, Hakenbeck R. 2003. The *Streptococcus pneumoniae cia* regulon: CiaR target sites and transcription profile analysis. *J Bacteriol* **185**:60–70. doi:10.1128/JB.185.1.60-70.2003

Mell JC, Shumilina S, Hall IM, Redfield RJ. 2011. Transformation of natural genetic variation into *Haemophilus influenzae* genomes. *PLoS Pathogens* **7**:e1002151. doi:10.1371/journal.ppat.1002151

Mellroth P, Daniels R, Eberhardt A, Rönnlund D, Blom H, Widengren J, Normark S, Henriques-Normark B. 2012. LytA, major autolysin of *Streptococcus pneumoniae*, requires access to nascent peptidoglycan. *Journal of Biological Chemistry* **287**:11018–11029. doi:10.1074/JBC.M111.318584/ATTACHMENT/8F67F731-D0C0-4B34-889A-534F3E51B2D1/MMC1.ZIP

Mirouze N, Bergé MA, Soulet AL, Mortier-Barrière I, Quentin Y, Fichant G, Granadel C, Noirot-Gros MF, Noirot P, Polard P, Martin B, Claverys JP. 2013. Direct involvement of DprA, the transformation-dedicated RecA loader, in the shut-off of pneumococcal competence. *Proc Natl Acad Sci U S A* **110**. doi:10.1073/pnas.1219868110

Moreillon P, Tomasz A, Tomasz A. 1988. Penicillin Resistance and Defective Lysis in Clinical Isolates of Pneumococci: Evidence for Two Kinds of Antibiotic Pressure Operating in the Clinical Environment. *The Journal of Infectious Diseases* **157**:1150–1157. doi:10.1093/INFDIS/157.6.1150

Morlot C, Noirclerc-Savoye M, Zapun A, Dideberg O, Vernet T. 2004. The d,d-carboxypeptidase PBP3 organizes the division process of *Streptococcus pneumoniae*. *Molecular Microbiology* **51**:1641–1648. doi:10.1046/j.1365-2958.2003.03953.x

Morlot C, Zapun A, Dideberg O, Vernet T. 2003. Growth and division of *Streptococcus pneumoniae*: localization of the high molecular weight penicillin-binding proteins during the cell cycle. *Molecular Microbiology* **50**:845–855. doi:10.1046/j.1365-2958.2003.03767.x

Morrison DA, Mortier-Barrière I, Attaiech L, Claverys JP. 2007. Identification of the major protein component of the pneumococcal eclipse complex. *Journal of Bacteriology* **189**:6497–6500. doi:10.1128/JB.00687-07

Moscoso M, Domenech M, García E. 2010. Vancomycin tolerance in clinical and laboratory *Streptococcus pneumoniae* isolates depends on reduced enzyme activity of the major LytA autolysin or cooperation between CiaH histidine kinase and capsular polysaccharide. *Molecular Microbiology* **77**.

Mouz N, di Guilmi AM, Gordon E, Hakenbeck R, Dideberg O, Vernet T. 1999. Mutations in the active site of penicillin-binding protein PBP2x from *Streptococcus pneumoniae*. Role in the specificity for beta-lactam antibiotics. *J Biol Chem* **274**:19175–80. doi:10.1074/jbc.274.27.19175

Mouz N, Gordon E, di Guilmi AM, Petit I, Pétillot Y, Dupont Y, Hakenbeck R, Vernet T, Dideberg O. 1998. Identification of a structural determinant for resistance to beta-lactam antibiotics in Gram-positive bacteria. *Proc Natl Acad Sci U S A* **95**:13403–6. doi:10.1073/PNAS.95.23.13403

Muller M, Marx P, Hakenbeck R, Bruckner R. 2011. Effect of new alleles of the histidine kinase gene *ciaH* on the activity of the response regulator CiaR in *Streptococcus pneumoniae* R6. *Microbiology (N Y)* **157**:3104–3112. doi:10.1099/mic.0.053157-0

Nagai K, Davies TA, Jacobs MR, Appelbaum PC. 2002. Effects of amino acid alterations in penicillin-binding proteins (PBPs) 1a, 2b, and 2x on PBP affinities of penicillin, ampicillin, amoxicillin, cefditoren, cefuroxime, cefprozil, and cefaclor in 18 clinical isolates of penicillin-susceptible, -intermediate, and -resistant pneumococci. *Antimicrobial Agents and Chemotherapy* **46**:1273–1280. doi:10.1128/AAC.46.5.1273-1280.2002

Nichol KA, Zhanel GG, Hoban DJ. 2002. Penicillin-binding protein 1A, 2B, and 2X alterations in Canadian isolates of penicillin-resistant *Streptococcus pneumoniae*. *Antimicrobial Agents and Chemotherapy* **46**:3261–3264. doi:10.1128/AAC.46.10.3261-3264.2002

Nunes S, Sá-Leão R, Carriço J, Alves CR, Mato R, Brito Avô A, Saldanha J, Almeida JS, Santos Sanches I, de Lencastre H. 2005. Trends in drug resistance, serotypes, and molecular types of *Streptococcus pneumoniae* colonizing preschool-age children attending day care centers in Lisbon, Portugal: A summary of 4 years of annual surveillance. *Journal of Clinical Microbiology* **43**:1285–1293. doi:10.1128/JCM.43.3.1285-1293.2005

O'Brien KL, Wolfson LJ, Watt JP, Henkle E, Deloria-Knoll M, McCall N, Lee E, Mulholland K, Levine OS, Cherian T. 2009. Burden of disease caused by *Streptococcus pneumoniae* in children younger than 5 years: global estimates. *The Lancet* **374**:893–902. doi:10.1016/S0140-6736(09)61204-6

Olivares A, Olivares Trejo J, Arellano-Galindo J, Zuñiga G, Escalona G, Carlos Vigueras J, Marín P, Xicohtencatl J, Valencia P, Velázquez-Guadarrama N. 2011. pep 27 and lytA in Vancomycin-Tolerant Pneumococci. *J Microbiol Biotechnol* **21**:1345–1351. doi:10.4014/jmb.1105.05045

Pankuch GA, Jacobs MR, Appelbaum PC. 1995. Comparative activity of ampicillin, amoxycillin, amoxycillin/clavulanate and cefotaxime against 189 penicillin-susceptible and -resistant pneumococci. *Journal of Antimicrobial Chemotherapy* **35**:883–888. doi:10.1093/jac/35.6.883

Pankuch GA, Jueneman SA, Davies TA, Jacobs MR, Appelbaum PC. 1998. In vitro selection of resistance to four beta-lactams and azithromycin in *Streptococcus pneumoniae*. *Antimicrob Agents Chemother* **42**:2914–8. doi:10.1128/AAC.42.11.2914

Pérez-Trallero E, Fernandez-Mazarrasa C, García-Rey C, Bouza E, Aguilar L, García-de-Lomas J, Baquero F. 2001. Antimicrobial susceptibilities of 1,684 *Streptococcus pneumoniae* and 2,039 *Streptococcus pyogenes* isolates and their ecological relationships: Results of a 1-year (1998-1999) multicenter surveillance study in Spain. *Antimicrobial Agents and Chemotherapy* **45**:3334–3340. doi:10.1128/AAC.45.12.3334-3340.2001

Pérez-Trallero E, García-De-La-Fuente C, García-Rey C, …., Rubio C. 2005. Geographical and ecological analysis of resistance, coresistance, and coupled resistance to antimicrobials in respiratory pathogenic bacteria in Spain. *Antimicrobial Agents and Chemotherapy* **49**:1965–1972. doi:10.1128/AAC.49.5.1965-1972.2005

Pérez-Trallero E, Marimón JM, Ercibengoa M, Giménez MJ, Coronel P, Aguilar L. 2007. Antimicrobial susceptibilities of amoxycillin-non-susceptible and susceptible isolates among penicillin-non-susceptible *Streptococcus pneumoniae*. *Clinical Microbiology and Infection* **13**:937–940. doi:10.1111/j.1469-0691.2007.01777.x

Pérez-Trallero E, Marimón JM, González A, García-Rey C, Aguilar L. 2003. Genetic relatedness of recently collected Spanish respiratory tract *Streptococcus pneumoniae* isolates with reduced susceptibility to amoxicillin. *Antimicrob Agents Chemother* **47**:3637–9. doi:10.1128/aac.47.11.3637-3639.2003

Pernot L, Chesnel L, Le Gouellec A, Croizé J, Vernet T, Dideberg OO, Dessen A. 2004. A PBP2x from a Clinical Isolate of *Streptococcus pneumoniae* Exhibits an Alternative Mechanism for Reduction of Susceptibility to β-Lactam Antibiotics. *Journal of Biological Chemistry* **279**:16463–16470. doi:10.1074/jbc.M313492200

Peters K, Schweizer I, Beilharz K, Stahlmann C, Veening JW, Hakenbeck R, Denapaite D. 2014. *Streptococcus pneumoniae* PBP2x mid-cell localization requires the C-terminal PASTA domains and is essential for cell shape maintenance. *Molecular Microbiology* **92**:733–755. doi:10.1111/mmi.12588

Philippe J, Gallet B, Morlot C, Denapaite D, Hakenbeck R, Chen Y, Vernet T, Zapun A. 2015. Mechanism of β-Lactam Action in *Streptococcus pneumoniae*: the Piperacillin Paradox. *Antimicrobial Agents and Chemotherapy* **59**:609–621. doi:10.1128/AAC.04283-14

Piotrowski A, Luo P, Morrison DA. 2009. Competence for Genetic Transformation in *Streptococcus pneumoniae*: Termination of Activity of the Alternative Sigma Factor ComX Is Independent of Proteolysis of ComX and ComW. *Journal of Bacteriology* **191**:3359. doi:10.1128/JB.01750-08

Potgieter E, Chalkley LJ. 1995. Relatedness among penicillin-binding protein 2b genes of *Streptococcus mitis*, *Streptococcus oralis*, and *Streptococcus pneumoniae*. *Microb Drug Resist* **1**:35–42. doi:10.1089/mdr.1995.1.35

Quevillon-Cheruel S, Campo N, Mirouze N, Mortier-Barrière I, Brooks MA, Boudes M, Durand D, Soulet AL, Lisboa J, Noirot P, Martin B, van Tilbeurgh H, Noirot-Gros MF, Claverys JP, Polard P. 2012. Structure-function analysis of pneumococcal DprA protein reveals that dimerization is crucial for loading RecA recombinase onto DNA during transformation. *Proc Natl Acad Sci U S A* **109**:E2466–E2475. doi:10.1073/pnas.1205638109

Reichmann P, König A, Liñares J, Alcaide F, Tenover FC, McDougal L, Swidsinski S, Hakenbeck R. 1997. A Global Gene Pool for High-Level Cephalosporin Resistance in Commensal *Streptococcus* Species and *Streptococcus pneumoniae*. *The Journal of Infectious Diseases* **176**:1001–1012. doi:10.1086/516532

Ruiz N. 2009. Streptococcus pyogenes YtgP (Spy_0390) Complements *Escherichia coli* Strains Depleted of the Putative Peptidoglycan Flippase MurJ. *Antimicrobial Agents and Chemotherapy* **53**:3604. doi:10.1128/AAC.00578-09

Salvadori G, Junges R, Morrison DA, Petersen FC. 2019. Competence in *Streptococcus pneumoniae* and close commensal relatives: Mechanisms and implications. *Frontiers in Cellular and Infection Microbiology*. doi:10.3389/fcimb.2019.00094

Sanbongi Y, Ida T, Ishikawa M, Osaki Y, Kataoka H, Suzuki T, Kondo K, Ohsawa F, Yonezawa M. 2004. Complete sequences of six penicillin-binding protein genes from 40 *Streptococcus pneumoniae* clinical isolates collected in Japan. *Antimicrobial Agents and Chemotherapy* **48**:2244–2250. doi:10.1128/AAC.48.6.2244-2250.2004

Scheffers D-J, Pinho MG. 2005. Bacterial Cell Wall Synthesis: New Insights from Localization Studies. *Microbiology and Molecular Biology Reviews* **69**:585–607. doi:10.1128/mmbr.69.4.585-607.2005

Schuster C, Dobrinski B, Hakenbeck R. 1990. Unusual septum formation in *Streptococcus pneumoniae* mutants with an alteration in the D,D-carboxypeptidase penicillin-binding protein 3. *Journal of Bacteriology* **172**:6499–6505. doi:10.1128/jb.172.11.6499-6505.1990

Schweizer I, Peters K, Stahlmann C, Hakenbeck R, Denapaite D. 2014. Penicillin-binding protein 2x of *Streptococcus pneumoniae*: The mutation Ala707Asp within the C-terminal PASTA2 domain leads to destabilization. *Microbial Drug Resistance*. Mary Ann Liebert, Inc. 140 Huguenot Street, 3rd Floor New Rochelle, NY 10801 USA. pp. 250–257. doi:10.1089/mdr.2014.0082

Shak JR, Vidal JE, Klugman KP. 2013. Influence of bacterial interactions on pneumococcal colonization of the nasopharynx. *Trends Microbiol* **21**:129–35. doi:10.1016/j.tim.2012.11.005

Sham LT, Butler EK, Lebar MD, Kahne D, Bernhardt TG, Ruiz N. 2014. MurJ is the flippase of lipid-linked precursors for peptidoglycan biogenesis. *Science* **345**:220. doi:10.1126/SCIENCE.1254522

Sham L-T, Tsui H-CT, Land AD, Barendt SM, Winkler ME. 2012. Recent advances in pneumococcal peptidoglycan biosynthesis suggest new vaccine and antimicrobial targets. *Curr Opin Microbiol* **15**:194–203. doi:10.1016/j.mib.2011.12.013

Sibold C, Henrichsen J, König A, Martin C, Chalkley L, Hakenbeck R. 1994. Mosaic *pbpX* genes of major clones of penicillin-resistant *Streptococcus pneumoniae* have evolved from *pbpX* genes of a penicillin-sensitive *Streptococcus oralis*. *Molecular Microbiology* **12**:1013–1023. doi:10.1111/j.1365-2958.1994.tb01089.x

Sifaoui F, Kitzis MD, Gutmann L. 1996. In vitro selection of one-step mutants of *Streptococcus pneumoniae* resistant to different oral β-lactam antibiotics is associated with alterations of PBP2x. *Antimicrobial Agents and Chemotherapy* **40**:152–156. doi:10.1128/AAC.40.1.152

Skwark MJ, Croucher NJ, Puranen S, Chewapreecha C, Pesonen M, Xu YY, Turner P, Harris SR, Beres SB, Musser JM, Parkhill J, Bentley SD, Aurell E, Corander J. 2017. Interacting networks of resistance, virulence and core machinery genes identified by genome-wide epistasis analysis. *PLoS Genetics* **13**. doi:10.1371/journal.pgen.1006508

Slager J, Aprianto R, Veening JW. 2019. Refining the pneumococcal competence regulon by RNA sequencing. *Journal of Bacteriology* **201**:e00780-18. doi:10.1128/JB.00780-18

Smith AM, Klugman KP. 2001. Alterations in MurM, a cell wall muropeptide branching enzyme, increase high-level penicillin and cephalosporin resistance in *Streptococcus pneumoniae*. *Antimicrobial Agents and Chemotherapy* **45**:2393–2396. doi:10.1128/AAC.45.8.2393-2396.2001

Soriano F, Cafini F, Aguilar L, Tarrago D, Alou L, Gimenez M-J, Gracia M, Ponte M-CMC, Leu D, Pana M, Letowska I, Fenoll A, Tarrag?? D, Alou L, Gim??nez MJ, Gracia M, Ponte M-CMC, Leu D, Pana M, Letowska I, Fenoll A. 2008. Breakthrough in penicillin resistance? *Streptococcus pneumoniae* isolates with penicillin/cefotaxime MICs of 16 mg/L and their genotypic and geographical relatedness. *Journal of Antimicrobial Chemotherapy* **62**:1234–1240. doi:10.1093/jac/dkn392

Stanhope MJ, Lefébure T, Walsh SL, Becker JA, Lang P, Pavinski Bitar PD, Miller LA, Italia MJ, Amrine-Madsen H. 2008. Positive selection in penicillin-binding proteins 1a, 2b, and 2x from *Streptococcus pneumoniae* and its correlation with amoxicillin resistance development. *Infection, Genetics and Evolution* **8**:331–339. doi:10.1016/J.MEEGID.2008.02.001

Stanhope MJ, Walsh SL, Becker JA, Miller LA, Lefébure T, Lang P, Bitar PDP, Amrine-Madsen H. 2007. The relative frequency of intraspecific lateral gene transfer of penicillin binding proteins 1a, 2b, and 2x, in amoxicillin resistant *Streptococcus pneumoniae*. *Infection, Genetics and Evolution* **7**:520–534. doi:10.1016/J.MEEGID.2007.03.004

Straume D, Stamsås GA, Håvarstein LS. 2015. Natural transformation and genome evolution in *Streptococcus pneumoniae*. *Infection, Genetics and Evolution* **33**:371–380. doi:10.1016/j.meegid.2014.10.020

Taguchi A, Welsh MA, Marmont LS, Lee W, Sjodt M, Kruse AC, Kahne D, Bernhardt TG, Walker S. 2019. FtsW is a peptidoglycan polymerase that is functional only in complex with its cognate penicillin-binding protein. *Nature Microbiology 2019 4:4* **4**:587–594. doi:10.1038/s41564-018-0345-x

Tait-Kamradt A, Cronan M, Dougherty TJ. 2009. Comparative genome analysis of high-level penicllin resistance in *Streptococcus pneumoniae*. *Microb Drug Resist* **15**:69–75.

Tam P-YI, Thielen BK, Obaro SK, Brearley AM, Kaizer AM, Chu H, Janoff EN. 2017. Childhood pneumococcal disease in Africa – a systematic review and meta-analysis of incidence,

serotype distribution, and antimicrobial susceptibility. *Vaccine* **35**:1817. doi:10.1016/J.VACCINE.2017.02.045

The European Committee on Antimicrobial Susceptibility Testing. 2022. Breakpoint tables for interpretation of MICs and zone diameters.

Tomasz A. 1968. Biological consequences of the replacement of choline by ethanolamine in the cell wall of Pneumococcus: chain formation, loss of transformability, and loss of autolysis. *Proc Natl Acad Sci U S A* **59**:86–93. doi:10.1073/pnas.59.1.86

Tomasz A, Waks S. 1975. Mechanism of action of penicillin: triggering of the pneumococcal autolytic enzyme by inhibitors of cell wall synthesis. *Proc Natl Acad Sci U S A* **72**:4162–4166. doi:10.1073/pnas.72.10.4162

Troeger C, Blacker B, Khalil IA, Rao PC, …, Reiner RC. 2018. Estimates of the global, regional, and national morbidity, mortality, and aetiologies of lower respiratory infections in 195 countries, 1990–2016: a systematic analysis for the Global Burden of Disease Study 2016. *The Lancet Infectious Diseases* **18**:1191–1210. doi:10.1016/S1473-3099(18)30310-4

Trzciński K, Thompson CM, Lipsitch M. 2004. Single-step capsular transformation and acquisition of penicillin resistance in *Streptococcus pneumoniae*. *Journal of Bacteriology* **186**:3447–3452. doi:10.1128/JB.186.11.3447-3452.2004

Vollmer, W., Massidda, O., & Tomasz, A. (2019). The cell wall of *Streptococcus pneumoniae*. *Microbiology spectrum*, 7(3), 7-3. doi:10.1128/microbiolspec.GPP3-0018-2018

Waxman DJ, Strominger JL. 1983. Penicillin-Binding Proteins and the Mechanism of Action of Beta-Lactam Antibiotics1. *Annual Review of Biochemistry* **52**:825–869. doi:10.1146/annurev.bi.52.070183.004141

Ween O, Gaustad P, Håvarstein LS. 1999. Identification of DNA binding sites for ComE, a key regulator of natural competence in *Streptococcus pneumoniae*. *Molecular Microbiology* **33**:817–827. doi:10.1046/j.1365-2958.1999.01528.x

Weiser JN, Ferreira DM, Paton JC. 2018. *Streptococcus pneumoniae*: transmission, colonization and invasion **16**. doi:10.1038/s41579-018-0001-8

Weng L, Piotrowski A, Morrison DA. 2013. Exit from Competence for Genetic Transformation in *Streptococcus pneumoniae* Is Regulated at Multiple Levels. *PLoS ONE* **8**:e64197. doi:10.1371/journal.pone.0064197

Wright AJ. 1999. The penicillinsMayo Clinic Proceedings. Elsevier. pp. 290–307. doi:10.4065/74.3.290

Wyres KL, Lambertsen LM, Croucher NJ, McGee L, von Gottberg A, Liñares J, Jacobs MR, Kristinsson KG, Beall BW, Klugman KP, Parkhill J, Hakenbeck R, Bentley SD, Brueggemann AB. 2013. Pneumococcal capsular switching: A historical perspective. *Journal of Infectious Diseases* **207**:439–449. doi:10.1093/infdis/jis703

Wyres KL, Lambertsen LM, Croucher NJ, McGee L, von Gottberg A, Liñares J, Jacobs MR, Kristinsson KG, Beall BW, Klugman KP, Parkhill J, Hakenbeck R, Bentley SD, Brueggemann AB. 2012. The multidrug-resistant PMEN1 pneumococcus is a paradigm for genetic success. *Genome Biology* **13**:R103. doi:10.1186/gb-2012-13-11-r103

Yang H, Zhou C, Dhar A, Pavletich NP. 2020. Mechanism of strand exchange from RecA–DNA synaptic and D-loop structures. *Nature* **586**:801–806. doi:10.1038/s41586-020-2820-9

Zapun A, Contreras-Martel C, Vernet T. 2008. Penicillin-binding proteins and β-lactam resistance. *FEMS Microbiology Reviews* **32**:361–385. doi:10.1111/J.1574-6976.2007.00095.X

Zerfaß I, Hakenbeck R, Denapaite D, Zerfass I, Hakenbeck R, Denapaite D. 2009. An important site in PBP2x of penicillin-resistant clinical isolates of *Streptococcus pneumoniae*: Mutational analysis of Thr338. *Antimicrobial Agents and Chemotherapy* **53**:1107–1115. doi:10.1128/AAC.01107-08

# Chapter 2

## The acquisition of clinically relevant amoxicillin resistance in *Streptococcus pneumoniae* requires ordered horizontal gene transfer of four loci

Paddy S. Gibson[1], Evan Bexkens[1], Sylvia Zuber[1], Lauren A. Cowley[2], Jan-Willem Veening[1,*]

[1] Department of Fundamental Microbiology, Faculty of Biology and Medicine, University of Lausanne, Biophore Building, CH-1015 Lausanne, Switzerland
[2] Department of Biology & Biochemistry, Milner Centre for Evolution, University of Bath, Claverton Down Campus, Bath BA2 7AY, United Kingdom

[*]Correspondence to Jan-Willem Veening: Jan-Willem.Veening@unil.ch, tel: +41 (0)21 6925625, Twitter handle: @JWVeening

*Preprinted in bioRxiv, under revision for PLOS Pathogens*

All experiments were performed by PG, or SZ and EB under the supervision of PG. Data analysis was performed by PG. Scripts for recombination detection were provided by LC and implemented by PG. Manuscript was written by PG with revisions and feedback by LC and JWV.

## Abstract

Understanding how antimicrobial resistance spreads is critical for optimal application of new treatments. In the naturally competent human pathogen *Streptococcus pneumoniae*, resistance to β-lactam antibiotics is mediated by recombination events in genes encoding the target proteins, resulting in reduced drug binding affinity. However, for the front-line antibiotic amoxicillin, the exact mechanism of resistance still needs to be elucidated. Through successive rounds of transformation with genomic DNA from a clinically resistant isolate, we followed amoxicillin resistance development. Using whole genome sequencing, we showed that multiple recombination events occurred at different loci during one round of transformation. We found examples of non-contiguous recombination, and demonstrated that this could occur either through multiple D-loop formation from one donor DNA molecule, or by the integration of multiple DNA fragments. We also show that the final minimum inhibitory concentration (MIC) differs depending on recipient genome, explained by differences in the extent of recombination at key loci. Finally, through back transformations of mutant alleles and fluorescently labelled penicillin (bocillin-FL) binding assays, we confirm that *pbp1a*, *pbp2b*, *pbp2x*, and *murM* are the main resistance determinants for amoxicillin resistance, and that the order of allele uptake is important for successful resistance evolution. We conclude that recombination events are complex, and that this complexity contributes to the highly diverse genotypes of amoxicillin-resistant pneumococcal isolates.

## Introduction

Genomic plasticity through frequent and large-scale recombination drives the evolution of antibiotic resistance in *Streptococcus pneumoniae* (the pneumococcus) (Salvadori et al., 2019). This naturally competent member of the human nasopharyngeal commensal microbiota opportunistically causes otitis media as well as severe invasive diseases such as pneumonia, bacteremia, and meningitis (O'Brien et al., 2009; Shak et al., 2013). Despite conjugate vaccine introduction, the species remains an important human pathogen, as vaccine-escape and antibiotic resistant variants constantly arise (Croucher et al., 2011; Wyres et al., 2013).

Variants occur primarily through natural transformation and homologous recombination of DNA from strains or closely related species that occupy the same niche, such as *S. mitis* and *S. oralis* (Croucher et al., 2012; Dowson et al., 1993; Sibold et al., 1994). One case study showed more than 7% of the genome had been transferred between two pneumococcal strains during the polyclonal infection of a pediatric patient over three months (Hiller et al., 2010). Early studies of transformation in the pneumococcus showed uptake of fragments ranging from 2-6 Kb (Gurney and Fox, 1968), but cell-to-cell contact was found to facilitate transfer of long DNA fragments (Cowley et al., 2018), and recombinant regions as large as 30 – 50 Kb in length have been observed in clinically relevant lineages such as PMEN-1 (Croucher et al., 2011; Wyres et al., 2013, 2012). Events such as these have played a significant role in shaping the pneumococcal pangenome (Donati et al., 2010).

Natural competence is activated when the competence stimulating peptide (CSP) interacts with the ComDE two-component system (Straume et al., 2015) (Figure 1) where ComE, phosphorylated by ComD, activates transcription of the genes encoding the alternative sigma factor *comX* (Martin et al., 2013; Slager et al., 2019; Ween et al., 1999). ComX then activates transcription of the late *com* genes necessary for DNA uptake and recombination. This includes the type IV-like pilus (ComGC), endonuclease EndA, and transport proteins ComFA, and ComEC (Bergé et al., 2013; Lacks and Greenberg, 1976; Lacks and Neuberger, 1975; Laurenceau et al., 2013; Rosenthal and Lacks, 1980). RecA and the transformation-dedicated DNA processing protein A (DprA) are essential for single-stranded DNA (ssDNA) uptake without degradation (Attaiech et al., 2011). Although not fully understood, DprA and RecA

are thought to polymerize on ssDNA upon cell entry, initiating the homology search, while additional DNA molecules are then bound by multiple SsbB proteins protecting them from degradation by endogenous nucleases (Attaiech et al., 2011; Morrison et al., 2007). It has been hypothesized that the accumulation of stable ssDNA-SsbB eclipse complexes in the cytoplasm enables successive recombination events during one competence window, increasing genetic plasticity (Attaiech et al., 2011). Sequestered ssDNA can then be accessed by the transformation-dedicated DNA processing protein A (DprA), which mediates the loading of RecA onto the pre-synaptic filament (Lisboa et al., 2014; Mortier-Barrière et al., 2007; Quevillon-Cheruel et al., 2012). DprA is also involved in competence shut-off, along with ComX and RpoD sigma factor competition, and CSP degradation by HtrA (Cassone et al., 2012; Martin et al., 2013; Mirouze et al., 2013; Piotrowski et al., 2009; Weng et al., 2013).

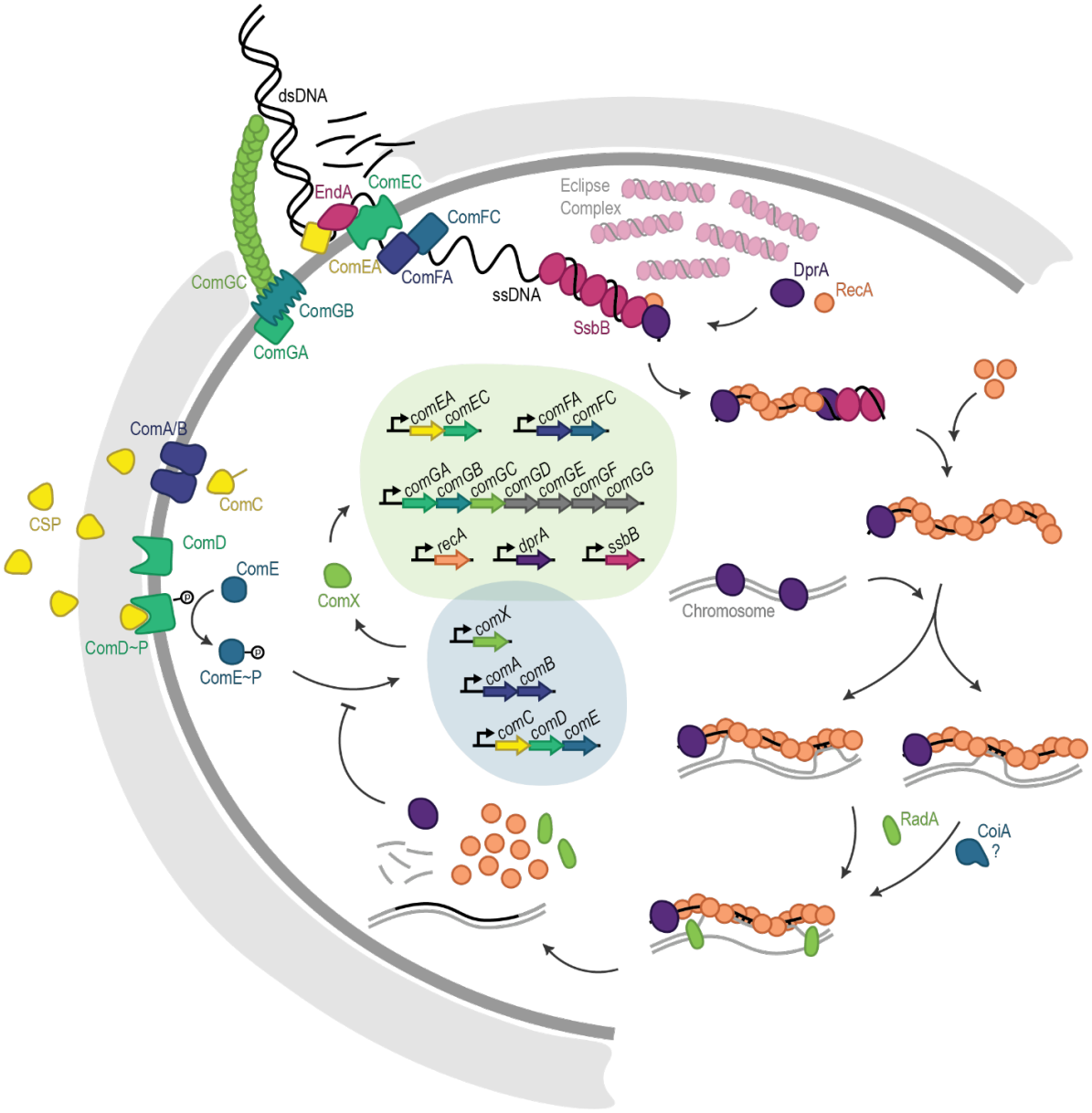


**Figure 1: DNA uptake and recombination during natural competence in *Streptococcus pneumoniae*.** Schematic overview of the regulatory steps required for the pneumococcus to uptake and recombine extracellular DNA. Competence is activated when CSP interacts with the ComDE two-component system, where phosphorylated ComE activates transcription of ComX and other early competence genes (darker grey bubble). This results in a positive feedback loop, where ComC is produced, then modified and exported from the cell by ComA/B as CSP. Meanwhile, ComX activates transcription of late competence genes, including the type IV-like pilus (ComGC), which brings DNA within reach of endonuclease EndA. EndA performs random nicks, then degrades one strand as the other is pulled into the cell and associated with DprA, RecA, and SsbB, to protect from degradation (exact mechanism not fully understood). DprA mediates loading of RecA onto SsbB-ssDNA eclipse complexes to form the presynaptic filament which then searches the chromosome for homology. RecA-ssDNA filaments may interact with the chromosome at multiple points, while successful base pairing between incoming and chromosomal DNA facilitates strand invasion and exchange. The helicase RadA facilitates D-loop extension, and CoiA is essential for successful recombination during transformation, although its exact role is not known. DprA is also involved in competence shut off, through blocking phosphorylation of ComE.

Competence is tightly controlled, with expression of most genes turned off within 20 minutes of CSP induction, providing a small window for DNA uptake and recombination (Alloing et al., 1998). To accelerate homology detection, the RecA-ssDNA presynaptic filament has been shown to interact with the chromosome in 3-dimensional space at multiple points of contact (Forget and Kowalczykowski, 2012; Wiktor et al., 2021; Yang et al., 2020). Displacement-loop (D-loop) formation is facilitated by base pairing between the chromosome and the ssDNA molecule, within the two DNA-binding sites of RecA (Bell and Kowalczykowski, 2016; Torres et al., 2019). Eight consecutive bases must be successfully paired before the DNA-DNA interaction is stabilized and strand exchange can occur (Hsieh et al., 1992; Mazin and Kowalczykowski, 1996). In *S. pneumoniae*, D-loop extension is promoted by RadA (DnaB-type helicase) which helps to unwind chromosomal DNA, extending recombination over long genomic distances (Marie et al., 2017), and while its function is not known, CoiA is essential for successful recombination (Desai and Morrison, 2007; Mortier-Barrière et al., 2007). Although initial testing is highly stringent, once crossover has started and the region of complementation is extended, stringency decreases, allowing some mismatches and thereby increasing desirable genetic variation (Carrasco et al., 2016; Danilowicz et al., 2015). This is aided by the generalized mismatch repair system in *S. pneumoniae* (hex) which is not induced during competence (Claverys and Lacks, 1986), is only able to identify mismatches in the donor-recipient heteroduplex before D-loop resolution (Claverys and Lacks, 1986; Gasc et al., 1989), and is easily overwhelmed by excess mismatches (Humbert et al., 1995).

Penicillin binding proteins (PBPs) are key β-lactam resistance determinants and are essential for bacterial cell wall synthesis by catalyzing the transglycosylation (TG) and transpeptidation (TP) reactions responsible for peptidoglycan (PGN) formation (Scheffers and Pinho, 2005). While highly conserved in penicillin (PEN) sensitive strains, PBPs of resistant isolates are highly variable, with up to 10% of amino acid changes (Hakenbeck et al., 2012). Significant amounts of this variation was recently confirmed to be acquired from *S. mitis* (Kalizang'oma et al., 2021). These large-scale changes alter the structure of the active sites, reducing β-lactam binding affinity (Hakenbeck et al., 2012). Amoxicillin (AMX) is the first line oral antibiotic prescribed for bacterial lower respiratory tract infections. AMX resistant strains first appeared in the mid-90s in the United States and France (Doern et al., 1996; Doit et al., 1999) and are

currently on the rise in Spain, a phenomenon which correlates with increased usage of oral AMX/clavulanic acid (Càmara et al., 2018). Early AMX resistant lineages were closely related to known PEN resistance clones already circulating in the population (Doit et al., 1999; Stanhope et al., 2007). Sequencing of *pbp* alleles from susceptible and resistant strains found high variation in *pbp2x* and *pbp1a*, while SNPs shared between AMX resistant isolates were only found in pbp2b (Cafini et al., 2006; Chesnel et al., 2005; du Plessis et al., 2002; Kosowska et al., 2004). However, no SNP or block of SNPs in any one *pbp*, when transferred to a susceptible strain, has been sufficient to confer resistance (Hakenbeck et al., 1998; Kosowska et al., 2004). This is not entirely surprising, as the transpeptidase activity of PBPs is an essential function, and modifications to the active site are likely to have deleterious effects which need to be compensated for (Albarracín Orio et al., 2011)(Albarracín Orio et al., 2011). One mechanism of fitness compensation appears to be through substitutions in MurM, which results in abnormally high proportions of branched muropeptides in the cell wall (Filipe et al., 2002; Filipe and Tomasz, 2000; Garcia-Bustos and Tomasz, 1990; Smith and Klugman, 2001). Branched muropeptides have been shown to have increased importance in strains depleted for Pbp2b, indicating a link between muropeptide composition and cell elongation (Berg et al., 2013). Other non-target proteins which have been implicated in resistance include CpoA (lafB) (Grebe et al., 1997) and CiaH (Guenzi et al., 1994).

Although multiple residues in Pbp1a, Pbp2x, and Pbp2b were found to be under positive selection in AMX resistant isolates (Stanhope et al., 2008), a specific block of ten substitutions in the 590-641 region of the Pbp2b TP domain is repeatedly associated with AMX resistance (Cafini et al., 2006; du Plessis et al., 2002; Kosowska et al., 2004). However, transformation of *pbp2x*, *pbp2b*, and *pbp1a* alleles to AMX susceptible strain R6 did not recreate the AMX resistance of the donor strain, and the addition of *murM* had no effect. Only when genomic DNA was used could the original resistance level be achieved, indicating the role of a non-*pbp* or *murM* resistance determinant (Chesnel et al., 2005; du Plessis et al., 2002), or unknown epistatic interactions (Arnold et al., 2018). Interestingly, other studies have found a correlation between *murM* mutations and AMX resistance, although their presence depended on the *pbp2b* allele (Cafini et al., 2006; Càmara et al., 2018). Taken together, these

studies strongly suggest the existence of multiple routes to AMX resistance and imply a tight link in the roles of Pbp2b and MurM in the mechanisms.

To study recombination and the development of AMX resistance in the pneumococcus in more detail and identify possible evolutionary routes towards AMX resistance, we sequentially transformed genomic DNA from a resistant clinical isolate (serotype 11A, ST6521, German National Reference Centre for Streptococci 2017, SN75752) into two different recipient strains coming from different clonal complexes (serotype 2 D39V and serotype 4 TIGR4). Whole genome sequencing showed recipient-dependent, genome-wide mutation uptake. In addition to identifying the necessary determinants for AMX resistance, we found a strong tendency towards the order of *pbp* and *murM* allele uptake. Long read Pacbio sequencing excluded a role for DNA methylation or genomic rearrangements or movement of genetic mobile elements as resistance determinants. We also investigated non-contiguous recombination, previously observed in *S. pneumoniae*, *Haemophilus influenzae*, and *Helicobacter pylori* (Croucher et al., 2012; Kulick et al., 2008; Mell et al., 2011), and propose a model for how these complex events occur. To conclude, we show that the uptake of four alleles from a resistant strain (*pbp2X*, *pbp2B*, *pbp1A* and *murM*), in a specific order, is required and sufficient for clinically relevant resistance development towards amoxicillin in sensitive *S. pneumoniae*.

## Results

***Serial transformation with genomic DNA from an AMX resistant strain increased AMX MIC***

In order to understand the sequence of recombination events leading to the development of AMX resistance, a susceptible *S. pneumoniae* strain D39V (minimum inhibitory concentration (MIC) 0.01 µg/mL) was transformed in two successive rounds with genomic DNA originating from AMX resistant clinical isolate 11A (MIC 4 µg/mL) followed by selection on a range of AMX concentrations above MIC (Figure 2A, Table 1). In the first round, ten colonies were picked at random from the highest AMX concentration with growth (0.03 µg/mL AMX). The MICs of these strains ranged from 0.047 – 0.125 µg/mL, 4 – 10 times that of wild-type D39V (Figure 2B, Table S1).

The second round of transformation resulted in 100 strains with MICs from 0.25 to 2 µg/mL (Figure 2B), lower than the donor strain, and a third round of transformation did not increase

the MIC further. Interestingly, five of the ten lineages had seven or more strains with MICs of 1 µg/mL or higher. In contrast, the AMR37 lineage resulted in MICs from 0.25 – 0.5 µg/mL, with one exception at 2 µg/mL. These lineage-dependent differences in AMX MIC range ($p$ = 5 x $10^{-4}$, Fisher's Exact Test) suggested that mutations acquired in the first round contributed to the recombination events which occurred in the second round, and thus to the MICs of the resulting strains.

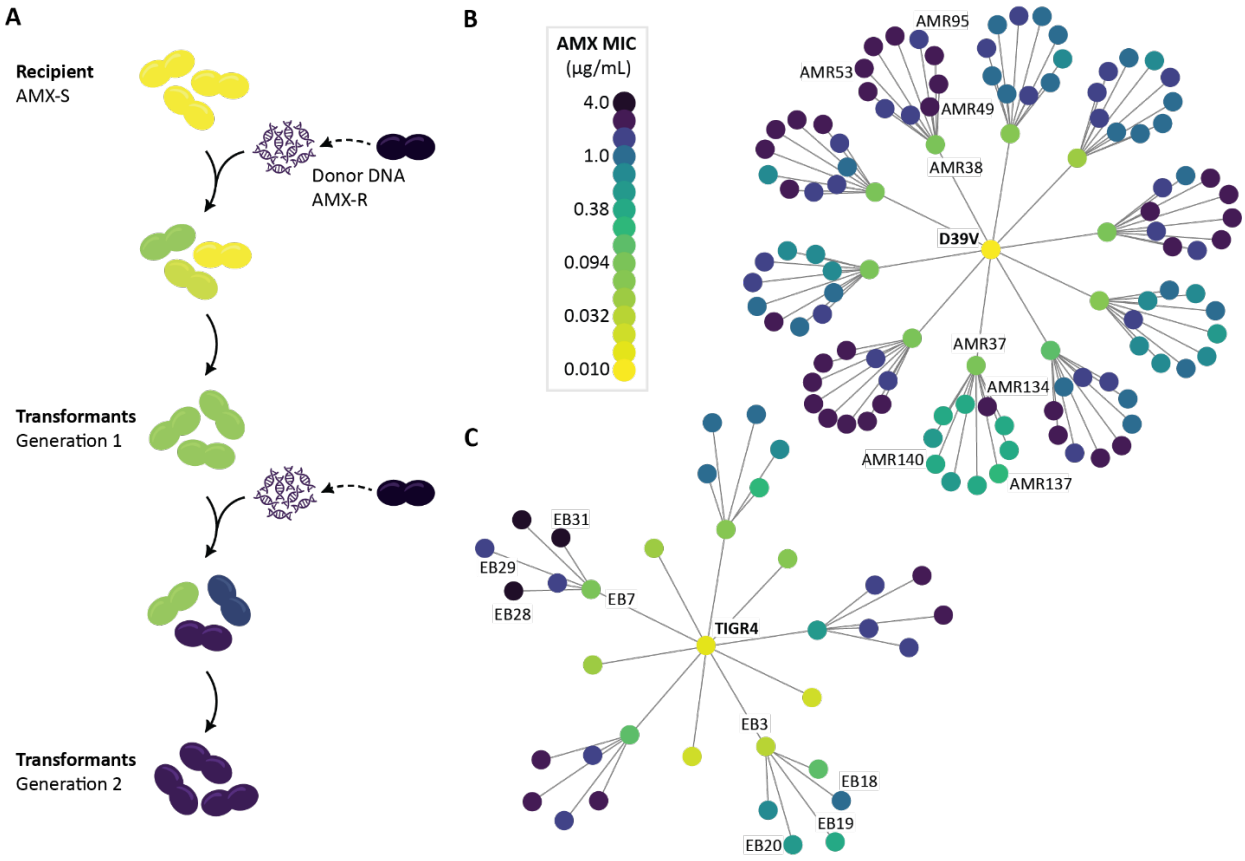


**Figure 2**: **Transformation as an experimental tool to track the evolutionary path to AMX resistance**. **(A)** Experimental design. Susceptible D39V and TIGR4 were transformed with genomic DNA from an AMX resistant clinical isolate then selected on a range of AMX concentrations. Ten colonies were picked at random from the highest concentration with growth (first round on 0.03 µg/mL and second round on 0.17 – 0.3 µg/mL, depending on MIC of the recipient strain). Isolated transformants with increased MICs were then subjected to a second round of transformation. **(B)** Pedigree chart of recombinant strains derived from D39V, and **(C)** from TIGR4. Color represents AMX MIC. Strains which were sequenced and used throughout the study are labelled.

Similar lineage-dependent MIC patterns were seen when TIGR4 was used as the recipient strain ($p$ = 1.00x$10^{-3}$, Fisher's Exact Test) (Figure 2B). Here, the AMX MICs of the first-generation ranged from 0.023 – 0.5 µg/mL, with one strain showing a more than 30-fold increase from wild-type TIGR4. In the second-generation, three recombinant strains reached

the same MIC as the donor strain (4 μg/mL), suggesting potential key differences in the recipient strain genomes, or deleterious epistatic effects of AMX resistance mutations which affected resistance development through recombination.

***Cell lysis upon AMX treatment correlated with PBP affinities***

To test whether transformed strains phenocopy the donor with regards to AMX resistance, phase contrast microscopy with an AMX concentration above the recipient MICs (1 μg/mL) was performed. A complete stall in growth was observed for both recipient strains and first-generation recombinant AMR38, with mild to severe lysis after 6 hrs of treatment (Figure 3A). In contrast, donor strain 11A grew to form a microcolony in this AMX concentration, while second-generation AMR53 grew more slowly and with abnormally elongated cells (Figure 3A). To test whether the increased resistance of AMR53 is related to alterations in the affinity of the PBPs towards AMX, we performed Bocillin-Fl labelling. Bocillin-Fl is a fluorescently labelled penicillin derivative that binds all six PBPs of *S. pneumoniae* (Zhao et al., 1999), and the intensity of labelling can be used as a proxy for the affinity of the PBP for β-lactam antibiotics (Kocaoglu et al., 2015). All six PBPs of D39V and TIGR4 had a high affinity for the fluorescently labelled penicillin (Figure3B). Interestingly, TIGR4 showed some evidence of Pbp1a degradation products that bound Bocillin-Fl with high affinity even though it is 99.7 % identical to D39V Pbp1a. In contrast, 11A showed an altered PBP pattern, where Pbp2b and Ppb1a showed complete loss of affinity, and Pbp2x was labelled more faintly and migrated more slowly (Figure 3B). Both first- and second-generation recombinants demonstrated a loss of affinity of Pbp2b and Pbp2x for Bocillin-FL, with Pbp1a in AMR53 also showing reduced affinity, and potentially some degradation (Figure 3B). Together, these characterizations demonstrate that transformed recipients phenocopy the donor AMX resistant strain and have acquired PBPs with reduced affinity towards bocillin-FL.

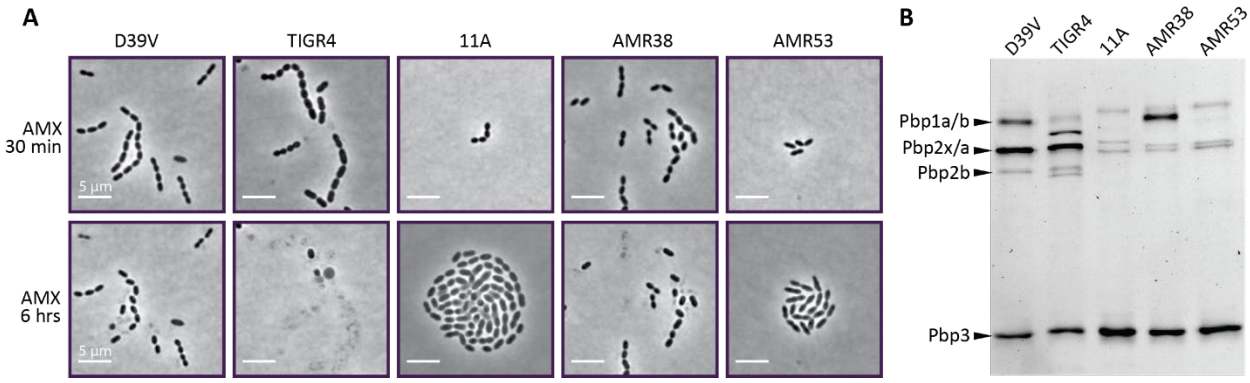


**Figure 3: Phenotypic characterization of key strains used in this study.** (**A**) Phase-contrast snapshots of recipient strains D39V and TIGR4, donor strain 11A, and recombinant strains AMR38 (generation 1) and AMR53 (generation 2) on C+Y agarose pads after 30 minutes and 6 hours of treatment with 1 µg/mL AMX. This concentration was above MIC for D39V, TIGR4, and AMR38, and lead to a complete stall in growth and partial lysis. Donor strain 11A grew well in this AMX concentration, although some heterogeneity in cell shape could be observed. Although lower than the AMX MIC for AMR53, this strain showed decreased growth and abnormally elongated cells, indicating cells were stressed. Scale bar is 5 µm. (B) Bocillin-FL binding patterns for the same five strains. Expected PBP band sizes for D39V are shown on the left. Image of Coomassie stained gel can be found in Figure S1)

### *Recombination events clustered around resistance-associated loci*

In order to examine the genetic differences in recombinant strains that may explain the differences in MIC, we selected eight recombinant strains from each experiment, and Illumina sequenced to ~600-fold mean coverage. For the D39V experiment, we chose AMR38 and three of its descent strains, as this lineage had the highest MICs. To contrast, we also chose AMR37 and three descendent strains, which had the lowest and most variable MICs in the second generation (Fig 2B). We used a similar selection criteria for the TIGR4 experiment, taking strains from the high MIC EB7 lineage, and from the low MIC EB3 lineage (Fig. 2C).

To be able to accurately map recipient to donor, we also performed long-read PacBio sequencing followed by short-read polishing on the 11A donor and TIGR4 recipient (an accurate genome map was already available for D39V (Slager et al., 2018)). Recombination was detected using SNPs, as described in Cowley et al. (2018). On average 0.38 % ± 0.22 % of the donor genome was transferred during a single transformation event, and the total percentage transferred after two rounds was 0.80 ± 0.05%. Although higher numbers of recombination events were detected in the D39V dataset, the average event length was larger in the TIGR4 dataset (D39V 0.79 Kb and TIGR4 2.29 Kb, Table S3 and S4), resulting in similar total amounts of donor genome transfer after two rounds of transformation (D39V 0.79 ±

0.23%, TIGR4 0.80 ± 0.16%, Table S3 and S4). Of note, the longest recorded recombination fragment was 4.00 Kb for D39V and 12.52 Kb for TIGR4.

Recombination events clustered around key loci for pneumococcal β-lactam resistance in both datasets; *pbp2x*, *pbp2b*, *pbp1a* and *murM* (Figure 4A and 5C). SNPs were also found at closely located loci, likely due to linkage. In the D39V strains, there was extensive recombination at distantly located sites. Examples include *ptvABC*, associated with vancomycin tolerance (Liu et al., 2017), and *murT*, which performs an amidation step essential for peptidoglycan crosslinking (Figueiredo et al., 2012; Münch et al., 2012).

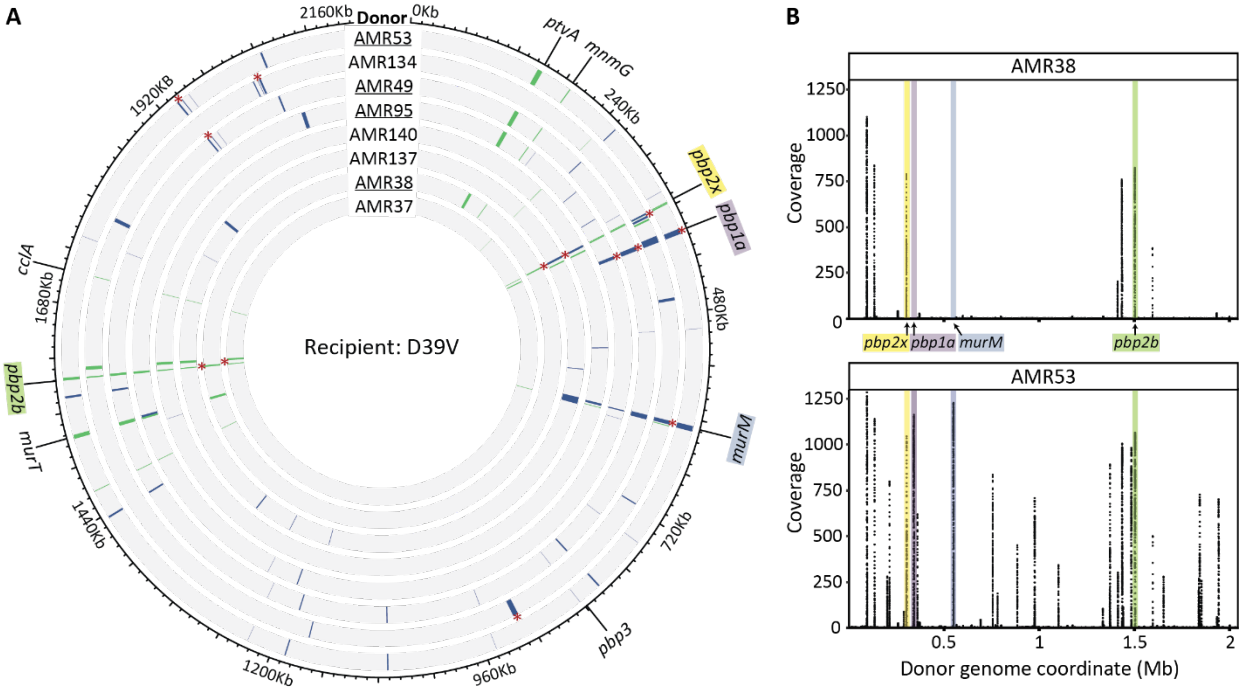


**Figure 4**: **Widespread transformation and uptake of 11A donor DNA in recipient D39V upon AMX selection**. **(A)** Circos plot with detected recombination events in D39V derived strains, arranged from lowest to highest MIC from the center. AMR38 and all derived strains are underlined, AMR37 and all derived strains are not. Grey indicates the sequences matches that of the recipient D39V, while recombination events are colored. Events acquired in the first round of transformation are shown in green, in the second round in blue, and lengths were increased to aid in visualization (see Table S3 for a list of all detected events). Recombination events determined to be non-contiguous are marked with (*). Non-contiguous events detected in the first-generation were removed from the data set on the second-generation strains, so are not marked. **(B)** Coverage of reads mapped competitively to the donor genome and plotted by coordinate beginning at the origin. Recombination events cluster at known β-lactam resistance determinants, *pbp2x*, *pbp2b*, *murM*, and *pbp1a*.

In contrast, of the six total recombination loci in the TIGR4 dataset, only three were located distally from the *pbp* and *murM* genes, and all were detected based on the presence of very few SNPs.

We hypothesised that differences in recombination patterns could have arisen from reduced similarity with the donor genome, however comparing total shared and unique SNPs did not suggest major differences in variability between the two recipient genomes (Figure 5A). When considering variation around key loci, we saw that the TIGR4 *pbp2b* region was more divergent from the donor than D39V. The quality of donor DNA used may have also played a role. Together, these results demonstrate that regardless of the recipient strain, four loci are consistently acquired in high AMX resistant recombinants, namely *pbp2x*, *pbp2b*, *pbp1a* and *murM* (Figure 5B).

Structural variation and base modification detection with PacBio sequencing revealed no major structural changes or differences in methylated motifs in the D39V recombinant strains. However, a local rearrangement was identified at the *hsdS-creX* locus in EB7, EB28, and EB29. In this region, spontaneous reshuffling of *hsdS* genes by CreX results in different methyltransferase specificity of the type I restriction modification system SpnD39III (Feng et al., 2014; Manso et al., 2014; Slager et al., 2018). TIGR4 was found to be predominantly in the B-configuration, EB7 and EB29 in the D-configuration, and EB28 in the C-configuration, while all D39V-derived strains and 11A were mostly in the F-configuration. Differences in methylated motifs have transcriptomic consequences (Manso et al., 2014), however MIC differences among these recombinants can largely be explained by SNPs in key loci for β-lactam resistance.

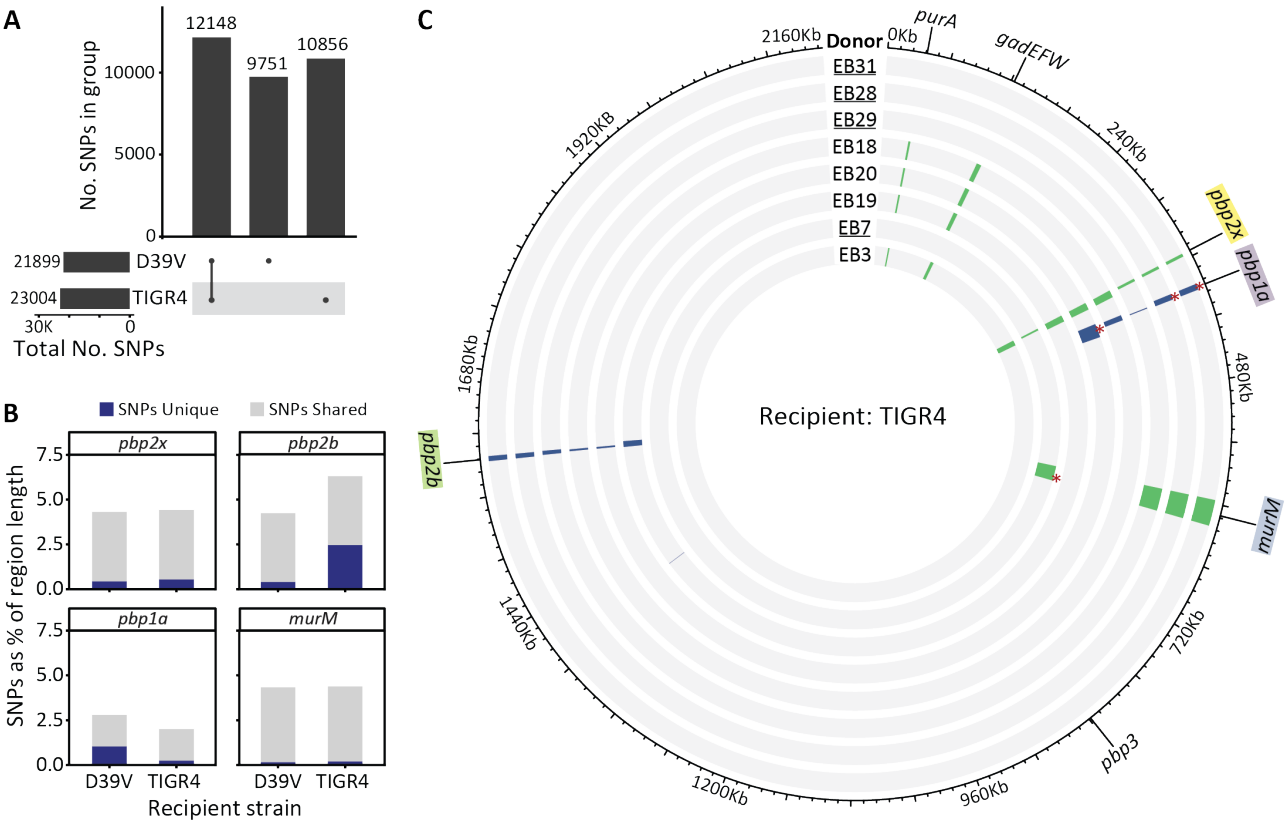


**Figure 5: Uptake of four donor fragments is sufficient for AMX resistance in TIGR4. (A)** Upset plot of shared and unique SNPs between each recipient and the donor. Bars on the left show the total number of SNPs for each recipient genome compared to the donor. In the central bar plot, from left to right, SNPs shared between D39V and TIGR4, SNPs found only in D39V, and SNPs found only in TIGR4. Although the two recipients differ from the donor strain by similar amounts of SNPs, only about half are unique. **(B)** SNP counts in pbp/murM genes, including 5 Kb up- and downstream. Number of SNPs unique to each recipient are shown in blue, and shared in light grey. **(C)** Circos plot showing detected recombination events in TIGR4 derived strains, arranged from lowest to highest MIC from inside to out. EB7 and all derived strains are underlined, EB3 and all derived strains are not. Grey indicates the sequences matches that of the recipient D39V, while recombination events are colored. Events acquired in the first round of transformation are shown in green, and in the second round in blue, and lengths were increased to aid in visualization (see Table S3 for a list of all detected events). Only six loci with recombination were identified in the entire data set, four of which are known β-lactam resistance determinants, *pbp2x*, *pbp2b*, *murM*, *pbp1a*.

### *Non-contiguous recombination events likely result from a single donor molecule*

Recombination is often thought of as a donor molecule forming a single D-loop at a homologous site on the recipient chromosome, which is then expanded in both directions until the requirement for homology is no longer met, at which point the interaction ends. However, we detected recombination events from one round of transformation located very close together on the chromosome, sometimes within the same gene but with separating recipient SNPs, a motif reminiscent of clinically resistant mosaic *pbp* alleles. This has also been noted previously in *in vitro* pneumococcal recombination studies and was hypothesized to

result from a single donor molecule (Croucher et al., 2012; Mortier-Barriere et al., 1997). To determine if events were significantly close together, forming a single non-contiguous recombination event, a bootstrapping approach was applied to the distances between novel recombination events within the same strain (Croucher et al., 2012). We found 37 events across all strains that could be amalgamated into single events under the assumptions of this approach (Figure S2, Table S4).

In addition, using PCR amplified fragments of the *pbp2x-mraY* locus from 11A, we were able to test, for the first time, whether non-contiguous recombination events occurred more frequently when the template was provided as a single molecule, or as two overlapping fragments. By ligating additional regions of non-homologous DNA, we also tested the effect of molecule length on recombination.

Transformation efficiency increased with length of both the overall molecule, and the homologous region (Figure 6A). This is in line with previous studies showing the importance of molecule length and homology in pneumococcal transformation (Kurushima et al., 2020; Morrison and Guild, 1972). We hypothesize that increased length may increase the likelihood of spontaneous contact with the ComGC pilus, while also decreasing the likelihood of homologous region fragmentation by EndA, prior to entry (Morrison and Guild, 1973). The efficiencies of the short overlapping fragments were lower than that of the long fragments, although increased slightly when transformed in combination.

Recombination occurred in all colonies sequenced. When two overlapping fragments were provided, uptake was often unequal, with either the upstream or downstream fragment incorporated more often. Recombination of both fragments was observed in 1/20 cases and was not observed when fragments were lengthened by non-homologous DNA (Figure S3A-H, Table S7).

Non-contiguous recombination was detected in all conditions, although the frequency of occurrence increased with length of homology (Figure 6C, Figure S3A-H, Table S7). It was observed both when the template was given as a single long fragment, and as two overlapping fragments.

Overall, the results suggested that the formation of multiple D-loops from either a single template molecule, or from multiple molecules, could lead to non-contiguous recombination

events (Figure 6D). However, given that longer homology and total molecule length increased the efficiency of transformation partly by reducing strand degradation (Morrison and Guild, 1972), there may have been more opportunity for complex recombination patterns to occur when longer fragments were taken up.

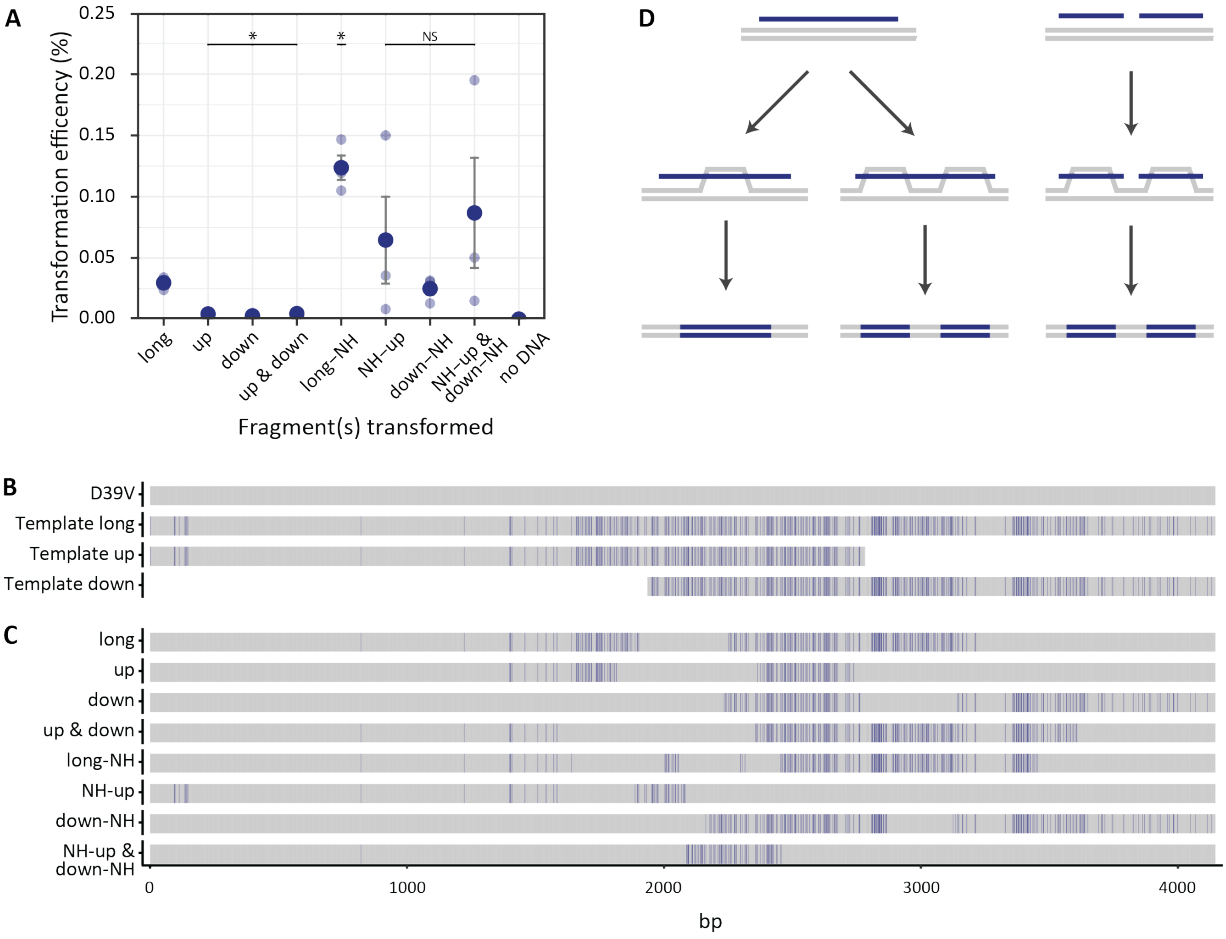


**Figure 6**: **Fragmented transformation of donor DNA predominantly originates from non-contiguous recombination events.** Three fragments were PCR amplified from the 11A strain *pbp2x* locus, one long 4.2 Kb fragment, and two overlapping short fragments (up 2837 bp, and down 2260 bp). In addition, the same fragments were ligated to stretches of non-homologous DNA, taking all total lengths to 6 Kb (long-NH, NH-up, and down-NH). **(A)** Efficiencies of transformation of fragments into D39V with selection on AMX (0.015 µg/mL). Statistically significant differences in efficiency compared to the long fragment was determined by *t* test with Benjamini-Hochberg correction for multiple testing. NS not significant, * indicates $p_{adj} < 0.05$. **(B)** Alignment of the homologous region of template fragments used in the experiment. Donor SNPs are shown in blue, while bases matching the recipient (D39V) are shown in grey. **(C)** Alignment of 4.2 Kb locus from colonies transformed with different fragments. Bases shared with donor but not with recipient are shown in blue. **(D)** Schematic showing hypothesized molecular mechanisms for non-contiguous and contiguous recombination. As shown in panel B, both events can take place, but based on transformation efficiencies, the process on the left with long donor DNA is more efficient.

***AMX resistant pbp and murM alleles are sufficient to explain AMX MICs***

Substitutions in all four proteins (Pbp1a, Pbp2b, Pbp2x and MurM) were required to reach an MIC close or equal to that of the donor strain (Figure S4, and Table S5), but the order of uptake varied both stochastically, and depending on the recipient genome. The correlation between allele uptake and MIC increase was consistent in the D39V background. First-generation strains had mutations in *pbp2b* and *pbp2x*, the two essential PBPs for cell growth (Berg et al., 2013). In the second-generation, all strains acquired mutations in *murM*, and those with MICs higher than 1 µg/mL also had mutations in *pbp1a*. In TIGR4, *pbp2x* alleles were also acquired in the first-generation, however *pbp2b* mutations only appeared after the second round of transformation. Mutations in *murM* were recombined in EB7 in the first round of transformation, then were inherited vertically in that lineage, but were not acquired by EB3 or any descendant strains (Figure 5C). Although *murM* mutations were not present in all strains with *pbp1a* modifications, strains with recombination events at all four loci had higher MICs (Figure 2C). This indicated that *murM* mutations may be less important for successful integration and selection for *pbp1a* mutations but are key for expression of the AMX resistant phenotype of the donor (Filipe et al., 2002; Filipe and Tomasz, 2000; Garcia-Bustos and Tomasz, 1990; Smith and Klugman, 2001).

An experiment was designed to test whether the order of allele uptake in D39V recombinant strains was crucial for AMX resistance development, and if PBP and MurM substitutions alone were sufficient to explain AMX MICs. Alleles of *pbp2x* and *pbp2b* from AMR37 (*pbp2x37*, *pbp2b37*) and AMR38 (*pbp2x38*, *pbp2b38*) were transformed into D39V and selected on AMX. Strains carrying either a recombinant *pbp2x* or *pbp2b* allele had E-test MICs up to 0.064 µg/mL. However, when both *pbp* alleles were integrated (D39V$^{2x38\text{-}2b38}$), the E-test result equalled that of the recombinant allele donor (Figure 7), suggesting that mutations outside these two loci were not involved in the observed reduction in AMX susceptibility in the first-generation strains.

To assess whether mutated *pbp2x* and *pbp2b* were critical for *murM* mutation uptake, D39V was transformed with *murM* from both AMR53 (*murM53*) and AMR95 (*murM95*) and MICs determined. Surprisingly, we were able to select for colonies with integration of the AMR53 *murM* allele (D39V$^{M53}$) resulting in an E-test result of 0.023 µg/mL, despite this protein not being a direct target of AMX (Figure 7 and Figure 8A.B). The genome was sequenced, and no spontaneous point mutations were identified in previously described resistance determinants

outside *murM* (Table S8). When transformed into the D39V$^{2x38\text{-}2b38}$, the E-test MICs reached 0.5 µg/mL and 0.38 µg/mL for AMR95 and AMR53 *murM* alleles (D39V$^{2x38\text{-}2b38\text{-}M95}$, D39V$^{2x38\text{-}2b38\text{-}M53}$), respectively. AMX susceptibility decreased substantially when all three genes were mutated, however failed to reach the final MIC of the recombinant allele donor, indicating the necessity of another resistance determinant (Figure 7).

*pbp1a* alleles from AMR53 and AMR95 (*pbp1a53*, *pbp1a95*) could not be successfully selected on AMX when transformed into D39V, either alone or in conjunction with a *murM* allele from the same donor. Indeed, Pbp1a is not a key target of AMX, and this result was not unexpected. We instead transformed a construct where a kanamycin resistance cassette was cloned behind *pbp1a*, with 1 Kb of homology up- and downstream. Growth in liquid culture of the resulting strains at AMX 0.01 µg/mL was similar to D39V (Figure 8A.B). Interestingly, successful integration occurred for both *pbp1a53* and *pbp1a95* when transformed into D39V$^{2x38\text{-}2b38}$ (D39V$^{2x38\text{-}2b38\text{-}1a53}$, D39V$^{2x38\text{-}2b38\text{-}1a95}$), suggesting that a mutated *murM* allele was not required for mutations in *pbp1a* to cause a selectable increase in AMX MIC. However, substitutions in Pbp2x, Pbp2b, and Pbp1a alone were insufficient to replicate the E-test results of the allele source strains (Figure 7).

We therefore transformed *murM* and *pbp1a* alleles from AMR53 and AMR95 into D39V$^{2x38\text{-}2b38}$ simultaneously, and found that selection was possible on higher concentrations of AMX (1 µg/mL) than for either gene alone (0.2 µg/mL). The resulting strains (D39V$^{2x38\text{-}2b38\text{-}M53\text{-}1a53}$, D39V$^{2x38\text{-}2b38\text{-}M95\text{-}1a95}$) had AMX resistance phenotypes matching those of AMR53 and AMR95, with E-test results of 2 µg/mL and 1.5 µg/mL respectively (Figure 7).

The strains containing all four genes from AMR53 and AMR95 were whole genome sequenced to check for spontaneous point mutations outside these loci. One non-synonymous mutation in *glnA* (glutamine synthase type I) was found in both strains. Downregulation of *glnA* has been linked to the pneumococcal penicillin stress response (el Khoury et al., 2017), but no differences in AMX survival were observed in these strains compared to the allele donors lacking the SNP.

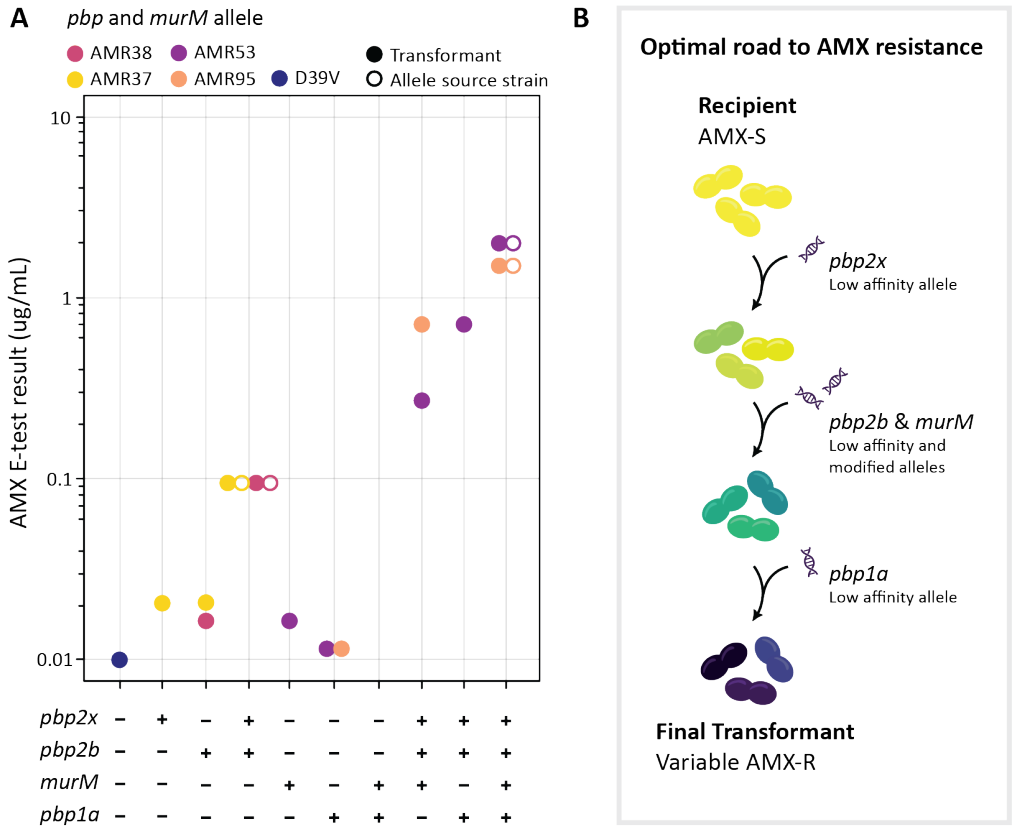


**Figure 7: Uptake of mosaic *pbp1a*, *pbp2b*, *pbp2x* and *murM* is required and sufficient for clinically relevant amoxicillin resistance in *S. pneumoniae*.** (A) AMX MICs determined by E-test for D39V transformant strains (solid circles) where *pbp* and *murM* alleles from different source strains (empty circles) were transformed in combination. Color shows allele source. (B) Schematic overview of the optimal road to AMX resistance development through horizontal gene transfer. Low affinity *pbp2x* was uptaken in the first round of transformation in both datasets, whereas donor *murM* and *pbp2b* alleles were acquired in the first or second round, depending on recipient and lineage. Low affinity *pbp1a* was recombined in the second round, and only found in strains with AMX MICs above 0.75 µg/mL. In principle uptake of low affinity and modified alleles could be achieved in a single (unlikely) or double step.

To quantify the affinities of resistant PBP alleles to β-lactam antibiotics, Bocillin-FL binding patterns were determined for allele swap strains and the source strains (Figure 8C.D). This confirmed that the recombinant PBPs had reduced penicillin binding affinities. For Pbp2b, both the AMR37 and AMR38 alleles resulted in almost complete loss of binding, and a band could not be quantified (Figure 8D). A large reduction in affinity was observed for Pbp2x38, larger than for Pbp2x37, which correlated to a small difference in growth at 0.1 µg/mL AMX between the two source strains (Figure 8A.B). This could be explained by 13 amino acid substitutions including S389L and T338A which were not present in the AMR37 allele but have previously been linked to reduced susceptibility to β-lactams (Kocaoglu et al., 2015; Kosowska et al., 2004).

Perhaps most interesting were the two low affinity Pbp1a alleles tested. In all strains containing *pbp1a95* (AMR95 derived), reduced band intensity was observed in the Pbp1a/Pbp1b size range, however, a faster migrating species was also detected. The *pbp1a95* allele contained a spontaneous point mutation (not present in the 11A donor) causing a premature stop codon. This resulted in the loss of 65 amino acids (of a total of 720) and put the predicted size at 73.1 kDa instead of 79.6 kDa. Reduced intensity at the expected Pbp1a/Pbp1b size range was also observed for the AMR53 allele (Pbp1a53) however, an additional Bocillin-FL-tagged species which migrated slightly faster than expected was also observed. The predicted protein length of Pbp1a53 is identical to D39V and the donor, with no premature stop codons identified. The additional band may indicate some degradation of this protein species, although the TP domain must still be available for Bocillin-FL binding. Together, these experiments demonstrate that transfer of the *pbp2X*, *pbp2B*, *pbp1a* and *murM* alleles of 11A into strain D39V is sufficient to explain the observed AMX resistance in transformants obtained using chromosomal DNA.

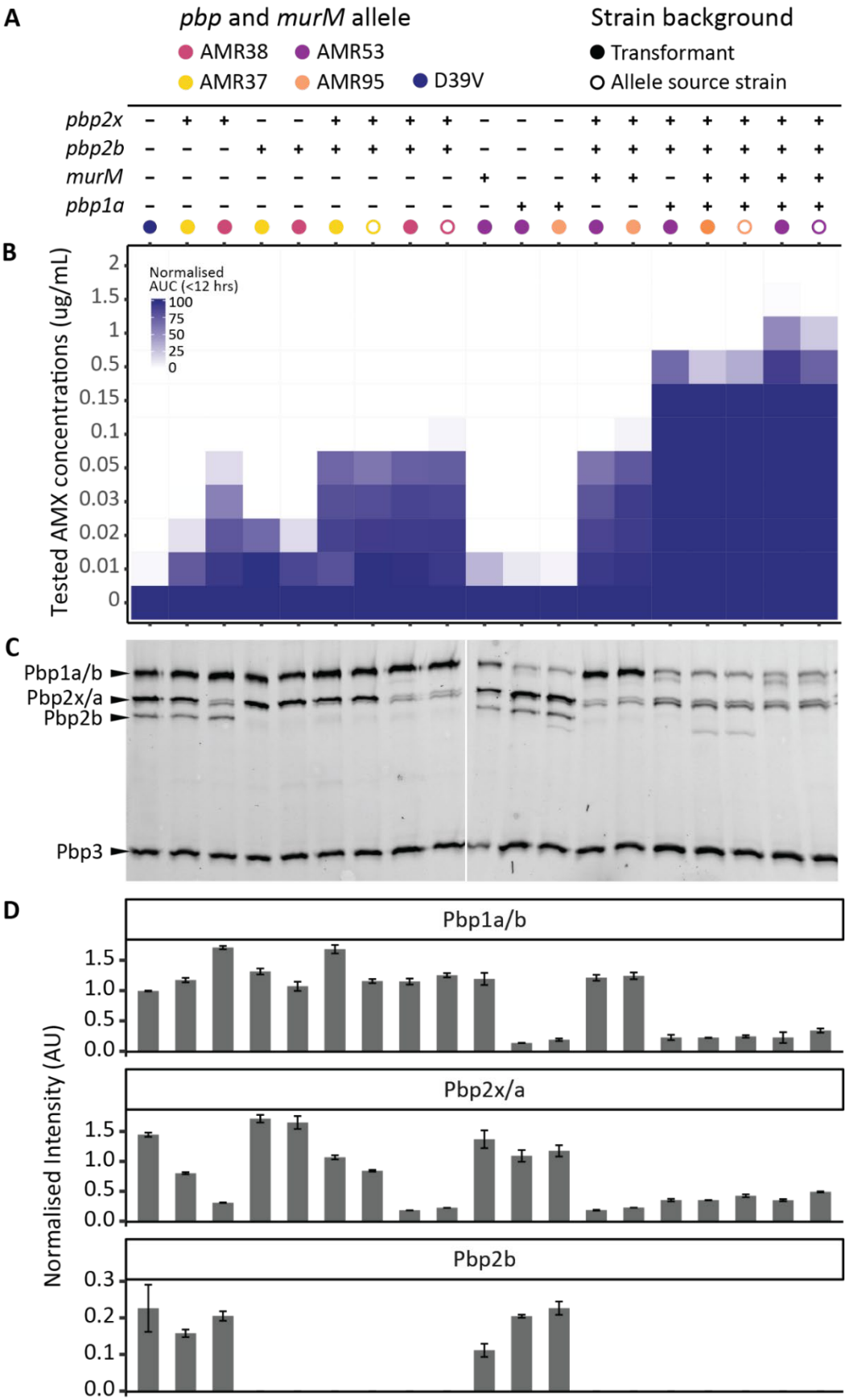


**Figure 8: Recombinant PBP proteins visualized by PBP-bocillin binding affinities.** Transformed AMX resistant strains produce mosaic PBPs with reduced affinity for Bocillin-FL. Each column shows the phenotypic

characterization of one *pbp* and *murM* allele swap strain. **(A)** Table showing the presence (+) and absence (-) of alleles from different source strains (colour). Allele source strains are also included and are indicated by the unfilled circles. **(B)** Survival in different AMX concentrations quantified by determining the area under the growth curve (AUC) after 12 hours growth in AMX normalized by AUC in the absence of AMX. **(C)** Bocillin-FL binding affinity gel. **(D)** Intensity of bands corresponding to Pbp1a/b, Pbp2x/a, and Pbp2b, normalized by the intensity of the Pbp3 band of the same lane, as this allele remained unmodified in all strains.

### *High AMX resistance in the D39V comes at a significant fitness loss*

Of the 16 recombinant strains sequenced, only EB31 and EB28 from the TIGR4 collection had the same AMX MIC as the donor strain, and a third round of transformation with gDNA into AMR53 failed to increase the MIC. The only region of mutations that EB28 and EB31 had in common that was not present in the highest MIC AMR strains, was a block of 10 mutations in the 590-641 region of Pbp2b (Figure 9C, Table S5). To test whether these substitutions were sufficient to explain the MIC difference, the *pbp2b* allele from EB31 (*pbp2b31*) was transformed into AMR53 and AMR95. The AMX E-test scores for the resulting strains were both 4-6 μg/mL. However, growth curves revealed a significant fitness loss, with a mean maximum specific growth rate of 0.11 μ/h for AMR95 decreasing almost 100-fold to 0.0036 μ/h for AMR95$^{2b31}$, which was exacerbated by the presence of AMX (Figure 9B). In contrast, AMR53$^{2b31}$ grew almost 3-fold slower than AMR53 (AMR53 0.12 μ/h, AMR53$^{2b31}$ 0.046 μ/h, Figure 9B), but showed a lytic phenotype in stationary phase. Interestingly, this strain outgrew the 11A donor in sublethal AMX concentrations (Figure 9A). The difference in growth rate between AMR95$^{2b31}$ and AMR53$^{2b31}$ was likely explained by the truncated Pbp1a95 protein. Significant modifications to the active sites of essential proteins often need to be compensated for, which may be impacted by the sub-optimal performance of other proteins in the system. Although the TP and TG domains of Pbp1a95 were intact, it is possible that the loss of 65 amino acids from the C-terminal resulted in an overall reduction in function, unrelated to its AMX binding affinity. This correlates with previous studies showing that compensation by substitutions in Pbp1A are required to mitigate fitness loss resulting from modifications to the Pbp2b active site (Albarracín Orio et al., 2011). Together, these experiments show that D39V is capable of reaching high AMX resistance, but that the absence of compensation by Pbp1A substitutions may result in significant fitness costs.

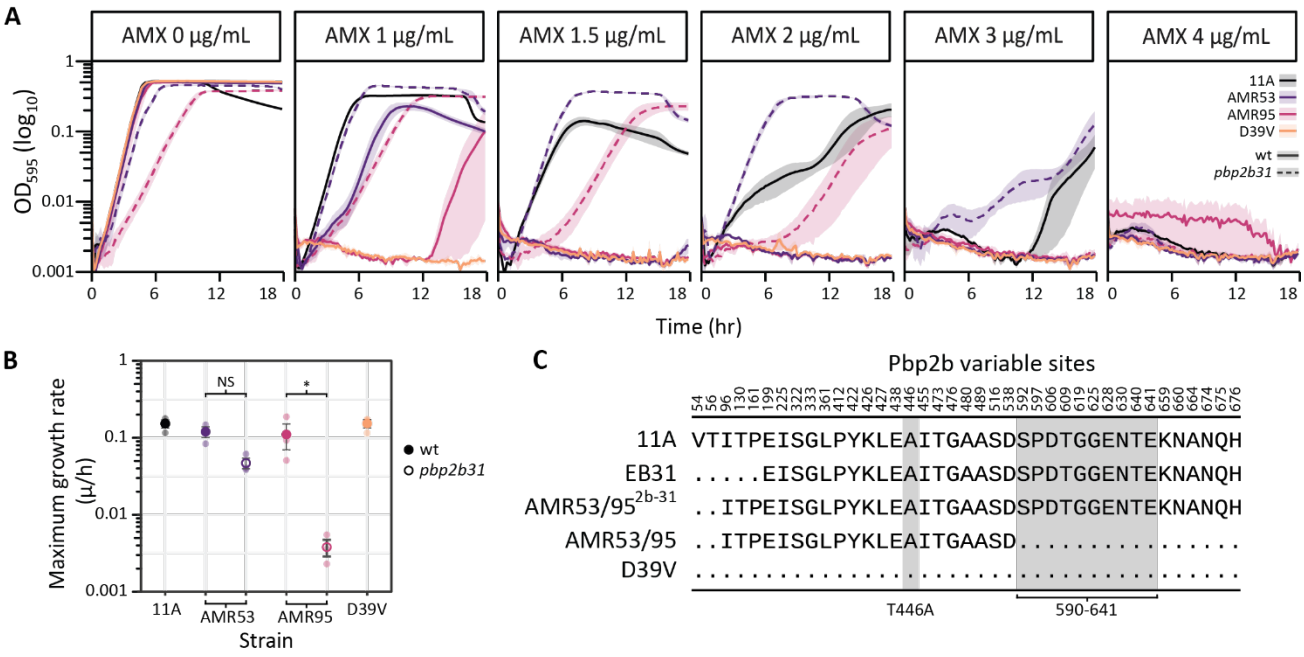


**Figure 9: Ten substitutions in Pbp2b 590-641 region essential for high AMX resistance. (A)** Growth of AMR53$^{2b31}$ and AMR95$^{2b31}$ (dotted lines) in different AMX concentrations. 11A, D39V, AMR53, and AMR95 (solid lines) are shown as controls. **(B)** Dot plot of maximum specific growth rates (µ/h) calculated from the AMX 0 µg/mL condition in triplicate (transparent circles). The mean for each strain is shown by an opaque circle, solid for wild-type (wt) strains and empty for AMR53$^{2b31}$ and AMR95$^{2b31}$. Color denotes strain background. Significance was determined by one-way ANOVA with a Tukey correction for multiple testing. **(C)** Amino acid sites in pbp2b which differ from D39V for strains 11A, EB31, AMR53 (identical to AMR95), and AMR53$^{2b31}$ (the result of transforming AMR53 or AMR95 with the EB31 pbp2b allele). Dots indicate the amino acid matches D39V, and key substitutions, T446A and a block of 10 between 590-641 (Cafini et al., 2006; du Plessis et al., 2002; Kosowska et al., 2004), are highlighted in grey.

## Discussion

Natural competence and homologous recombination in *S. pneumoniae* allow for enormous genomic plasticity which contributes to the rapid development of vaccine-escape and antibiotic resistant isolates. In one round of transformation, more than 29 recombination events can occur in a single cell (Cowley et al., 2018), while events up to 50 Kb in length have been identified in clinical isolates (Wyres et al., 2013), allowing for significant remodelling at multiple loci simultaneously. Indeed, here we show a two-step sequential transformation experiment with up to 20 individual recombination events around the genome and lengths up to 13 Kb, resulting in an average donor genome transfer per step of 0.38%. This allows for huge genomic diversity, which, when placed under selective pressure, can lead to the rapid spread of antibiotic resistance-associated genotypes (Chewapreecha et al., 2014).

β-lactam resistance in the pneumococcus relies on DNA movement between closely related strains and species within the same niche, allowing tens of substitutions to accumulate in the target proteins (Hakenbeck et al., 2012). It has previously been shown through in vitro transformation experiments into laboratory strains that the main determinants of β-lactam resistance are modified alleles of *pbp2x*, *pbp2b*, *pbp1a*, and *murM* (Fani et al., 2014; Smith and Klugman, 2001; Trzciński et al., 2004). For the front-line antibiotic AMX, resistance has also been associated with mutations in these genes although the relative importance of the changes in each locus is not well understood (Cafini et al., 2006; Chesnel et al., 2005; du Plessis et al., 2002; Garcia-Bustos and Tomasz, 1990; Kosowska et al., 2004; Smith and Klugman, 2001). We confirmed the requirement for mutations in all four genes and showed that subtle differences between alleles could cause noticeable changes in both AMX-dependent fitness and the penicillin-binding affinity of PBPs.

In addition, a specific order of mutation uptake for penicillin resistance has been demonstrated in both *Staphylococcus aureus* and the pneumococcus (Demerec, 1945; Hotchkiss, 1951; Shockley and Hotchkiss, 1970). For AMX this order was found to be *pbp2x*, *pbp2b*, then *pb1a*, with the role of *murM* unable to be confirmed in that experimental system (du Plessis et al., 2002). Here, we confirm that substitutions in Pbp2x are a critical first step for AMX resistance, perhaps reflecting the protein's high affinity for the antibiotic (Kocaoglu et al., 2015) (Figure 7C), and that the T338A substitution is required for resistance to fully develop. We also show that mutations in both *pbp2b* and *murM* are essential intermediary steps, and that a modified *pbp1a* allele is crucial for high-level AMX resistance. It is however important to note that these experiments were performed using high concentrations of naked DNA as a model, while in the nasopharynx genetic exchange likely occurs via fratricide or from small quantities of free environmental DNA (Eldholm et al., 2009; Johnsborg et al., 2008). In addition, previous studies have strongly implied the existence of multiple mechanisms of AMX resistance in *S. pneumoniae*, associated with different *pbp2b* and *murM* alleles (Cafini et al., 2006; Càmara et al., 2018; du Plessis et al., 2002), and that by using a single donor strain we were limited to the study of only one. However, we confirmed that a previously described block of ten substitutions in the 590-641 region of the Pbp2b TP domain (Cafini et al., 2006; du Plessis et al., 2002; Kosowska et al., 2004) was essential to reconstruct the AMX MIC of the serotype 11A ST6521 donor strain in D39V and TIGR4.

Perhaps most interestingly, we also show that the loss of 65 amino acids from the C-terminus of Pbp1a results in a significant fitness cost in the presence of these additional Pbp2b substitutions, highlighting the importance of interactions and fitness loss compensation between essential cell-wall synthesis proteins (Albarracín Orio et al., 2011).

In addition to these experiments demonstrating the evolutionary route to clinical AMX resistance, we show that non-contiguous recombination could result from either a single, or multiple, donor DNA molecules. It is easy to imagine a long ssDNA-RecA presynaptic filament interacting with the chromosome at multiple points in the 3-dimensional cellular space (Forget and Kowalczykowski, 2012; Yang et al., 2020)(Figure 1 model), which then initiates the formation of several D-loops simultaneously as homologous DNA-DNA interactions stabilize (Bell and Kowalczykowski, 2016; Hsieh et al., 1992; Mazin and Kowalczykowski, 1996). On the other hand, SsbB coated ssDNA sequestered in the cytoplasm could provide a pool from which multiple donor molecules homologous for the same chromosomal region could be sourced (Attaiech et al., 2011). However, we also observed that both transformation efficiency and non-contiguous event occurrence increased with length of homology and total length of the donor molecule, suggesting that single donor molecule events may simply be more likely. This concurs with the previous observation of transforming DNA concentration-independent differences in recombination event density, which would not have been expected under a multiple donor molecule hypothesis (Croucher et al., 2012). Recombination structures such as these have also been observed in *H. influenzae*, with the authors noting that localized clustering of long tracts of donor sequence appeared too close to have occurred by chance (Mell et al., 2011). They hypothesized incoming DNA degradation via cytosolic or translocation endonucleases resulted in these clusters. In addition, mismatch repair via the Hex system could in principle be responsible for the reversion of small numbers of point mutations between non-contiguous recombination segments, although the system was likely saturated in our model (Humbert et al., 1995). In order to untangle the different possible mechanisms of non-contiguous recombination from other effects on transformation efficiency, testing mixtures of different donor fragment lengths might be necessary.

Altering the active sites of essential proteins in cell division is risky and requires a delicate balance between antibiotic avoidance and fitness loss. Accumulation of sufficient mutations in the appropriate order is aided both by the simultaneous recombination of multiple donor

fragments distally around the genome, and by the occurrence of complex non-contiguous events. The experimental transformation experiments combined with whole genome sequencing as performed here provide valuable insights into viable and non-viable evolutionary paths toward AMX resistance development in the pneumococcus. The strong co-dependence among different proteins and their alleles creates significant challenges for complete understanding of resistance mechanisms, and emphasizes the importance of combining data from phenotypic, molecular, genomic, and genome-wide association studies.

## Methods

### *Bacterial strains, growth conditions, and antibiotics*

*S. pneumoniae* strains are shown in Table 1 and Table S1. Bacteria were cultured in liquid C+Y medium with no shaking at 37°C. C+Y media was adapted from Adams and Roe (Martin et al., 1995).

For transformation, *S. pneumoniae* was grown in C+Y (pH 6.8) at 37°C to $OD_{595}$ 0.1. Competence was induced by addition of 100 ng/ml synthetic CSP-1 (D39V) or CSP-2 (TIGR4) and 12 min incubation at 37°C. DNA uptake occurred during 20 min at 30°C, followed by dilution and recovery for 1.5 hr. Transformants were selected by plating inside Columbia agar supplemented with 3% defibrinated sheep blood (CBA, Thermo Scientific) containing the appropriate antibiotic and incubated at 37°C in 5% $CO_2$ overnight. Successful transformants were confirmed by PCR and Sanger sequencing (Microsynth).

Strains were stocked at $OD_{595}$ 0.3 in C + Y with 15% glycerol at -80°C.

AMX (Sigma Aldrich) powder was dissolved initially in 100% DMSO. This solution was diluted in molecular grade water with 4% DMSO to two concentrations, 100 µg/mL and 1 mg/mL, and stored at -80°C.

**Table 1**: Key strains used in this study. The full collection of recombinant strains and their AMX MIC can be found in Table S1

| Strain Name | Strain ID | Genotype and relevant characteristics | AMX MIC (µg/mL) | reference |
|---|---|---|---|---|
| D39V | VL1 | Serotype 2 laboratory strain, AMX susceptible | 0.001 | Slager et al., 2018 |
| TIGR4 | VL2177 | Serotype 4 laboratory strain, AMX susceptible | 0.016 | Tettelin et al., 2001 |
| 11A | SN75752 VL1313 | Serotype 11A ST6521 clinical isolate, AMX resistant | 4 | German National Reference Center for Streptococci |
| AMR37 | VL4481 | D39V; recombinant strain, generation 1 | 0.094 | This study |
| AMR38 | VL4482 | D39V; recombinant strain, generation 1 | 0.094 | This study |
| AMR53 | VL3196 | D39V; recombinant strain, generation 2 | 2 | This study |
| AMR95 | VL4484 | D39V; recombinant strain, generation 2 | 1.5 | This study |
| EB31 | VL4495 | TIGR4; recombinant strain, generation 2 | 4 | This study |
| D39V$^{2x37}$ | VL4496 | D39V; *pbp2x37* | 0.023 | This study |
| D39V$^{2x38}$ | VL4302 | D39V; *pbp2x38* | 0.064 | This study |
| D39V$^{2b37}$ | VL4497 | D39V; *pbp2b37* | 0.023 | This study |
| D39V$^{2b38}$ | VL4498 | D39V; *pbp2b38* | 0.023 | This study |
| D39V$^{2x37\text{-}2b37}$ | VL4499 | D39V; *pbp2x37*; *pbp2b37* | 0.094 | This study |
| D39V$^{2x38\text{-}2b38}$ | VL3895 | D39V; *pbp2x38*; *pbp2b38* | 0.094 | This study |
| D39V$^{M53}$ | VL3960 | D39V; *murM53* | 0.023 | This study |
| D39V$^{1a53}$ | VL4159 | D39V; *pbp1a53* | 0.016 | This study |
| D39V$^{1a95}$ | VL4160 | D39V; *pbp1a95* | 0.016 | This study |
| D39V$^{2x38\text{-}2b38\text{-}M53}$ | VL3961 | D39V; *pbp2x38*; *pbp2b38*; *murM53* | 0.38 | This study |
| D39V$^{2x38\text{-}2b38\text{-}M95}$ | VL3962 | D39V; *pbp2x38*; *pbp2b38*; *murM95* | 0.5 | This study |
| D39V$^{2x38\text{-}2b38\text{-}1a53}$ | VL3896 | D39V; *pbp2x38*; *pbp2b38*; *pbp1a53* | 0.75 | This study |
| D39V$^{2x38\text{-}2b38\text{-}M53\text{-}1a53}$ | VL3963 | D39V; *pbp2x38*; *pbp2b38*; *murM53*; *pbp1a53* | 2 | This study |
| D39V$^{2x38\text{-}2b38\text{-}M95\text{-}1a95}$ | VL4500 | D39V; *pbp2x38*; *pbp2b38*; *murM95*; *pbp1a95* | 1.5 | This study |
| AMR53$^{2b31}$ | VL4174 | AMR53; *pbp2b31* | 6 | This study |
| AMR95$^{2b31}$ | VL4184 | AMR95; *pbp2b31* | 6 | This study |

***Minimum Inhibitory Concentrations (MICs)***

Bacteria were grown in C+Y broth to $OD_{595}$ 0.1, then AMX MIC was determined using E-tests (Biomeriaux, Lyon) on Mueller Hinton agar containing 5% defibrinated sheep's blood. MICs were read after 18 h incubation at 37°C and 5% $CO_2$.

Strains with MICs below the limit of the E-tests (0.016 μg/mL) were tested in Mueller Hinton cation-adjusted broth with 5% defibrinated sheep's blood using the broth micro-dilution method (Charles et al., 2016). Briefly, bacteria were streaked onto MH2-blood plates and grown overnight. Colonies were picked from plates and resuspended in PBS (pH 7.4) to McFarlane standard 0.5. This inoculum was diluted 100-fold into 96-well plates containing MH2-blood broth and AMX (in 2-fold concentration steps) then plated on agar plates as a control for contamination and cell density. Plates were incubated for 18 hours at 37°C and 5% $CO_2$. MIC was defined as the lowest concentration of antibiotic where visible α-haemolysis occupied approximately less than 10% of the surface area of the well. Due to a high level of subjectivity, MIC determination was repeated twice on different days, and MIC calls were confirmed by a second person in each case.

***Growth curves and analysis***

Strains were precultured in C+Y broth to OD 0.1, then diluted 100-fold into 96-well microtiter plates, containing fresh C+Y and AMX. The $OD_{595}$ was measured every 10 min for 12 hr in a plate reader (Infinite F200, Tecan) with incubation at 37°C. All strains were tested in triplicate Area under the curve was determined using TecanExtracter (Dénéréaz, unpublished). The AUC of each replicate was divided by that of the no antibiotic control for each strain, to normalize for strain-dependent differences in growth. The mean and standard error of the mean (SEM) of the normalized AUC was determined for three biological replicates.

Statistical significance of maximum specific growth rate (μ/h) was determined using one-way ANOVA with a Tukey correction for multiple testing.

***Bocillin-FL binding assay***

Bocillin-FL is a fluorescently labelled penicillin molecule which can be used to visualise and quantify PBP-penicillin binding affinity *in vitro*. Strains were grown to OD 0.2 in 4 mL C+Y, washed and resuspended in phosphate buffered saline (PBS), then incubated for 30 min at 37C in 5 μg/mL bocillin-FL (Invitrogen). Cells were washed in ice cold PBS, then lysed by

sonication (10 x 1s pulses at 30% power). The cell lysate was spun down and supernatant removed to collect the membrane fraction, which was homogenized by sonication (1s pulse at 10%). Total protein concentration was determined by nanodrop, then samples were diluted in NuPAGE LDS sample buffer (Life Technologies) with 10 mM DTT and incubated at 95°C for 5 min. Samples were loaded into two 15-well Novex™ WedgeWell™ 10% Tris-Glycine 1.0 mm Mini Protein Gels (Invitrogen), to a total protein amount of approximately 1.8 mg in a maximum volume of 30 µL. Where necessary, gels were imaged simultaneously on an Amersham Typhoon (GE Healthcare) with Cy2 DIGE filter setup. Bands were quantified using ImageQuant (GE Healthcare). As all strains tested had identical Pbp3 proteins, the intensities of the Pbp1a/b, Pbp2x/a, and Pbp2b bands were divided by the Pbp3 band intensity of the corresponding sample for normalisation. Imaging and quantification were performed in duplicate. Coomassie Blue staining was also performed, to confirm equal sample loading.

***Phase-contrast time-lapse microscopy***

For time-lapse microscopy, cells were pre-cultured in liquid C + Y medium at 37°C and spotted on a low-melting 1.2% C + Y agarose patch, with or without AMX at 1 µg/mL. Phase-contrast pictures were taken every 10 min as described (de Jong et al., 2011) using a Leica DMi8 with a 100x phase contrast objective.

***Isolation of genomic DNA***

10 mL of $OD_{595}$ 0.2 culture was pelleted by centrifugation, then resuspended in Nuclei Lysis solution (Promega) supplemented with 0.05% SDS, 0.025% deoxycholate (DOC), and 200 µg/mL RNase A. This was incubated at 37°C for 20 minutes, 80°C for 5 minutes, then 37° C for 10 minutes. Protein Precipitation Solution (Promega) was added to the lysate, vortexed vigorously, then incubated on ice for 10 minutes. The precipitated protein was pelleted by centrifugation and the supernatant transferred into isopropanol to precipitate the DNA, which was then collected by centrifugation. DNA was washed once in 70% ethanol before air drying and resuspension in the appropriate buffer (either TE buffer or molecular grade water). DNA was run on a 1% agarose gel to confirm no significant degradation had occurred, and stored at 4°C.

***Serial Transformation of S. pneumoniae with genomic DNA***

AMX susceptible recipient strains were transformed with 100 µg/mL genomic DNA isolated from AMX resistant strain 11A (Table 1) as above, with the following modifications. DNA uptake occurred during 30 min, followed by recovery for 2 hrs. Transformants were selected by plating inside Columbia agar supplemented with 5% defibrinated sheep blood and a range of AMX (0.03 µg/mL). Ten colonies were then picked at random and streaked onto CBA plates containing AMX. The next day, single colonies were grown up in C+Y with AMX and stocked. MICs were determined for these 10 strains, which were then subjected to another round of transformation and selection on a range of AMX concentrations (0.17 - 0.5 µg/mL), and 5-10 single colonies were picked for each of the 10 strains transformed. These were isolated, and MICs determined, as above. To test for significant differences between MICs of second-generation strains in different lineages, a Fisher's Exact Test with Monte Carlo p-value simulation was used.

To control for spontaneous mutations arising during transformation and recombination, cells transformed with either no DNA, or with D39V genomic DNA, were also plated in CBA with AMX (0.03). Neither resulted in visible colonies.

***Whole genome sequencing and quality control***

Genomic DNA from recombinant strains from each recipient background, as well as 11A and TIGR4 were Illumina sequenced (PE150, Novogene and Eurofins Genomics), with a mean coverage of 600-fold. Reads were trimmed using Trimmomatic (Bolger et al., 2014), then assembled using SPAdes (Nurk et al., 2013). Assembly quality was assessed with Quast (Gurevich et al., 2013), and read depth was determined in samtools (Li et al., 2009). Previously published D39V Illumina reads were filtered as above and used where necessary (GEO accessions GSE54199 and GSE69729) (Slager et al., 2014). Allelic exchange strains ($D39V^{M53}$, $D39V^{2x38\text{-}2b38\text{-}M53\text{-}1a53}$, $D39V^{1a53}$, $D39V^{2x38\text{-}2b38\text{-}M95\text{-}1a95}$) were treated in the same way, then variants were called using bbmap (Bushnell, 2013), Freebayes (Garrison and Marth, 2012), and vcftools (Danecek et al., 2011), in order to check for random mutations arising elsewhere in the genome.

11A, TIGR4, and a subset of recombinant strains were sent for PacBio sequencing (Sequel I and II, Lausanne Genomic Technologies Facility). Demultiplexing and quality control were

performed using SMRTlink (PacBio), then reads shorter than 1000 bp were removed with filtlong (Wick, 2017). Recombinant strain reads were mapped to the recipient reference genome using NGMLR and structural variants (SVs) called with sniffles with default settings, except with read mapping quality > 40 and read depth > 50 (Sedlazeck et al., 2018). Imprecise SVs were then filtered out. DNA methylation detection was performed using motifMaker (Clark et al., 2012).

Raw read files are deposited with NCBI Sequence Read Archive under BioProject PRJNA789167 (Individual SRA accession numbers for recombinant strains can be found in Table S4).

***Hybrid assemblies of reference genomes***

As PacBio sequencing depth was greater than 200x, genomes were assembled in a long-read only manner using Trycycler (Wick et al., 2021), followed by short-read polishing.

Briefly, filtered reads were subsampled 12 times and *de novo* assembled in four different assemblers, flye (Kolmogorov et al., 2019), raven (Wang et al., 2018), wtdbg2 (Ruan and Li, 2020), and miniasm plus minipolish (Li, 2018, 2016). Some assemblies were removed during the Trycycler cluster and reconcile steps, leaving the final consensus sequence to be built from seven to eight assemblies. The consensus assembly was subjected to rounds of polishing with PacBio reads using pbmm2 and pbgcpp (PacBio Toolkit), followed by one round of short-read polishing with Pilon (Walker et al., 2014).

Genomes were annotated in Prokka (Seemann, 2014) using Barrnap and Aragorn (Laslett and Canback, 2004; Seemann, 2019) and are deposited at NCBI under BioProject PRJNA789167 (accession numbers currently in process).

***Recombination detection with NGS***

Competitive mapping of filtered illumina reads onto a pseudogenome containing both recipient and donor chromosomes was used for crude visualization of recombination loci (bbmap) (Matthey et al., 2019). In order to characterize these loci more accurately, filtered reads of recombinant and recipient strains were mapped onto the 11A hybrid genome assembly using smalt, then variants were called with bcftools (Li, 2011). SNPs were filtered as described previously (Cowley et al. 2018), and used to build a consensus alignment of donor, recipient, and recombinant strains. The consensus alignment was run through a python script

designed to identify SNPs between recombinant and donor which are not shared with the recipient genome. Once identified, the match was extended until the donor and recombinant sequences are no longer identical, then the start, end, and length of detected recombination events are extracted (Cowley et al 2018).

***Identifying non-contiguous recombination events***

Many recombination events were located very close together, with sometimes only a few recipient allele SNPs separating the two, suggesting a single donor DNA molecule as the source. To determine if events were significantly close together, a bootstrapping approach was applied (Croucher et al., 2012). Firstly, the distances between one recombination event and each of the other recombination events in a single genome were calculated. The circular chromosome gives two values, and the shortest distance between any two events was added to the test population. This was calculated for every sequenced strain in the D39V and TIGR4 recombinants, and for second-generation strains any prior events carried through from the first-generation were removed from the dataset. The shortest recombination distance within a strain became the test value ($d_{test}$), and then the test population was sampled (with replacement).

The distribution of a bootstrapped sample (same size as the test population) was used to test the hypothesis that $d_{test}$ was significantly shorter than expected under the null hypothesis that recombination events are located at random around the chromosome. A Holm correction was applied to account for multiple testing, based on the number of recombination events in the strain. Bootstrap tests were performed one thousand times for each $d_{test}$ value and considered significantly short if the null hypothesis was rejected at least 95% of the time. If a $d_{test}$ value was significant, then the distance between the next shortest pairing within the strain became $d_{test}$, and was tested in the same fashion. This continued until a $d_{test}$ where the null hypothesis could not be rejected.

When recombination events were considered significantly close together, they were linked together into non-contiguous recombination events.

***Confirming the origins of non-contiguous recombination events in vivo***

A 4.25 Kb region of the 11A genome spanning *pbp2x* was used to test the origin of non-contiguous recombination. This region included an 846 bp stretch with SNPs conferring a

small decrease in AMX susceptibility sufficient for selection. One long fragment spanning the entire region was amplified with OVL5375 and OVL5378. Two shorter fragments were then amplified, an upstream fragment (Up) with OVL5379 and OVL5375 (2.84 Kb) and a downstream fragment (Down) with OVL5376 and OVL5378 (2.26 Kb), which overlapped at the SNPs determined to be necessary for selection (Table S2, S5). The three donor DNA templates used in the experiment and their SNPs are shown in Figure 6C (Table S6).

D39V was transformed as above, with equimolar quantities of each fragment separately, as well as a combination of the two short fragments, and a negative control with no DNA. Transformants were selected on AMX (0.015 µg/mL), and the transformation efficiency was determined by dividing by the total viable count. Individual colonies were restreaked on AMX, then single colonies were picked and the 4.25 Kb region of interest was amplified and Sanger sequenced (Microsynth, Table S2 oligos). Nucleotide sequences were aligned in Mega (Kumar et al., 2018).

As molecule length affects transformation efficiency (Keller et al., 2019; Kurushima et al., 2020; Lee et al., 1998), an additional experiment was performed, where the amplified fragments were all extended to 6 Kb by the addition of non-homologous DNA amplified from *E. coli* and ligated to one end using Golden Gate assembly with BsmBI and T4 DNA ligase (NEB, Vazyme). All oligos and the corresponding templates used in the cloning for these experiments are outlined in Table S6, and a comprehensive oligo list can be found in Table S2. The assemblies were then amplified to ensure high quality of transforming fragments, resulting in three fragments of equal size, with differing lengths of homologous regions to the *pbp2x* locus. These were then transformed, amplified, and Sanger sequenced as above, and the transformation efficiency determined.

***Gene and protein alignments***

Nucleotide sequences of *pbp* and *murM* genes were translated using Emboss:TransSeq (Madeira et al., 2019). Alignments were performed with Muscle (Edgar, 2004). Phylogenetic trees were produced using concatenated protein alignments of Pbp2x, Pbp2b, Pbp1a, and MurM as input for FastTree (default settings), and visualised in ITOL (Letunic and Bork, 2021; Price et al., 2009).

***Amplification and transformation of pbp and murM loci for allelic exchange experiments***

Genes for *pbps* were amplified with Phanta Max Super-Fidelity DNA Polymerase (Vazyme) and primers ordered from Sigma (Table S2). Equimolar quantities of PCR products were used for transformation. To avoid transforming mutations in *murN* alongside those in *murM*, alleles at this locus were cloned into a construct with D39V flanking sequences. The upstream and downstream fragments were amplified from D39V with OVL5540/OVL5779 and OVL5780/OVL5541 respectively, and the *murM* allele from AMR53 or AMR95 with OVL5777/OVL5778. Fragments were then assembled using BsmBI and T4 DNA ligase.

*pbp2x* and *pbp2b* alleles from AMR37 and AMR38 were transformed into D39V as above, selected on 0.012 µg/mL, 0.015 µg/mL, 0.02 µg/mL AMX, and confirmed by Sanger sequencing. D39V$^{2x38\text{-}2b38}$ (Table 1) was then used as the recipient for *murM* and *pbp1a* alleles from AMR53 and AMR95, with selection on 0.2 µg/mL, 0.5 µg/mL and 1 µg/mL AMX.

## Acknowledgements

We would like to thank Mark van der Linden at the German National Reference Center for Streptococci for the 11A (SN75752) clinical isolate, and the Lausanne Genomic Technologies Facility for their valuable work in PacBio sequencing and data quality control. We would also like to thank Arnau Domenech Pena, Alice Wallef, Vincent de Bakker, Julien Denereaz, and the rest of the Veening Lab for their help, contributions, and feedback.

P.G. was supported by the University of Lausanne Faculty of Biology and Medicine PhD fellowship. Work in the Veening lab is supported by the Swiss National Science Foundation (SNSF) (project grant 310030_192517), SNSF JPIAMR grant (40AR40_185533), SNSF NCCR 'AntiResist' (51NF40_180541) and ERC consolidator grant 771534-PneumoCaTChER.

## References


Albarracín Orio AG, Piñas GE, Cortes PR, Cian MB, Echenique J. 2011. Compensatory evolution of pbp mutations restores the fitness cost imposed by β-lactam resistance in *Streptococcus pneumoniae*. *PLoS Pathogens* **7**:e1002000. doi:10.1371/journal.ppat.1002000

Alloing G, Martin B, Granadel C, Claverys JP. 1998. Development of competence in *Streptococcus pneumoniae*: Pheromone autoinduction and control of quorum sensing by the oligopeptide permease. *Molecular Microbiology* **29**:75–83. doi:10.1046/J.1365-2958.1998.00904.X

Arnold BJ, Gutmann MU, Grad YH, Sheppard SK, Corander J, Lipsitch M, Hanage WP. 2018. Weak epistasis may drive adaptation in recombining bacteria. *Genetics* **208**:1247–1260. doi:10.1534/genetics.117.300662

Attaiech L, Olivier A, Mortier-Barrière I, Soulet AL, Granadel C, Martin B, Polard P, Claverys JP. 2011. Role of the single-stranded DNA-binding protein SsbB in pneumococcal transformation: Maintenance of a reservoir for genetic plasticity. *PLoS Genetics* **7**:e1002156. doi:10.1371/journal.pgen.1002156

Bell JC, Kowalczykowski SC. 2016. RecA: Regulation and Mechanism of a Molecular Search Engine. *Trends in Biochemical Sciences*. doi:10.1016/j.tibs.2016.04.002

Berg KH, Stamsås GA, Straume D, Håvarstein LS. 2013. Effects of low PBP2b levels on cell morphology and peptidoglycan composition in *Streptococcus pneumoniae* R6. *Journal of Bacteriology* **195**:4342–4354. doi:10.1128/JB.00184-13

Bergé MJ, Kamgoué A, Martin B, Polard P, Campo N, Claverys J-P. 2013. Midcell Recruitment of the DNA Uptake and Virulence Nuclease, EndA, for Pneumococcal Transformation. *PLOS Pathogens* **9**:e1003596. doi:10.1371/JOURNAL.PPAT.1003596

Bolger AM, Lohse M, Usadel B. 2014. Trimmomatic: a flexible trimmer for Illumina sequence data. *Bioinformatics* **30**:2114–20. doi:10.1093/bioinformatics/btu170

Bushnell B. 2013. BBMap download | SourceForge.net. *SourceForge*. https://sourceforge.net/projects/bbmap/

Cafini F, del Campo R, Alou L, Sevillano D, Morosini MI, Baquero F, Prieto J, García E, Casal J, Fenoll A, de la Campa AG, Bouza E, Baquero F, Soriano F, Pallarés R, Liñares J, Garau J, Lacasa JM, Latorre C, Pérez-Trallero E, García de Lomas J, Fleites A. 2006. Alterations of the penicillin-binding proteins and murM alleles of clinical *Streptococcus pneumoniae* isolates with high-level resistance to amoxicillin in Spain. *Journal of Antimicrobial Chemotherapy* **57**:224–229. doi:10.1093/jac/dki442

Càmara J, Cubero M, Martín-Galiano AJ, García E, Grau I, Nielsen JB, Worning P, Tubau F, Pallarés R, Domínguez MÁ, Kilian M, Liñares J, Westh H, Ardanuy C. 2018. Evolution of the β-lactam-resistant *Streptococcus pneumoniae* PMEN3 clone over a 30 year period in Barcelona, Spain. *Journal of Antimicrobial Chemotherapy* **73**:2941–2951. doi:10.1093/jac/dky305

Carrasco B, Serrano E, Sánchez H, Wyman C, Alonso JC. 2016. Chromosomal transformation in Bacillus subtilis is a non-polar recombination reaction. *Nucleic Acids Research* **44**:2754–2768. doi:10.1093/nar/gkv1546

Cassone M, Gagne AL, Spruce LA, Seeholzer SH, Sebert ME. 2012. The HtrA protease from *Streptococcus pneumoniae* digests both denatured proteins and the competence-stimulating peptide. *J Biol Chem* **287**:38449–59. doi:10.1074/jbc.M112.391482

Charles MK, Berenger BM, Turnbull L, Rennie R, Fuller J. 2016. Variability of β-lactam susceptibility testing for *Streptococcus pneumoniae* using 4 commercial test methods and broth microdilution. *Diagnostic Microbiology and Infectious Disease* **84**:240–245. doi:10.1016/J.DIAGMICROBIO.2015.11.014

Chesnel L, Carapito R, Croizé J, Dideberg O, Vernet T, Zapun A. 2005. Identical penicillin-binding domains in penicillin-binding proteins of *Streptococcus pneumoniae* clinical isolates with different levels of beta-lactam resistance. *Antimicrob Agents Chemother* **49**:2895–2902. doi:10.1128/AAC.49.7.2895

Chewapreecha C, Harris SR, Croucher NJ, Turner C, Marttinen P, Cheng L, Pessia A, Aanensen DM, Mather AE, Page AJ, Salter SJ, Harris D, Nosten F, Goldblatt D, Corander J, Parkhill J, Turner P, Bentley SD. 2014. Dense genomic sampling identifies highways of pneumococcal recombination. *Nature Genetics* **46**:305–309. doi:10.1038/ng.2895

Clark TA, Murray IA, Morgan RD, Kislyuk AO, Spittle KE, Boitano M, Fomenkov A, Roberts RJ, Korlach J. 2012. Characterization of DNA methyltransferase specificities using single-molecule, real-time DNA sequencing. *Nucleic Acids Research* **40**. doi:10.1093/nar/gkr1146

Claverys JP, Lacks SA. 1986. Heteroduplex deoxyribonucleic acid base mismatch repair in bacteria. *Microbiological Reviews*. doi:10.1128/mmbr.50.2.133-165.1986

Cowley LA, Petersen FC, Junges R, Jimson D. Jimenez M, Morrison DA, Hanage WP. 2018. Evolution via recombination: Cell-to-cell contact facilitates larger recombination events in *Streptococcus pneumoniae*. *PLOS Genetics* **14**:e1007410. doi:10.1371/journal.pgen.1007410

Croucher NJ, Harris SR, Barquist L, Parkhill J, Bentley SD. 2012. A high-resolution view of genome-wide pneumococcal transformation. *PLoS Pathogens* **8**:e1002745. doi:10.1371/journal.ppat.1002745

Croucher NJ, Harris SR, Fraser C, Quail MA, Burton J, van der Linden M, McGee L, von Gottberg A, Song JH, Ko KS, Pichon B, Baker S, Parry CM, Lambertsen LM, Shahinas D, Pillai DR, Mitchell TJ, Dougan G, Tomasz A, Klugman KP, Parkhill J, Hanage WP, Bentley SD. 2011. Rapid pneumococcal evolution in response to clinical interventions. *Science (1979)* **331**:430–434. doi:10.1126/SCIENCE.1198545

Danecek P, Auton A, Abecasis G, Albers CA, Banks E, DePristo MA, Handsaker RE, Lunter G, Marth GT, Sherry ST, McVean G, Durbin R. 2011. The variant call format and VCFtools. *Bioinformatics* **27**:2156–2158. doi:10.1093/bioinformatics/btr330

Danilowicz C, Yang D, Kelley C, Prévost C, Prévost P, Prentiss M. 2015. The poor homology stringency in the heteroduplex allows strand exchange to incorporate desirable mismatches without sacrificing recognition in vivo. *Nucleic Acids Research* **43**:6473–6485. doi:10.1093/nar/gkv610

Demerec M. 1945. Production of Staphylococcus strains resistant to various concentrations of penicillin. *Proceedings of the National Academy of Sciences* **31**:16–24.

Desai B v, Morrison DA. 2007. Transformation in *Streptococcus pneumoniae*: Formation of eclipse complex in a *coiA* mutant implicates CoiA in genetic recombination. *Molecular Microbiology* **63**:1107–1117. doi:10.1111/j.1365-2958.2006.05558.x

Doern G v, Brueggemann A, Holley HP, Rauch AM. 1996. Antimicrobial resistance of *Streptococcus pneumoniae* recovered from outpatients in the United States during the winter months of 1994 to 1995: results of a 30-center national surveillance study. *Antimicrob Agents Chemother* **40**:1208–13. doi:10.1128/AAC.40.5.1208

Doit C, Loukil C, Fitoussi F, Geslin P, Bingen E. 1999. Emergence in France of Multiple Clones of Clinical*Streptococcus pneumoniae* Isolates with High-Level Resistance to Amoxicillin. *Antimicrobial Agents and Chemotherapy* **43**:1480–1483. doi:10.1128/AAC.43.6.1480

Donati C, Hiller NL, Tettelin H, Muzzi A, Croucher NJ, Angiuoli S v., Oggioni M, Dunning Hotopp JC, Hu FZ, Riley DR, Covacci A, Mitchell TJ, Bentley SD, Kilian M, Ehrlich GD, Rappuoli R, Moxon ER, Masignani V. 2010. Structure and dynamics of the pan-genome of *Streptococcus pneumoniae* and closely related species. *Genome Biology* **11**:R107. doi:10.1186/gb-2010-11-10-r107

Dowson CG, Coffey TJ, Kell C, Whiley RA. 1993. Evolution of penicillin resistance in *Streptococcus pneumoniae*; the role of *Streptococcus mitis* in the formation of a low affinity PBP2B in *S. pneumoniae*. *Molecular Microbiology* **9**:635–643. doi:10.1111/j.1365-2958.1993.tb01723.x

du Plessis M, Bingen E, Klugman KP, Plessis M du, Bingen E, Klugman KP, du Plessis M, Bingen E, Klugman KP. 2002. Analysis of Penicillin-Binding Protein Genes of Clinical Isolates of *Streptococcus pneumoniae* with Reduced Susceptibility to Amoxicillin. *Antimicrobial Agents and Chemotherapy* **46**:2349–2357. doi:10.1128/AAC.46.8.2349

Edgar RC. 2004. MUSCLE: Multiple sequence alignment with high accuracy and high throughput. *Nucleic Acids Research* **32**:1792–1797. doi:10.1093/nar/gkh340

el Khoury JY, Boucher N, Bergeron MG, Leprohon P, Ouellette M. 2017. Penicillin induces alterations in glutamine metabolism in *Streptococcus pneumoniae*. *Scientific Reports* **7**. doi:10.1038/s41598-017-15035-y

Eldholm V, Johnsborg O, Haugen K, Ohnstad HS, Havastein LS. 2009. Fratricide in *Streptococcus pneumoniae*: Contributions and role of the cell wall hydrolases CbpD, LytA and LytC. *Microbiology (N Y)* **155**:2223–2234. doi:10.1099/MIC.0.026328-0

Fani F, Leprohon P, Zhanel GG, Bergeron MG, Ouellette M. 2014. Genomic analyses of DNA transformation and penicillin resistance in *Streptococcus pneumoniae* clinical isolates. *Antimicrobial Agents and Chemotherapy* **58**:1397–1403. doi:10.1128/AAC.01311-13

Feng Z, Li J, Zhang JR, Zhang X. 2014. Qdnamod: A statistical model-based tool to reveal intercellular heterogeneity of DNA modification from SMRT sequencing data. *Nucleic Acids Research* **42**:13488–13499. doi:10.1093/nar/gku1097

Figueiredo TA, Sobral RG, Ludovice AM, de Almeida JMF, Bui NK, Vollmer W, de Lencastre H, Tomasz A. 2012. Identification of Genetic Determinants and Enzymes Involved with the Amidation of Glutamic Acid Residues in the Peptidoglycan of *Staphylococcus aureus*. *PLOS Pathogens* **8**:e1002508. doi:10.1371/JOURNAL.PPAT.1002508

Filipe SR, Severina E, Tomasz A. 2002. The murMN operon: A functional link between antibiotic resistance and antibiotic tolerance in *Streptococcus pneumoniae*. *Proceedings of the National Academy of Sciences* **99**:1550–1555. doi:10.1073/PNAS.032671699

Filipe SR, Tomasz A. 2000. Inhibition of the expression of penicillin resistance in *Streptococcus pneumoniae* by inactivation of cell wall muropeptide branching genes. *Proceedings of the National Academy of Sciences* **97**:4891–4896. doi:https://doi.org/10.1073/pnas.080067697

Forget AL, Kowalczykowski SC. 2012. Single-molecule imaging of DNA pairing by RecA reveals a three-dimensional homology search. *Nature 2012 482:7385* **482**:423–427. doi:10.1038/nature10782

Garcia-Bustos J, Tomasz A. 1990. A biological price of antibiotic resistance: major changes in the peptidoglycan structure of penicillin-resistant pneumococci. *Proc Natl Acad Sci U S A* **87**:5415–9. doi:10.1073/pnas.87.14.5415

Garrison E, Marth G. 2012. Haplotype-based variant detection from short-read sequencing. *arXiv.org*.

Gasc AM, Sicard AM, Claverys JP. 1989. Repair of single- and multiple-substitution mismatches during recombination in *Streptococcus pneumoniae*. *Genetics* **121**:29–36. doi:10.1093/genetics/121.1.29

Grebe T, Paik J, Hakenbeck R. 1997. A novel resistance mechanism against β-lactams in *Streptococcus pneumoniae* involves CpoA, a putative glycosyltransferase. *Journal of Bacteriology* **179**:3342–3349. doi:10.1128/jb.179.10.3342-3349.1997

Guenzi E, Gasc A-M, Sicard MA, Hakenbeck R. 1994. A two-component signal-transducing system is involved in competence and penicillin susceptibility in laboratory mutants of *Streptococcus pneumoniae*. *Molecular Microbiology* **12**:505–515. doi:10.1111/j.1365-2958.1994.tb01038.x

Gurevich A, Saveliev V, Vyahhi N, Tesler G. 2013. QUAST: quality assessment tool for genome assemblies. *Bioinformatics* **29**:1072–1075. doi:10.1093/bioinformatics/btt086

Gurney T, Fox MS. 1968. Physical and genetic hybrids formed in bacterial transformation. *Journal of Molecular Biology* **32**:83–100. doi:10.1016/0022-2836(68)90147-2

Hakenbeck R, Brückner R, Denapaite D, Maurer P. 2012. Molecular mechanisms of β-lactam resistance in *Streptococcus pneumoniae*. *Future Microbiology*. doi:10.2217/fmb.12.2

Hakenbeck R, Nig AK, Kern I, van der Linden M, Keck W, Billot-Klein D, Legrand R, Schoot B, Gutmann L. 1998. Acquisition of Five High-Mr Penicillin-Binding Protein Variants during Transfer of High-Level Beta-Lactam Resistance from *Streptococcus mitis* to *Streptococcus pneumoniae*. *Journal of Bacteriology* **180**:1831–1840.

Hiller NL, Ahmed A, Powell E, Martin DP, Eutsey R, Earl J, Janto B, Boissy RJ, Hogg J, Barbadora K, Sampath R, Lonergan S, Post JC, Hu FZ, Ehrlich GD. 2010. Generation of Genic Diversity among *Streptococcus pneumoniae* Strains via Horizontal Gene Transfer during a Chronic Polyclonal Pediatric Infection. *PLOS Pathogens* **6**:e1001108. doi:10.1371/JOURNAL.PPAT.1001108

Hotchkiss RD. 1951. Transfer of penicillin resistance in pneumococci by the deoxyribonucleate derived from resistant cultures. *Cold Spring Harb Symp Quant Biol* **16**:457–461. doi:10.1101/SQB.1951.016.01.032

Hsieh P, Camerini-Otero CS, Camerini-Otero RD. 1992. The synapsis event in the homologous pairing of DNAs: RecA recognizes and pairs less than one helical repeat of DNA. *Proc Natl Acad Sci U S A* **89**:6492–6496. doi:10.1073/pnas.89.14.6492

Humbert O, Prudhomme M, Hakenbeck R, Dowson CG, Claverys JP. 1995. Homeologous recombination and mismatch repair during transformation in *Streptococcus pneumoniae*: Saturation of the Hex mismatch repair system. *Proc Natl Acad Sci U S A* **92**:9052–9056. doi:10.1073/pnas.92.20.9052

Johnsborg O, Eldholm V, Bjørnstad ML, Håvarstein LS. 2008. A predatory mechanism dramatically increases the efficiency of lateral gene transfer in *Streptococcus pneumoniae* and related commensal species. *Molecular Microbiology* **69**:245–253. doi:10.1111/j.1365-2958.2008.06288.x

Kalizang'oma A, Chaguza C, Gori A, Davison C, Beleza S, Antonio M, Beall B, Goldblatt D, Kwambana-Adams B, Bentley SD, Heyderman RS. 2021. *Streptococcus pneumoniae* serotypes that frequently colonise the human nasopharynx are common recipients of penicillin-binding protein gene fragments from *Streptococcus mitis*. *Microbial Genomics* **7**:000622. doi:10.1099/mgen.0.000622

Keller LE, Rueff A-SS, Kurushima J, Veening J-WW. 2019. Three new integration vectors and fluorescent proteins for use in the opportunistic human pathogen *Streptococcus pneumoniae*. *Genes (Basel)* **10**:394. doi:10.3390/genes10050394

Kocaoglu O, Tsui H-CCT, Winkler ME, Carlson EE. 2015. Profiling of β-lactam selectivity for penicillin-binding proteins in *Streptococcus pneumoniae* D39. *Antimicrobial Agents and Chemotherapy* **59**:3548–3555. doi:10.1128/AAC.05142-14

Kolmogorov M, Yuan J, Lin Y, Pevzner PA. 2019. Assembly of long, error-prone reads using repeat graphs. *Nature Biotechnology* **37**:540–546. doi:10.1038/s41587-019-0072-8

Kosowska K, Jacobs MR, Bajaksouzian S, Koeth L, Appelbaum PC. 2004. Alterations of Penicillin-Binding Proteins 1A, 2X, and 2B in *Streptococcus pneumoniae* Isolates for Which Amoxicillin MICs Are Higher than Penicillin MICs **48**. doi:10.1128/AAC.48.10.4020-4022.2004

Kulick S, Moccia C, Didelot X, Falush D, Kraft C, Suerbaum S. 2008. Mosaic DNA imports with interspersions of recipient sequence after natural transformation of Helicobacter pylori. *PLoS ONE* **3**:e3797. doi:10.1371/journal.pone.0003797

Kumar S, Stecher G, Li M, Knyaz C, Tamura K. 2018. MEGA X: Molecular evolutionary genetics analysis across computing platforms. *Molecular Biology and Evolution* **35**:1547–1549. doi:10.1093/molbev/msy096

Kurushima J, Campo N, van Raaphorst R, Cerckel G, Polard P, Veening JW. 2020. Unbiased homeologous recombination during pneumococcal transformation allows for multiple chromosomal integration events. *Elife* **9**:1–70. doi:10.7554/ELIFE.58771

Lacks S, Greenberg B. 1976. Single-strand breakage on binding of DNA to cells in the genetic transformation of Diplococcus pneumoniae. *Journal of Molecular Biology* **101**:255–275. doi:10.1016/0022-2836(76)90376-4

Lacks S, Neuberger M. 1975. Membrane location of a deoxyribonuclease implicated in the genetic transformation of Diplococcus pneumoniae. *Journal of Bacteriology* **124**:1321–1329. doi:10.1128/jb.124.3.1321-1329.1975

Laslett D, Canback B. 2004. ARAGORN, a program to detect tRNA genes and tmRNA genes in nucleotide sequences. *Nucleic Acids Research* **32**:11–16. doi:10.1093/nar/gkh152

Laurenceau R, Péhau-Arnaudet G, Baconnais S, Gault J, Malosse C, Dujeancourt A, Campo N, Chamot-Rooke J, le Cam E, Claverys JP, Fronzes R. 2013. A Type IV Pilus Mediates DNA

Binding during Natural Transformation in *Streptococcus pneumoniae*. *PLoS Pathogens* **9**:e1003473. doi:10.1371/journal.ppat.1003473

Lee MS, Seok C, Morrison DA. 1998. Insertion-duplication mutagenesis in *Streptococcus pneumoniae*: Targeting fragment length is a critical parameter in use as a random insertion tool. *Applied and Environmental Microbiology* **64**:4796–4802. doi:10.1128/aem.64.12.4796-4802.1998

Letunic I, Bork P. 2021. Interactive tree of life (iTOL) v5: An online tool for phylogenetic tree display and annotation. *Nucleic Acids Research* **49**:W293–W296. doi:10.1093/nar/gkab301

Li H. 2018. Minimap2: Pairwise alignment for nucleotide sequences. *Bioinformatics* **34**:3094–3100. doi:10.1093/bioinformatics/bty191

Li H. 2016. Minimap and miniasm: Fast mapping and de novo assembly for noisy long sequences. *Bioinformatics* **32**:2103–2110. doi:10.1093/bioinformatics/btw152

Li H. 2011. A statistical framework for SNP calling, mutation discovery, association mapping and population genetical parameter estimation from sequencing data. *Bioinformatics* **27**:2987–2993. doi:10.1093/bioinformatics/btr509

Li H, Handsaker B, Wysoker A, Fennell T, Ruan J, Homer N, Marth G, Abecasis G, Durbin R, 1000 Genome Project Data Processing Subgroup. 2009. The Sequence Alignment/Map format and SAMtools. *Bioinformatics* **25**:2078–2079. doi:10.1093/bioinformatics/btp352

Lisboa J, Andreani J, Sanchez D, Boudes M, Collinet B, Liger D, Tilbeurgh H van, Guérois R, Quevillon-Cheruel S. 2014. Molecular determinants of the DprA-RecA interaction for nucleation on ssDNA. *Nucleic Acids Research* **42**:7395–7408. doi:10.1093/nar/gku349

Liu X, Li JW, Feng Z, Luo Y, Veening JW, Zhang JR. 2017. Transcriptional repressor PtvR regulates phenotypic tolerance to vancomycin in *Streptococcus pneumoniae*. *Journal of Bacteriology* **199**:54–71. doi:10.1128/JB.00054-17

Madeira F, Park Y mi, Lee J, Buso N, Gur T, Madhusoodanan N, Basutkar P, Tivey ARN, Potter SC, Finn RD, Lopez R. 2019. The EMBL-EBI search and sequence analysis tools APIs in 2019. *Nucleic Acids Research* **47**:W636–W641. doi:10.1093/nar/gkz268

Manso AS, Chai MH, Atack JM, Furi L, de Ste Croix M, Haigh R, Trappetti C, Ogunniyi AD, Shewell LK, Boitano M, Clark TA, Korlach J, Blades M, Mirkes E, Gorban AN, Paton JC, Jennings MP, Oggioni MR. 2014. A random six-phase switch regulates pneumococcal virulence via global epigenetic changes. *Nature Communications* **5**:1–9. doi:10.1038/ncomms6055

Marie L, Rapisarda C, Morales V, Bergé M, Perry T, Soulet AL, Gruget C, Remaut H, Fronzes R, Polard P. 2017. Bacterial RadA is a DnaB-Type helicase interacting with RecA to promote

bidirectional D-loop extension. *Nature Communications* **8**:1–14. doi:10.1038/ncomms15638

Martin B, Garcia P, Castanié M -P, Claverys J -P. 1995. The *recA* gene of *Streptococcus pneumoniae* is part of a competence-induced operon and controls lysogenic induction. *Molecular Microbiology* **15**:367–379. doi:10.1111/j.1365-2958.1995.tb02250.x

Martin B, Soulet AL, Mirouze N, Prudhomme M, Mortier-Barrière I, Granadel C, Noirot-Gros MF, Noirot P, Polard P, Claverys JP. 2013. ComE/ComE~P interplay dictates activation or extinction status of pneumococcal X-state (competence). *Molecular Microbiology* **87**:394–411. doi:10.1111/mmi.12104

Matthey N, Stutzmann S, Stoudmann C, Guex N, Iseli C, Blokesch M. 2019. Neighbor predation linked to natural competence fosters the transfer of large genomic regions in vibrio cholerae. *Elife* **8**. doi:10.7554/eLife.48212

Mazin A v, Kowalczykowski SC. 1996. The specificity of the secondary DNA binding site of RecA protein defines its role in DNA strand exchange. *Proc Natl Acad Sci U S A* **93**:10673–10678. doi:10.1073/pnas.93.20.10673

Mell JC, Shumilina S, Hall IM, Redfield RJ. 2011. Transformation of natural genetic variation into *Haemophilus influenzae* genomes. *PLoS Pathogens* **7**:e1002151. doi:10.1371/journal.ppat.1002151

Mirouze N, Bergé MA, Soulet AL, Mortier-Barrière I, Quentin Y, Fichant G, Granadel C, Noirot-Gros MF, Noirot P, Polard P, Martin B, Claverys JP. 2013. Direct involvement of DprA, the transformation-dedicated RecA loader, in the shut-off of pneumococcal competence. *Proc Natl Acad Sci U S A* **110**. doi:10.1073/pnas.1219868110

Morrison DA, Guild WR. 1973. Breakage prior to entry of donor DNA in Pneumococcus transformation. *BBA Section Nucleic Acids And Protein Synthesis* **299**:545–556. doi:10.1016/0005-2787(73)90226-8

Morrison DA, Guild WR. 1972. Transformation and deoxyribonucleic acid size: extent of degradation on entry varies with size of donor. *J Bacteriol* **112**:1157–1168. doi:10.1128/jb.112.3.1157-1168.1972

Morrison DA, Mortier-Barrière I, Attaiech L, Claverys JP. 2007. Identification of the major protein component of the pneumococcal eclipse complex. *Journal of Bacteriology* **189**:6497–6500. doi:10.1128/JB.00687-07

Mortier-Barriere I, Humbert O, Martin B, Prudhomme M, Claverys JP. 1997. Control of recombination rate during transformation of *Streptococcus pneumoniae*: An overview. *Microbial Drug Resistance* **3**:233–242. doi:10.1089/mdr.1997.3.233

Mortier-Barrière I, Velten M, Dupaigne P, Mirouze N, Piétrement O, McGovern S, Fichant G, Martin B, Noirot P, le Cam E, Polard P, Claverys JP. 2007. A Key Presynaptic Role in

Transformation for a Widespread Bacterial Protein: DprA Conveys Incoming ssDNA to RecA. *Cell* **130**:824–836. doi:10.1016/j.cell.2007.07.038

Münch D, Roemer T, Lee SH, Engeser M, Sahl HG, Schneider T. 2012. Identification and in vitro Analysis of the GatD/MurT Enzyme-Complex Catalyzing Lipid II Amidation in *Staphylococcus aureus*. *PLOS Pathogens* **8**:e1002509. doi:10.1371/JOURNAL.PPAT.1002509

Nurk S, Bankevich A, Antipov D, Gurevich A, Korobeynikov A, Lapidus A, Prjibelsky A, Pyshkin A, Sirotkin A, Sirotkin Y, Stepanauskas R, McLean J, Lasken R, Clingenpeel SR, Woyke T, Tesler G, Alekseyev MA, Pevzner PA. 2013. Assembling genomes and mini-metagenomes from highly chimeric reads. Deng M., Jiang R., Sun F., Zhang X. (Eds) *Research in Computational Molecular Biology.* Springer, Berlin, Heidelberg. pp. 158–170. doi:10.1007/978-3-642-37195-0_13

O'Brien KL, Wolfson LJ, Watt JP, Henkle E, Deloria-Knoll M, McCall N, Lee E, Mulholland K, Levine OS, Cherian T. 2009. Burden of disease caused by *Streptococcus pneumoniae* in children younger than 5 years: global estimates. *The Lancet* **374**:893–902. doi:10.1016/S0140-6736(09)61204-6

Piotrowski A, Luo P, Morrison DA. 2009. Competence for Genetic Transformation in *Streptococcus pneumoniae*: Termination of Activity of the Alternative Sigma Factor ComX Is Independent of Proteolysis of ComX and ComW. *Journal of Bacteriology* **191**:3359. doi:10.1128/JB.01750-08

Price MN, Dehal PS, Arkin AP. 2009. Fasttree: Computing large minimum evolution trees with profiles instead of a distance matrix. *Molecular Biology and Evolution* **26**:1641–1650. doi:10.1093/molbev/msp077

Quevillon-Cheruel S, Campo N, Mirouze N, Mortier-Barrière I, Brooks MA, Boudes M, Durand D, Soulet AL, Lisboa J, Noirot P, Martin B, van Tilbeurgh H, Noirot-Gros MF, Claverys JP, Polard P. 2012. Structure-function analysis of pneumococcal DprA protein reveals that dimerization is crucial for loading RecA recombinase onto DNA during transformation. *Proc Natl Acad Sci U S A* **109**:E2466–E2475. doi:10.1073/pnas.1205638109

Rosenthal AL, Lacks SA. 1980. Complex structure of the membrane nuclease of *Streptococcus pneumoniae* revealed by two-dimensional electrophoresis. *Journal of Molecular Biology* **141**:133–146. doi:10.1016/0022-2836(80)90381-2

Ruan J, Li H. 2020. Fast and accurate long-read assembly with wtdbg2. *Nature Methods* **17**:155–158. doi:10.1038/s41592-019-0669-3

Salvadori G, Junges R, Morrison DA, Petersen FC. 2019. Competence in *Streptococcus pneumoniae* and close commensal relatives: Mechanisms and implications. *Frontiers in Cellular and Infection Microbiology*. doi:10.3389/fcimb.2019.00094

Scheffers D-J, Pinho MG. 2005. Bacterial Cell Wall Synthesis: New Insights from Localization Studies. *Microbiology and Molecular Biology Reviews* **69**:585–607. doi:10.1128/mmbr.69.4.585-607.2005

Sedlazeck FJ, Rescheneder P, Smolka M, Fang H, Nattestad M, von Haeseler A, Schatz MC. 2018. Accurate detection of complex structural variations using single-molecule sequencing. *Nature Methods* **15**:461–468. doi:10.1038/s41592-018-0001-7

Seemann T. 2019. GitHub - tseemann/barrnap: Bacterial ribosomal RNA predictor. *GitHub*. https://github.com/tseemann/barrnap

Seemann T. 2014. Prokka: Rapid prokaryotic genome annotation. *Bioinformatics* **30**:2068–2069. doi:10.1093/bioinformatics/btu153

Shak JR, Vidal JE, Klugman KP. 2013. Influence of bacterial interactions on pneumococcal colonization of the nasopharynx. *Trends Microbiol* **21**:129–35. doi:10.1016/j.tim.2012.11.005

Shockley TE, Hotchkiss RD. 1970. Stepwise introduction of transformable penicillin resistance in Pneumococcus. *Genetics* **64**:397–408. doi:10.1093/genetics/64.3-4.397

Sibold C, Henrichsen J, König A, Martin C, Chalkley L, Hakenbeck R. 1994. Mosaic pbpX genes of major clones of penicillin-resistant *Streptococcus pneumoniae* have evolved from *pbpX* genes of a penicillin-sensitive *Streptococcus oralis*. *Molecular Microbiology* **12**:1013–1023. doi:10.1111/j.1365-2958.1994.tb01089.x

Slager J, Aprianto R, Veening JW. 2019. Refining the pneumococcal competence regulon by RNA sequencing. *Journal of Bacteriology* **201**:e00780-18. doi:10.1128/JB.00780-18

Slager J, Aprianto R, Veening JW. 2018. Deep genome annotation of the opportunistic human pathogen *Streptococcus pneumoniae* D39. *Nucleic Acids Research* **46**:9971–9989. doi:10.1093/nar/gky725

Slager J, Kjos M, Attaiech L, Veening JW. 2014. Antibiotic-induced replication stress triggers bacterial competence by increasing gene dosage near the origin. *Cell* **157**:395–406. doi:10.1016/j.cell.2014.01.068

Smith AM, Klugman KP. 2001. Alterations in MurM, a cell wall muropeptide branching enzyme, increase high-level penicillin and cephalosporin resistance in *Streptococcus pneumoniae*. *Antimicrobial Agents and Chemotherapy* **45**:2393–2396. doi:10.1128/AAC.45.8.2393-2396.2001

Stanhope MJ, Lefébure T, Walsh SL, Becker JA, Lang P, Pavinski Bitar PD, Miller LA, Italia MJ, Amrine-Madsen H. 2008. Positive selection in penicillin-binding proteins 1a, 2b, and 2x from *Streptococcus pneumoniae* and its correlation with amoxicillin resistance development. *Infection, Genetics and Evolution* **8**:331–339. doi:10.1016/J.MEEGID.2008.02.001

Stanhope MJ, Walsh SL, Becker JA, Miller LA, Lefébure T, Lang P, Bitar PDP, Amrine-Madsen H. 2007. The relative frequency of intraspecific lateral gene transfer of penicillin binding proteins 1a, 2b, and 2x, in amoxicillin resistant *Streptococcus pneumoniae*. *Infection, Genetics and Evolution* **7**:520–534. doi:10.1016/J.MEEGID.2007.03.004

Straume D, Stamsås GA, Håvarstein LS. 2015. Natural transformation and genome evolution in *Streptococcus pneumoniae*. *Infection, Genetics and Evolution* **33**:371–380. doi:10.1016/j.meegid.2014.10.020

Torres R, Serrano E, Alonso JC. 2019. Bacillus subtilis RecA interacts with and loads RadA/Sms to unwind recombination intermediates during natural chromosomal transformation. *Nucleic Acids Research* **47**:9198–9215. doi:10.1093/nar/gkz647

Trzciński K, Thompson CM, Lipsitch M. 2004. Single-step capsular transformation and acquisition of penicillin resistance in *Streptococcus pneumoniae*. *Journal of Bacteriology* **186**:3447–3452. doi:10.1128/JB.186.11.3447-3452.2004

Walker BJ, Abeel T, Shea T, Priest M, Abouelliel A, Sakthikumar S, Cuomo CA, Zeng Q, Wortman J, Young SK, Earl AM. 2014. Pilon: An integrated tool for comprehensive microbial variant detection and genome assembly improvement. *PLoS ONE* **9**:e112963. doi:10.1371/journal.pone.0112963

Wang H, Marcišauskas S, Sánchez BJ, Domenzain I, Hermansson D, Agren R, Nielsen J, Kerkhoven EJ. 2018. RAVEN 2.0: A versatile toolbox for metabolic network reconstruction and a case study on Streptomyces coelicolor. *PLoS Computational Biology* **14**:e1006541. doi:10.1371/journal.pcbi.1006541

Ween O, Gaustad P, Håvarstein LS. 1999. Identification of DNA binding sites for ComE, a key regulator of natural competence in *Streptococcus pneumoniae*. *Molecular Microbiology* **33**:817–827. doi:10.1046/j.1365-2958.1999.01528.x

Weng L, Piotrowski A, Morrison DA. 2013. Exit from Competence for Genetic Transformation in *Streptococcus pneumoniae* Is Regulated at Multiple Levels. *PLoS ONE* **8**:e64197. doi:10.1371/journal.pone.0064197

Wick R. 2017. rrwick/Filtlong: quality filtering tool for long reads. *GitHub*. https://github.com/rrwick/Filtlong

Wick RR, Judd LM, Cerdeira LT, Hawkey J, Méric G, Vezina B, Wyres KL, Holt KE. 2021. Trycycler: consensus long-read assemblies for bacterial genomes. *Genome Biology* **22**:1–17. doi:10.1186/s13059-021-02483-z

Wiktor J, Gynnå AH, Leroy P, Larsson J, Coceano G, Testa I, Elf J. 2021. RecA finds homologous DNA by reduced dimensionality search. *Nature* **597**:426–429. doi:10.1038/s41586-021-03877-6

Wyres KL, Lambertsen LM, Croucher NJ, McGee L, von Gottberg A, Liñares J, Jacobs MR, Kristinsson KG, Beall BW, Klugman KP, Parkhill J, Hakenbeck R, Bentley SD, Brueggemann AB. 2013. Pneumococcal capsular switching: A historical perspective. *Journal of Infectious Diseases* **207**:439–449. doi:10.1093/infdis/jis703

Wyres KL, Lambertsen LM, Croucher NJ, McGee L, von Gottberg A, Liñares J, Jacobs MR, Kristinsson KG, Beall BW, Klugman KP, Parkhill J, Hakenbeck R, Bentley SD, Brueggemann AB. 2012. The multidrug-resistant PMEN1 pneumococcus is a paradigm for genetic success. *Genome Biology* **13**:R103. doi:10.1186/gb-2012-13-11-r103

Yang H, Zhou C, Dhar A, Pavletich NP. 2020. Mechanism of strand exchange from RecA–DNA synaptic and D-loop structures. *Nature* **586**:801–806. doi:10.1038/s41586-020-2820-9

Zhao G, Meier TI, Kahl SD, Gee KR, Blaszczak LC. 1999. BOCILLIN FL, a sensitive and commercially available reagent for detection of penicillin-binding proteins. *Antimicrobial Agents and Chemotherapy* **43**:1124–1128. doi:10.1128/aac.43.5.1124

## Supplementary Figures

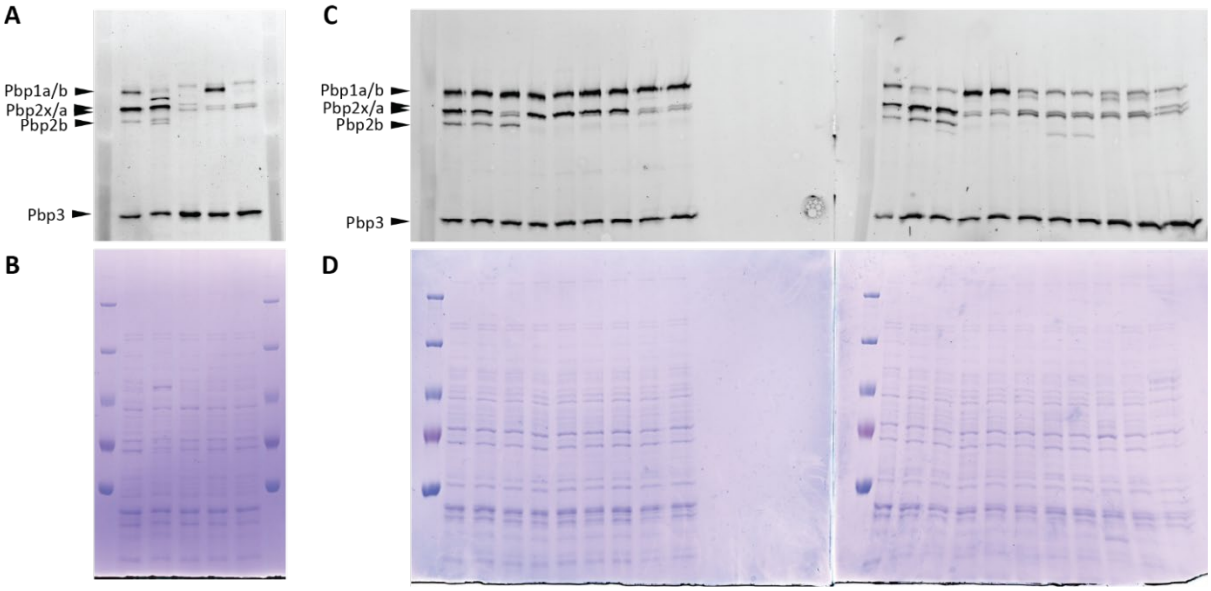


**Figure S1: Fluorescence and coomassie stained images of Bocillin-FL gels**. (A) Bocillin-FL labelled cell extracts imaged in an Amersham Typhoon with Cy2 filter setup showing PBP binding affinities, from Figure 3. (B) Coomassie stain of Bocillin-FL gel from Figure 3. (C) Bocillin-FL labelled cell extracts imaged in an Amersham Typhoon Cy2 filter setup from Figure 8. (D) Coomassie stain of Bocillin-FL gel from Figure 8.

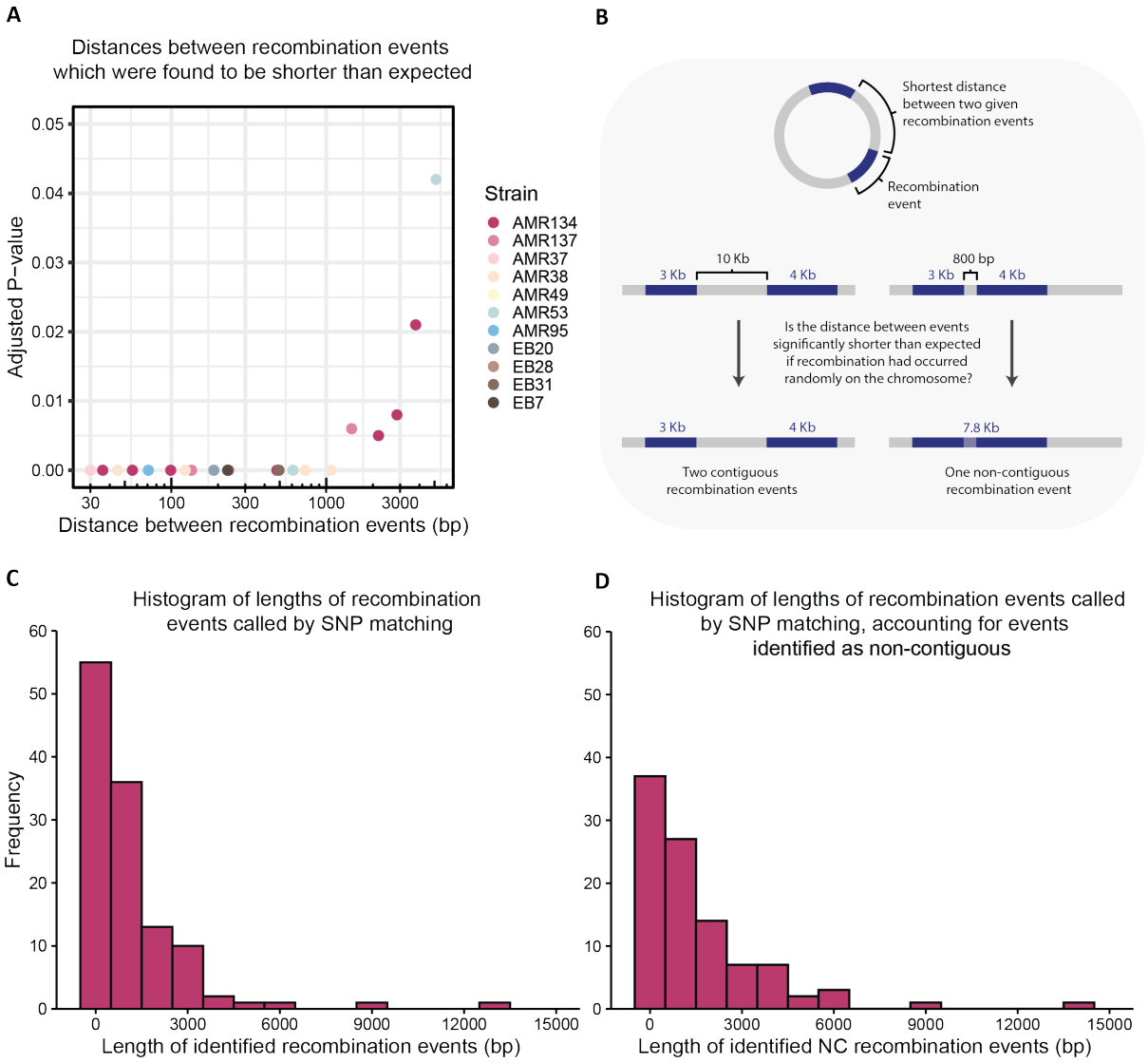


**Figure S2: Identification of non-contiguous recombination from sequenced recombinant strains using a bootstrapping method** (Croucher et al. 2012). (A) Distances between recombination events which were found to shorter than expected under a null hypothesis where events occur randomly around the chromosome. (B) Schematic showing how events were treated if they were found to be closer to each other than expected. (C) Histogram of recombination events length across all sequenced recombinant strains if non-contiguous recombination is not taken into account. (D) Histogram of recombination events length across all sequenced recombinant strains if non-contiguous recombination is accounted for.

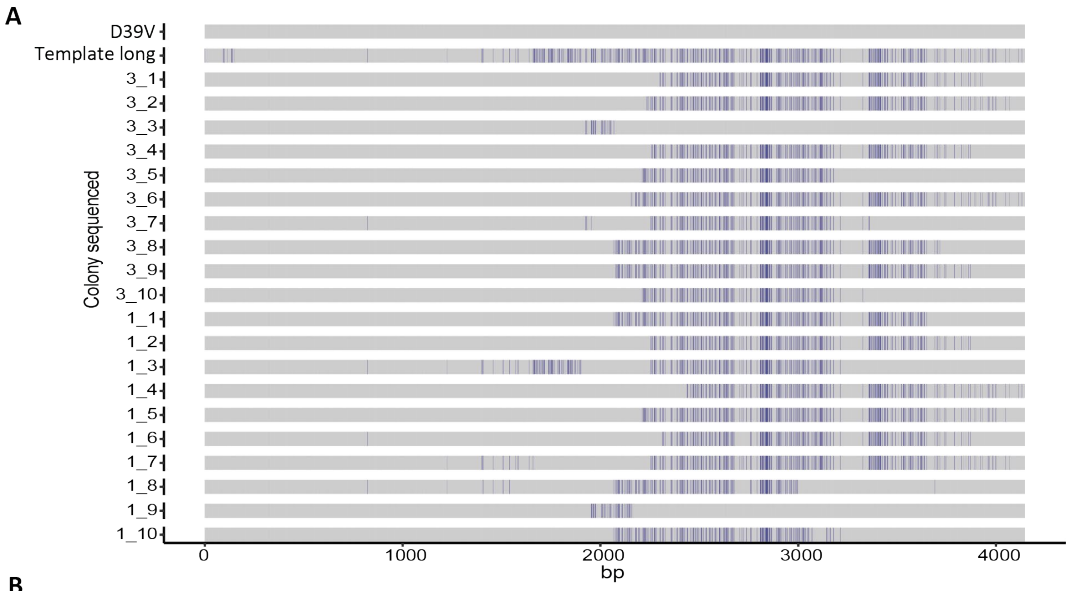
A
D39V
Template long
3_1
3_2
3_3
3_4
3_5
3_6
3_7
3_8
3_9
3_10
1_1
1_2
1_3
1_4
1_5
1_6
1_7
1_8
1_9
1_10
Colony sequenced
0
1000
2000
3000
4000
bp

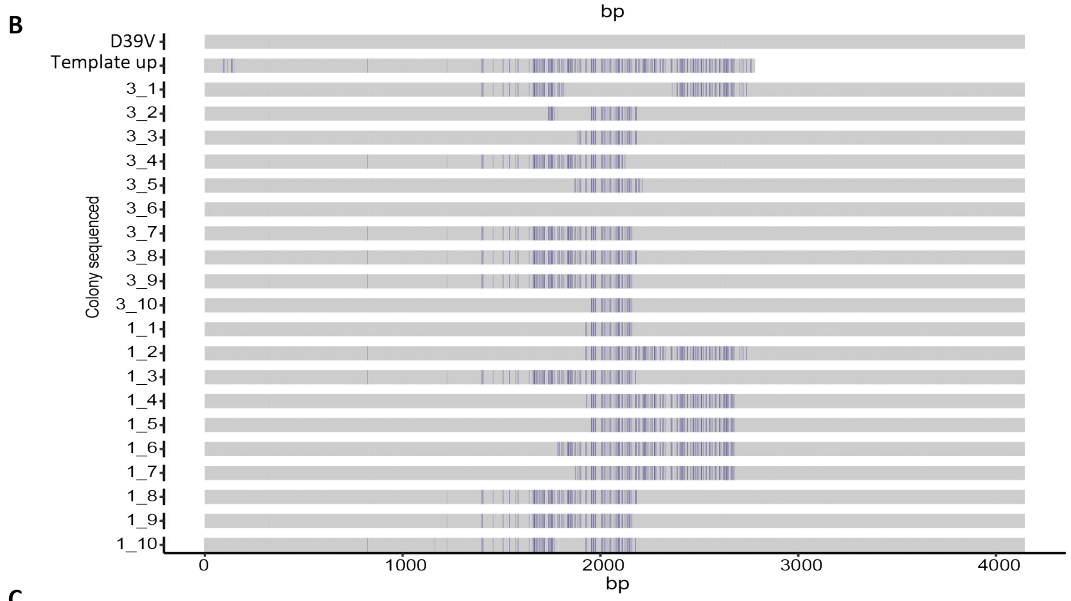
B
D39V
Template up
3_1
3_2
3_3
3_4
3_5
3_6
3_7
3_8
3_9
3_10
1_1
1_2
1_3
1_4
1_5
1_6
1_7
1_8
1_9
1_10
Colony sequenced
0
1000
2000
3000
4000
bp

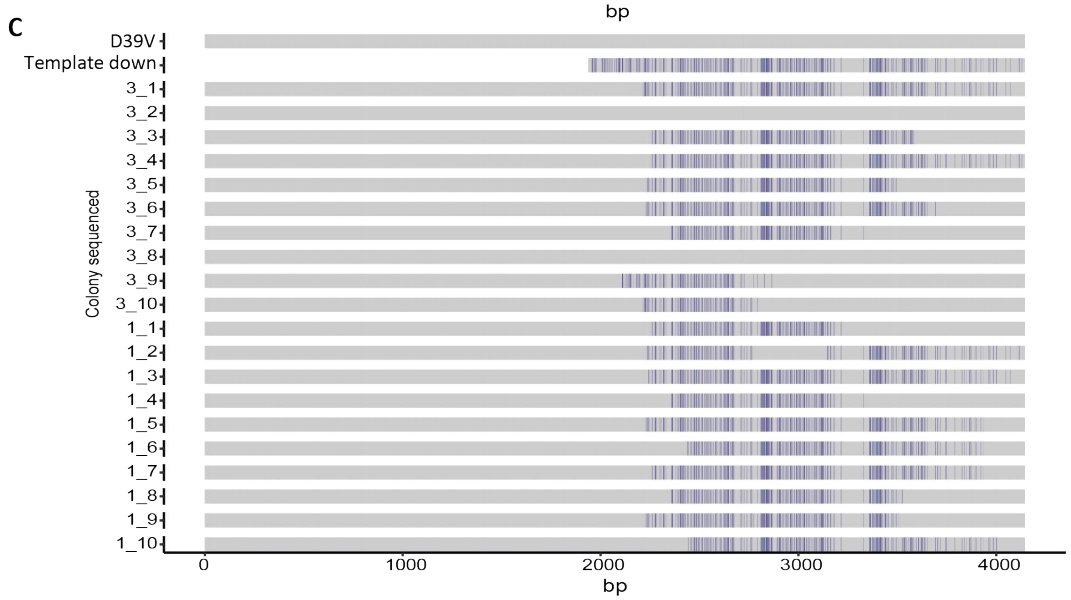
C
D39V
Template down
3_1
3_2
3_3
3_4
3_5
3_6
3_7
3_8
3_9
3_10
1_1
1_2
1_3
1_4
1_5
1_6
1_7
1_8
1_9
1_10
Colony sequenced
0
1000
2000
3000
4000
bp

**D**

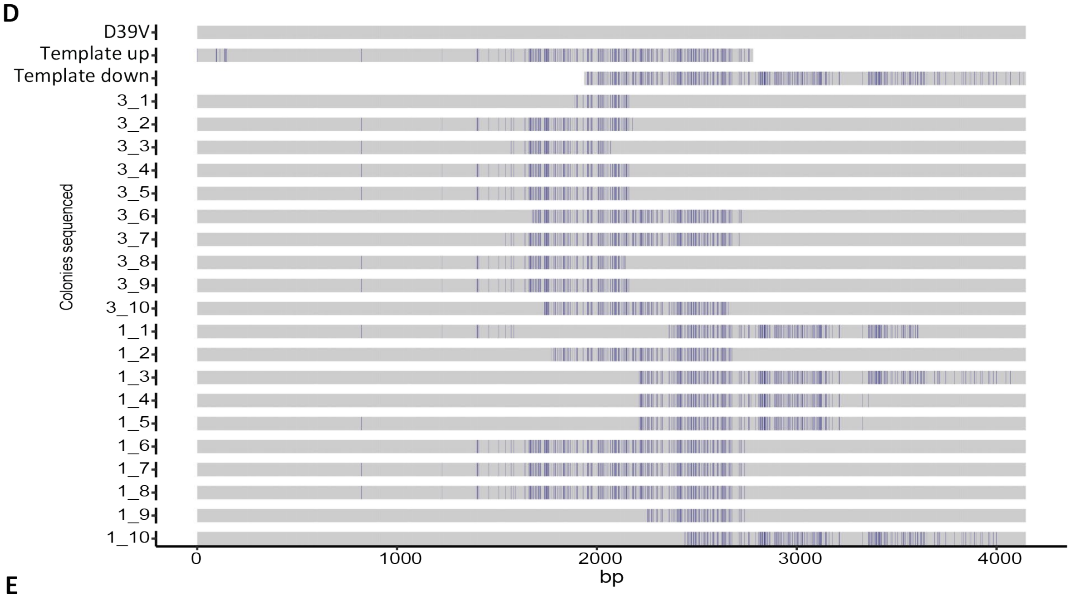
D39V
Template up
Template down
3_1
3_2
3_3
3_4
3_5
3_6
3_7
3_8
3_9
3_10
1_1
1_2
1_3
1_4
1_5
1_6
1_7
1_8
1_9
1_10
Colonies sequenced
0
1000
2000
3000
4000
bp

**E**

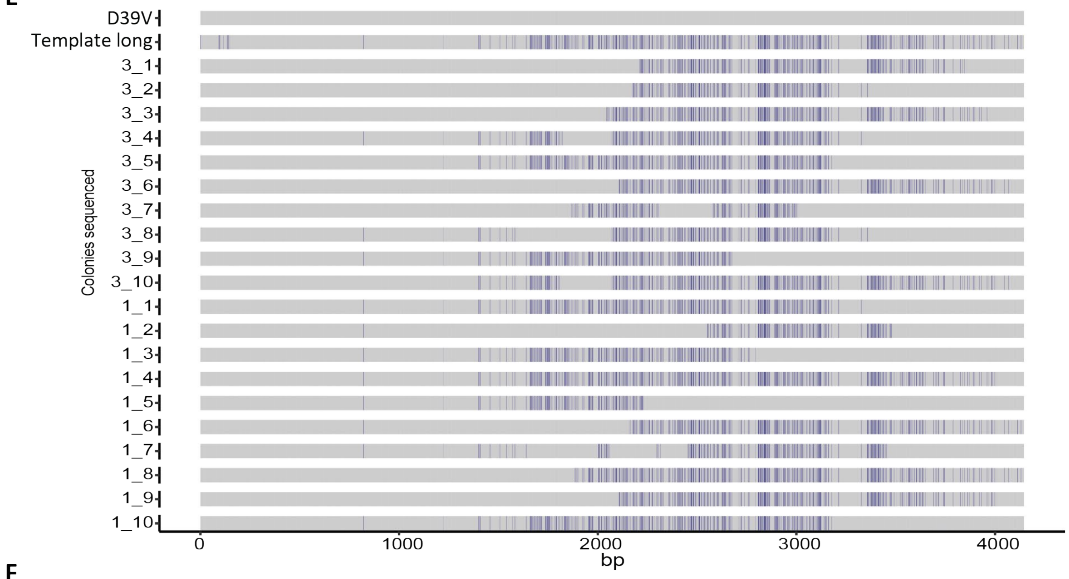
D39V
Template long
3_1
3_2
3_3
3_4
3_5
3_6
3_7
3_8
3_9
3_10
1_1
1_2
1_3
1_4
1_5
1_6
1_7
1_8
1_9
1_10
Colonies sequenced
0
1000
2000
3000
4000
bp

**F**

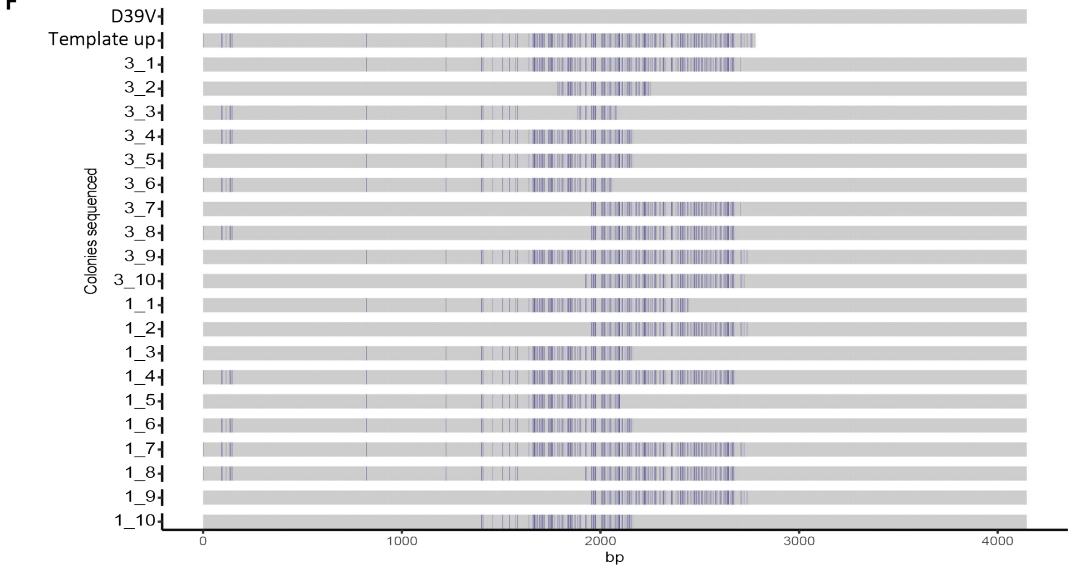
D39V
Template up
3_1
3_2
3_3
3_4
3_5
3_6
3_7
3_8
3_9
3_10
1_1
1_2
1_3
1_4
1_5
1_6
1_7
1_8
1_9
1_10
Colonies sequenced
0
1000
2000
3000
4000
bp

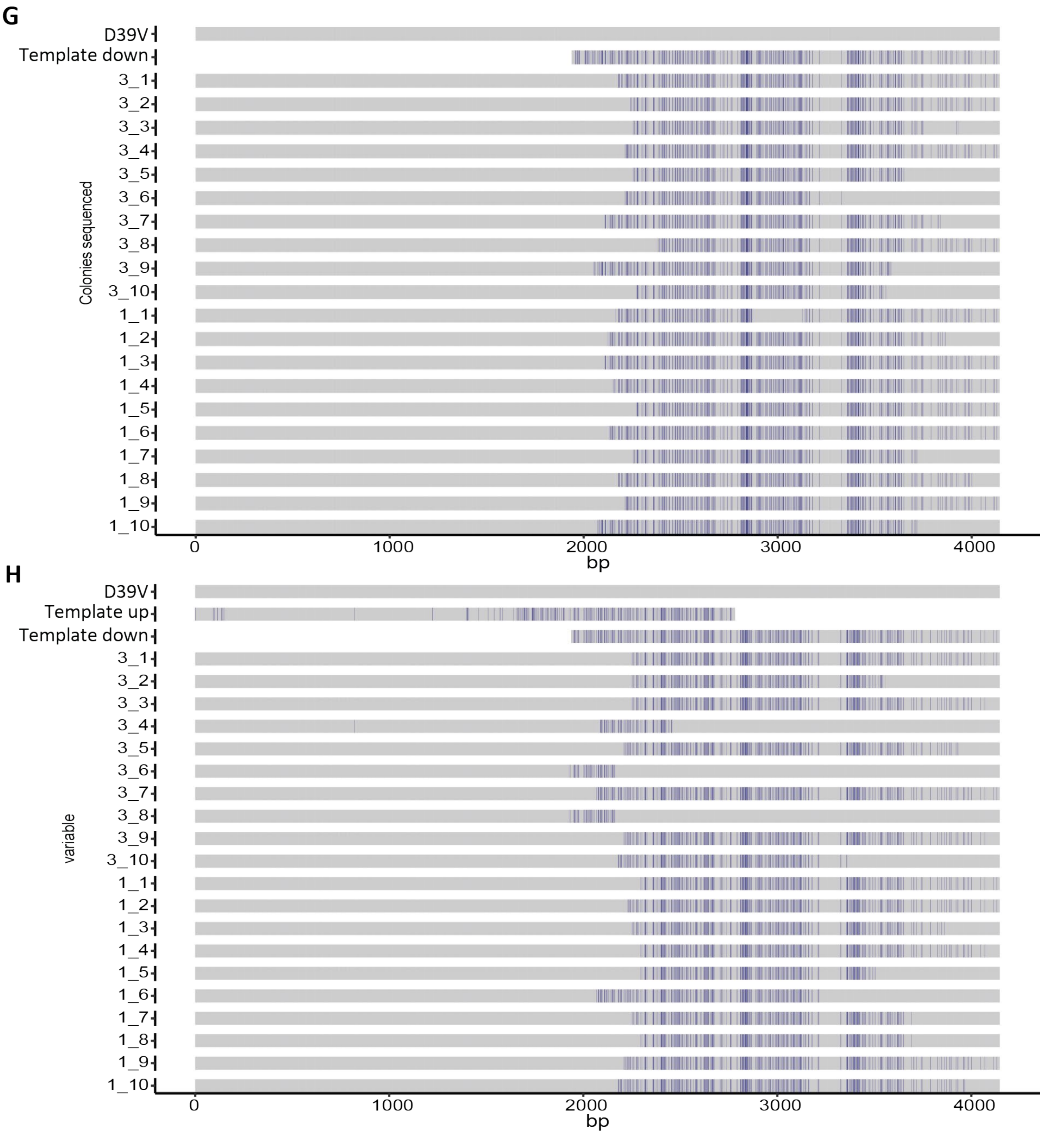


**Figure S3: Alignments of pbp2x-mraY from colonies isolated after transformation with different length and combinations of donor fragments to explain the occurrence of non-contiguous recombination.** Facets show colonies selected from different donor templates which correspond to Figure 6. Bases which match the recipient (D39V) are coloured grey, those which match the donor (11A) are shown in blue. (A) Long, (B) Up, (C) Down, (D) Up & Down, (E) Long-NH, (F) NH-Up, (G) Down-NH, and (H) NH-Up and Down-NH.

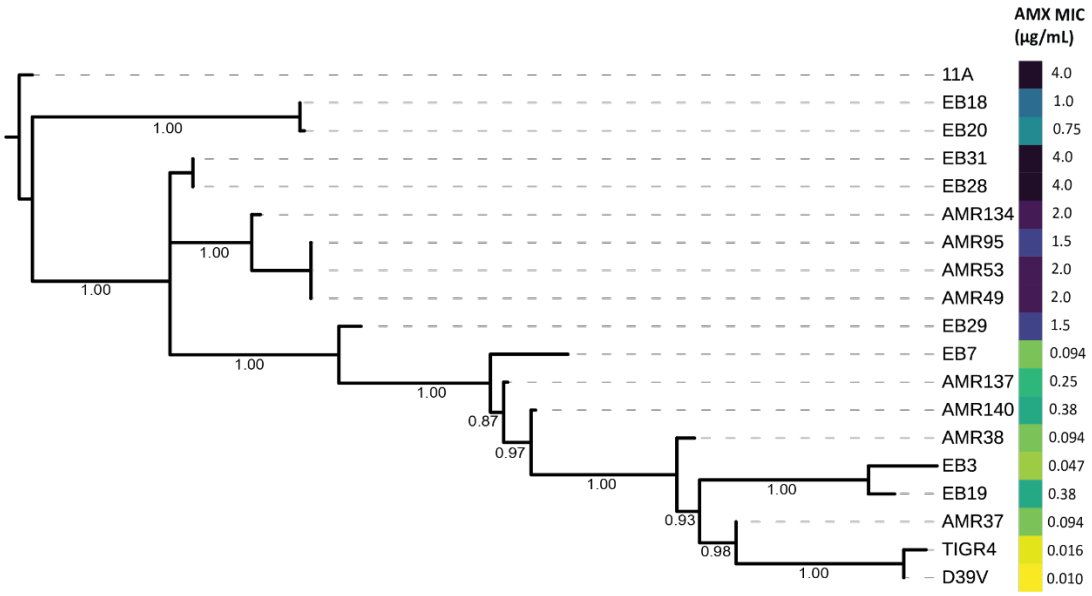


**Figure S4: Dendrogram of strain relationships built from amino acid sequences of Pbp and murM proteins**. Alignments of Pbp1a, Pbp2b, Pbp2x, and MurM amino acid sequences were used to construct a phylogenetic tree of donor, recipient, and recombinant strains. AMX MICs are shown on the right, colour scale represents MIC and corresponds to figure 2, where yellow is an AMX MIC of 0.01 µg/mL and dark purple is an MIC of 4 µg/mL.

## Supplementary Tables

**Table S1**: **Recombinant strains isolated in sequential rounds of transformation with AMX resistant DNA and their associated MICs**.

| Strain number | Parental strain | Generation | AMX MIC (μg/mL) |
|---|---|---|---|
| AMR34 | D39 | 1 | 0.094 |
| AMR35 | D39 | 1 | 0.064 |
| AMR36 | D39 | 1 | 0.125 |
| AMR37 | D39 | 1 | 0.094 |
| AMR38 | D39 | 1 | 0.094 |
| AMR39 | D39 | 1 | 0.094 |
| AMR40 | D39 | 1 | 0.094 |
| AMR41 | D39 | 1 | 0.094 |
| AMR42 | D39 | 1 | 0.047 |
| AMR43 | D39 | 1 | 0.064 |
| AMR44 | AMR34 | 2 | 1.5 |
| AMR45 | AMR34 | 2 | 1 |
| AMR46 | AMR34 | 2 | 2 |
| AMR47 | AMR34 | 2 | 2 |
| AMR48 | AMR34 | 2 | 2 |
| AMR49 | AMR38 | 2 | 2 |
| AMR50 | AMR38 | 2 | 2 |
| AMR51 | AMR38 | 2 | 1.5 |
| AMR52 | AMR38 | 2 | 1.5 |
| AMR53 | AMR38 | 2 | 2 |
| AMR54 | AMR40 | 2 | 2 |
| AMR55 | AMR41 | 2 | 2 |
| AMR56 | AMR41 | 2 | 2 |
| AMR57 | AMR41 | 2 | 2 |
| AMR58 | AMR41 | 2 | 1.5 |
| AMR59 | AMR41 | 2 | 1.5 |
| AMR60 | AMR41 | 2 | 2 |
| AMR61 | AMR41 | 2 | 2 |
| AMR62 | AMR41 | 2 | 2 |
| AMR63 | AMR41 | 2 | 2 |
| AMR64 | AMR41 | 2 | 2 |
| AMR65 | AMR43 | 2 | 1.5 |
| AMR66 | AMR34 | 2 | 2 |
| AMR67 | AMR34 | 2 | 1.5 |
| AMR68 | AMR34 | 2 | 2 |
| AMR69 | AMR34 | 2 | 1.5 |
| AMR70 | AMR34 | 2 | 2 |
| AMR71 | AMR35 | 2 | 1 |
| AMR72 | AMR35 | 2 | 0.75 |
| AMR73 | AMR35 | 2 | 1 |

| | | | |
|---|---|---|---|
| AMR74 | AMR35 | 2 | 0.5 |
| AMR75 | AMR35 | 2 | 0.75 |
| AMR76 | AMR35 | 2 | 1 |
| AMR77 | AMR35 | 2 | 0.75 |
| AMR78 | AMR35 | 2 | 0.75 |
| AMR79 | AMR35 | 2 | 1.5 |
| AMR80 | AMR35 | 2 | 0.75 |
| AMR81 | AMR36 | 2 | 1.5 |
| AMR82 | AMR36 | 2 | 1 |
| AMR83 | AMR36 | 2 | 1 |
| AMR84 | AMR36 | 2 | 2 |
| AMR85 | AMR36 | 2 | 2 |
| AMR86 | AMR36 | 2 | 1.5 |
| AMR87 | AMR36 | 2 | 2 |
| AMR88 | AMR36 | 2 | 2 |
| AMR89 | AMR36 | 2 | 1 |
| AMR90 | AMR36 | 2 | 1.5 |
| AMR91 | AMR38 | 2 | 2 |
| AMR92 | AMR38 | 2 | 2 |
| AMR93 | AMR38 | 2 | 2 |
| AMR94 | AMR38 | 2 | 2 |
| AMR95 | AMR38 | 2 | 1.5 |
| AMR96 | AMR39 | 2 | 0.75 |
| AMR97 | AMR39 | 2 | 1 |
| AMR98 | AMR39 | 2 | 0.5 |
| AMR99 | AMR39 | 2 | 1 |
| AMR100 | AMR39 | 2 | 2 |
| AMR101 | AMR39 | 2 | 1 |
| AMR102 | AMR39 | 2 | 1.5 |
| AMR103 | AMR39 | 2 | 1.5 |
| AMR104 | AMR39 | 2 | 0.75 |
| AMR105 | AMR39 | 2 | 0.75 |
| AMR106 | AMR40 | 2 | 1.5 |
| AMR107 | AMR40 | 2 | 1 |
| AMR108 | AMR40 | 2 | 1.5 |
| AMR109 | AMR40 | 2 | 1.5 |
| AMR110 | AMR40 | 2 | 2 |
| AMR111 | AMR40 | 2 | 0.75 |
| AMR112 | AMR40 | 2 | 2 |
| AMR113 | AMR40 | 2 | 2 |
| AMR114 | AMR40 | 2 | 2 |
| AMR115 | AMR42 | 2 | 1 |
| AMR116 | AMR42 | 2 | 1.5 |
| AMR117 | AMR42 | 2 | 1 |
| AMR118 | AMR42 | 2 | 0.75 |
| AMR119 | AMR42 | 2 | 1 |

| | | | |
|---|---|---|---|
| AMR120 | AMR42 | 2 | 1 |
| AMR121 | AMR42 | 2 | 1.5 |
| AMR122 | AMR42 | 2 | 1 |
| AMR123 | AMR42 | 2 | 1.5 |
| AMR124 | AMR42 | 2 | 1 |
| AMR125 | AMR43 | 2 | 0.75 |
| AMR126 | AMR43 | 2 | 1 |
| AMR127 | AMR43 | 2 | 1 |
| AMR128 | AMR43 | 2 | 1 |
| AMR129 | AMR43 | 2 | 1 |
| AMR130 | AMR43 | 2 | 1.5 |
| AMR131 | AMR43 | 2 | 1.5 |
| AMR132 | AMR43 | 2 | 1.5 |
| AMR133 | AMR43 | 2 | 1 |
| AMR134 | AMR37 | 2 | 2 |
| AMR135 | AMR37 | 2 | 0.38 |
| AMR136 | AMR37 | 2 | 0.38 |
| AMR137 | AMR37 | 2 | 0.25 |
| AMR138 | AMR37 | 2 | 0.38 |
| AMR139 | AMR37 | 2 | 0.5 |
| AMR140 | AMR37 | 2 | 0.38 |
| AMR141 | AMR37 | 2 | 0.5 |
| AMR142 | AMR37 | 2 | 0.38 |
| AMR143 | AMR37 | 2 | 0.38 |
| EB1 | TIGR4 | 1 | 0.5 |
| EB2 | TIGR4 | 1 | 0.023 |
| EB3 | TIGR4 | 1 | 0.047 |
| EB4 | TIGR4 | 1 | 0.023 |
| EB5 | TIGR4 | 1 | 0.125 |
| EB6 | TIGR4 | 1 | 0.047 |
| EB7 | TIGR4 | 1 | 0.094 |
| EB8 | TIGR4 | 1 | 0.064 |
| EB9 | TIGR4 | 1 | 0.047 |
| EB10 | TIGR4 | 1 | 0.064 |
| EB11 | TIGR4 | 1 | 0.032 |
| EB12 | EB1 | 2 | 1.5 |
| EB13 | EB1 | 2 | 1.5 |
| EB14 | EB1 | 2 | 1.5 |
| EB15 | EB1 | 2 | 2 |
| EB16 | EB1 | 2 | 2 |
| EB17 | EB3 | 2 | 0.125 |
| EB18 | EB3 | 2 | 1 |
| EB19 | EB3 | 2 | 0.38 |
| EB20 | EB3 | 2 | 0.75 |
| EB21 | EB3 | 2 | 0.5 |
| EB22 | EB5 | 2 | 2 |

| | | | |
|---|---|---|---|
| EB23 | EB5 | 2 | 1.5 |
| EB24 | EB5 | 2 | 2 |
| EB25 | EB5 | 2 | 1.5 |
| EB26 | EB5 | 2 | 2 |
| EB27 | EB7 | 2 | 1.5 |
| EB28 | EB7 | 2 | 4 |
| EB29 | EB7 | 2 | 1.5 |
| EB30 | EB7 | 2 | 4 |
| EB31 | EB7 | 2 | 4 |
| EB32 | EB8 | 2 | 0.25 |
| EB33 | EB8 | 2 | 1 |
| EB34 | EB8 | 2 | 1 |
| EB35 | EB8 | 2 | 0.75 |
| EB36 | EB8 | 2 | 1 |

**Table S2**: **Primers used in this study.**

| **Primers to amplify *pbp* alleles in *S. pneumoniae*** | | |
|---|---|---|
| **Primer name** | **5'-3' sequence** | **Description** |
| OVL1814 | GCAGACCAAGCTCTTGCAAGTGCAGAATG | Forward primer to amplify *pbp2x* |
| OVL1815 | GCTGTTTGACATCCTCATGCATCTGCTGGCCTG | Reverse primer to amplify *pbp2x* |
| OVL1086 | TACCGTCGTCTCGCATAATTTCCTTTCTAATTCATTGGATG | Forward primer to amplify *pbp2b* |
| OVL540 | CAGTAGATCTAGGAGGTTAGAAATGAGACTGATTTGTATGAG | Reverse primer to amplify *pbp2b* |
| OVL5542 | GCCAAGGCGAGCATCACTG | Forward primer to amplify *pbp1a* |
| OVL5543 | CCAACGACAGCCTCAAGCCC | Reverse primer to amplify *pbp1a* |
| **Primers to amplify *murM* alleles flanked by D39V homologous regions in *S. pneumoniae*** | | |
| **Primer name** | **5'-3' sequence** | **Description** |
| OVL5540 | GTGATTCGGCCAATGCAG | Forward primer for upstream homologous region from D39V |
| OVL5779 | GGTTTCCGTCTCCTTTCCTACTCTCTTTCCTCCAG | Reverse primer for upstream homologous region from D39V, with BsmBI cut site |
| OVL5777 | GGTTTCCGTCTCCGAAATGTACCGTTATCAAATTGG | Forward primer for *murM* allele from AMR53 and AMR95, with BsmBI cut site |
| OVL5778 | GGTTTCCGTCTCCACTTACTTTCTATGTTTTTTTC | Reverse primer for *murM* allele from AMR53 and AMR95, with BsmBI cut site |
| OVL5780 | GGTTTCCGTCTCCAAGTATATGGCACTAACAACACTC | Forward primer for downstream homologous region from D39V, with BsmBI cut site |
| OVL5541 | GGAGTAGCCATAGTATGG | Reverse primer for downstream homologous region from D39V |
| **Primers to amplify fragments for cloning a kanamycin resistance casette behind *pbp1a* in *S. pneumoniae*** | | |
| **Primer name** | **5'-3' sequence** | **Description** |

| | | |
|---|---|---|
| OVL848 | CTTGTTGTGACAGATGAGTCTGGCAAG | Forward primer for upstream homology |
| OVL849 | GGAAGTCGTCTCCTTCATTTATCATCCAGA TTTTTCTGG | Reverse primer for upstream homology with BsmBI recognition site |
| OVL850 | GGAAGTCGTCTCCTGAAACAATTCATCCAG TAAAATAT AATATTTT | Forward primer for *kan*$^R$ with BsmBI recognition site |
| OVL851 | GGAAGTCGTCTCCAATGGCTAAAATGAGA ATATCACC | Reverse primer for *kan*$^R$ with BsmBI recognition site |
| OVL852 | GGAAGTCGTCTCGCATTTATGGTTGTGCTG GTTGA | Forward primer for downstream homology with BsmBI recognition site |
| OVL853 | CTGCGCCTAATCAAGTATCTGAGCATTAGC | Reverse primer for downstream homology |
| **Primers to amplify fragments for detemining recombination dynamics in *S. pneumoniae* and *E. coli*** | | |
| **Primer name** | **5'-3' sequence** | **Description** |
| OVL5375 | GTGTTCAGGAAATTGATGG | Forward primer for long donor DNA fragment |
| OVL5376 | GTAACTATGAGCCAGG | Forward primer for short (downstream) donor DNA fragment |
| OVL5378 | CATCAGGGTGCCATTC | Reverse primer for long donor DNA fragment |
| OVL5379 | CTGAAGCCCGCTCCAAG | Reverse primer for short (upstream) donor DNA fragment |
| OVL5557 | ATCCGACGTCTCGGGCATCAGGGTGCCA TTCTTAC | Reverse primer for long donor DNA fragment, with BsmBI recognition site for ligation to non-homologous DNA |
| OVL5558 | ATCCGACGTCTCCTGCCAATGGCATGGAA TCG | Forward primer for non-homologous DNA fragment, with BsmBI recognition site for ligation to donor DNA |
| OVL5559 | CGTTGGTAAGACAACCTCCAGCGC | Forward primer for non-homologous DNA fragment |
| OVL5560 | CATCTCCGTCTCGTACGTGTTCAGGAAATT GATGG | Forward primer for short (upstream) donor DNA fragment, with BsmBI recognition site for ligation to non-homologous DNA |
| OVL5561 | CGAAGTAACAACAATAATGCGTGC | Forward primer for non-homologous DNA fragment (short, upstream) |
| OVL5562 | CATCTCCGTCTCCCGTAAATTCCGCCGCGGG | Reverse primer for non-homologous DNA fragment (short, upstream), with BsmBI recognition site for ligation to donor DNA |
| OVL5563 | CAGTAGCGTCTCCTGCCGTCGATACCCGCA GTATATATCG | Forward primer for non-homologous DNA fragment (short, downstream), with BsmBI recognition site for ligation to donor DNA |
| OVL5564 | CGATACGATTACGATAC | Reverse primer for non-homologous DNA fragment (short, downstream) |

**Table S3**: **List of all recombination events identified in transformants using SNPs.**

| Strain | Event Number | Unique_ID | Start | End | Length |
|---|---|---|---|---|---|
| AMR134 | 1 | AMR134_1 | 354,799 | 354,808 | 10 |
| AMR134 | 2 | AMR134_2 | 354,907 | 355,727 | 821 |
| AMR134 | 3 | AMR134_3 | 358,589 | 359,725 | 1,137 |
| AMR134 | 4 | AMR134_4 | 386,356 | 390,350 | 3,995 |
| AMR134 | 5 | AMR134_5 | 461,315 | 462,935 | 1,621 |
| AMR134 | 6 | AMR134_6 | 609,019 | 609,046 | 28 |
| AMR134 | 7 | AMR134_7 | 609,082 | 609,221 | 140 |
| AMR134 | 8 | AMR134_8 | 609,277 | 611,459 | 2,183 |
| AMR134 | 9 | AMR134_9 | 714,881 | 715,473 | 593 |
| AMR134 | 10 | AMR134_10 | 909,342 | 911,190 | 1,849 |
| AMR134 | 11 | AMR134_11 | 911,670 | 913,539 | 1,870 |
| AMR134 | 12 | AMR134_12 | 1,163,261 | 1,163,793 | 533 |
| AMR134 | 13 | AMR134_13 | 1,787,417 | 1,789,496 | 2,080 |
| AMR134 | 14 | AMR134_14 | 2,024,320 | 2,024,866 | 547 |
| AMR134 | 15 | AMR134_15 | 2,030,025 | 2,030,172 | 148 |
| AMR134 | 16 | AMR134_16 | 2,032,347 | 2,033,364 | 1,018 |
| AMR137 | 1 | AMR137_1 | 353,399 | 353,399 | 1 |
| AMR137 | 2 | AMR137_2 | 353,534 | 354,622 | 1,089 |
| AMR137 | 3 | AMR137_3 | 354,857 | 355,727 | 871 |
| AMR137 | 4 | AMR137_4 | 556,660 | 557,143 | 484 |
| AMR137 | 5 | AMR137_5 | 609,625 | 615,306 | 5,682 |
| AMR137 | 6 | AMR137_6 | 1,169,879 | 1,170,151 | 273 |
| AMR137 | 7 | AMR137_7 | 1,243,179 | 1,243,450 | 272 |
| AMR137 | 8 | AMR137_8 | 1,311,771 | 1,312,586 | 816 |
| AMR137 | 9 | AMR137_9 | 1,800,852 | 1,800,852 | 1 |
| AMR137 | 10 | AMR137_10 | 1,868,953 | 1,871,228 | 2,276 |
| AMR137 | 11 | AMR137_11 | 2,133,770 | 2,134,278 | 509 |
| AMR140 | 1 | AMR140_1 | 354,220 | 355,660 | 1,441 |
| AMR140 | 2 | AMR140_2 | 519,460 | 520,087 | 628 |
| AMR140 | 3 | AMR140_3 | 608,713 | 610,325 | 1,613 |
| AMR140 | 4 | AMR140_4 | 1,519,415 | 1,519,442 | 28 |
| AMR37 | 1 | AMR37_1 | 244,929 | 244,929 | 1 |
| AMR37 | 2 | AMR37_2 | 355,756 | 356,161 | 406 |
| AMR37 | 3 | AMR37_3 | 362,436 | 363,397 | 962 |
| AMR37 | 4 | AMR37_4 | 614,225 | 614,591 | 367 |
| AMR37 | 5 | AMR37_5 | 1,595,802 | 1,596,469 | 668 |
| AMR37 | 6 | AMR37_6 | 1,596,499 | 1,596,747 | 249 |
| AMR37 | 7 | AMR37_7 | 1,606,184 | 1,608,129 | 1,946 |
| AMR37 | 8 | AMR37_8 | 1,716,569 | 1,716,811 | 243 |
| AMR38 | 1 | AMR38_1 | 149,673 | 152,390 | 2,718 |
| AMR38 | 2 | AMR38_2 | 189,668 | 190,127 | 460 |
| AMR38 | 3 | AMR38_3 | 354,220 | 354,622 | 403 |

| | | | | | |
|---|---|---|---|---|---|
| AMR38 | 4 | AMR38_4 | 355,351 | 355,651 | 301 |
| AMR38 | 5 | AMR38_5 | 355,696 | 356,161 | 466 |
| AMR38 | 6 | AMR38_6 | 1,467,866 | 1,468,148 | 283 |
| AMR38 | 7 | AMR38_7 | 1,530,905 | 1,533,081 | 2,177 |
| AMR38 | 8 | AMR38_8 | 1,595,802 | 1,597,225 | 1,424 |
| AMR38 | 9 | AMR38_9 | 1,597,348 | 1,597,646 | 299 |
| AMR49 | 1 | AMR49_1 | 256,265 | 256,710 | 446 |
| AMR49 | 2 | AMR49_2 | 341,229 | 341,229 | 1 |
| AMR49 | 3 | AMR49_3 | 388,040 | 390,904 | 2,865 |
| AMR49 | 4 | AMR49_4 | 391,514 | 391,654 | 141 |
| AMR49 | 5 | AMR49_5 | 499,430 | 499,430 | 1 |
| AMR49 | 6 | AMR49_6 | 609,304 | 612,216 | 2,913 |
| AMR49 | 7 | AMR49_7 | 750,319 | 750,319 | 1 |
| AMR49 | 8 | AMR49_8 | 813,809 | 814,602 | 794 |
| AMR49 | 9 | AMR49_9 | 841,600 | 841,600 | 1 |
| AMR49 | 10 | AMR49_10 | 947,221 | 947,323 | 103 |
| AMR49 | 11 | AMR49_11 | 1,069,235 | 1,069,877 | 643 |
| AMR49 | 12 | AMR49_12 | 1,184,232 | 1,184,814 | 583 |
| AMR49 | 13 | AMR49_13 | 1,228,734 | 1,228,734 | 1 |
| AMR49 | 14 | AMR49_14 | 1,435,227 | 1,436,164 | 938 |
| AMR49 | 15 | AMR49_15 | 1,575,877 | 1,576,978 | 1,102 |
| AMR49 | 16 | AMR49_16 | 1,756,708 | 1,756,708 | 1 |
| AMR49 | 17 | AMR49_17 | 1,938,647 | 1,939,478 | 832 |
| AMR49 | 18 | AMR49_18 | 1,944,594 | 1,944,911 | 318 |
| AMR49 | 19 | AMR49_19 | 1,954,165 | 1,954,206 | 42 |
| AMR49 | 20 | AMR49_20 | 2,045,640 | 2,046,589 | 950 |
| AMR53 | 1 | AMR53_1 | 256,265 | 256,710 | 446 |
| AMR53 | 2 | AMR53_2 | 341,229 | 341,229 | 1 |
| AMR53 | 3 | AMR53_3 | 388,040 | 390,904 | 2,865 |
| AMR53 | 4 | AMR53_4 | 391,514 | 391,654 | 141 |
| AMR53 | 5 | AMR53_5 | 499,430 | 499,430 | 1 |
| AMR53 | 6 | AMR53_6 | 609,304 | 612,216 | 2,913 |
| AMR53 | 7 | AMR53_7 | 750,319 | 750,319 | 1 |
| AMR53 | 8 | AMR53_8 | 813,809 | 814,602 | 794 |
| AMR53 | 9 | AMR53_9 | 841,600 | 841,600 | 1 |
| AMR53 | 10 | AMR53_10 | 947,221 | 947,323 | 103 |
| AMR53 | 11 | AMR53_11 | 1,069,235 | 1,069,877 | 643 |
| AMR53 | 12 | AMR53_12 | 1,184,232 | 1,184,814 | 583 |
| AMR53 | 13 | AMR53_13 | 1,228,734 | 1,228,734 | 1 |
| AMR53 | 14 | AMR53_14 | 1,435,227 | 1,436,164 | 938 |
| AMR53 | 15 | AMR53_15 | 1,575,877 | 1,576,978 | 1,102 |
| AMR53 | 16 | AMR53_16 | 1,756,708 | 1,756,708 | 1 |
| AMR53 | 17 | AMR53_17 | 1,938,647 | 1,939,478 | 832 |
| AMR53 | 18 | AMR53_18 | 1,944,594 | 1,944,911 | 318 |
| AMR53 | 19 | AMR53_19 | 1,954,165 | 1,954,206 | 42 |
| AMR53 | 20 | AMR53_20 | 2,045,640 | 2,046,589 | 950 |

| | | | | | |
|---|---|---|---|---|---|
| AMR95 | 1 | AMR95_1 | 202,345 | 202,345 | 1 |
| AMR95 | 2 | AMR95_2 | 282,398 | 282,637 | 240 |
| AMR95 | 3 | AMR95_3 | 328,995 | 329,262 | 268 |
| AMR95 | 4 | AMR95_4 | 388,706 | 390,833 | 2,128 |
| AMR95 | 5 | AMR95_5 | 390,904 | 390,904 | 1 |
| AMR95 | 6 | AMR95_6 | 609,911 | 610,589 | 679 |
| AMR95 | 7 | AMR95_7 | 622,425 | 622,425 | 1 |
| AMR95 | 8 | AMR95_8 | 1,198,176 | 1,198,779 | 604 |
| AMR95 | 9 | AMR95_9 | 1,243,450 | 1,243,450 | 1 |
| AMR95 | 10 | AMR95_10 | 1,534,349 | 1,534,424 | 76 |
| AMR95 | 11 | AMR95_11 | 2,068,094 | 2,070,615 | 2,522 |
| EB3 | 1 | EB3_1 | 35,799 | 36,933 | 1,135 |
| EB3 | 2 | EB3_2 | 125,178 | 128,057 | 2,880 |
| EB3 | 3 | EB3_3 | 355,444 | 360,250 | 4,807 |
| EB7 | 1 | EB7_1 | 354,799 | 356,191 | 1,393 |
| EB7 | 2 | EB7_2 | 602,748 | 615,271 | 12,524 |
| EB7 | 3 | EB7_3 | 615,502 | 616,674 | 1,173 |
| EB18 | 1 | EB18_1 | 388,182 | 391,310 | 3,129 |
| EB18 | 2 | EB18_2 | 1,595,773 | 1,596,817 | 1,045 |
| EB19 | 1 | EB19_1 | 1,401,978 | 1,402,044 | 67 |
| EB19 | 2 | EB19_2 | 1,595,941 | 1,600,237 | 4,297 |
| EB20 | 1 | EB20_1 | 389,212 | 398,477 | 9,266 |
| EB20 | 2 | EB20_2 | 398,665 | 398,665 | 1 |
| EB20 | 3 | EB20_3 | 1,595,668 | 1,596,747 | 1,080 |
| EB28 | 1 | EB28_1 | 387,327 | 390,179 | 2,853 |
| EB28 | 2 | EB28_2 | 390,674 | 390,904 | 231 |
| EB28 | 3 | EB28_3 | 1,594,460 | 1,596,817 | 2,358 |
| EB29 | 1 | EB29_1 | 389,852 | 390,272 | 421 |
| EB29 | 2 | EB29_2 | 1,595,193 | 1,597,357 | 2,165 |
| EB31 | 1 | EB31_1 | 387,327 | 390,179 | 2,853 |
| EB31 | 2 | EB31_2 | 390,674 | 390,904 | 231 |
| EB31 | 3 | EB31_3 | 1,594,460 | 1,596,817 | 2,358 |

**Table S4**: **Summary statistics for the characterisation of SNP and recombination results for sequenced recombinant strains**. (A) All predicted events detected when compared to parent strain genome. Potential non-contiguity not accounted for. (B) Total Dna transferred during the final round of transformation for that strain. (*) All DNA or SNPs transferred into the original recipient (D39V or TIGR4), through one or two rounds of transformation (depending on the generation). SRA accession numbers for raw Illumina and PacBio reads used for analysis are also provided.

| Strain Name | Strain ID | Parent Strain | # recombination events (A) | Total DNA transferred (bp)(B) | Mean length of recombination events (bp) | Standard error of the mean length (SEM, bp) | Number of events longer than 2kb | Number of events longer than 10kb | Number of events predicted to be involved a NCR event | Total DNA transferred (% of donor genome, cumulative)* | # SNPs transferred (cumulative)* | # SNPs transferred (cumulative)*/ total SNPs | Illumina data SRA Accession numbers | PacBio data SRA Accession numbers |
|---|---|---|---|---|---|---|---|---|---|---|---|---|---|---|
| AMR37 | VL4481 | D39V | 8 | 4842 | 605 | 217.48 | 0 | 0 | 2 | 0.23 | 250 | 0.013 | SRR17236832 | - |
| AMR38 | VL4482 | D39V | 9 | 8532 | 948 | 310.01 | 2 | 0 | 5 | 0.4 | 382 | 0.020 | SRR17236837 | SRR17236833 |
| AMR49 | VL4483 | AMR38 | 20 | 12676 | 634 | 192.39 | 4 | 0 | 4 | 0.99 | 815 | 0.042 | SRR17236831 | - |
| AMR53 | VL3196 | AMR38 | 20 | 12574 | 634 | 192.39 | 4 | 0 | 4 | 0.99 | 813 | 0.041 | SRR17236830 | SRR17236829 |
| AMR95 | VL4484 | AMR38 | 11 | 6521 | 593 | 269.41 | 4 | 0 | 2 | 0.7 | 694 | 0.035 | SRR17236856 | SRR17236855 |
| AMR134 | VL4485 | AMR37 | 16 | 18573 | 1161 | 266.27 | 3 | 0 | 9 | 1.09 | 893 | 0.046 | SRR17236854 | - |
| AMR137 | VL4486 | AMR37 | 11 | 12274 | 1116 | 495.64 | 2 | 0 | 3 | 0.8 | 703 | 0.036 | SRR17236853 | - |
| AMR140 | VL4487 | AMR37 | 4 | 3710 | 928 | 368.82 | 0 | 0 | 0 | 0.4 | 525 | 0.027 | SRR17236852 | - |
| EB3 | VL4488 | TIGR4 | 3 | 8822 | 2941 | 1060.45 | 2 | 0 | 0 | 0.41 | 407 | 0.020 | SRR17236851 | - |
| EB7 | VL4489 | TIGR4 | 3 | 15090 | 5030 | 3747.54 | 1 | 1 | 2 | 0.7 | 744 | 0.037 | SRR17236850 | SRR17236849 |
| EB18 | VL4490 | EB3 | 2 | 4175 | 2087 | 1042.00 | 3 | 0 | 0 | 0.6 | 739 | 0.036 | SRR17236848 | - |
| EB19 | VL4491 | EB3 | 2 | 4365 | 2182 | 2115.00 | 3 | 0 | 0 | 0.61 | 711 | 0.035 | SRR17236847 | - |
| EB20 | VL4492 | EB3 | 3 | 10347 | 3449 | 2925.13 | 3 | 0 | 2 | 0.89 | 783 | 0.039 | SRR17236844 | - |
| EB28 | VL4493 | EB7 | 3 | 5,442 | 1814 | 804.30 | 3 | 1 | 2 | 0.95 | 1211 | 0.060 | SRR17236843 | SRR17236842 |
| EB29 | VL4494 | EB7 | 2 | 2,586 | 1293 | 872.00 | 2 | 1 | 0 | 0.82 | 1037 | 0.051 | SRR17236841 | SRR17236840 |
| EB31 | VL4495 | EB7 | 3 | 5,442 | 1814 | 804.30 | 3 | 1 | 2 | 0.95 | 1211 | 0.060 | SRR17236839 | - |

| | Mean total DNA transferred (% of donor genome, cumulative)* | SEM |
|---|---|---|
| Overview D39V derived generation 2 strains | 0.828333333 | 0.103518651 |
| Overview TIGR4 derived generation 2 strains | 0.803333333 | 0.0657098 |

**Table S5**: **Key amino acid substitutions in PBPs and MurM of recombinant strains**. Substitutions listed have been associated with β-lactam resistance in the literature previously. Cells coloured green have the same allele as D39V, those coloured blue have the same allele as 11A. Strain AMX MICs are also indicated for reference.

| | | Pbp2x | | | | | | Pbp2b | | | | | Pbp1a | | | | | | | | MurM | | MurN | | |
|---|---|---|---|---|---|---|---|---|---|---|---|---|---|---|---|---|---|---|---|---|---|---|---|---|---|
| Strain | MIC | 337 – 338 | 389 | 394 – 397 | 514 | 546 – 549 | 605 | 199 | 446 | 476 | 489 | No. substitutions 590-541 | 103 | 351 | 371 | 432 | 512 | 540 | 574-577 | 609 | 101 | Allele source | 142 | 241 | 256 |
| D39V | 0.01 | ST | S | HSSN | N | LKSG | N | D | T | E | T | 0 | T | S | T | P | E | S | TSQF | N | V | D39V | T | D | N |
| TIGR4 | 0.016 | ST | S | HSSN | N | LKSG | N | D | T | E | T | 0 | T | S | T | P | E | T | TSQF | N | A | TIGR4 | T | D | N |
| EB3 | 0.047 | ST | L | HSSN | H | VKSG | T | D | T | E | T | 0 | T | S | T | P | E | T | TSQF | N | A | TIGR4 | T | D | N |
| AMR37 | 0.094 | ST | S | HSSN | H | VKSG | T | D | A | G | A | 0 | T | S | T | P | E | S | TSQF | N | V | D39V | T | D | N |
| AMR38 | 0.094 | SA | L | HSSN | H | VKSG | T | E | A | G | A | 0 | T | S | T | P | E | S | TSQF | N | V | D39V | I | E | K |
| EB7 | 0.094 | SA | L | HSSN | H | VKSG | T | D | T | E | T | 0 | T | S | T | P | E | T | TSQF | N | A | Donor | I | E | K |
| AMR137 | 0.25 | SA | L | HSSN | H | VKSG | T | D | A | G | A | 0 | T | S | T | P | E | S | TSQF | N | A | Donor | T | D | N |
| AMR140 | 0.38 | SA | L | HSSN | H | VKSG | T | D | A | G | A | 0 | T | S | T | P | E | S | TSQF | N | A | Donor* | T | D | N |
| EB19 | 0.38 | ST | L | HSSN | H | VKSG | T | E | A | G | A | 0 | T | S | T | P | E | T | TSQF | N | A | TIGR4 | T | D | N |
| EB20 | 0.75 | ST | L | HSSN | H | VKSG | T | D | A | G | A | 0 | S | A | A | T | K | T | NTGY | D | A | TIGR4 | T | D | N |
| EB18 | 1 | ST | L | HSSN | H | VKSG | T | E | A | G | A | 0 | S | A | A | T | K | T | NTGY | D | A | TIGR4 | T | D | N |
| EB29 | 1.5 | SA | L | HSSN | H | VKSG | T | E | A | G | A | 10 | T | S | T | P | E | T | TSQY | N | A | Donor | I | E | K |
| AMR95 | 1.5 | SA | L | HSSN | H | VKSG | T | E | A | G | A | 0 | S | A | A | T | K | T | NTGY | D | A | Donor | T | D | N |
| AMR134 | 2 | SA | L | HSSN | H | VKSG | T | D | A | G | A | 0 | T | A | A | T | K | T | NTGY | D | A | Donor | I | D | N |
| AMR49 | 2 | SA | L | HSSN | H | VKSG | T | E | A | G | A | 0 | S | A | A | T | K | T | NTGY | D | A | Donor | I | E | K |
| AMR53 | 2 | SA | L | HSSN | H | VKSG | T | E | A | G | A | 0 | S | A | A | T | K | T | NTGY | D | A | Donor | I | E | K |
| EB28 | 4 | SA | L | HSSN | H | VKSG | T | E | A | G | A | 10 | S | A | A | T | K | T | NTGY | D | A | Donor | I | E | K |
| EB31 | 4 | SA | L | HSSN | H | VKSG | T | E | A | G | A | 10 | S | A | A | T | K | T | NTGY | D | A | Donor | I | E | K |
| VL1313 | 4 | SA | L | HSSN | H | VKSG | T | E | A | G | A | 10 | S | A | A | T | K | T | NTGY | D | A | Donor | I | E | K |

**Table S6**: **Cloning design for fragments used to test for single-molecule non-contiguous recombination at the *pbp2x-mraY* locus**.

| **Primers to amplify fragments for detemining recombination dynamics in *S. pneumoniae* and *E. coli*** | | | |
|---|---|---|---|
| **Fragment name** | **Forward Primer** | **Reverse Primer** | **Template** |
| Long | OVL5375 | OVL5378 | 11A |
| Up | OVL5379 | OVL5375 | 11A |
| Down | OVL5376 | OVL5378 | 11A |
| long-NH | OVL5375 | OVL5557 | 11A |
| | OVL5558 | OVL5559 | *E. coli* BL21 |
| NH-up | OVL5561 | OVL5562 | *E. coli* BL21 |
| | OVL5560 | OVL5379 | 11A |
| down-NH | OVL5376 | OVL5557 | 11A |
| | OVL5563 | OVL5564 | *E. coli* BL21 |

**Table S7**: **Summary statistics from colonies isolated after transformation with different length and combinations of donor fragments to explain the occurrence of non-contiguous recombination.**

| **Fragment(s) transformed** | **Total length of fragment** | **Length of homologous region** | **No. transformants sequenced** | **No. where donor mutations were detected** | **No. with non-contiguous recombination** | **% NCR occurrence** | **Both fragments recombined** |
|---|---|---|---|---|---|---|---|
| Long | 4251 | 4251 | 20 | 20 | 5 | 25 | - |
| Up | 2837 | 2837 | 20 | 20 | 2 | 10 | - |
| Down | 2260 | 2260 | 20 | 18 | 1 | 5.56 | - |
| Up & down | - | - | 20 | 20 | 1 | 5 | 1 |
| long-NH | 6000 | 4251 | 20 | 20 | 5 | 25 | - |
| NH-up | 6000 | 2837 | 20 | 20 | 3 | 15 | - |
| down-NH | 6000 | 2260 | 20 | 20 | 2 | 10 | - |
| NH-up & down-NH | - | - | 20 | 20 | 1 | 5 | 0 |

**Table S8**: **SNPs detected in D39V$^{M53}$** .

| Genome | Location (bp) | Gene_ID (if in coding region) | Predicted function (if in coding region) | Amino acid change |
|---|---|---|---|---|
| VL3960 (D39V$^{M53}$) | 319066 | cps2E | Capsule synthesis | Y428H |
| VL3960 (D39V$^{M53}$) | 576394 | prtA | Serine protease PrtA precursor | E1997G |
| VL3960 (D39V$^{M53}$) | 659823 | SPV_2214 | transposase, truncated ISSpn2. | - |
| VL3960 (D39V$^{M53}$) | 1356494 | SPV_1342 | ISSpn8 transposase, partial | - |
| VL3960 (D39V$^{M53}$) | 1738914 | plcR | transcriptional regulator | I215V |
| VL3960 (D39V$^{M53}$) | 1876322 | hexA | DNA mismatch repair protein HexA | L25W |

# Chapter 3

## Membrane protein BeaU is important for LytA-dependent autolysis and β-lactam susceptibility in *Streptococcus pneumoniae*

Paddy S. Gibson[1], Auriane N. Form[1], Nina L. Tang[1,2], Vincent de Bakker[1], Xue Liu[1,3], Jan-Willem Veening[1,*]

[1] Department of Fundamental Microbiology, Faculty of Biology and Medicine, University of Lausanne, Biophore Building, CH-1015 Lausanne, Switzerland

[2] Laboratory of Parasitic Diseases, National Institute of Allergy and Infectious Diseases, Bethesda, Maryland, USA

[3] Guangdong Key Laboratory for Genome Stability and Human Disease Prevention, Department of Pharmacology, International Cancer Center, Shenzhen University Health Science Center, 518060 Shenzhen, China

[*]Correspondence to Jan-Willem Veening: Jan-Willem.Veening@unil.ch, tel: +41 (0)21 6925625, Twitter handle: @JWVeening

Experiments were performed by PG, or NT and AF under the supervision of PG, with the exception of the *ΔbeaU* mutant CRISPRi-seq which was performed by XL. Data analysis was performed by PG, with CRISPRi-seq scripts developed by VDB and XL. JWV provided conceptual input for experimental design. PG wrote this chapter and produced all figures with feedback from JWV.

## Abstract

The opportunistic human pathogen *Streptococcus pneumoniae* typically undergoes mass population autolysis after reaching stationary phase in liquid culture or during β-lactam therapy. The autolysin responsible, LytA, has since been identified as a key virulence factor in this species, with deletion mutants shown to be severely attenuated in infection models. Despite its importance in the ability of *S. pneumoniae* to cause invasive infection, both how LytA is exported from the cell and how its activity is regulated is not understood.

Here, we apply CRISPRi-seq in conjunction with amoxicillin-induced autolysis to screen for novel regulators of this important pathway. We identify β-lactam susceptibility and autolysis associated protein BeaU. Cells mutated for *beaU* demonstrate increased and premature lysis in stationary phase as well as during exposure to β-lactam antibiotics. Importantly, we show that increased lysis in absence of BeaU is dependent on LytA. BeaU localizes to the membrane and has its C-terminus intracellularly, and in-silico modelling suggests it may form dimers or trimers. A genome-wide synthetic lethal screen suggests that BeaU has a function associated with cell wall synthesis proteins, where its deletion alters the cell wall structure in a way that increases susceptibility of the peptidoglycan to the LytA autolysin.

## Introduction

*Streptococcus pneumoniae* is a commensal member of the human nasopharyngeal microflora, and a leading cause of otitis media, pneumonia, meningitis, and septicemia. Although colonization of the nasopharyngeal epithelium is usually asymptomatic (Nunes et al., 2005), local spread and dissemination mediated by several virulence factors can lead to severe disease in vulnerable populations. A critical pneumococcal virulence factor is choline binding protein (CBP) and major autolysin, LytA. Responsible for the classical stationary phase autolysis typical of *S. pneumoniae* batch cultured in liquid media (Avery and Cullen, 1923; Garcia et al., 1985; Howard and Gooder, 1974; Tomasz, 1968), LytA-negative mutants show attenuated virulence in sepsis, pneumonia, and meningitis murine infection models (Berry et al., 1989; Berry and Paton, 2000; Canvin et al., 1995; Hirst et al., 2008). Exactly why an autolysin protein is required for successful host invasion remains a topic of some debate. A prevailing theory is that LytA-mediated autolysis releases inflammatory cell wall debris and microbial proteins, such as cytolytic toxin pneumolysin (Ply), required for epithelial invasion and aiding in avoidance of the host immune response (Lock et al., 1992; Tuomanen, 1999). However, LytA was also found to be responsible for capsule shedding prior to epithelial cell invasion, a ploy which results in free capsule "decoys" for host antimicrobial peptides and supports epithelial cell adherence, without inducing autolysis (Beiter et al., 2008; Cundell et al., 1995; Kietzman et al., 2016; Llobet et al., 2008).

Although LytA activity is important for pneumococcal survival in the host and its ability to cause invasive disease, autolysis is a double-edged sword, and loss of control can have lethal consequences (Uehara and Bernhardt, 2011; Vollmer et al., 2008). This can be observed upon treatment with β-lactam antibiotics, where the inhibition of penicillin binding proteins (PBPs) stalls cell wall synthesis, triggering LytA-dependent autolysis (Cho et al., 2014; Tomasz and Waks, 1975). Although isolates tolerant to penicillin and vancomycin often display defective lysis, this is rarely due to modifications to LytA itself, and rather to unidentified autolysin regulatory elements (Liu and Tomasz, 1985; Moreillon et al., 1988; Moscoso et al., 2010; Novak et al., 1999; Olivares et al., 2011).

LytA has an *N*-acetylmuramoyl L-alanine amidase domain at the N-terminus which acts on peptidoglycan (PG), cleaving the amide bond between glycan strand and peptide (Howard

and Gooder, 1974; Vollmer et al., 2008). Non-covalent bonds between the C-terminal choline binding domain (CBD) and teichoic acid-bound phosphorylcholine are essential for both LytA dimerization and its lytic activity (Briese and Hakenbeck, 1985; Fernández-Tornero et al., 2001; Holtje and Tomasz, 1975; Tomasz, 1968), while exposure to high concentrations of choline inhibits autolysis (Giudicelli and Tomasz, 1984). LytA is expressed throughout growth but remains cytoplasmic during exponential phase, before slowly shifting to the cell wall fraction upon entrance to stationary phase and prior to onset of autolysis (Flores-Kim et al., 2019; Mellroth et al., 2012). It does not possess a signal peptide (Diaz et al., 1989; García et al., 1986), and how it reaches the cell exterior to access the cleavage substrate is not known. In addition, how the timing of LytA transfer is controlled during the cell cycle and what stops lysis from occurring earlier remains elusive. One hypothesis is that actively growing cells are protected by capped PG, which blocks access of extracellular LytA, sourced from spontaneous neighbouring cell lysis during exponential growth, to its substrate. When cell wall synthesis machinery is stopped, such as in stationary phase or during β-lactam treatment, LytA can then access the uncapped nascent PG (Bonnet et al., 2018; Mellroth et al., 2012). Cell lysis would release intracellular LytA in the growth medium, causing a lytic cascade in neighbouring cells and eventually population autolysis. Alternatively, Flores-Kim et al. (2019) propose a significant role for teichoic acids in LytA regulation, where the autolysin is sequestered on lipoteichoic acid (LTA) throughout exponential growth. Upon entrance into stationary phase, FtsH-mediated degradation of LTA synthase TacL is triggered, resulting in a shift towards wall teichoic acid (WTA) synthesis through reduced substrate competition, forcing LytA to switch to WTA binding and bringing it into proximity with its PG substrate. While both hypotheses have merit and could be complementary, neither fully explain how LytA escapes the cytoplasm in the first place, and both are dependent on presently undefined regulatory proteins or systems.

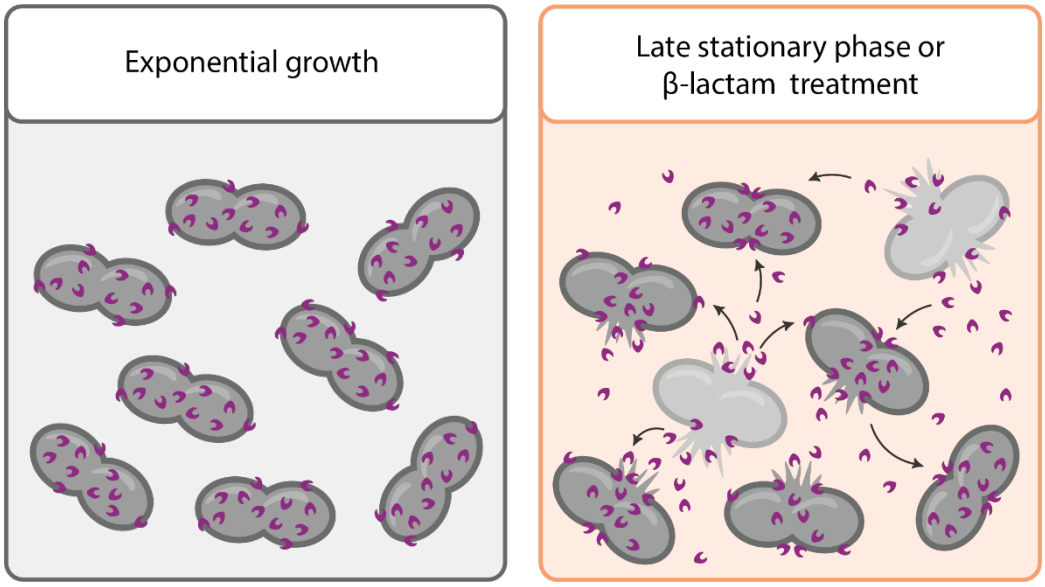


**Figure 1: Overview of what is known and hypothesized about the regulation of LytA in S. pneumoniae.** LytA is found in high concentrations in the cytoplasm during exponential growth, with some proteins localizing to the cell membrane/wall, likely through interactions with LTA. As it does not possess a signal peptide, there is a hypothesis that the cell membrane-associated LytA comes from the lysis of other cells in the population during normal cell turnover during growth

Here, we applied clustered regularly-interspaced short palindromic repeat interference sequencing (CRISPRi-seq) (Liu et al., 2021) in combination with the frontline antibiotic amoxicillin (AMX) in order to identify novel proteins that contribute to the regulation of β-lactam-induced autolysis in *S. pneumoniae*. AMX is one of the most commonly prescribed antibiotics worldwide, particularly for upper respiratory tract infections, and resistance to this drug is increasing in correlation with its high usage (Càmara et al., 2018; Doern et al., 1996; Doit et al., 1999). Here, we show that CRISPRi-seq can be used to identify factors affecting cell fitness in an autolytic bottleneck. Moreover, we identified SPV_1662, hereafter called BeaU for membrane protein associated with beta-lactam susceptibility and autolysis, a protein of previously unknown function which upon deletion increases both late stationary phase and β-lactam induced lysis, and propose a model explaining this phenotype.

## Results

### *CRISPRi-seq to identify genes important in control of autolysis*

We took advantage of the ability of cell-wall targeting antibiotics to trigger LytA-dependent lysis in *S. pneumoniae* to identify novel proteins which may contribute to autolysis regulation. We utilised CRISPRi-seq to identify operons in the pneumococcal genome which have differential effects on cell fitness during an AMX-induced population bottleneck. In this system, nuclease-inactive Cas9 (dCas9) is expressed from an IPTG-inducible promoter ($P_{lac}$) while single guide RNAs (sgRNAs) are constitutively expressed. Each mutant cell contains one operon-targeting sgRNA and are cultured in a pool containing all 1498 mutants (Liu et al., 2021).

After induction (IPTG 40 μM, 2hrs), the CRISPRi-seq library was exposed to the minimum inhibitory concentration (MIC, 0.01 μg/mL) of AMX for this strain for two hours. This concentration and duration of treatment was determined to be sufficient to kill 99% of cells (Fig 2AB). The population was then allowed to recover in fresh growth medium to sufficient levels for DNA isolation and sequencing ($OD_{595}$ 0.4). The control treatment was subjected to the same dilution and resuspension steps, but without addition of AMX. As a result, it reached the final OD faster and was not subjected to a bottleneck. Differential fitness of operons was determined from enrichment or depletion of sgRNAs in the AMX condition compared to the no treatment control, measured by calculating the $\log_2$ fold change in sgRNA abundance in non-induced versus induced samples. Significance was determined from the adjusted *p* value for the interaction between IPTG induction and AMX treatment ($p < 0.05$, Fig 2D).

Repression of 128 operons were found to have significant effects on cell fitness during AMX treatment, many of which were known members of cell wall biogenesis pathways. The sgRNA targeting the gene for AMX target Pbp2b was found to be significantly less abundant in the presence of the antibiotic, demonstrating the additive effect on fitness of reduced protein expression with concurrent direct protein inhibition (Fig 2D). In contrast, key target Pbp2x was not identified in the screen, likely because repression causes a severe fitness defect even in the absence of AMX (Dénéréaz and Veening, unpublished). Additional markers of screen success were the operons encoding endolytic murein transglycosylase *mltG* and RNA-binding protein *eloR,* where gene repression resulted in

increased fitness in presence of AMX (Fig 2D). This correlated with previous studies in which this complex was found to be synthetic viable in the absence of Pbp2b (Stamsås et al., 2017; Tsui et al., 2016; Winther et al., 2021). Conversely, reduced expression of *lytA* was not found to significantly impact fitness in AMX, despite a 1.16 $\log_2$ fold change value for the targeting sgRNA interaction effect, although this may be explained by substantial variation in read counts between replicates for this sgRNA strain.

One of the top hits from the screen was *spv_1662*, a gene of unknown function (hereafter called *beaU* for reasons explained below). This phenotype was confirmed in a single CRISPRi-sgRNA strain and repression of *beaU* led to significant decreased fitness in the presence of AMX (Fig 2D). Interestingly, *beaU* was also identified by CRISPRi-seq to be more essential in a superinfection model than in C + Y growth medium (Liu et al., 2021). Together, these results demonstrate that CRISPRi-seq can be used to identify genes involved in tolerance to AMX and control of autolysis (see below).

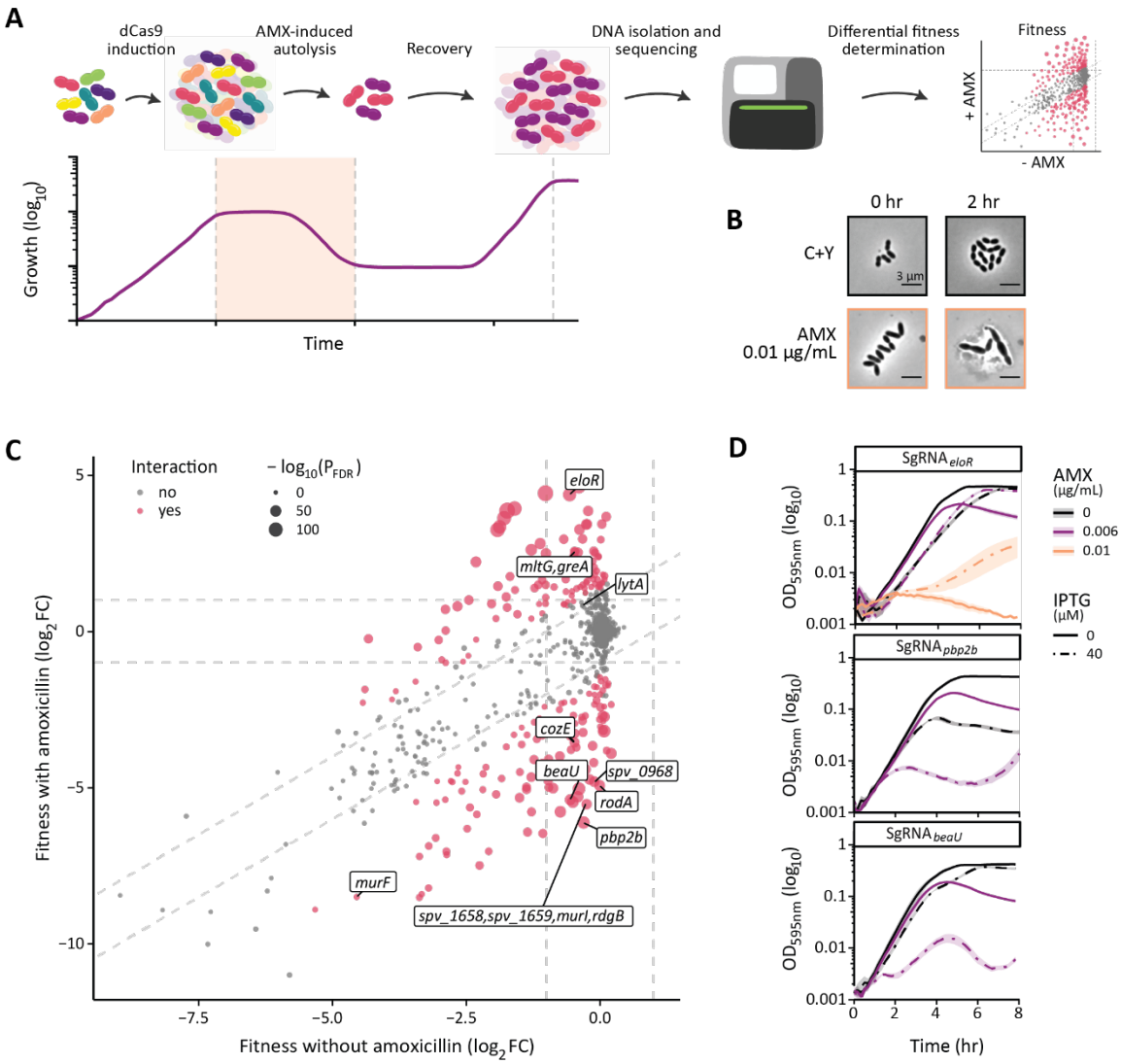


**Figure 2: AMX-induced bottleneck was used as the stressor for CRISPRi-seq to identify novel regulators of β-lactam-induced lysis.** (A) Schematic of the CRISPRi-seq experimental workflow including a representative growth curve of the bacterial population during treatment. The CRISPRi library was precultured in 40 uM IPTG to induce dCas9, with a non-induced control of media only (induction). After 2 hrs, both induced and non-induced samples were divided in two, and one tube of each was treated with 0.01 µg/mL AMX, then all four samples were incubated for another 2 hrs (AMX-induced autolysis). After the bottleneck, all samples were resuspended in a large volume of fresh media and grown to early stationary phase (recovery), before DNA isolation and sequencing. The differential fitness of each sgRNA operon target with and without the AMX treatment was then determined. (B) Phase contrast microscopy images of *S. pneumoniae* D39V cells in the absence and presence of AMX 0.01 µg/mL, at timepoints 0 and 2 hr. (C) sgRNA strain fitness in presence (y axis) and absence (x axis) of AMX-induced bottleneck. Fitness is measured as the $\log_2$ fold change of sgRNA read counts between induced and non-induced samples for that treatment. Point colour indicates whether the interaction between induction and AMX treatment was considered significant (pink, *p*-adjusted < 0.05) or non-significant (grey), and size is determined by the -$\log_{10}$ transformed *p*-adjusted, where larger points indicate smaller *p* values (D) Growth of

$P_{lac}$-*dcas9* strains each containing an sgRNA targeting (from top to bottom) *eloR*, *pbp2b*, and *beaU*. They were grown with (solid line) and without (dashed line) 40 mM IPTG, with 0 µg/mL (black), sublethal (purple, 0.006 µg/mL), and MIC (orange, 0.01 µg/mL) concentrations of AMX. sgRNA strains where fitness was found in the CRISPRi-seq screen to decrease under AMX-induced bottleneck (sgRNA$^{pbp2b}$, and sgRNA$^{beaU}$) were only tested in 0 µg/mL and sublethal AMX.

### *Depletion of BeaU increases both late-stationary phase and β-lactam-induced autolysis in an AMX-susceptible background*

To confirm that decreased survival in the presence of AMX was caused by repression of *beaU* alone, and not by polar effects of dCas9-DNA binding on downstream or upstream gene expression, we tested an inducible *beaU* complementation strain in the presence and absence of the antibiotic. This was particularly important as *beaU* is a small gene (249 bp) located directly upstream of the glutamate racemase encoding *murI* (Fig 3A). MurI catalyses the racemization of L-glutamine to D-glutamine, a necessary step in the synthesis of peptidoglycan subunits (Fisher, 2008), the repression of which could hypothetically explain reduced cell fitness in combination with AMX treatment. In addition, autolysis in C + Y medium occurs some hours after stationary phase is reached, but longer growth time is not possible with the CRISPRi system in the pneumococcus due to the accumulation of suppressor mutations in dCas9.

*beaU* is in a single gene operon immediately downstream from trehalose metabolism genes *treP* and *treC* (Fig 3A). It has a transcriptional start site preceded by an RpoD-binding site and is followed immediately by a transcriptional terminator (95% efficiency), indicating it is largely transcribed as a monocistronic message (Slager et al., 2018). Interestingly, there is no terminator between the CcpA- and TreR-controlled *trePC* operon, suggesting that *beaU* expression may be affected by the relative abundancies of glucose and trehalose. Growth in different trehalose concentrations did not affect lysis in the *ΔbeaU* strain (Fig S1). It is not considered essential for cell growth in C + Y medium at 37°C and so we were able to exchange *beaU* with an erythromycin resistance marker (ery$^{R}$). We then complemented the deletion with an IPTG-inducible copy of *beaU* inserted at the ectopic ZIP locus (Keller et al., 2019) (Fig 3B). Depletion of *beaU* had no effect on cell shape in the absence of antibiotics when imaged in exponential growth (Fig 3C). Under AMX treatment, cell abnormalities such as elongated cells and septation defects were observed in both IPTG conditions.

Depleting *beaU* had no effect on the initial growth rate of D39V. However, autolysis occurred earlier in stationary phase and progressed more quickly, resulting in a large difference in $OD_{595}$ at 24 hrs (Fig 3D). In addition, AMX-induced lysis was initiated at a lower $OD_{595}$ when *beaU* was depleted. The autolysis defects could be complemented by induction of $P_{lac}$-*beaU* with 100 µM IPTG in both cases, while 10 µM had almost no effect.

As early autolysis in the BeaU depleted strain was triggered by both late stationary phase and AMX treatment, we grew the inducible strain with cefotaxime (CTX) and tetracycline, to test the specificity of the response. We found that BeaU depletion resulted in increased autolysis in the presence of sublethal CTX, but not tetracycline (Fig 3D). Together, these characterizations demonstrate an association between cell wall damage and increased autolysis due to BeaU depletion.

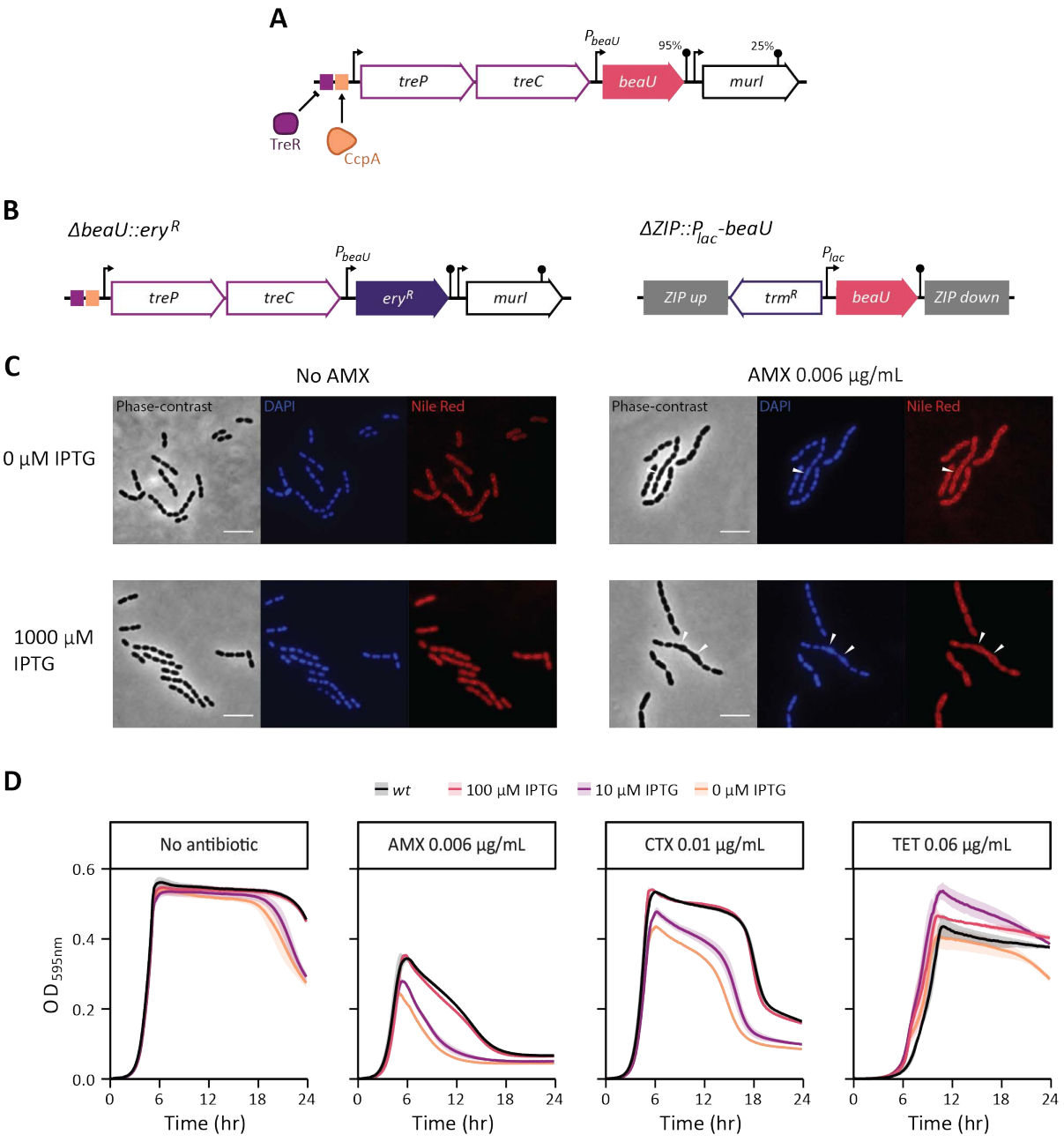


**Figure 3: Depletion of *beaU* increases both late stationery and β-lactam induced autolysis.** (A) Schematic showing the genomic context of *beaU*, located at position D39V.0:1673888..1674136 (- strand) . It has its own transcriptional start site and terminator with 95% efficiency, likely limiting transcriptional readthrough into the downstream glutamate racemase encoding gene *murI*. *murI* has a weak internal terminator (25% efficiency) and is transcribed in an operon with *rdgB* and two genes of unknown function (not depicted). Upstream of *beaU* is the CcpA and TreR regulated *treP* and *treC* operon encoding proteins for the metabolism of trehalose as an alternative energy source to glucose. There is no terminator between *treC* and *beaU*, indicating glucose- and trehalose-dependent transcriptional readthrough. (B) Schematic showing construction of the *beaU* deletion, and complementation with an IPTG inducible copy at the ectopic ZIP locus (Keller et al., 2019). (C) Phase-contrast and fluorescent microscopy snapshots of *D39V*; $P_{lac}$-*beaU; ΔbeaU* cultured with and without 1000 µM IPTG, and

in the absence and presence of 0.006 μg/mL AMX, then stained with DAPI and Nile-Red. (D) Growth of D39V (AMX susceptible wild-type *S. pneumoniae*) and the D39V; $P_{lac}$-*beaU; ΔbeaU* strain in the absence of antibiotic treatment, and in sublethal AMX (0.006 μg/mL), CTX (0.01 μg/mL), and tetracycline (0.06 μg/mL) with a range of IPTG concentrations. $OD_{595}$ is plotted on a linear scale to better observe autolysis. Lines show the mean of two replicates and shading represents the SEM. Increased autolysis was observed when BeaU was depleted in the presence of AMX and CTX and could be complemented with 100 μM IPTG.

***Increased lysis because of beaU deletion is dependent on major autolysin LytA***

LytA is known to be triggered upon entrance to late stationary phase, and by cell wall targeting antibiotics (Howard and Gooder, 1974; Tomasz and Waks, 1975). To confirm that increased lysis in an *beaU* depletion was mediated by LytA, we tested whether deleting *lytA* could block lysis onset when *beaU* is absent. We also tested the effect of deleting *lytB*, an alternative pneumococcal murein hydrolase essential for daughter cell separation during cell division (Garcia et al., 1999). Deletion strains were grown in the absence and presence of sublethal AMX concentrations. To quantify autolysis across many strains, the area under the curve was determined for the range of timepoints between 12 - 24 hr (Fig 4A-C), and significant differences in AUC were tested for using a two-way ANOVA with Tukey correction for multiple testing (Table S1).

Surprisingly, the severe lysis defect of the D39V *ΔbeaU* strain was partially corrected by the co-deletion of *lytB* when growth was assayed in the absence of AMX (Fig 4A). Co-deleting *lytA* with *beaU* resulted in a complete loss of stationary phase autolysis. Interestingly, when assayed in the presence of sublethal AMX, deleting *lytB* did not fully correct the *ΔbeaU* lysis phenotype, whereas deleting *lytA* blocked the lytic activity of AMX in both the D39V *wt* and *ΔbeaU* backgrounds. Regardless of AMX treatment and *beaU* genotype, deleting both *lytA* and *lytB* resulted in the same growth phenotype as deleting *lytA* alone, indicating that lysis in the absence of LytB is mediated by LytA.

We also tested the combinatorial effects of deleting *lytA*, *lytB*, and *beaU* in AMX resistant VL4174 cells (Fig 4B). Cells of this strain began to lyse earlier than D39V and deleting *ΔbeaU* did not increase lysis. Deleting *lytB* had an insignificant effect on lysis in the VL4174;*ΔbeaU* genetic background ($p > 0.05$), whereas deleting *lytA* removed the lytic phenotype of the

strain, regardless of *beaU* presence in the genome. The same pattern was observed in the presence of sublethal AMX.

Taken together, the data suggests that while removing LytB from the cell may be beneficial in a *⊿beaU* background, the mechanism of lysis occurs through LytA. We hypothesize an indirect effect of *ΔlytB*, where increased cell chaining as a consequence of unseparated PG increased cell wall stability, thereby reducing the effect of *ΔbeaU*, but in an insufficient manner to overcome AMX-induced lysis.

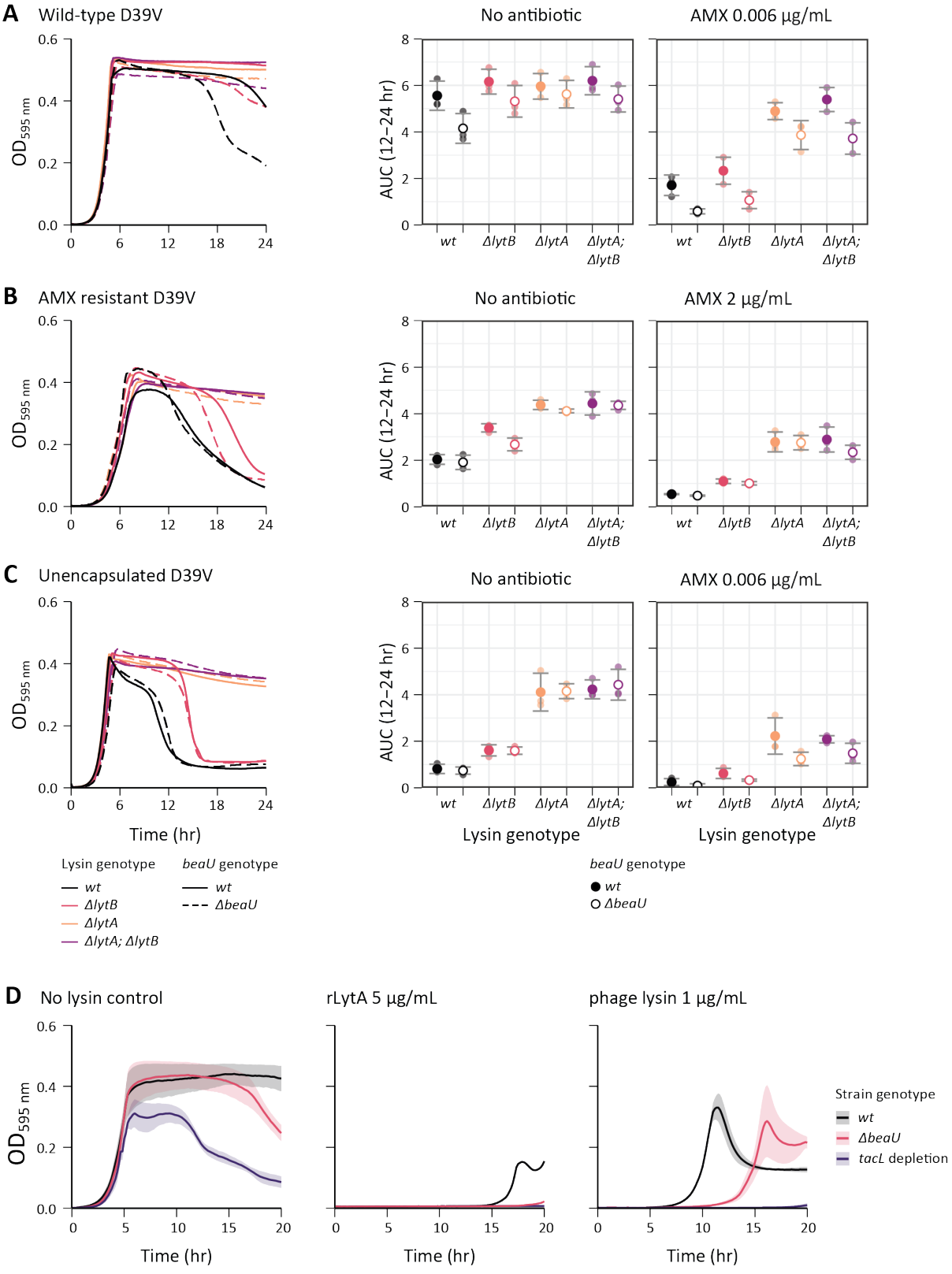


**Figure 4: Autolysis caused by deletion of beaU is dependent on presence of major autolysin LytA.** *lytA* and *lytB* were deleted in *wt* (solid line) and Δ*beaU* (dashed line) backgrounds of (A) wild-type D39V, (B) AMX resistant D39V (VL4174), and (C) Unencapsulated D39V (*Δcps*). Growth curves without antibiotic are on the left and display the mean of three replicates. As a measure of autolysis, the area under the curve for 12 – 24 hrs was

determined for all strains in the absence and presence of sublethal AMX and results are shown on the right for all strains. Replicates are indicated by translucent circles and means by opaque circles. *beaU* genotype is indicated by solid (+*beaU*) and empty (-*beaU*) circles. Error bars represent standard deviation and colour indicates *lytA* and *lytB* genotype. Growth curves in AMX treatment are shown in Fig S2. Statistical significance was tested using a two-way ANOVA with Tukey correction for multiple testing (Table S1). (D) Growth of wild-type and *ΔbeaU* D39V under treatment with recombinant LytA protein (rLytA), and with phage lysin (Cpl-1). The D39V; $P_{lac}$-*tacL; ΔtacL* strain (VL4665) was used as a control, as TacL depletion is reported to increase LytA susceptibility (Flores-Kim et al., 2019). Due to technical constrains, the rLytA experiment could only be performed once, although increased sensitivity in the *ΔbeaU* strain is visible. Treatment with 1 µg/mL phage lysin was replicated twice and the *ΔbeaU* strain also showed increased lysis.

### *Deletion of beaU does not increase lysis in unencapsulated D39V*

Removal of the capsule increases stationary phase lysis in the pneumococcus. We thus tested for an additive effect of deleting *beaU* in a D39V capsule mutant (*Δcps*). In this strain, lysis began with the onset of stationary phase, earlier than for both *wt* encapsulated D39V and VL4174, and deleting *beaU* did not further increase the autolytic phenotype (Fig 4C).

We then tested the effect of co-deleting *lytA* and *lytB* with *beaU* in the *Δcps* background. Deleting *lytB* delayed the onset of lysis by more than 6 hrs in both the *wt* and *ΔbeaU* contexts. As in D39V and VL4174, deletion of *lytA* blocked lysis from occurring at all within the 24hr assayed timeframe. This confirms that the *ΔbeaU* lysis phenotype is LytA-dependent, and further supports the hypothesis that reduced PG hydrolysis by LytB reduces lysis by LytA.

### *Deletion of beaU increases susceptibility to extracellular LytA protein and phage lysin*

The dependence of *ΔbeaU*-associated autolysis on the presence of *lytA* could suggest both direct or indirect regulation of autolysin activity by BeaU. To test this, we treated wild-type D39V and the *ΔbeaU* mutant with recombinant purified LytA protein (rLytA), which has been shown to induce lysis in *ΔlytA* mutants (Mellroth et al., 2012). As a control, we used a *tacL* depletion strain precultured in the absence of inducer (VL4665), which is reported to be highly sensitive to LytA (Flores-Kim et al., 2019). Unfortunately, due to difficulties purifying rLytA, we were only able to perform this experiment once, but preliminary data indicated that deletion of *beaU* resulted in increased lysis upon addition of extracellular LytA to the growth

medium (Fig 4D). To explore this phenotype further, we also tested the three strains with purified phage lysin Cpl-1. Here, we also showed that the *ΔbeaU* mutant was also more susceptible to lysis induced by the phage lysin, although not as susceptible as the *tacL* depletion strain (Fig 4D). Although these results do suggest an indirect effect of BeaU on LytA activity, in order to confirm this hypothesis the experiments need to be repeated in *lytA* deletion strains.

***BeaU is an internal protein and localizes to the cell membrane***

BeaU is a small protein, only 82 amino acids in length, and was predicted by TMHMM 2.0 to have a short transmembrane domain spanning from Leu4 to Arg26, with the N-terminus outside the cell. PneumoExpress RNA-seq data shows it is relatively highly expressed in a constitutive manner (Fig S3) (Aprianto et al., 2018). We used *AlphaFold2* to predict structural features of the peptide. BeaU was predicted to form three α-helices, including the predicted transmembrane domain at the N-terminus, which are separated by flexible linkers (Fig 5AB). Repeated predictions of the structure placed the two shorter helices in near-identical orientations to each other while showing some mobility relative in position to the aforementioned transmembrane helix. This speaks for a reasonably robust orientation of these intracellular helices relative to each other with flexibility in their anchoring to the membrane, forming an overall "arrow" shaped structure (Fig S4AB). Plotting the electrostatic charge over the surface of the protein demonstrated the nonpolar nature of the N-helix with some charge carrying residues located at the cytoplasmic terminus (Fig S4C). The transmembrane domain of the predicted structure gave a length of ~3 Å, with the N-terminus was predicted to be outside the cell, and the C-terminus in the cytoplasm (Fig 5B).

Given a torsional distortion of the N-terminal transmembrane domain, we were curious whether this feature of the protein might accommodate multimerization of BeaU. Thus, in addition to predicting the tertiary structure of BeaU as a monomer, we employed *AlphaFold2-Multimer* to predict the structure in a dimeric and trimeric form (Fig 5CD). Models for both predictions showed some plausibility (as judged by Predicted Average Error values between predictions (PAE), Fig S4DE)), with membrane-spanning helices bundled together and C-terminal helices arranging to point outwards from the central axis of the multimer. Testing higher order multimers did not produce confident predictions, with PAE values showing large

variance in the placement of dimeric and trimeric units within these predictions (Fig S4FG). *AlphaFold2* predicts structures indiscriminate of solvent, and so these multimeric predictions must be taken under advisement, as stabilizing effects of protein-membrane interactions present *in-vivo* might be mimicked by multimeric assemblies *in-silico*. Experimental confirmation is thus required to confirm if and which assemblies BeaU preferentially forms in the cell.

To confirm the transmembrane protein prediction, we tagged BeaU with monomeric superfolder GFP (m(sf)GFP) and imaged its localization using fluorescence microscopy. We tested both N-terminal and C-terminal fusions, either at the native locus under the control of $P_{beaU}$, or at the ectopic ZIP locus expressed from $P_{lac}$ (Keller et al., 2019). The N-terminal fusions appeared non-functional, resulting in small foci around the cell and at the poles, suggesting protein aggregation/degradation (Fig S5A). If the N-terminus is indeed found inside the membrane at the interface between the inner and outer lipid layers, the fusion of m(SF)GFP may have interfered with the ability of the protein to traverse with the membrane, explaining the poor localization. In contrast, the C-terminal fusions localized evenly to the cell membrane around the entire cell, with no preference for a specific location (Fig 5E). In some cells fluorescence appeared brighter at the septum, but this may be due to the double membrane layer that occurs as cells prepare to divide. These experiments confirmed the predicted membrane localization and suggested that an untagged N-terminus was important for protein localization.

We then designed an experiment using the Nano-Glo® HiBiT extracellular detection assay to confirm the prediction that BeaU is oriented with the C-terminus inside the cytoplasm. BeaU was fused with the HiBit peptide tag under the control of $P_{lac}$ at the ectopic CIL locus (Keller et al., 2019; Schwinn et al., 2018). The HiBit peptide tag forms a complex with the LgBit peptide if accessible, resulting in an enzyme which breaks down the NanoGlo reagent and emitting light. As the LgBit was added to the extracellular buffer and does not permeate the cell membrane, the light reaction would only be detected if the HiBit tagged terminus was outside the cell. After validating the system on a known membrane protein (Fig S5B), both N- and C-terminal fusions were tested. As a positive control, both strains were tested as whole cells, and as lysates, where both N- and C- terminals would be available to interact with the LgBit peptide.

Although the induced N-terminal fusion did not produce high luminescence compared to the non-induced controls, even when cells were lysed, the differences were statistically significant for both cell preparations (intact: $p_{adj}$ = 0.0028, lysed: $p_{adj}$ = 0.042). The low luminescence measurements may suggest protein misfolding or degradation, presumably related to tagging the protein at the membrane permeating N-terminus, as observed with GFP fusions (Fig S5A). The C-terminal fusion did not result in significantly more luminescence than the non-induced control in the whole cell samples ($p_{adj}$ = 1), however, when lysed, significantly more luminescence was produced ($p_{adj}$ = 0.026). This indicated that the C-terminal HiBit tag was only available to interact with the LgBit peptide when the extracellular buffer could access the inside of the membrane.

To summarise, BeaU is a small, constitutively expressed protein that localises to the cell membrane with the C-terminus sitting intracellularly and may exist in a multimeric form (Fig. 7 with model of localization).

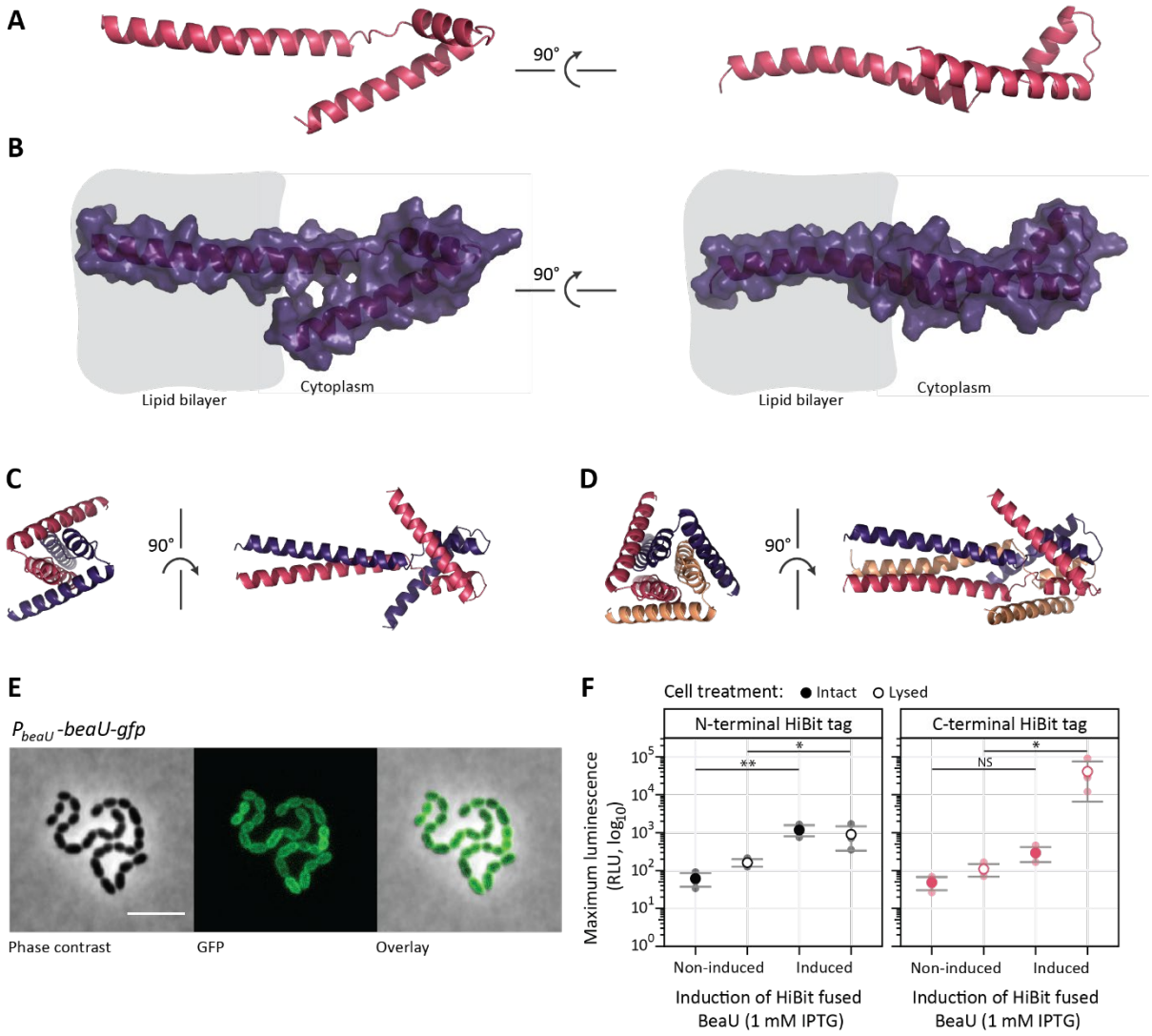


**Figure 5: BeaU is a cell membrane localised internal protein which may exist as a monomer, dimer, or trimer.** (A) Cartoon and (B) surface model of the AlphaFold2-predicted structure of BeaU monomer, with 90° rotation. The predicted membrane domain of BeaU is estimated to be ~3 Å, similar to other membrane-spanning proteins of the pneumococcus. (C) AlphaFold2 predicted structure of BeaU as a dimer. (D) Predicted structure of BeaU as a trimer. All PAE errors from AlphaFold2 models are shown in Fig S4. (E) Phase-contrast and fluorescent microscopy snapshots of BeaU tagged at the C-terminus with GFP, under the control of $P_{beaU}$. Scale bar is 5 µm. BeaU-GFP localized to the cell membrane. BeaU N-terminal fusions did not function well (Fig S5A) (F) Luminescence of Nano-Glo® HiBit-tagged BeaU. N-terminus tagged cells are shown in black, and C-terminus in pink. Samples were either left whole (solid circles) or lysed (empty circles), in order to compare luminescence when the tags were localized with BeaU vs free in solution with cellular debris. Results from four replicates are shown in translucent circles. Statistical significance was assessed using and ANOVA with Tukey correction for multiple testing, NS not significate, * $p_{adj} < 0.05$, and ** $p_{adj} < 0.005$.

***CRISPRi-seq predicts genetic interactions of beaU with cell wall and cell division proteins***

BeaU is highly conserved in strains of *S. pneumoniae*, but has no homology with characterized proteins of known function, and no predicted enzymatic domain. To look for genetic interactions which may provide clues as to the pathway BeaU is involved in, we performed CRISPRi-seq in both D39V and *ΔbeaU* strains. The D39V CRISPRi pooled library was transformed into a *ΔbeaU* background also containing *bgaA::*$P_{lac}$*-dcas9*, then both CRISPRi libraries were grown in the presence and absence of IPTG and the sgRNAs sequenced. Differential fitness of operons was established by the enrichment or depletion of sgRNAs in *ΔbeaU* compared to wild-type D39V, measured in the same manner as the original AMX CRISPRi-seq screen. Significance was determined from the adjusted *p* value for the interaction between strain background and IPTG induction ($p_{adj} < 0.05$, Fig 6A).

The screen identified 12 operons which were differentially fit in *ΔbeaU* compared to the wild-type (Fig 6A, Table S2). This including many cell wall synthesis and cell division-associated proteins, as well as some of unknown function. Two genes, *cozEa* and *lafB*, were found to be essential in D39V, but became non-essential in the absence of *beaU* (Fig 6B). LafB (CpoA) is an intracellular glycosyltransferase thought to be associated with the LTA synthesis pathway (Edman et al., 2003; Reichmann and Gründling, 2011), while CozEa is a part of the MreCD complex directing cell elongation and essential for the septal localization of Pbp1A (Fenton et al., 2016). CozEa is hypothesized to monitor cell size and shape through penicillin binding protein regulation, although a role in membrane fluidity has also been hypothesized (Gallay and Veening, unpublished).

The other 10 hits were all predicted to be more essential in the *ΔbeaU* mutant compared to D39V. This included operons encoding septal-localized cell division proteins DivIB, DivIC, and EzrA (Noirclerc-Savoye et al., 2005), and LytR (Fig S6). LytR is essential for the attachment of TA to the cell wall thereby forming WTA (Ye et al., 2018; Minhas and Veening, unpublished). Particularly relevant to BeaU is its involvement in LytA activation, hypothesized to occur through cell wall structure alterations.

In addition, several hypothetical protein-encoding genes were identified. Interestingly, one of these was *spv_0968* ($p_{adj} = 2.77 \times 10^{-3}$), found in the original CRISPRi-seq screen to become more essential in AMX (Fig 2B, Fig S6). It is a GNAT-family acetyltransferase with a cytoplasmic localisation and has previously been found to be downregulated during

penicillin treatment (Rogers et al., 2007).

In addition to predicting genetic interactions via CRISPRi-seq, we also performed a pull-down assay with GFP tagged BeaU (C-terminal fusion), to attempt to identify direct protein-protein interactions (data not shown). Unfortunately, likely due to technical difficulties caused by membrane protein solubilization, the initial attempt appeared highly non-specific, with many membrane proteins identified with varying abundancies. The only common theme were four proteins involved in acetoin metabolism, but a preliminary growth assay to test the effect of different glucose and acetoin experiments did not show any effect on *ΔbeaU* autolysis (Fig S6).

Overall, the predicted genetic interaction comprise a series of operons associated with septal cell division, or with cell wall synthesis, suggesting a possible function for BeaU in one of these important cellular pathways. The results of the CRISPRi-seq screen remain to be validated, and further characterisation is required to identify whether the predicted interactions are direct or indirect.

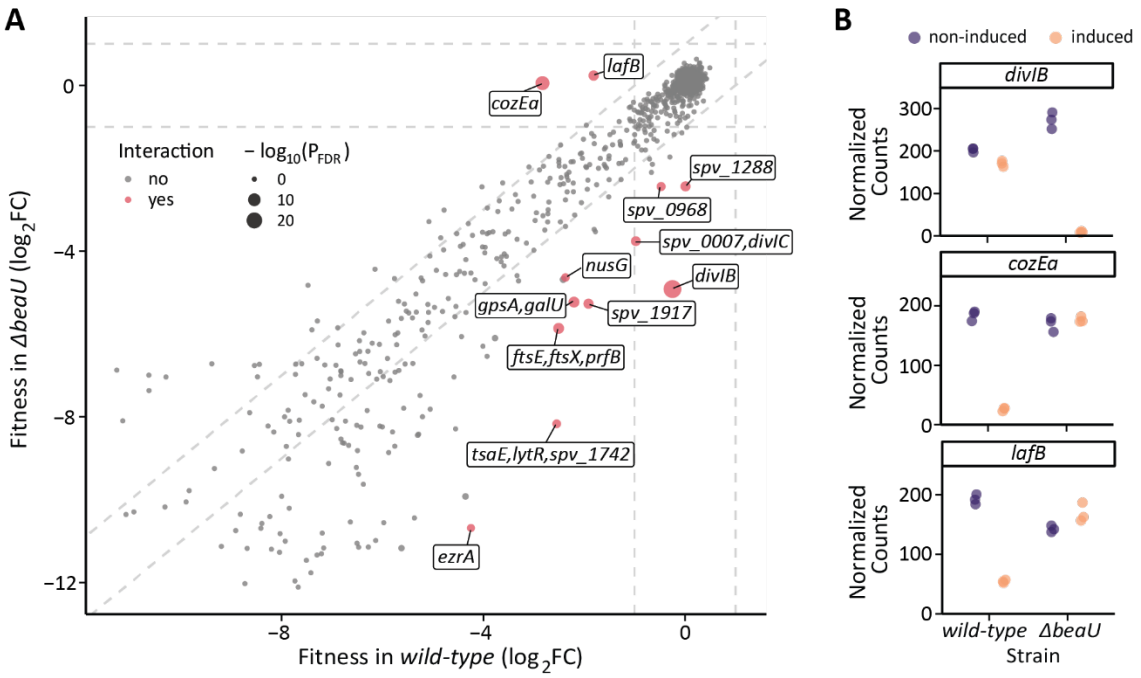


**Figure 6: CRISPRi-seq in *ΔbeaU* genetically links *beaU* to operons involved in call wall synthesis and cell division to be.** (A) Fitness, measured as the $\log_2$ fold change of sgRNA read counts between induced and non-induced

samples, in *ΔbeaU* (y axis) over fitness in wild-type D39V (x axis). Each point represents an operon in the genome-wide screen, and colour indicates if the interaction between induction and strain was significant (pink, *p*-adjusted < 0.05) or non-significant (grey). Point size is determined by the $-\log_{10}$ transformed *p*-adjusted, where larger points indicate smaller *p* values. 12 operons were found to have differential effects on fitness in the *ΔbeaU* strain and are labelled on the plot. (See Table S2 for details) (B) Normalized sgRNA counts of three top hits for for non-induced and induced samples in the wild-type and *ΔbeaU* strains. Repression of *divIB* caused significantly more negative effects on fitness in *ΔbeaU* compared to the wild-type ($p_{adj} < 1 \times 10^{-9}$), while *cozE* and *lafB* repression had significant beneficial effects on fitness in the *ΔbeaU* strain ($p_{adj} < 1 \times 10^{-9}$, and $p_{adj} = 2.7 \times 10^{-4}$, respectively).

## Discussion

The major pneumococcal autolysin LytA is an essential virulence factor for the successful transition from beneficial colonizer to harmful invader performed by opportunistic pathogen *S. pneumoniae*. LytA binds to teichoic acid bound phosphorylcholine residues in the cell wall, which both aids in dimerization and brings the N-terminal amidase domain within reach of its substrate, the amide bond between glycan strand and peptide of PG (Howard and Gooder, 1974; Vollmer et al., 2008). Choline is critical for its activity, with lysis inhibited when concentrations are both too high or too low (Briese and Hakenbeck, 1985; Giudicelli and Tomasz, 1984; Tomasz, 1968).

Although LytA is constitutively expressed throughout the cell cycle it does not initiate lysis until late stationary phase in liquid batch culture, revealing tight control over its autolytic activity (Avery and Cullen, 1923). Loss of control has lethal consequences, exemplified by the effect of cell wall-targeting antibiotic treatment, where stalled PG synthesis triggers LytA-dependent autolysis (Cho et al., 2014; Tomasz and Waks, 1975).

The onset of autolysis in late stationary phase correlates with a shift in LytA localization, from the cytoplasm to the cell wall fraction (Flores-Kim et al., 2019; Mellroth et al., 2012). However, in the absence of a signal peptide or known exporter, how this occurs and exactly what triggers this shift is unknown (Diaz et al., 1989). Here, we used CRISPRi-seq in combination with AMX treatment to identify a novel protein associated with autolysis, BeaU. BeaU is a small peptide of 80 amino acids, which localizes to the cell membrane with the C-terminus sitting intracellularly (Fig 5). Using *AlphaFold2-multimer*, we show that dimer or trimer forms

of BeaU are plausible, although further experiments to elucidate the multimeric state, such as *in vivo* crosslinking, would be necessary to confirm the *in-silico* modeling.

Deletion of *beaU* resulted in increased susceptibility to β-lactam antibiotics, as well as earlier onset of stationary phase lysis, both of which were shown to be LytA-dependent (Fig 4A-C). LytA dependence could indicate either a direct or indirect role for BeaU in its regulation. A preliminary assay with purified rLytA protein treatment showed increased susceptibility upon *beaU* deletion to extracellular LytA, indicating that any regulatory function is taking place outside of the cell (Fig 4D). One possibility is a direct interaction of the N-terminus of BeaU with LytA, although this seems unlikely given that only four amino acids of BeaU are predicted to be outside the membrane, and LytA is known to be associated with choline residues on LTA and WTA, suggesting some distance between proteins (Giudicelli and Tomasz, 1984). However, a direct BeaU-LytA interaction could be tested for using a split luciferase assay, where BeaU is tagged at the N-terminus with a luciferase fragment, and the complementary fragment fused to LytA. Emission of light can then be measured if the luciferase fragments are brought close enough together to reconstitute the enzyme, although strict controls would be necessary to confirm the N-terminal BeaU-luciferase fusion localizes correctly (Kato and Jones, 2010).

The alternative hypothesis is that the absence of BeaU modifies the cell wall structure in a way that increases the ability of LytA to interact with its enzymatic substrate. This is supported by the increased susceptibility of the *ΔbeaU* mutant to phage lysin, although this experiment should be repeated in *ΔlytA* mutants to control for potential combinatorial effects of the two lysins. Predicted genetic interactions with LTA synthesis protein *lafB*, cell elongation factor *cozEa*, and divisome members *divIB* and *divIC* also correlate with this hypothesis, although *in vivo* confirmation of CRISPRi-seq hits remains to be performed (Fig 6).

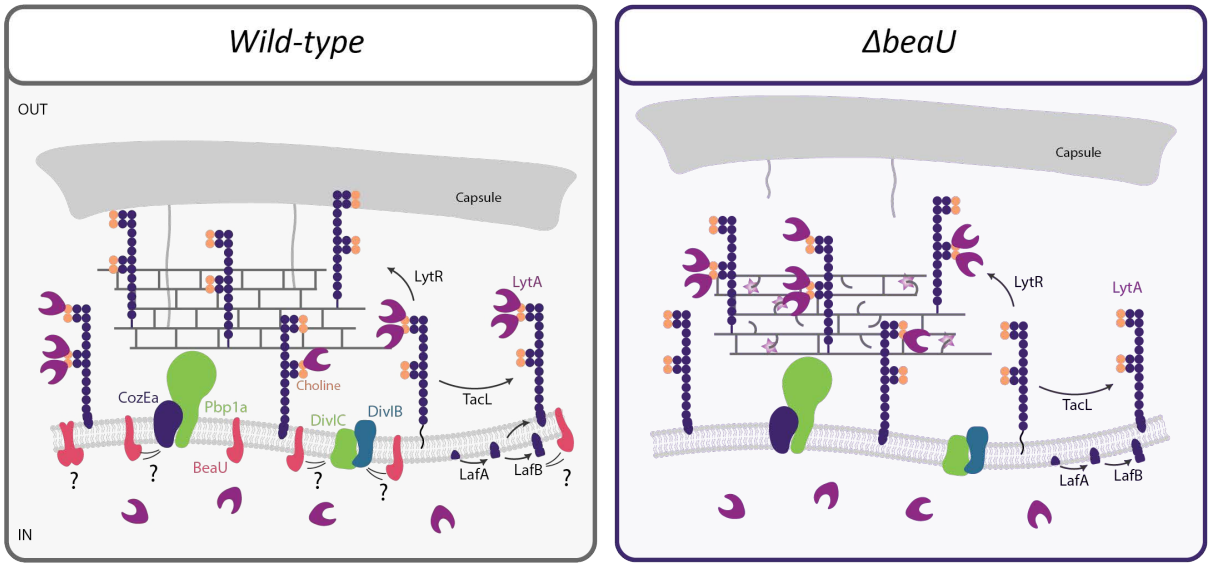


**Figure 7: Schematic showing the hypothesised role of BeaU in controlling autolysis in the pneumococcus**. Pneumococcal cells autolyze by the action of LytA in stationary phase, presumably to shed their capsule and cause inflammation in the host through release of pneumolysin and other antigens such as cell wall fragments. Cell wall targeting antibiotics stimulate LytA-dependent autolysis by a yet unknown mechanism. Here, we discovered the protein BeaU as important in autolysis control, as mutants prematurely lyse in late stationary phase in a LytA-dependent manner. The exact mode of action of BeaU in autolysis control is unknown. However, we show that BeaU has a short transmembrane domain at its N-terminus with its C-terminus residing intracellularly. It may exist as a monomer, dimer, or trimer. Predicted genetic interactions include *cozEa*, *divIB*, *divIC*, *lafB*, and *lytR*, but remain to be confirmed experimentally. Together, our data strongly suggests that BeaU is an indirect regulator of autolysis.

In principle, alterations to either phosphorylcholine present on LTA or WTA could impact the amidase activity of LytA (Fig. 7). It has previously been hypothesized that mature PG is capped, which, alongside the continuous activity of cell wall synthesis proteins at the septum during active growth, restricts LytA access to the glycan-peptide amide bond. When synthesis is stalled, then LytA can access uncapped nascent peptidoglycan at the septum (Bonnet et al., 2018; Mellroth et al., 2012). If the predicted genetic interactions with PG synthesis and division related genes are confirmed, this could suggest BeaU is involved in PG synthesis, either through direct protein-protein interactions, or as some sort of general support structure in the cell membrane. In this case, deletion of *beaU* may affect the activity of PG synthesizing enzymes in the membrane, allowing LytA better access to nascent PG. We plan to perform PG digestion combined with high-performance liquid chromatography to explore any differences in muropeptide composition between wild-type D39V compared to the *ΔbeaU* mutant (Hakenbeck et al., 1998).

Another study has hypothesized that LytA is sequestered on phosphorylcholine residues on the LTA during early stationary phase, and that LTA synthesis via TacL is then downregulated. This then allows for increased WTA synthesis and forces a shift of LytA from LTA towards WTA as the relative abundancies change, allowing access to the substrate (Flores-Kim et al., 2019). Interestingly, using CRISPRi-seq, we found that repression of *lafB* had a beneficial effect on fitness in a *ΔbeaU* mutant, indicating a reduction in essentiality in the absence of BeaU. LafB is a glycosyltransferase involved in glycolipid formation. The LTA anchor is thought to be glucosyl-diacylglycerol (Glc-DAG), with glucose group added to DAG by LafA(Chapter 1, Fig 1). LafB then produces GalGlc-DAG but its importance for LTA production in the pneumococcus is not known (Denapaite et al., 2012; Ho et al., 2008). In contrast, LytR, required for TA anchoring to the cell wall, became more essential in the *ΔbeaU* mutant. This could suggest that a shift from LTA to WTA synthesis is required in the *ΔbeaU* mutant, which may explain the increased autolysis phenotype.

Although the results from the CRISPRi-seq screen in the *ΔbeaU* mutant suggest several hypotheses to be explored, these genetic interactions are currently predictions and remain to be confirmed. The 12 operons identified as differentially fit in the mutant vs wild-type strain will be individually cloned as complements in the absence and presence of *beaU*. The predicted fitness effects can then be quantified, and growth can be assayed in the presence and absence of LytA-inducing conditions to further explore the roles of these proteins in BeaU function. In addition, it will be important to determine if the interactions with BeaU are indirect, or due to direct protein-protein contact. A split luciferase assay as well as fluorescently tagged protein co-localizations can be employed to explore any confirmed targets.

The use of CRISPRi-seq in combination with AMX-induced autolysis has allowed us to identify BeaU, a novel membrane protein hypothesized to play a role in the regulation of LytA-dependent autolysis. Control of the major pneumococcal autolysin is tightly linked to the cell wall and its synthesis, but is not well understood (Fig. 7). Identifying novel proteins such as BeaU that may be involved in these pathways furthers our knowledge of both important antibiotic targets and essential virulence factors of *S. pneumoniae*.

## Methods

### *Bacterial strains, growth conditions, and antibiotics*

*S. pneumoniae* strains (Table 1) were cultured in liquid C+Y medium, adapted from Adams and Roe (Martin et al., 1995), at 37°C with no shaking.

For transformation, *S. pneumoniae* culture in C+Y (pH 6.8) at $OD_{595}$ 0.1 was treated with 100 ng/ml synthetic CSP-1 for 12 min at 37°C, then incubated with DNA at 30°C for 20 min. After 1.5 hrs of recovery at 37°C, transformants were selected in Columbia agar supplemented with 3% defibrinated sheep blood (CBA, Thermo Scientific) and the appropriate antibiotic. Incubation occurred at 37°C in 5% $CO_2$ overnight. Successful transformants were confirmed by PCR and Sanger sequencing (Microsynth). Antibiotics used for selection were spectinomycin (100 µg/ml, spc), erythromycin (0.5 µg/ml, ery), chloramphenicol (3 µg/ml, chl), tetracycline (0.5 µg/ml, tet), kanamycin (250 µg/ml, kan), and gentamycin (80 µg/ml, gen). Strains were stocked at $OD_{595}$ 0.3 in C + Y with 15% glycerol at -80°C.

AMX (Sigma Aldrich) powder was dissolved initially in 100% DMSO. This solution was diluted in molecular grade water with 4% DMSO to two concentrations, 100 µg/mL and 1 mg/mL, and stored at -80°C.

**Table 1**: Strains used in study.

| Strain ID | Genotype and relevant characteristics | Reference |
|---|---|---|
| D39V | Serotype 2 laboratory strain | (Slager et al., 2018) |
| VL333 | *DCI23; prs1::F6-lacI (gen)* | (Synefiaridou and Veening, 2021) |
| VL1998 | *DCI23; bgaA::Plac-dCas9sp (tet); prs1::F6-lacI (gen)* | (Liu et al., 2021) |
| CRSP82 | *VL1998; $P_3$-sgRNA$^{eloR}$* | (Liu et al., 2021) |
| CRSP67 | *VL1998; $P_3$-sgRNA$^{pbp2b}$* | (Liu et al., 2021) |
| CRSP71 | *VL1998; $P_3$-sgRNA$^{beaU}$* | (Liu et al., 2021) |
| VL3460 | *D39V; ΔbeaU* | This study |
| VL4023 | *D39V; ZIP::Plac-beaU (spc); ΔbeaU::ery; prs1::F6-lacI-tetR (gen)* | This study |
| VL3660 | *D39V; Δcps* | (Synefiaridou and Veening, 2021) |
| VL4174 | AMX resistant D39V (recombinant pbp1a, pbp1b, pbp2x, murM) | (Gibson et al., 2021) |
| VL4742 | *D39V; ΔlytA::spc* | Laboratory collection |
| VL559 | *D39V; ΔlytB::chl* | Laboratory collection |
| VL5132 | *D39V; ΔlytA::spc; ΔlytB::chl* | This study |
| VL4453 | *D39V; ΔlytA::spc; ΔbeaU::ery* | This study |
| VL4454 | *D39V; ΔlytB::chl; ΔbeaU::ery* | This study |
| VL5118 | *D39V; ΔlytA::spc; ΔlytB::chl; ΔbeaU::ery* | This study |
| VL5119 | *VL3660; ΔlytA::spc* | This study |
| VL5129 | *VL3660; ΔlytB::chl* | This study |
| VL5106 | *VL3660; ΔbeaU::ery* | This study |
| VL5130 | *VL3660; ΔlytA::spc; ΔlytB::chl* | This study |

| | | |
|---|---|---|
| VL5120 | *VL3660; ΔlytA::spc; ΔbeaU::ery* | This study |
| VL5112 | *VL3660; ΔlytB::chl; ΔbeaU::ery* | This study |
| VL5131 | *VL3660; ΔlytA::spc; ΔlytB::chl; ΔbeaU::ery* | This study |
| VL5114 | *VL4174; ΔlytA::spc* | This study |
| VL5122 | *VL4174; ΔlytB::chl* | This study |
| VL5113 | *VL4174; ΔbeaU::ery* | This study |
| VL5133 | *VL4174; ΔlytA::spc; ΔlytB::chl* | This study |
| VL5115 | *VL4174; ΔlytA::spc; ΔbeaU::ery* | This study |
| VL5134 | *VL4174; ΔlytB::chl; ΔbeaUF::ery* | This study |
| VL5135 | *VL4174; ΔlytA::spc; ΔlytB::chl; ΔbeaU::ery* | This study |
| VL4665 | *D39V; ZIP::Plac-tacL (tmp), bgaA::PssbB-luc (tet); prs1::PF6-lacI-tetR (gen); tacL::ery* | Laboratory collection |
| VL4502 | *D39V; prs1::lacI-tetR (gen); beaU::eryR; CIL::Plac-Hibit-beaU(kan)* | This study |
| VL4503 | *D39V; prs1::lacI-tetR (gen); beaU::eryR; CIL::Plac-beaU-Hibit (kan)* | This study |
| VL4461 | *D39V; beaU::beaU-msfGFP (spc)* | This study |
| VL4477 | *D39V; prs1::lacI-tetR(gen); ZIP::Plac-GFP-beaU (spc); ΔbeaU::ery* | This study |
| VL4038 | *DCI23; ΔbeaU::ery* | This study |

***CRISPRi-seq screening***

For an operon-wide study of amoxicillin stress on *S. pneumoniae*, the recently developed CRISPRi-seq technique was performed (de Bakker et al., 2022; Liu et al., 2021). A D39V library of 1499 single guide RNAs (sgRNA) targeting almost all operons in the genome was used, with *dcas9* under control of the IPTG-inducible promoter $P_{lac}$ (Liu et al., 2021).

The library was pre-cultured to $OD_{595}$ 0.1, diluted 20-fold in C+Y +/- IPTG (40 μM) and incubated 2 hrs. To test survival in an AMX bottleneck, induced and non-induced cultures were split into two tubes of 2mL C + Y (IPTG where appropriate), and one tube of each was treated with AMX 0.01 μg/mL for two hours, a treatment determined to be sufficient to kill 99% of cells. Cells were washed, then grown to $OD_{595}$ 0.4 in 10 mL fresh C + Y. Final cell cultures were pelleted for genomic DNA isolation. The protocol was replicated four times.

Cultures were pelleted by centrifugation, then resuspended in Nuclei Lysis solution (Promega) supplemented with 0.05 % SDS, 0.025 % deoxycholate (DOC), and 200 μg/mL RNase A. This was incubated at 37°C for 20 minutes, 80°C for 5 minutes, then 37°C for 10 minutes. Protein Precipitation Solution (Promega) was added to the lysate, vortexed vigorously, then incubated on ice for 10 minutes. The precipitated protein was pelleted by centrifugation and the supernatant transferred into isopropanol to precipitate the DNA, which was then collected by centrifugation. DNA was washed once in 70% ethanol before air drying and resuspension in the appropriate buffer (either TE buffer or molecular grade water). DNA was run on a 1% agarose gel to confirm no significant degradation had occurred, and stored at 4°C.

Library sgRNAs for each sample were amplified from genomic DNA with 12 cycles of PCR, with primers designed to bind to the Illumina read 1 and read 2 elements, which are on the plasmid on either side of the sgRNA. In addition, each primer had Illumina barcodes included, unique pairs were used for every replicate (32 sets), allowing de-multiplexing after the sequencing run (Liu et al., 2021). PCR products were quantified, diluted, and denatured according to the Illumina standard protocol. All replicates for both experimental approaches were sequenced concurrently using a high-output 300 cycle kit on an Illumina Miniseq sequencer for a 150bp paired end run.

20 bp sgRNA sequences were extracted from each read, quality checked, and counted in 2Fast2Q using default settings (Bravo et al., 2021). Raw count data was normalized and analyzed using DESeq2 (Anders and Huber, 2010), where a generalized linear model was used to test the interaction effect between AMX and IPTG on sgRNA abundance. A significant interaction indicates that the presence of IPTG has a different effect on cells treated with AMX compared to non-AMX treated cells and is tested for each sgRNA in the pool. Results were filtered on both the significance of this interaction (FDR adjusted $p < 0.05$), and on the size of the fold-change in sgRNA abundancy between plus AMX and minus AMX in the presence of IPTG ($log_2$fold-change > 2) (de Bakker et al., 2022). The hits were then short listed for confirmation based on gene products and the literature.

Selected hits were confirmed by cloning individual sgRNAs into the same *S. pneumoniae* background as the pooled library. Strains were tested by inducing for two hours with IPTG, diluting to $OD_{595}$ 0.001 in fresh C + Y with or without AMX and grown in a plate reader to determine growth curves. The amoxicillin concentration used depended on whether downregulation of the operon had caused a fitness loss (0.006 µg/mL) or a fitness gain (0.01 µg/mL) in the presence of the antibiotic.

CRISPRi-seq to compare operon fitness in wild-type D39V vs the *ΔbeaU* mutant was performed similarly, with some modifications. The sgRNA library was introduced into strain *ΔbeaU::ery, bgaA::Plac-dcas9(sp)(tet); prs1::PF6-lacI-tetR (gen)* (VL4038, Table 1) as was done previously for D39V (Liu et al., 2021). Both libraries were precultured to $OD_{595}$ 0.1, diluted 20-fold into fresh media +/- 1mM IPTG then grown to $OD_{595}$ 0.1, before being diluted 20-fold into fresh media (+/- IPTG as required) again. Samples were grown to $OD_{595}$ 0.4, and pelleted. From this point samples were processed in the same way as above. The experiment was performed in triplicate.

***Bioinformatic protein characterization***

Proteins of unknown functions identified in the CRISPRi-seq screen were run through TMHMM pred to identify any putative transmembrane domains, and signal 6.0 for signal peptide sequences. StringDB was used to search for any known genetic or protein interactions. BeaU (SPV_1662) was modelled using the Alphafold2 Colab notebook (dpmd.ai/alphafold-colab) (Evans et al., 2021; Jumper et al., 2021). It was performed in both monomer and multimer mode with the published D39V sequence as input (Slager et al., 2018).

***Cloning***

All constructs were assembled from PCR products using a one-pot Golden Gate assembly (Engler et al., 2009). The type II restriction enzyme used was BsmBI in all cases. Primers used for amplification can be found in Table S3, and are organized by construct for ease of use.

***Growth curves and analysis***

Strains were precultured in C + Y broth to OD 0.1, then diluted 100-fold into 96-well microtiter plates, containing fresh C + Y with antibiotics and IPTG to appropriate concentrations as required. The $OD_{595}$ was measured every 10 min for 24 hr in a plate reader (Infinite F200, Tecan) with incubation at 37°C. All conditions were tested in duplicate or triplicate.

Experiments with purified lysins were performed in the same way, and lysin was added right before initiating the plate reader experiment.

Area under the curve (AUC) for the 12-24 hour autolysis timeframe was determined using TecanExtracter (Dénéréaz, unpublished). The mean and standard error of the mean (SEM) of the normalized AUC was determined for three biological replicates.

Statistical significance of AUC was determined using one-way ANOVA with a Tukey correction for multiple testing.

***Microscopy***

For time-lapse microscopy, cells were pre-cultured in liquid C + Y medium at 37°C and spotted on a low-melting 1.2% C + Y agarose patch, with or without AMX at the appropriate concentration. Phase contrast and fluorescent images were taken every 10 min as described (de Jong et al., 2011) using a Leica DMi8 with a 100x phase contrast objective. GFP fluorescence was detected using 100ms exposure.

For still images stained with DAPI and Nile red, cells were pre-cultured in the same way, then 1 µl of 1 mg/ml Nile red was added to the tube, and incubated at room temperature for 4 min. Then, 1 µl of 1 mg/ml DAPI was added and the mix was incubated for one more minute. Cells were centrifuged and resuspended in fresh PBS, before spotting on a low-melting 1.2% C + Y agarose patch with or without IPTG or AMX. Phase contrast, DAPI and Nile red images were obtained with a Leica DMi8 and 100x phase contrast objective.

Images were processed using ImageJ.

***Nano-Glo HiBiT extracellular detection assay***

*S. pneumoniae* HiBit fusion strains VL4502 and VL4503 for BeaU, VL4058 and VL4059 for control protein Spv_0963, and negative control D39V were used in the assay. Strains were diluted 10-fold in C+Y +/- IPTG (1 mM), then grown to $OD_{595}$ 0.3. Half of each culture was then incubated with phage lysin Cpl-1 (8 µg/ml) for 20min at 37°C, while the remaining aliquot was left intact. Reagents from the Nano-Glo® HiBiT extracellular detection assay (Promega) were prepared in a 96-well black-wall plate according to kit instructions, then samples were mixed into the appropriate wells. Luminescence was read every 5 min for 30 min with 1 s integration time at 30°C in a Tecan plate reader.

## Acknowledgments

We would like to thank Gregory Resch for the purified phage lysin (Cpl-1), as well as Josué Flores Kim, Thomas Bernhardt, and David Rudner for the purified rLytA which made these experiments possible. We would also like to thank Julien Dénéréaz, Florian Bock, and Clement Gallay for their invaluable expertise, and the entire Veening and Gruber labs for their creative input.

P.G. was supported by the University of Lausanne Faculty of Biology and Medicine PhD fellowship. Work in the Veening lab is supported by the Swiss National Science Foundation (SNSF) (project grant 310030_192517), SNSF JPIAMR grant (40AR40_185533), SNSF NCCR 'AntiResist' (51NF40_180541) and ERC consolidator grant 771534-PneumoCaTChER.

## References

Anders S, Huber W. 2010. Differential expression analysis for sequence count data. *Genome Biology* **11**:R106. doi:10.1186/gb-2010-11-10-r106

Aprianto R, Slager J, Holsappel S, Veening JW. 2018. High-resolution analysis of the pneumococcal transcriptome under a wide range of infection-relevant conditions. *Nucleic Acids Research* **46**:9990–10006. doi:10.1093/nar/gky750

Avery OT, Cullen GE. 1923. Studies on the enzymes of pneumococcus: IV. Bacteriolytic enzyme. *Journal of Experimental Medicine* **38**:199–206. doi:10.1084/jem.38.2.199

Beiter K, Wartha F, Hurwitz R, Normark S, Zychlinsky A, Henriques-Normark B. 2008. The capsule sensitizes *Streptococcus pneumoniae* to α-defensins human neutrophil proteins 1 to 3. *Infection and Immunity* **76**:3710–3716. doi:10.1128/IAI.01748-07

Berry AM, Lock RA, Hansman D, Paton JC. 1989. Contribution of autolysin to virulence of *Streptococcus pneumoniae*. *Infection and Immunity* **57**:2324–2330. doi:10.1128/iai.57.8.2324-2330.1989

Berry AM, Paton JC. 2000. Additive attenuation of virulence of *Streptococcus pneumoniae* by mutation of the genes encoding pneumolysin and other putative pneumococcal virulence proteins. *Infection and Immunity* **68**:133–140. doi:10.1128/IAI.68.1.133-140.2000

Bonnet J, Durmort C, Mortier-Barrière I, Campo N, Jacq M, Moriscot C, Straume D, Berg KH, Håvarstein L, Wong YS, Vernet T, di Guilmi AM. 2018. Nascent teichoic acids insertion

into the cell wall directs the localization and activity of the major pneumococcal autolysin LytA. *Cell Surface* **2**:24–37. doi:10.1016/j.tcsw.2018.05.001

Bravo AM, Typas A, Veening J-W. 2021. 2FAST2Q: A general-purpose sequence search and counting program for FASTQ files. *bioRxiv* 2021.12.17.473121. doi:10.1101/2021.12.17.473121

Briese T, Hakenbeck R. 1985. Interaction of the pneumococcal amidase with lipoteichoic acid and choline. *European Journal of Biochemistry* **146**:417–427. doi:10.1111/j.1432-1033.1985.tb08668.x

Càmara J, Cubero M, Martín-Galiano AJ, García E, Grau I, Nielsen JB, Worning P, Tubau F, Pallarés R, Domínguez MÁ, Kilian M, Liñares J, Westh H, Ardanuy C. 2018. Evolution of the β-lactam-resistant *Streptococcus pneumoniae* PMEN3 clone over a 30 year period in Barcelona, Spain. *Journal of Antimicrobial Chemotherapy* **73**:2941–2951. doi:10.1093/jac/dky305

Canvin JR, Marvin AP, Sivakumaran M, Paton JC, Boulnois GJ, Andrew PW, Mitchell TJ. 1995. The Role of Pneumolysin and Autolysin in the Pathology of Pneumonia and Septicemia in Mice Infected with a Type 2 Pneumococcus. *Journal of Infectious Diseases* **172**:119–123. doi:10.1093/infdis/172.1.119

Cho H, Uehara T, Bernhardt TG. 2014. Beta-Lactam Antibiotics Induce a Lethal Malfunctioning of the Bacterial Cell Wall Synthesis Machinery. *Cell* **159**:1300–1311.

Cundell DR, Weiser JN, Shen J, Young A, Tuomanen EI. 1995. Relationship between colonial morphology and adherence of *Streptococcus pneumoniae*. *Infection and Immunity* **63**:757–761. doi:10.1128/iai.63.3.757-761.1995

de Bakker V, Liu X, Bravo AM, Veening JW. 2022. CRISPRi-seq for genome-wide fitness quantification in bacteria. *Nature Protocols*. doi:10.1038/s41596-021-00639-6

Denapaite D, Brückner R, Hakenbeck R, Vollmer W. 2012. Biosynthesis of teichoic acids in *Streptococcus pneumoniae* and closely related species: Lessons from genomes. *Microbial Drug Resistance* **18**:344–358. doi:10.1089/MDR.2012.0026/ASSET/IMAGES/LARGE/FIGURE4.JPEG

Diaz E, Garcia E, Ascaso C, Mendez E, Lopez R, Garcia JL. 1989. Subcellular localization of the major pneumococcal autolysin: A peculiar mechanism of secretion in Escherichia coli. *Journal of Biological Chemistry* **264**:1238–1244. doi:10.1016/s0021-9258(19)85077-9

Doern G v, Brueggemann A, Holley HP, Rauch AM. 1996. Antimicrobial resistance of *Streptococcus pneumoniae* recovered from outpatients in the United States during the winter months of 1994 to 1995: results of a 30-center national surveillance study. *Antimicrob Agents Chemother* **40**:1208–13. doi:10.1128/AAC.40.5.1208

Doit C, Loukil C, Fitoussi F, Geslin P, Bingen E. 1999. Emergence in France of Multiple Clones of Clinical *Streptococcus pneumoniae* Isolates with High-Level Resistance to Amoxicillin. *Antimicrobial Agents and Chemotherapy* **43**:1480–1483. doi:10.1128/AAC.43.6.1480

Edman M, Berg S, Storm P, Wikström M, Vikström S, Öhman A, Wieslander Å. 2003. Structural features of glycosyltransferases synthesizing major bilayer and non bilayer-prone membrane lipids in *Acholeplasma laidlawii* and *Streptococcus pneumoniae*. *Journal of Biological Chemistry* **278**:8420–8428. doi:10.1074/jbc.M211492200

Engler C, Gruetzner R, Kandzia R, Marillonnet S. 2009. Golden gate shuffling: A one-pot DNA shuffling method based on type IIs restriction enzymes. *PLoS ONE* **4**:e5553. doi:10.1371/journal.pone.0005553

Evans R, O'Neill M, Pritzel A, Antropova N, Senior AW, Green T, Žídek A, Bates R, Blackwell S, Yim J, Ronneberger O, Bodenstein S, Zielinski M, Bridgland A, Potapenko A, Cowie A, Tunyasuvunakool K, Jain R, Clancy E, Kohli P, Jumper J, Hassabis D. 2021. Protein complex prediction with AlphaFold-Multimer, bioRxiv. Cold Spring Harbor Laboratory. doi:10.1101/2021.10.04.463034

Fenton AK, Mortaji L el, Lau DTC, Rudner DZ, Bernhardt TG. 2016. CozE is a member of the MreCD complex that directs cell elongation in *Streptococcus pneumoniae*. *Nature Microbiology* **2**:1–10. doi:10.1038/nmicrobiol.2016.237

Fernández-Tornero C, López R, García E, Giménez-Gallego G, Romero A. 2001. A novel solenoid fold in the cell wall anchoring domain of the pneumococcal virulence factor LytA. *Nature Structural Biology* **8**:1020–1024. doi:10.1038/nsb724

Fisher SL. 2008. Glutamate racemase as a target for drug discovery. *Microbial Biotechnology*. doi:10.1111/j.1751-7915.2008.00031.x

Flores-Kim J, Dobihal GS, Fenton A, Rudner DZ, Bernhardt TG. 2019. A switch in surface polymer biogenesis triggers growth-phase-dependent and antibiotic-induced bacteriolysis. *Elife* **8**. doi:10.7554/eLife.44912

Garcia E, Gareia -Luis, Garcia P. 1985. Cloning and expression of the pneumococcal autolysin gene in Escherichia coil **201**:225–230.

García P, García J, García E, López R. 1986. Nucleotide sequence and expression of the pneumococcal autolysin gene from its own promoter in Escherichia coli. *Gene* **43**:265–272. doi:10.1016/0378-1119(86)90215-5

Garcia P, Gonzalez MP, Garcia E, Lopez R, Garcia JL. 1999. LytB, a novel pneumococcal murein hydrolase essential for cell separation. *Molecular Microbiology* **31**:1275–1277. doi:10.1046/J.1365-2958.1999.01238.X

Gibson PS, Bexkens E, Zuber S, Cowley L, Veening J-W. 2021. The acquisition of clinically relevant amoxicillin resistance in *Streptococcus pneumoniae* requires ordered horizontal gene transfer of four loci. *bioRxiv* 2021.12.17.473165. doi:10.1101/2021.12.17.473165

Giudicelli S, Tomasz A. 1984. Attachment of pneumococcal autolysin to wall teichoic acids, an essential step in enzymatic wall degradation. *Journal of Bacteriology* **158**:1188–1190. doi:10.1128/jb.158.3.1188-1190.1984

Hakenbeck R, Nig AK, Kern I, van der Linden M, Keck W, Billot-Klein D, Legrand R, Schoot B, Gutmann L, König A, Kern I, van der Linden M, Keck W, Billot-Klein D, Legrand R, Schoot B, Gutmann L. 1998. Acquisition of Five High-M r Penicillin-Binding Protein Variants during Transfer of High-Level beta-Lactam Resistance from *Streptococcus mitis* to *Streptococcus pneumoniae*. *Journal of Bacteriology* **180**:1831–1840.

Hirst RA, Gosai B, Rutman A, Guerin CJ, Nicotera P, Andrew PW, O'Callaghan C. 2008. *Streptococcus pneumoniae* deficient in pneumolysin or autolysin has reduced virulence in meningitis. *Journal of Infectious Diseases* **197**:744–751. doi:10.1086/527322

Ho SS, Cartee RT, Pritchard DG, Nahm MH. 2008. A new model of pneumococcal lipoteichoic acid structure resolves biochemical, biosynthetic, and serologic inconsistencies of the current model. *J Bacteriol* **190**:2379–2387. doi:10.1128/JB.01795-07

Holtje J v., Tomasz A. 1975. Lipoteichoic acid: a specific inhibitor of autolysin activity in pneumococcus. *Proc Natl Acad Sci U S A* **72**:1690–1694. doi:10.1073/pnas.72.5.1690

Howard L v., Gooder H. 1974. Specificity of the autolysin of Streptococcus (Diplococcus) pneumoniae. *Journal of Bacteriology* **117**:796–804. doi:10.1128/jb.117.2.796-804.1974

Jumper J, Evans R, Pritzel A, Green T, Figurnov M, Ronneberger O, Tunyasuvunakool K, Bates R, Žídek A, Potapenko A, Bridgland A, Meyer C, Kohl SAA, Ballard AJ, Cowie A, Romera-Paredes B, Nikolov S, Jain R, Adler J, Back T, Petersen S, Reiman D, Clancy E, Zielinski M, Steinegger M, Pacholska M, Berghammer T, Bodenstein S, Silver D, Vinyals O, Senior AW, Kavukcuoglu K, Kohli P, Hassabis D. 2021. Highly accurate protein structure prediction with AlphaFold. *Nature* **596**:583–589. doi:10.1038/s41586-021-03819-2

Kato N, Jones J. 2010. The split luciferase complementation assay. *Methods Mol Biol* **655**:359–376. doi:10.1007/978-1-60761-765-5_24

Keller LE, Rueff AS, Kurushima J, Veening JW. 2019. Three new integration vectors and fluorescent proteins for use in the opportunistic human pathogen *Streptococcus pneumoniae*. *Genes (Basel)* **10**:394. doi:10.3390/genes10050394

Kietzman CC, Gao G, Mann B, Myers L, Tuomanen EI. 2016. Dynamic capsule restructuring by the main pneumococcal autolysin LytA in response to the epithelium. *Nature Communications* **7**. doi:10.1038/NCOMMS10859

Liu HH, Tomasz A. 1985. Penicillin Tolerance in Multiply Drug-Resistant Natural Isolates of *Streptococcus pneumoniae*. *The Journal of Infectious Diseases* **152**:365–372. doi:10.1093/INFDIS/152.2.365

Liu X, Kimmey JM, Matarazzo L, de Bakker V, van Maele L, Sirard JC, Nizet V, Veening JW. 2021. Exploration of Bacterial Bottlenecks and *Streptococcus pneumoniae* Pathogenesis by CRISPRi-Seq. *Cell Host and Microbe* **29**:107-120.e6. doi:10.1016/j.chom.2020.10.001

Llobet E, Tomás JM, Bengoechea JA. 2008. Capsule polysaccharide is a bacterial decoy for antimicrobial peptides. *Microbiology (N Y)* **154**:3877–3886. doi:10.1099/mic.0.2008/022301-0

Lock RA, Hansman D, Paton JC. 1992. Comparative efficacy of autolysin and pneumolysin as immunogens protecting mice against infection by *Streptococcus pneumoniae*. *Microbial Pathogenesis* **12**:137–143. doi:10.1016/0882-4010(92)90116-6

Martin B, Garcia P, Castanié M -P, Claverys J -P. 1995. The recA gene of *Streptococcus pneumoniae* is part of a competence-induced operon and controls lysogenic induction. *Molecular Microbiology* **15**:367–379. doi:10.1111/j.1365-2958.1995.tb02250.x

Mellroth P, Daniels R, Eberhardt A, Rönnlund D, Blom H, Widengren J, Normark S, Henriques-Normark B. 2012. LytA, major autolysin of *Streptococcus pneumoniae*, requires access to nascent peptidoglycan. *Journal of Biological Chemistry* **287**:11018–11029. doi:10.1074/JBC.M111.318584/ATTACHMENT/8F67F731-D0C0-4B34-889A-534F3E51B2D1/MMC1.ZIP

Moreillon P, Tomasz A, Tomasz A. 1988. Penicillin Resistance and Defective Lysis in Clinical Isolates of Pneumococci: Evidence for Two Kinds of Antibiotic Pressure Operating in the Clinical Environment. *The Journal of Infectious Diseases* **157**:1150–1157. doi:10.1093/INFDIS/157.6.1150

Moscoso M, Domenech M, García E. 2010. Vancomycin tolerance in clinical and laboratory *Streptococcus pneumoniae* isolates depends on reduced enzyme activity of the major LytA autolysin or cooperation between CiaH histidine kinase and capsular polysaccharide. *Molecular Microbiology* **77**.

Noirclerc-Savoye M, le Gouëllec A, Morlot C, Dideberg O, Vernet T, Zapun A. 2005. In vitro reconstitution of a trimeric complex of DivIB, DivIC and FtsL, and their transient co-localization at the division site in *Streptococcus pneumoniae*. *Molecular Microbiology* **55**:413–424. doi:10.1111/j.1365-2958.2004.04408.x

Novak R, Henriques B, Charpentier E, Normark S, Tuomanen E. 1999. Emergence of vancomycin tolerance in *Streptococcus pneumoniae*. *Nature* **399**:590–593. doi:10.1038/21202

Nunes S, Sá-Leão R, Carriço J, Alves CR, Mato R, Brito Avô A, Saldanha J, Almeida JS, Santos Sanches I, de Lencastre H. 2005. Trends in drug resistance, serotypes, and molecular types of *Streptococcus pneumoniae* colonizing preschool-age children attending day care centers in Lisbon, Portugal: A summary of 4 years of annual surveillance. *Journal of Clinical Microbiology* **43**:1285–1293. doi:10.1128/JCM.43.3.1285-1293.2005

Olivares A, Olivares Trejo J, Arellano-Galindo J, Zuñiga G, Escalona G, Carlos Vigueras J, Marín P, Xicohtencatl J, Valencia P, Velázquez-Guadarrama N. 2011. *pep27* and *lytA* in Vancomycin-Tolerant Pneumococci. *J Microbiol Biotechnol* **21**:1345–1351. doi:10.4014/jmb.1105.05045

Reichmann NT, Gründling A. 2011. Location, synthesis and function of glycolipids and polyglycerolphosphate lipoteichoic acid in Gram-positive bacteria of the phylum Firmicutes. *FEMS Microbiology Letters*. doi:10.1111/j.1574-6968.2011.02260.x

Rogers PD, Liu TT, Barker KS, Hilliard GM, English BK, Thornton J, Swiatlo E, McDaniel LS. 2007. Gene expression profiling of the response of *Streptococcus pneumoniae* to penicillin. *Journal of Antimicrobial Chemotherapy* **59**:616–626. doi:10.1093/jac/dkl560

Schwinn MK, Machleidt T, Zimmerman K, Eggers CT, Dixon AS, Hurst R, Hall MP, Encell LP, Binkowski BF, Wood K v. 2018. CRISPR-Mediated Tagging of Endogenous Proteins with a Luminescent Peptide. *ACS Chemical Biology* **13**:467–474. doi:10.1021/acschembio.7b00549

Slager J, Aprianto R, Veening JW. 2018. Deep genome annotation of the opportunistic human pathogen *Streptococcus pneumoniae* D39. *Nucleic Acids Research* **46**:9971–9989. doi:10.1093/nar/gky725

Stamsås GA, Straume D, Ruud Winther A, Kjos M, Frantzen CA, Håvarstein LS. 2017. Identification of EloR (Spr1851) as a regulator of cell elongation in *Streptococcus pneumoniae*. *Molecular Microbiology* **105**:954–967. doi:10.1111/mmi.13748

Synefiaridou D, Veening JW. 2021. Harnessing CRISPR-Cas9 for Genome Editing in *Streptococcus pneumoniae* D39V. *Applied and Environmental Microbiology* **87**:1–15. doi:10.1128/AEM.02762-20

Tomasz A. 1968. Biological consequences of the replacement of choline by ethanolamine in the cell wall of Pneumococcus: chain formation, loss of transformability, and loss of autolysis. *Proc Natl Acad Sci U S A* **59**:86–93. doi:10.1073/pnas.59.1.86

Tomasz A, Waks S. 1975. Mechanism of action of penicillin: triggering of the pneumococcal autolytic enzyme by inhibitors of cell wall synthesis. *Proc Natl Acad Sci U S A* **72**:4162–4166. doi:10.1073/pnas.72.10.4162

Tsui HCT, Zheng JJ, Magallon AN, Ryan JD, Yunck R, Rued BE, Bernhardt TG, Winkler ME. 2016. Suppression of a deletion mutation in the gene encoding essential PBP2b reveals a new

lytic transglycosylase involved in peripheral peptidoglycan synthesis in *Streptococcus pneumoniae* D39. *Molecular Microbiology* **100**:1039–1065. doi:10.1111/mmi.13366

Tuomanen E. 1999. Molecular and cellular biology of pneumococcal infection. *Current Opinion in Microbiology* **2**:35–39. doi:10.1016/S1369-5274(99)80006-X

Uehara T, Bernhardt TG. 2011. More than just lysins: peptidoglycan hydrolases tailor the cell wall. *Current Opinion in Microbiology* **14**:698–703. doi:10.1016/J.MIB.2011.10.003

Vollmer W, Joris B, Charlier P, Foster S. 2008. Bacterial peptidoglycan (murein) hydrolases. *FEMS Microbiology Reviews*. doi:10.1111/j.1574-6976.2007.00099.x

Winther AR, Kjos M, Herigstad ML, Håvarstein LS, Straume D. 2021. EloR Interacts with the Lytic Transglycosylase MltG at Midcell in *Streptococcus pneumoniae* R6. *Journal of Bacteriology* **203**. doi:10.1128/JB.00691-20

Ye W, Zhang J, Shu Z, Yin Y, Zhang X, Wu K. 2018. Pneumococcal LytR protein is required for the surface attachment of both capsular polysaccharide and teichoic acids: Essential for pneumococcal virulence. *Frontiers in Microbiology* **9**:1199. doi:10.3389/fmicb.2018.01199

## Supplementary Figures

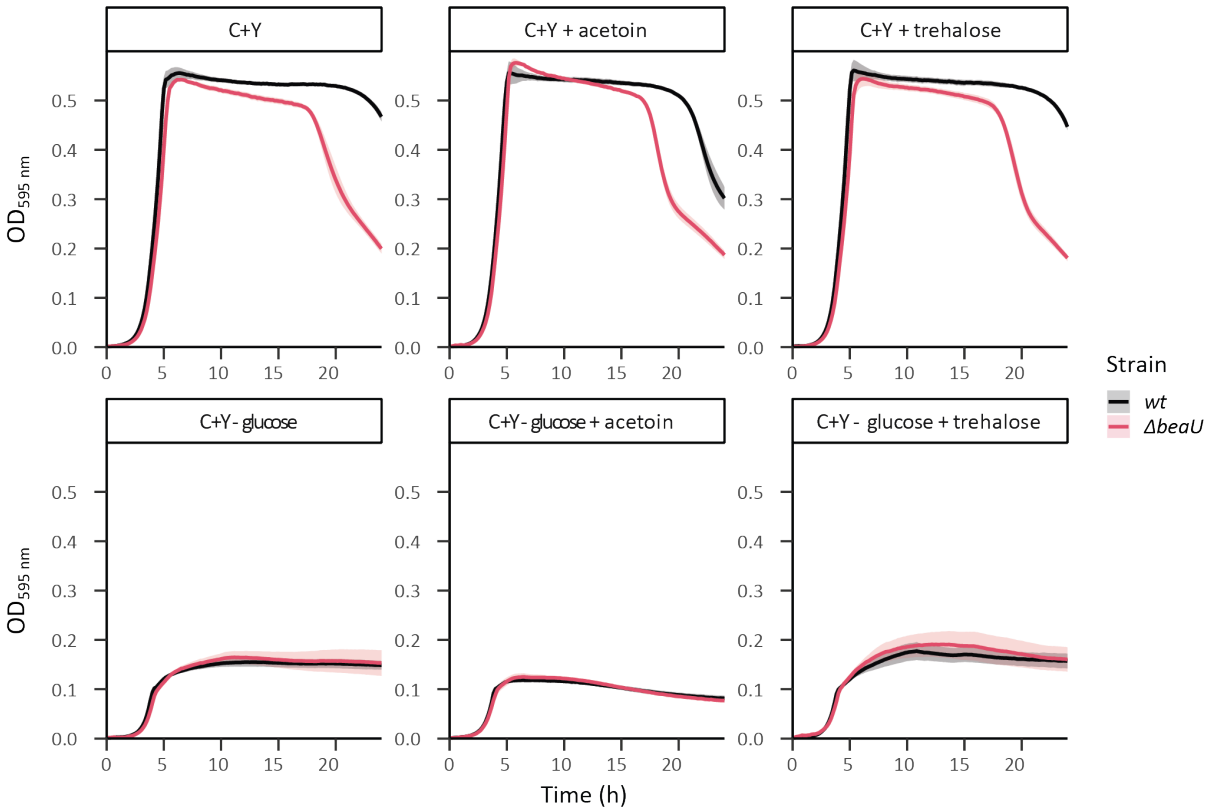


**Figure S1: Growth of D39V and ΔbeaU in C + Y medium supplemented with acetoin or trehalose.** Growth in the absence of glucose also shown (second row).

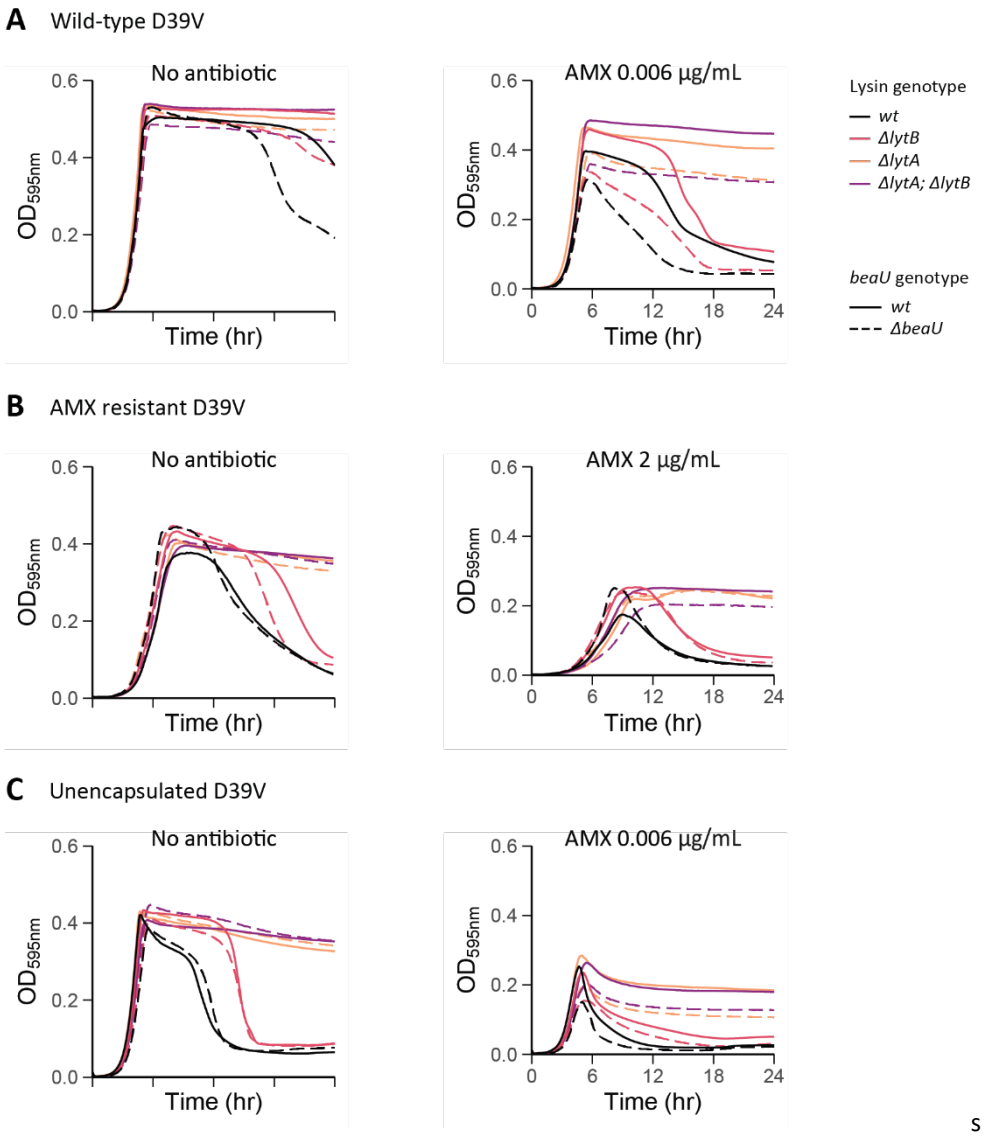


**Figure S2: AMX-induced lysis of ΔbeaU mutants is dependent on LytA.** Growth curves of *ΔlytA*, *ΔlytB*, and *ΔbeaU* mutants in (A) D39V, (B) AMX resistant D39V (VL4174), and (C) *Δcps* D39V (VL3660) in the presence of sublethal AMX. Corresponds to AUC data shown in Fig 4A-C.

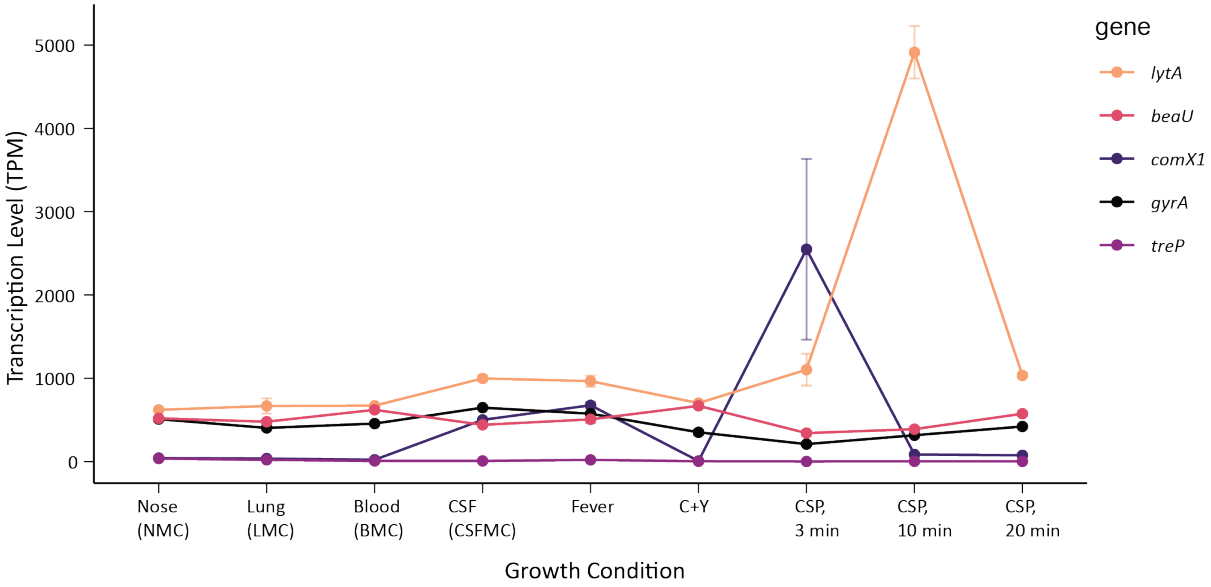


**Figure S3: Transcription levels of *beaU* in different growth conditions**. Transcription levels of *lytA*, *gyrA*, *comX1* (transcription activated upon competence), *treP* (located upstream of *beaU*) are shown for comparison. Transcription is measured as transcripts per million (TPM) (Aprianto et al., 2018).

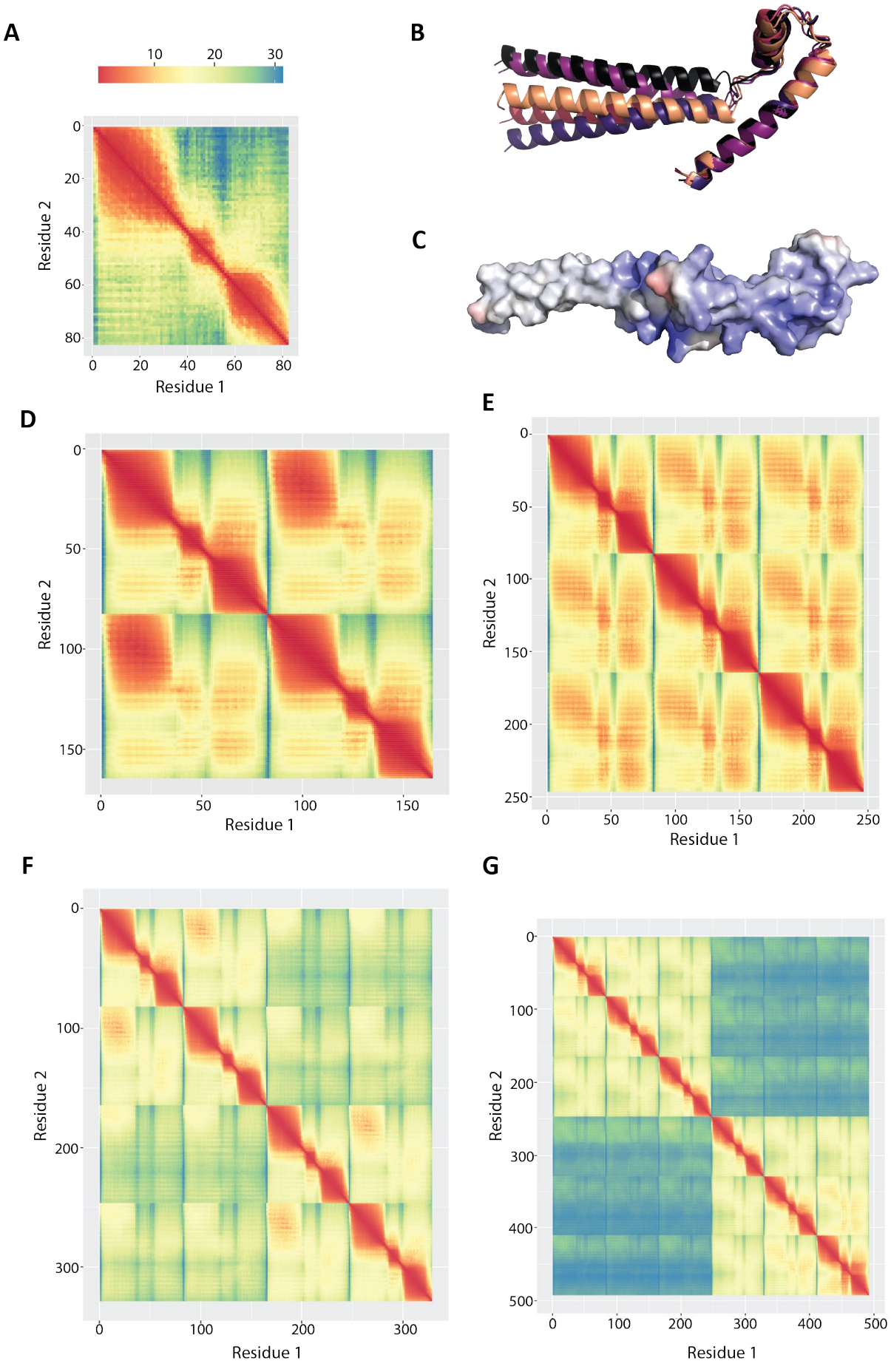
A
10
20
30
Residue 2
Residue 1
B
C
D
Residue 2
Residue 1
E
Residue 2
Residue 1
F
Residue 2
Residue 1
G
Residue 2
Residue 1

**Figure S4: in silico modelling of BeaU shows positive charge at C-terminus and reveals potential multimer formation.** (A) PAE heat map shows high confidence in the model predicted by *Alphafold2*. (B) Several iterations of the *Alphafold2* prediction of BeaU as a monomer show very similar models, with some flexibility in the linkers between α-helices. (C) Plot of the electrostatic charge over the surface of BeaU. The nonpolar nature of the predicted transmembrane N-helix is shown, with some charge carrying residues located at the cytoplasmic C-terminus. (D) *AlphaFold2-multimer* was used to model BeaU as a dimer, (E) trimer, (F) tetramer, and (G) hexamer. Heatmaps of the PAE values show high confidence in the dimer and trimer predictions, while tetramer and hexamer predictions simply showed bundling of dimer and trimer units. The accuracy of the prediction would need to be confirmed *in vivo*. Associated with Fig. 5A-D.

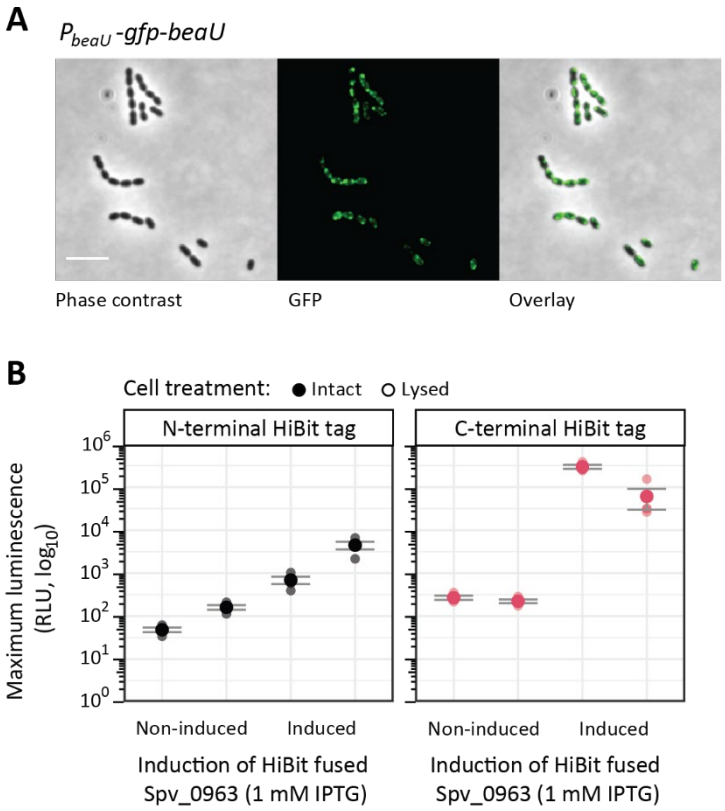


**Figure S5: Validation of HiBit and GFP fusions used in the study.** (A) N-terminal GFP fusion with BeaU showed poor localization, with foci occurring at the poles, suggesting protein degradation. (B) RLU plots of the NanoLuc HiBit Extracellular assay performed with known membrane protein SPV_0963, to validate the protocol prior to testing with BeaU. Associated with Fig. 5EF.

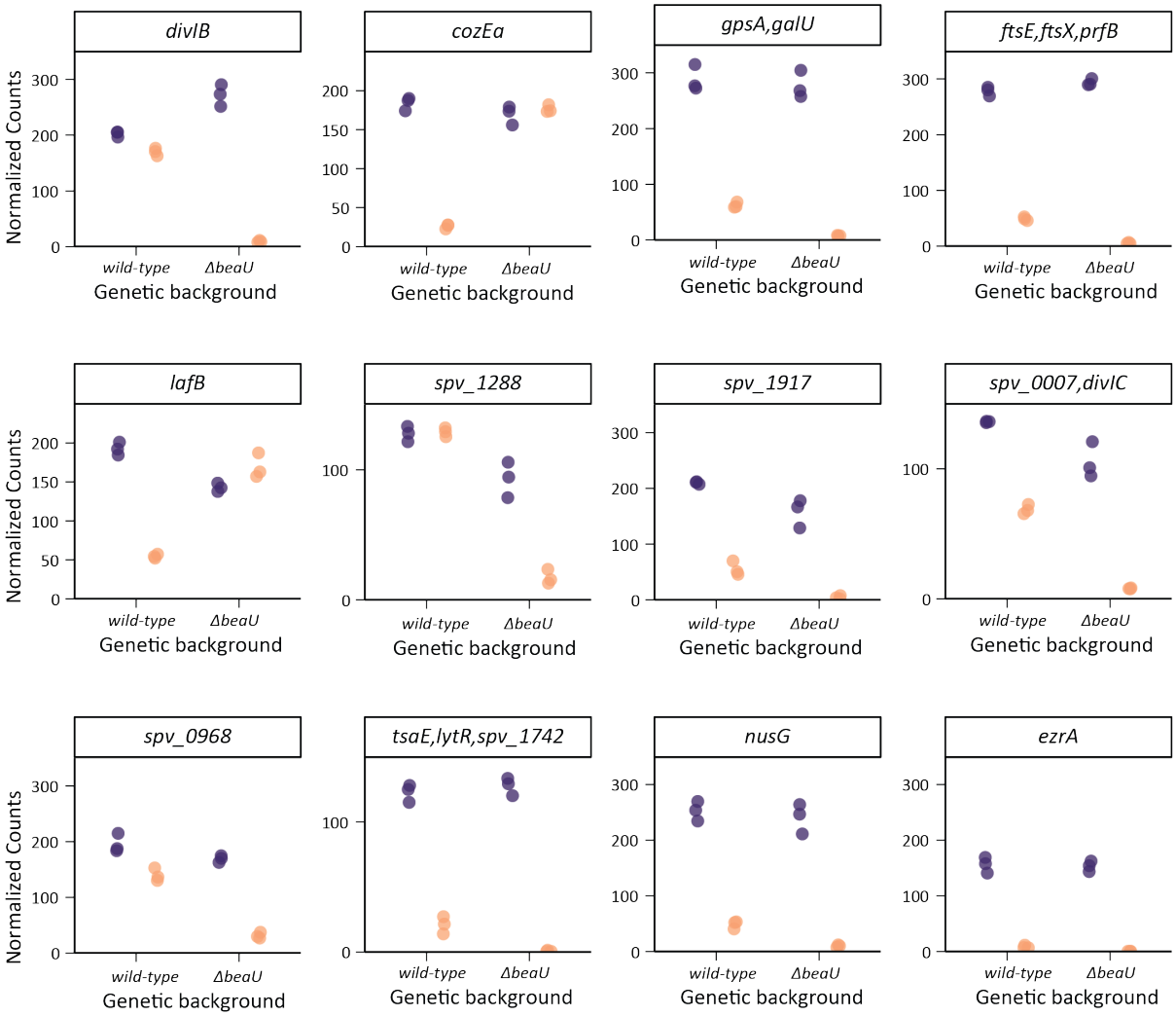


**Figure S6: Normalized read count plots of the 12 operons identified by CRISPRi-seq in the *ΔbeaU* mutant.** Values for each operon in induced (orange) and non-induced (purple) samples of the wild-type D39V and *ΔbeaU* CRISPRi libraries are shown. Associated with Fig 6.

## Supplementary Tables

**Table S1: Significance of lysis effects observed in the presence or absence of lysins in wild-type or ΔbeaU backgrounds .** An ANOVA with Tukey HSD correction for multiple testing was used to test for significant effects of lytA and lytB presence in wild-type or *ΔbeaU* backgrounds of D39V, VL3660, and VL4174. The adjusted *p*-values for each combination are shown here.

| **D39V** | | |
|---|---|---|
| **Contrast (lysin.*beaU* genotype)** | **0 AMX** $p_{adj}$ | **0.006 µg/mL AMX** $p_{adj}$ |
| wt.wt - lytB.wt | 0.22 | 0.49 |
| wt.wt - lytA.wt | 0.17 | 7.26E-09 |
| wt.wt - lytA_lytB.wt | 0.16 | 2.94E-09 |
| wt.wt - wt.ΔbeaU | 0.04 | 5.52E-05 |
| wt.wt - lytB.ΔbeaU | 1.00 | 0.41 |
| wt.wt - lytA.ΔbeaU | 1.00 | 2.48E-04 |
| wt.wt - lytA_lytB.ΔbeaU | 1.00 | 8.30E-05 |
| lytB.wt - lytA.wt | 1.00 | 1.56E-07 |
| lytB.wt - lytA_lytB.wt | 1.00 | 5.56E-08 |
| lytB.wt - wt.ΔbeaU | 0.01 | 5.87E-04 |
| lytB.wt - lytB.ΔbeaU | 0.04 | 5.52E-05 |
| lytB.wt - lytA.ΔbeaU | 0.57 | 8.55E-03 |
| lytB.wt - lytA_lytB.ΔbeaU | 0.59 | 2.72E-03 |
| lytA.wt - lytA_lytB.wt | 1.00 | 1.00 |
| lytA.wt - wt.ΔbeaU | 7.99E-03 | 8.07E-10 |
| lytA.wt - lytB.ΔbeaU | 0.42 | 7.42E-09 |
| lytA.wt - lytA.ΔbeaU | 0.04 | 5.52E-05 |
| lytA.wt - lytA_lytB.ΔbeaU | 0.51 | 0.06 |
| lytA_lytB.wt - wt.ΔbeaU | 7.47E-03 | 4.17E-10 |
| lytA_lytB.wt - lytB.ΔbeaU | 0.40 | 3.53E-09 |
| lytA_lytB.wt - lytA.ΔbeaU | 0.47 | 6.55E-03 |
| lytA_lytB.wt - lytA_lytB.ΔbeaU | 0.04 | 5.52E-05 |
| wt.ΔbeaU - lytB.ΔbeaU | 0.22 | 0.49 |
| wt.ΔbeaU - lytA.ΔbeaU | 0.17 | 7.26E-09 |
| wt.ΔbeaU - lytA_lytB.ΔbeaU | 0.16 | 2.94E-09 |
| lytB.ΔbeaU - lytA.ΔbeaU | 1.00 | 1.56E-07 |
| lytB.ΔbeaU - lytA_lytB.ΔbeaU | 1.00 | 5.56E-08 |
| lytA.ΔbeaU - lytA_lytB.ΔbeaU | 1.00 | 1.00 |
| **AMX resistant D39V (VL4174)** | | |
| **Contrast (lysin.*beaU* genotype)** | **0 AMX** $p_{adj}$ | **2 µg/mL AMX** $p_{adj}$ |

| | | |
|---|---|---|
| wt.wt - lytB.wt | 6.98E-05 | 0.07 |
| wt.wt - lytA.wt | 4.99E-10 | 9.84E-10 |
| wt.wt - lytA_lytB.wt | 1.66E-10 | 3.23E-09 |
| wt.wt - wt.ΔbeaU | 0.23 | 0.78 |
| wt.wt - lytB.ΔbeaU | 0.02 | 0.66 |
| wt.wt - lytA.ΔbeaU | 1.49E-07 | 1.18E-07 |
| wt.wt - lytA_lytB.ΔbeaU | 4.55E-08 | 3.96E-07 |
| lytB.wt - lytA.wt | 1.17E-05 | 9.65E-08 |
| lytB.wt - lytA_lytB.wt | 2.11E-06 | 4.21E-07 |
| lytB.wt - wt.ΔbeaU | 4.00E-05 | 0.04 |
| lytB.wt - lytB.ΔbeaU | 0.23 | 0.78 |
| lytB.wt - lytA.ΔbeaU | 4.01E-03 | 1.17E-05 |
| lytB.wt - lytA_lytB.ΔbeaU | 7.95E-04 | 4.93E-05 |
| lytA.wt - lytA_lytB.wt | 0.98 | 0.98 |
| lytA.wt - wt.ΔbeaU | 1.99E-09 | 8.19E-09 |
| lytA.wt - lytB.ΔbeaU | 9.44E-06 | 4.80E-07 |
| lytA.wt - lytA.ΔbeaU | 0.23 | 0.78 |
| lytA.wt - lytA_lytB.ΔbeaU | 1.00 | 0.73 |
| lytA_lytB.wt - wt.ΔbeaU | 7.52E-10 | 2.39E-08 |
| lytA_lytB.wt - lytB.ΔbeaU | 2.34E-06 | 1.73E-06 |
| lytA_lytB.wt - lytA.ΔbeaU | 0.38 | 1.00 |
| lytA_lytB.wt - lytA_lytB.ΔbeaU | 0.23 | 0.78 |
| wt.ΔbeaU - lytB.ΔbeaU | 6.98E-05 | 0.07 |
| wt.ΔbeaU - lytA.ΔbeaU | 4.99E-10 | 9.84E-10 |
| wt.ΔbeaU - lytA_lytB.ΔbeaU | 1.66E-10 | 3.23E-09 |
| lytB.ΔbeaU - lytA.ΔbeaU | 1.17E-05 | 9.65E-08 |
| lytB.ΔbeaU - lytA_lytB.ΔbeaU | 2.11E-06 | 4.21E-07 |
| lytA.ΔbeaU - lytA_lytB.ΔbeaU | 0.98 | 0.98 |

**Unencapsulated D39V (VL3660)**

| **Contrast (lysin.*beaU* genotype)** | **0 AMX** | **0.006 µg/mL AMX** |
|---|---|---|
| | $p_{adj}$ | $p_{adj}$ |
| wt.wt - lytB.wt | 0.04 | 0.83 |
| wt.wt - lytA.wt | 2.85E-10 | 1.29E-05 |
| wt.wt - lytA_lytB.wt | 1.05E-10 | 8.19E-06 |
| wt.wt - wt.ΔbeaU | 1.00 | 0.05 |
| wt.wt - lytB.ΔbeaU | 0.10 | 0.99 |
| wt.wt - lytA.ΔbeaU | 7.38E-09 | 0.01 |
| wt.wt - lytA_lytB.ΔbeaU | 2.82E-09 | 8.00E-03 |
| lytB.wt - lytA.wt | 3.37E-08 | 2.26E-04 |
| lytB.wt - lytA_lytB.wt | 9.60E-09 | 1.38E-04 |
| lytB.wt - wt.ΔbeaU | 0.17 | 0.09 |

| | | |
|---|---|---|
| lytB.wt - lytB.ΔbeaU | 1.00 | 0.05 |
| lytB.wt - lytA.ΔbeaU | 6.68E-07 | 0.13 |
| lytB.wt - lytA_lytB.ΔbeaU | 2.08E-07 | 0.09 |
| lytA.wt - lytA_lytB.wt | 0.99 | 1.00 |
| lytA.wt - wt.ΔbeaU | 1.09E-08 | 4.22E-06 |
| lytA.wt - lytB.ΔbeaU | 1.07E-06 | 3.96E-05 |
| lytA.wt - lytA.ΔbeaU | 1.00 | 0.05 |
| lytA.wt - lytA_lytB.ΔbeaU | 0.99 | 0.66 |
| lytA_lytB.wt - wt.ΔbeaU | 4.10E-09 | 2.96E-06 |
| lytA_lytB.wt - lytB.ΔbeaU | 3.28E-07 | 2.70E-05 |
| lytA_lytB.wt - lytA.ΔbeaU | 1.00 | 0.43 |
| lytA_lytB.wt - lytA_lytB.ΔbeaU | 1.00E+00 | 0.05 |
| wt.ΔbeaU - lytB.ΔbeaU | 0.04 | 0.83 |
| wt.ΔbeaU - lytA.ΔbeaU | 2.85E-10 | 1.29E-05 |
| wt.ΔbeaU - lytA_lytB.ΔbeaU | 1.05E-10 | 8.19E-06 |
| lytB.ΔbeaU - lytA.ΔbeaU | 3.37E-08 | 2.26E-04 |
| lytB.ΔbeaU - lytA_lytB.ΔbeaU | 9.60E-09 | 1.38E-04 |
| lytA.ΔbeaU - lytA_lytB.ΔbeaU | 0.99 | 1.00 |

**Table S2: $Log_2$ fold-change and $p_{adj}$ for the interaction effect of IPTG induction and strain background in the *ΔbeaU* CRISPRi-seq screen.**

| sgRNA target | log2FoldChange | log2FoldChange_SE | *p* | $p_{adj}$ |
|---|---|---|---|---|
| *divIB* | -4.66 | 3.16E-01 | 2.27E-31 | 3.41E-28 |
| *cozEa* | 2.87 | 2.30E-01 | 8.37E-17 | 6.27E-14 |
| *gpsA,galU* | -2.97 | 3.55E-01 | 7.21E-09 | 2.70E-06 |
| *ftsE,ftsX,prfB* | -3.29 | 4.10E-01 | 6.99E-09 | 2.70E-06 |
| *lafB* | 2.03 | 2.02E-01 | 9.10E-08 | 2.73E-05 |
| *spv_1288* | -2.42 | 2.91E-01 | 2.49E-07 | 6.22E-05 |
| *spv_1917* | -3.28 | 4.66E-01 | 3.04E-07 | 6.50E-05 |
| *spv_0007,divIC* | -2.72 | 3.73E-01 | 1.03E-06 | 1.92E-04 |
| *spv_0968* | -1.93 | 2.30E-01 | 1.66E-05 | 2.77E-03 |
| *tsaE,lytR,spv_1742* | -5.40 | 1.26E+00 | 4.56E-05 | 6.83E-03 |
| *nusG* | -2.19 | 3.34E-01 | 1.07E-04 | 1.46E-02 |
| *ezrA* | -5.48 | 2.36E+00 | 2.90E-04 | 3.62E-02 |

**Table S3: Oligos used in the study**

| **Primers to clone *ΔbeaU::ery*** | | |
|---|---|---|
| **Primer name** | **5'-3' sequence** | **Description** |
| OVL4160 | GATCCGTCTCATCCTGTTTCTTTTTGAGTCCCTTT | Reverse primer for upstream homology with BsaI recognition site |
| OVL2933 | GATCGGTCTCGAGGAATTTTCATATGAACAAAAATATAAAATATT CTCAA | Forward primer for *ery* with BsaI recognition site |
| OVL2934 | GATCGGTCTCGTTATTTCCTCCCGTTAAATAATAGA TAACTATTAAAAAT | Reverse primer for *ery* with BsaI recognition site |
| OVL4155 | GATCGGTCTCGATAAATAAGGAAAAGTCTGGGATGAAAG | Forward primer for downstream homology with BsaI recognition site |
| **Primers to clone *ZIP::$P_{lac}$-beaU (spc)*** | | |
| **Primer name** | **5'-3' sequence** | **Description** |
| OVL4495 | ATGCCTCGTCTCCTCCTTAATTGTGAGCGCTCACAATTAG | Reverse primer for upstream homology, *spc*, and $P_{lac}$with BsmBI recognition site from strain |
| OVL4507 | ACAGGTCGTCTCGAGGAAACAGGAGAAAAATGATGGATTTAC | Forward primer for *beaU* with BsmBI recognition site |
| OVL4508 | ACAGGTCGTCTCGCTTATTATTTTTTCTTTTTATTGTTAGCAAGGGC | Reverse primer for *beaU* with BsmBI recognition site |
| OVL4496 | ATGCCTCGTCTCCTAAGGATCCCTCCAGTAACTCGAG | Forward primer for terminator and downstream |

| | | |
|---|---|---|
| | | homology with BsmBI recognition site |
| **Primers to clone *beaU::beaU-m(sf)GFP* C terminal fusion at native locus** | | |
| **Primer name** | **5'-3' sequence** | **Description** |
| OVL6516 | CGGTCAGTTCGTTCAGTACAAGG | Reverse primer for upstream homology with BsmBI recognition site |
| OVL6517 | ATCGAGCGTCTCCTTAGGGGGATCATAGCCAAAGCCATTTTCACCC | Forward primer for *beaU-m(sf)GFP* with BsmBI recognition site from strain VL4473 |
| OVL6518 | ATCGAGCGTCTCCTAGATTTTTTCTTTTTATTGTTAGCAAGGG | Reverse primer for *beaU-m(sf)GFP* with BsmBI recognition site from strains VL4473 |
| OVL6519 | CCCAGGCTGACCTTAACTGGCGC | Forward primer for downstream homology with BsmBI recognition site |
| **Primers to clone *ZIP::m(sf)GFP-beaU* N terminal fusion at ectopic locus** | | |
| **Primer name** | **5'-3' sequence** | **Description** |
| OVL6319 | TAGCGACGTCTCGTCCAGCTTTAGCTGCAGCTTCTCC | Reverse primer for upstream homology, *spc*, $P_{lac}$, and m(sf)GFP with BsmBI recognition site from strain VL4475 |
| OVL6320 | TAGCGACGTCTCCTGGAGATTTACTTTTAGCAATTGTATTGATTG | Forward primer for *beaU* with BsmBI recognition site |
| OVL6321 | TAGCGACGTCTCCTTTCTTTTTATTGTTAGCAAGGGC | Reverse primer for *beaU* with BsmBI recognition site |
| OVL6322 | TAGCGACGTCTCGGAAAAAATAATAACTCGAGAAAAAAA AACCGCGCC | Forward primer for terminator and downstream homology with BsmBI recognition site from strain VL4475 |
| **Primers to clone *ZIP::beaU-HiBit* C terminal fusion at ectopic locus** | | |
| **Primer name** | **5'-3' sequence** | **Description** |
| OVL6980 | TTGGAGCGTCTCCCATAACTACTCCTCCTGATCTTAATTGT GAGCG | Reverse primer for upstream homology, *spc*, and $P_{lac}$ with BsmBI recognition site from strain VL4059 |
| OVL6981 | TTGGAGCGTCTCGTATGGATTTACTTTTAGCAATTGTATTGATTGTGC | Forward primer for *beaU* with BsmBI recognition site |
| OVL6982 | TTGGAGCGTCTCGCCTTTTTTCTTTTTATTGTTAGCAAGGG | Reverse primer for *beaU* with BsmBI recognition site |
| OVL6983 | TTGGAGCGTCTCCAAGGTGATGGTGGTTCTGGTGGTGGTGG | Forward primer for *HiBit*, terminator, and downstream homology with BsmBI recognition site from strain VL4059 |
| **Primers to clone *ZIP::HiBit-beaU* N terminal fusion at ectopic locus** | | |

| Primer name | 5'-3' sequence | Description |
|---|---|---|
| OVL6976 | ATGTCCCGTCTCGTCAGAACCACCACCACCAGAACC | Reverse primer for upstream homology, *spc*, $P_{lac}$-Hibit with BsmBI recognition site from strain VL4058 |
| OVL6977 | ATGTCCCGTCTCCCTGATTTACTTTTAGCAATTGTATTGATTGTGC | Forward primer for *beaU* with BsmBI recognition site |
| OVL6978 | ATGTCCCGTCTCCGAGTTATTTTTTCTTTTTATTGTTAGCAAGG | Reverse primer for *beaU* with BsmBI recognition site |
| OVL6979 | ATGTCCCGTCTCGACTCGAGAAAGTGTAAGCAATTCTGC | Forward primer for terminator and downstream homology with BsmBI recognition site from strain VL4058 |
| **Primers for transformation fragments from laboratory strains** | | |
| **Primer name** | **5'-3' sequence** | **Description** |
| OVL3171 | TCATTCCTCAATCTATATAACATAGC | Forward primer to amplify lytA::spc including homolgous regions up and downstream |
| OVL3172 | GATGAGTTCAATTGTATCTATCGGC | Reverse primer to amplify lytA::spc including homolgous regions up and downstream |
| OVL5202 | TTGGTCAAGATCCAGATTTGGCTTAT | Forward primer to amplify lytB::chl including homolgous regions up and downstream |
| OVL5207 | CTTGACTGATTTGATTGAAGAAACCA | Reverse primer to amplify lytB::chl including homolgous regions up and downstream |
| OVL1005 | GAAACAGATTTTATCTGCTTTATATCG | Forward primer to amplify ZIP locus |
| OVL1004 | ATCAGAAAGCAAACTAGAAAGTTATG | Reverse primer to amplify ZIP locus |
| OVL552 | CTTATTTAGGGCTTGGAAGA | Forward primer to amplify CIL locus |
| OVL553 | GACTCCGCTTTACGTCAAC | Reverse primer to amplify CIL locus |
| OVL4159 | TTCACGCATTCCCATGCA | Forward primer to amplify *beaU* locus including homolgous regions up and downstream |
| OVL4156 | CACTCCGATTTTCCCACC | Reverse primer to amplify *beaU* locus including homolgous regions up and downstream |

# Chapter 4

## Contribution of hyperactive CiaH substitutions to amoxicillin susceptibility and the cell wall stress response in *Streptococcus pneumoniae*

Paddy S. Gibson[1], Arnau Domenech[1], Jan-Willem Veening[1,*]

[1] Department of Fundamental Microbiology, Faculty of Biology and Medicine, University of Lausanne, Biophore Building, CH-1015 Lausanne, Switzerland

[*]Correspondence to Jan-Willem Veening: Jan-Willem.Veening@unil.ch, tel: +41 (0)21 6925625, Twitter handle: @JWVeening

This chapter was written and all experiments performed by PG, under the mentorship of AD and JWV.

## Abstract

Bacteria use two-component signal transduction systems (TCS) to sense and respond to changeable environmental conditions. The most well-studied TCS in the human pathogen *Streptococcus pneumoniae* is CiaRH, thought to modify expression of its regulon in response to cell wall stress. Previously, substitutions in the histidine kinase CiaH have been identified in laboratory mutants selected on cefotaxime and piperacillin. Here, we show selection of *ciaH* mutations following selection on amoxicillin for the first time. We confirmed that two substitutions in CiaH, one proximal to the conserved histidine, and the other resulting in a C-terminal eight amino acid truncation, were responsible for the decrease in amoxicillin susceptibility. Using a CiaR-dependent promoter fused to a luciferase reporter, we show that these substitutions correspond to increased gene expression in the CiaRH regulon. We then utilized clustered regularly-interspaced short palindromic repeat interference (CRISPRi) repression to attempt to identify which member(s) of the CiaRH regulon were responsible for decreased amoxicillin susceptibility, and show potential roles for at least four members. This work confirms previous studies showing that CiaRH is an active player in the pneumococcal cell wall stress response, and that its regulatory role is complex and multifaceted.

## Introduction

Two-component signal transduction systems (TCS) are important for bacteria to sense and respond to environmental change. The nasopharyngeal colonizer and opportunistic human pathogen *Streptococcus pneumoniae* possesses 13 TCS, which enable it to flourish in different host conditions (Lange et al., 1999; Throup et al., 2000). Highly conserved among both commensal and pathogenic Streptococcal species is CiaRH, a TCS that responds to cell wall stress, critical for an upper respiratory tract pathogen often exposed to broad-spectrum peptidoglycan-targeting antibiotics such as amoxicillin (AMX) (Guenzi et al., 1994). CiaRH was first identified and characterized in laboratory mutants with reduced susceptibility to cefotaxime (CTX), but has since been linked to competence, biofilm formation, vancomycin tolerance, oxidative stress, and virulence (Blanchette-Cain et al., 2013; Ibrahim et al., 2004; Martin et al., 2000; Moscoso et al., 2010). In murine models it was found to contribute to successful lung and nasopharyngeal colonization (Marra et al., 2002; Sebert et al., 2002; Throup et al., 2000). In addition, in the absence of a functional CiaRH system, cells cannot tolerate the large-scale modifications to essential penicillin binding protein Pbp2x necessary for β-lactam resistance (Mascher et al., 2006; Peters et al., 2021).

CiaH is an EnvZ subgroup histidine kinase found in the cell membrane. It has an extracellular sensor domain at the N-terminus flanked by two small putative transmembrane domains. Once an external stimulus is detected, the C-terminal cytoplasmic kinase autophosphorylates, then donates a phosphoryl group from its conserved histidine to an aspartic acid residue of the cognate response regulator CiaR (Giammarinaro et al., 1999). However, a clear signal to which CiaH responds has not yet been described. It was found to be differentially expressed under vancomycin and penicillin exposures, but the baseline expression from CiaR-dependent promoters is very high regardless of the environment, and no condition has been identified where CiaR is in the off state (el Khoury et al., 2017; Haas et al., 2005; Halfmann et al., 2011). This is indicative of strong evolutionary selection towards high CiaR-dependent gene expression even in the absence of cell wall stress. In addition, CiaH is known to act as phosphatase instead of a kinase in specific growth media, deactivating CiaR and downregulating expression (Halfmann et al., 2011). In this condition, acetyl phosphate (AcP) acts as a phosphoryl group donor for CiaR, an interaction that is dependent on acetate kinase AckA (Marx et al., 2015). Recently AckA was shown to interact directly with CiaR and to

negatively affect AcP-dependent CiaR phosphorylation (Kaiser et al., 2020). Response regulator control by many different proteins other than the associated histidine kinase has been described in other bacterial species, and it is not unlikely that additional phosphodonors or phosphoreceptors for CiaRH remain to be discovered (He et al., 2021).

CiaRH affects the expression of at least 21 operons in the pneumococcal genome (Mascher et al., 2003; Slager et al., 2019) (Table S2). This includes protease HtrA, which has been shown to contribute to competence shut off via degradation of the competence stimulating peptide CSP (Cassone et al., 2012; Giammarinaro et al., 1999; Sebert et al., 2005). While critical for the enormous genetic plasticity of Streptococcal species, competence imposes severe stress on the cell wall and CiaRH is necessary for its timely completion (Dagkessamanskaia et al., 2004). Interestingly, CiaRH also regulates the uptake and metabolism of choline, an essential amino acid for the pneumococcus, enabling a rapid response to fluctuating environmental concentrations key for colonization and virulence (Brundish and Baddiley, 1968; Johnston et al., 2016; Rane and Subbarow, 1940; Tomasz, 1967). Choline is used to decorate teichoic acids, which can then be bound by choline binding proteins such as major pneumococcal autolysin LytA, indicating a link between CiaR-dependent regulation and lysis phenotypes (Howard and Gooder, 1974; Tomasz, 1968). Indeed, CiaRH deletion mutants show increased stationary phase lysis, while vancomycin tolerance conferred by substitutions in CiaH can be overcome by increased LytA dosage (Moscoso et al., 2010). Five of the strongest promoters in the CiaRH regulon encode small RNAs (csRNAs), and have been associated with stationary phase lysis, competence, and β-lactam resistance phenotypes, although often only in the presence of hyperactive mutations in CiaH (Halfmann et al., 2007; Marx et al., 2010; Schnorpfeil et al., 2013; Tsui et al., 2010).

β-lactam resistance in *S. pneumoniae* is mostly mediated by substantial modification to the transpeptidase active sites of the antibiotic targets, penicillin binding proteins (PBPs), acquired through horizontal gene transfer (see also Chapter 2). However, in laboratory selected mutants, resistance to both CTX and piperacillin (PIP) have been attributed to single point substitutions in CiaH (Lalble and Hakenbeck, 1987). Most substitutions are located close to the conserved histidine and cause substantial increases in transcription from CiaR-dependent promoters along with complete loss of natural competence (Muller et al., 2011). In 2010, *ciaH* mutations were associated with a resistance phenotype in a clinical isolate for the first time, with the resulting CiaR activation hypothesized to help the multidrug resistant

isolate cope with adverse conditions during antibiotic treatment (Moscoso et al., 2010). In contrast to laboratory selected mutants, CiaH substitutions found in clinical strains result in only moderate increases in the activity of CiaR-dependent promoters, perhaps unsurprising given the fitness defects associated with loss of competence resulting from hyperactivation of CiaR (Muller et al., 2011).

The main determinants for AMX resistance in clinical isolates are *pbp2x*, *pbp2b*, *pbp1a* and *murM* (Gibson et al., 2021). Here, we show that AMX treatment can select for point mutations in *pbp2b* and *ciaH*. We confirm that these *ciaH* mutations result in upregulation of CiaR-dependent promoters, and using CRISPRi, we attempt to identify which members of the CiaRH regulon are responsible for the reduction in AMX susceptibility.

## Results

***Amoxicillin treatment selects for hyperactive CiaH substitutions***

The evolution of AMX resistance through random point mutations accumulated in laboratory experiments is notoriously difficult. Here, we selected for only very small decreases in AMX susceptibility, which allowed us to isolate several mutants of a susceptible laboratory strain (VL2675, D39V background) (Table 1). The *ciaH* gene of isolated strains were Sanger sequenced, and those with unique mutations used for the study. Resistance determinants *pbp2x* and *pbp2b* were also sequenced for isolates with no mutations in *ciaH*. *pbp2b* but not *pbp2x* mutations were identified. One isolate had acquired the T446A substitution in the transpeptidase domain of Pbp2b. This substitution has been described both in AMX resistant clinical isolates and in laboratory selected strains with reduced PIP susceptibility (Kosowska et al., 2004; Lalble and Hakenbeck, 1987). This isolate was used in the following experiments as a control strain with reduced susceptibility to AMX but no *ciaH* mutation.

Mutations resulting in two different CiaH substitutions were found in the population. One, T241P, was described previously in the same study with PIP selection, and consequently also reduced cefotaxime susceptibility (Muller et al., 2011). It is located proximal to the conserved histidine of CiaH (H226) and has been associated with increased activity from CiaR-dependent promoters (Muller et al., 2011). The other, a point mutation at the C-terminus resulting in an early stop codon and subsequent eight amino acid truncation, has not been described before (Fig. 1A). It is not immediately clear how this truncation might affect protein activity.

**Table 1: *ciaH* mutants and control strains used in the study**. Genotype and resulting CiaH substitutions are shown. A *pbp2b* mutant was also isolated and used as a control for decreased AMX susceptibility in the absence of *ciaH* mutations.

| Strain | Genotype | CiaH substitution |
|---|---|---|
| D39V | Serotype 2 laboratory strain | WT |
| VL2675 | *D39V; bgaA::PhtrA-luc-tet* | WT |
| 28E2 | *VL2675; pbp2b$^{T446A}$* | WT |
| 28F3 | *VL2675; ciaH$^{T241P}$* | T241P |
| 28F6 | *VL2675; ciaH$^{Q437*}$* | Q437* |
| D39V-CiaH$^{28F3}$ | *VL2675; ciaH$^{T241P}$* | T241P |
| D39V-CiaH$^{28F6}$ | *VL2675; ciaH$^{Q437*}$* | Q437* |
| PG45 | *D39V; bgaA::Plac-dcas9; prsI::lacI; ciaH::ciaH$^{wt}$-ery$^{R}$* | WT |
| PG47 | *D39V; bgaA::Plac-dcas9; prsI::lacI; ciaH::ciaH$^{T241P}$-ery$^{R}$* | T241P |

To test the extent of the reduced AMX susceptibility, we grew the isolated mutants alongside the wild-type in a range of AMX concentrations (Fig. 1B). Wild-type VL2675 experienced reduced growth at 0.008 µg/mL and was fully inhibited at 0.012 µg/mL AMX. In contrast, *pbp2b* mutant strain 28E2 (*pbp2b$^{T446A}$*) only experienced a small growth defect in 0.016 µg/mL, with higher concentrations required for complete inhibition. Of the two *ciaH* mutants, 28F3 (*ciaH$^{T241P}$*) displayed the greatest reduction in AMX susceptibility, with growth observed in some replicates at 0.016 µg/mL. 28F6 (*ciaH$^{Q437*}$*) was inhibited at 0.016 µg/mL and had a severe growth defect in 0.012 µg/mL AMX. This confirms previous studies showing that not all CiaH substitutions are equal, and that those closest to H226 have the largest effect on β-lactam susceptibility (Muller et al., 2011). Importantly, the *ciaH$^{Q437*}$* and *pbp2b* mutants grew as the wild-type in the absence of AMX, whereas the *ciaHT241P* mutant grew more slowly. This suggests a negative effect on fitness from the T241P substitution, but not from Q437*.

***Hyperactive CiaH mutants demonstrate heterogeneous cell morphologies***

As CiaH is involved in the cell wall stress response, and many members of its regulon are associated with the cell wall in some way (Table S2)(Slager et al., 2019), mutants were imaged in phase-contrast microscopy (Fig. 1C). The *pbp2b* mutant cells were consistent in size and shape, although appeared rounder than the wild-type. Modification of an amino acid so close to the transpeptidase active site may have a negative effect on enzymatic activity, which could translate to reduced elongation as Pbp2b is associated with longitudinal peptidoglycan crosslinking (Berg et al., 2013).

Interestingly, both *ciaH* mutants displayed heterogeneity in cell size and shape, a phenotype which has not been shown before. To quantify this, cell widths were measured for each strain and F-tests applied to test for significant differences in variation between each mutant and the wild-type (Fig. 1D). We found that the *ciaH* mutants were significantly more heterogeneous in cell width than the wild-type ($p < 1 \times 10^{-5}$ for both), while there was no significant difference in cell width variation of *pbp2b* mutant cells.

Together this shows that mutants with altered CiaH have reduced AMX susceptibility in the pneumococcus, as well as significant heterogeneity in cell morphology.

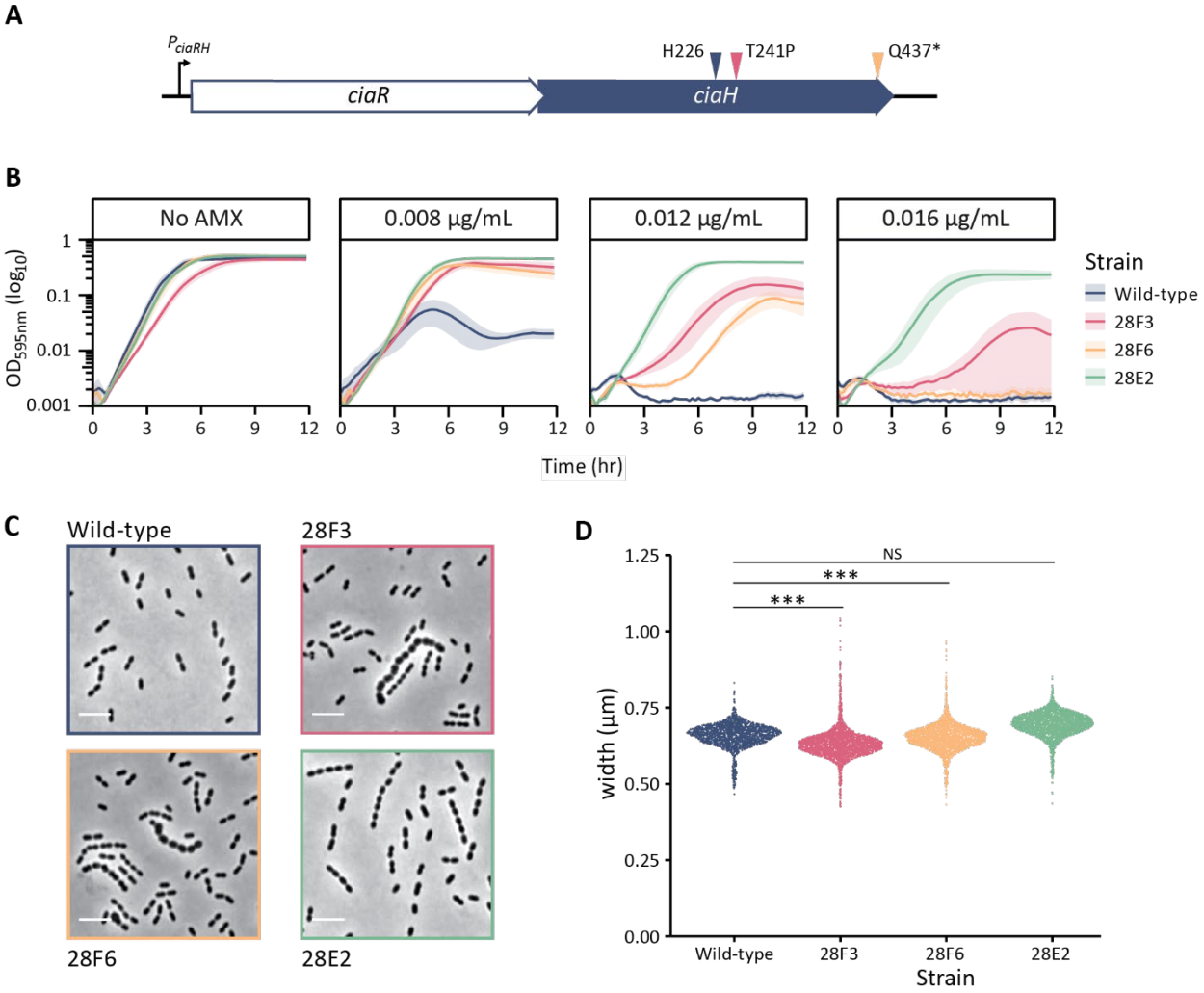


**Figure 1: Substitutions in CiaH result in decreased AMX susceptibility and increased variability in cell size**. (A) Schematic of the *ciaRH* operon with location of the conserved histidine (H226) codon and point mutations resulting in CiaH substitutions indicated. (B) Growth of wild-type (VL2675), 28F3 (*ciaH*$^{T241P}$), 28F6 (*ciaH*$^{Q437*}$), and 28E2 (*pbp2b*$^{T446A}$) in a range of AMX concentrations. (C) Phase contrast microscopy images of the four strains grown in the absence of AMX. Scale bar represents 5 µm. (D) Distribution of cell widths for wild-type VL2675 and each mutant from phase contrast images. Over 2500 cells were measured for each strain and F-tests were used to determine if there was a significant difference in variance between each mutant and the wild-type. NS not significant, *** indicates $p < 10^{-5}$.

### *CiaH substitutions sufficient to confer a decrease in AMX susceptibility*

To confirm that the *ciaH* point mutations alone were sufficient to explain the AMX susceptibility phenotype, we cloned an erythromycin resistance marker behind *ciaH* on the genome. This construct was then used to transform wild-type VL2675 with the *ciaH* alleles of the 28F3 and 28F6 mutants while selecting for erythromycin-resistance (Table 1). The wild-type strains and allele swapped mutants were then grown in AMX (Fig. 2AB).

Transfer of *ciaH*$^{T241P}$ resulted in the same growth defect as 28F3 in the absence of AMX, pinpointing this mutation in the fitness reduction (Fig. 2A). Although 28F3 and D39V-CiaH$^{28F3}$ grew similarly in 0.008 µg/mL AMX, at 0.012 µg/mL, the allele swapped strain experienced a longer lag phase than the original mutant, taking almost twice as long to reach the same stationary phase $OD_{595}$. This could suggest the presence of another point mutation in the 28F3 genome that has not been identified, but whole genome sequencing would be necessary to confirm this hypothesis. In contrast, transfer of the *ciaH*$^{Q437*}$ allele resulted in very similar growth phenotypes to the original mutant (23F6) in all AMX concentrations, albeit with some increased heterogeneity in 0.012 µg/mL AMX. We thus confirmed that mutations in *ciaH* are sufficient to cause a decrease in AMX susceptibility, although in some cases there may be other unknown determinants necessary for expression of the full phenotype.

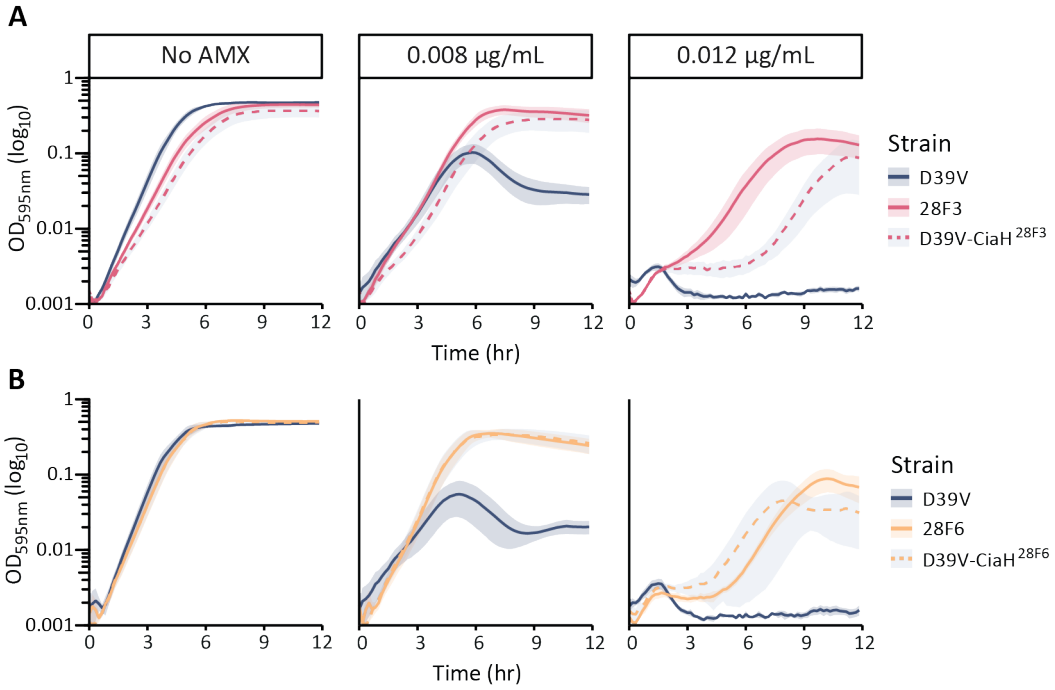


**Figure 2: *ciaH* point mutations sufficient to confer most, if not all, of the reduced AMX susceptibility phenotype**. *ciaH* mutants were transformed back into wild-type VL2675, then grown along side VL2675 and the respective mutant strain in a range of AMX concentrations. (A) 28F3 with CiaH$^{T241P}$, and (B) 28F6 with CiaH$^{Q437*}$.

### *Substitutions in CiaH correlate with increased activity from a CiaR-dependent promoter*

Previously described CiaH substitutions, including T241P, have been linked to hyperactive CiaR activity, presumably caused by increased phosphorylation by the CiaH mutant (Guenzi et al., 1994; Muller et al., 2011). In order to be able to test this for our mutants, the wild-type

strain used for mutant selection had a luciferase gene behind the CiaR-dependent *htrA* promoter introduced at the ectopic locus *bgaA*. We grew the *ciaH* mutants alongside the two control strains VL2675 and 28E2 in the presence of luciferin and measured both $OD_{595}$ and luminescence (RLU) (Fig. 3A). We then calculated the maximum RLU ($RLU_{max}$) for each strain over the course of the experiment and tested for significant differences between each mutant and the wild-type (Fig. 3B).

VL2675 provided a baseline for normal $P_{htrA}$ expression, which could then be compared against the mutants. As expected, the *pbp2b* mutant strain 28E2 did not produce higher levels of luminescence compared to the wild-type ($p_{adj}$ = 1, $t$ = -1.142). In contrast, both *ciaH* mutant strains produced 5 – 10-fold more luminescence than the wild-type *ciaH* strain (28F3: $p_{adj}$ = 0.00658, $t$ = -20.446. 28F6: $p_{adj}$ = 00.00838, $t$ = -16.765). Interestingly, the T241P substitution appears to have a stronger effect on CiaR-dependent expression, with a mean $RLU_{max}$ of ~60,000 AU compared to ~30,000 AU for the Q437* strain. This suggests that while both substitutions result in hyperactive phosphorylation from CiaH, the extent of the hyperactivity differs, and correlates with the respective effects on fitness from each substitution.

It has previously been observed that CiaH activity depends on growth media, with reduced activity in hyperactive *ciaH* mutants in media such as THY and BHI compared to C + Y (Halfmann et al., 2011). To test if this was the case in our system, we grew both VL2675 and the 28F3 mutant with luciferase reporter in BHI medium. To control for measurement and activity of the luciferase enzyme in this medium, we included a D39V background strain with luciferase under the control of the highly constitutive $P_3$ promoter (Kjos et al., 2016). Indeed, this strain did luminesce highly in the experimental conditions tested, significantly more than VL2675 ($p_{adj}$ = 0.002336255, $t$ = -27.628). Production of luminescence in 28F3 was still significantly higher than for VL2675 in BHI with a 2.3-fold difference ($p_{adj}$ = 0.001201852, $t$ = -32.906), although much lower than for the same strain in C + Y (mean BHI $RLU_{max}$ = 13,000 AU) (Fig. 3C). This indicated that despite differences in growth media composition, $CiaH^{T241P}$ still increased CiaR activity.

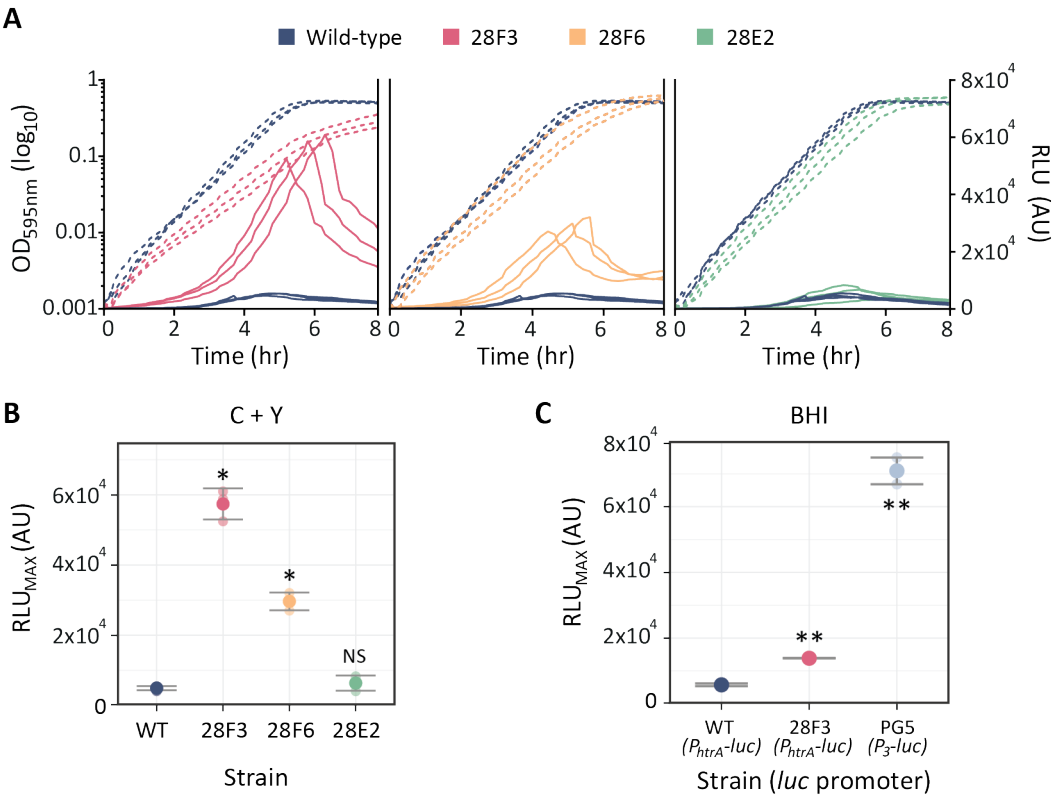


**Figure 3: CiaH substitutions result in increased expression from CiaR-dependent promoter, $P_{htrA}$.** A luciferase gene was cloned behind $P_{htrA}$ and used as a proxy for gene expression of the CiaRH regulon in the absence and presence of CiaH substitutions. (A) Growth and relative luminescence (RLU) of wild-type (blue), 28F3 (pink), 28F6 (orange), and 28E2 (green) grown in C + Y medium. (B) Maximum RLU for each strain over the 8 hr experiment in C + Y medium, and (C) for VL2675, 28F3, and D39V*; $P_3$-luc* (light blue) in BHI medium. Opaque circles show the mean of three replicates, which are represented by translucent circles. The difference in $RLU_{max}$ between each strain and wild-type for each medium was tested by *t* test, with a Bonferroni correction for multiple testing. NS not significant, * indicates $p_{adj} < 5 \times 10^{-2}$, and ** indicates $p_{adj} < 5 \times 10^{-3}$. As expected, in C + Y the two CiaH substitutions show a significant difference in $RLU_{max}$ compared to the wild-type, while the Pbp2b substitution had no effect. In BHI, luminescence from $P_{htrA}$ in 28F3 was much lower than in C + Y, although still significantly higher than for D39V.

### *Variable effects of CRISPRi repression on CiaRH regulated operons under AMX treatment*

CiaRH is predicted to regulate the expression of 21 operons, including itself (Table S2). These operons comprise a wide variety of cellular functions including competence shut off, choline metabolism and chromosome partitioning, as well as several genes for proteins of unknown function. In addition, six csRNAs are encoded in the regulon, five of which have been associated with the expression of different phenotypes themselves (Schnorpfeil et al., 2013). To identify which members of the CiaRH regulon were responsible for decreased AMX susceptibility in the presence of hyperactive CiaH substitutions, we used CRISPRi repression to unlink transcriptional control of each operon from CiaRH.

In these experiments, dCas9 expression was controlled by an IPTG inducible $P_{lac}$ promoter, while the sgRNA was constitutively expressed from the ectopic ZIP locus (Liu et al., 2017). This was performed in two different backgrounds, *ciaH*$^{wt}$ (PG45) and *ciaH*$^{T241P}$ (PG47). Final sgRNA strains were grown in C + Y, in the absence and presence of IPTG, and a range of AMX concentrations (Fig. 4). This allowed us to observe individual effects of each operon on AMX susceptibility in the context of CiaH$^{wt}$ and CiaH$^{T241P}$.

Expression of dCas9 in the two backgrounds had no effect on growth in the absence or presence of AMX (Fig. S1). sgRNAs targeting essential gene *pbp2b*, and highly transcribed gene *hlpA* were used to confirm dCas9 functionality (Fig. S1).

Repression of the *ciaRH* operon resulted in decreased survival in some AMX concentrations (0.008 μg/mL and 0.01 μg/mL) in the *ciaH*$^{wt}$ strain, demonstrating a correlation of reduced CiaRH with increased AMX susceptibility (Fig. 4A). This was not observed in the presence of T241P substitution, and luminescence in the T241P strain was high in all conditions (data not shown). Taken together, this confirms that CiaR activity is important for tolerating AMX-induced stress, but that repression of *ciaRH* in this system was insufficient to reduce the effect of CiaH$^{T241P}$.

Three operons in the regulon are considered essential for *S. pneumoniae* D39V to grow in laboratory conditions. As expected, IPTG treatment of strains with sgRNA targeting these operons had to be optimized and were reduced to the highest concentration that still allowed some growth. Interestingly, for all three operons, presence of IPTG had a deleterious effect on growth in AMX, regardless of *ciaH* allele (Fig. 4B, Fig. S2). This may suggest an additive effect, where the stress of reduced expression of essential proteins combined with AMX treatment negatively affected growth. It may be that in this case, overexpression of these operons would provide more information as to whether the growth defects are a direct effect of protein presence in response to AMX stress, or simply a result of cumulative stress. This might be particularly interesting for the *lic1* operon, which encodes proteins for the uptake and metabolism of choline. The importance of choline for the lytic activity of LytA, including upon β-lactam treatment, is well documented (Howard and Gooder, 1974; Tomasz, 1968; Chapter 3).

The effects of non-essential operon repression were variable (Fig. 4CD). No sgRNA strains showed large decreases in survival in AMX when operons were repressed, for example, repression of teichoic acid synthesis-involved *dlt* operon (Fig. 4C, Fig. S3). However, repressing *prsA* had a slightly beneficial effect on growth in AMX (Fig. 4D). PrsA is a putative parvulin-type peptidyl-prolyl isomerase (Slager et al., 2018). These enzymes are ubiquitous among Gram-positive bacteria, and important for the correct folding and secretion of extracellular proteins such as some virulence factors and the PBPs (Ünal and Steinert, 2014).

Six csRNAs are encoded by the CiaRH regulon, five of which have previously been linked to β-lactam sensitivity and autolysis (Halfmann et al., 2007; Schnorpfeil et al., 2013). In our system, repression of csRNAs *ccnB* and *ccnC* caused increased AMX susceptibility, although in the *ciaH*$^{T241P}$ mutant background only (Fig. 4EF). Thus, decreasing transcription from baseline wild-type expression did not make cells more susceptible to AMX, but that increased expression of *ccnB* and *ccnC* was important for the phenotype. The regulons of pneumococcal csRNAs are not well described but have been associated with competence and the cell wall. Larger effects may have been seen if csRNAs had been repressed in combination, in accordance with previous studies showing highly additive effects of all five csRNAs (Schnorpfeil et al., 2013).

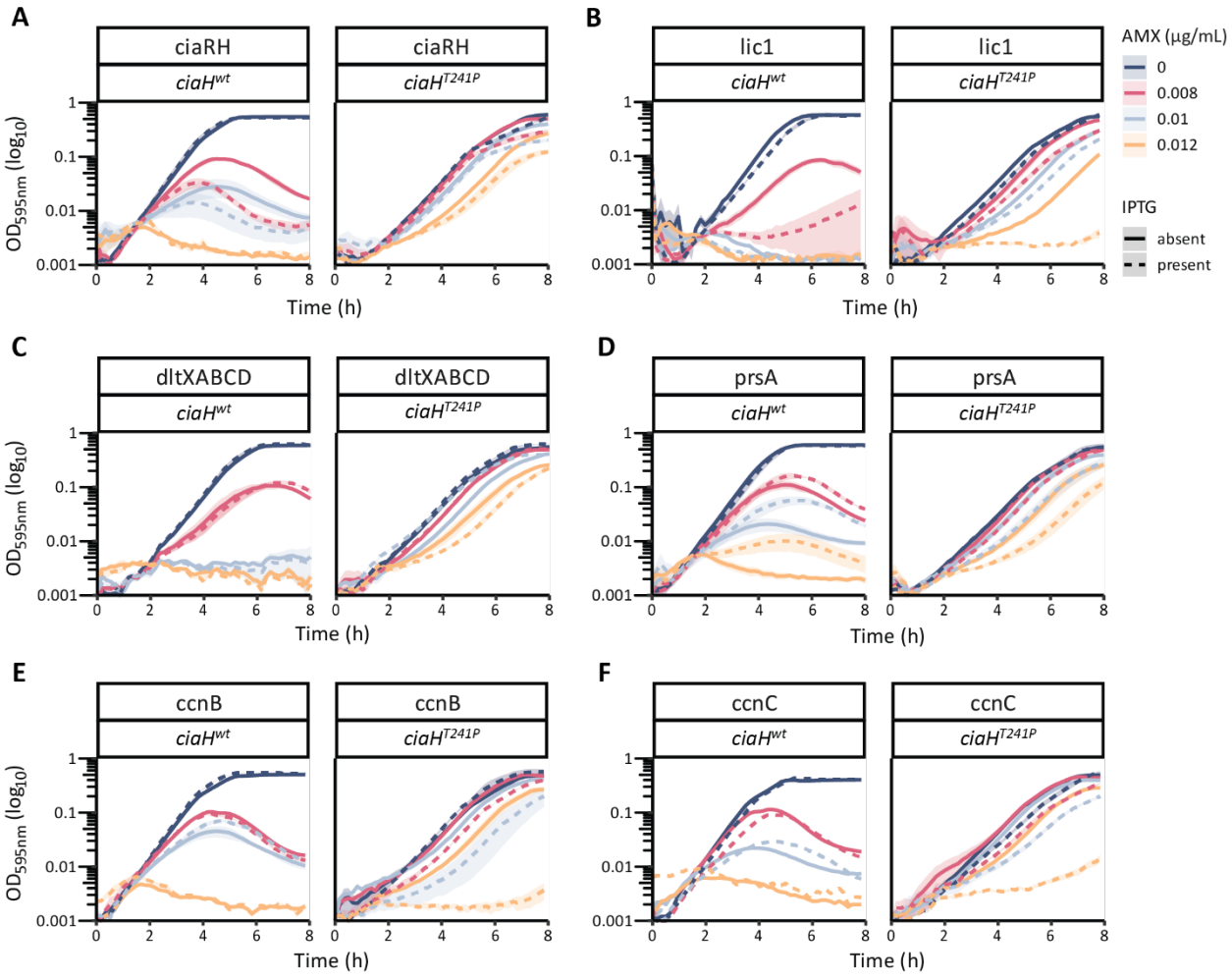


**Figure 4: CRISPRi repression via CRISPRi of operons in the CiaRH regulon in the absence and presence of AMX.** sgRNA targeting individual operons in the CiaRH regulon were introduced in strains carrying *dcas9* under control Plac, and either the *ciaH*$^{wt}$ or *ciaH*$^{T241P}$ alleles. The final strains were grown in the presence and absence of the inducer IPTG, and in a range of AMX concentrations. IPTG 1 mM was used for most strains, although was reduced upon optimization for operons essential in C + Y, including to 0.01 mM for *lic1*. All growth curves can be found in Fig. S1, S2, S3, and S4. Shown here are the growth curves for strains with sgRNA targeting (A) *ciaRH*, (B) the *lic1* operon with genes *tarI, tarJ, licA, licB*, and *licC*, (C) *prsA*, (D) the *dltX, dltA, dltB, dltC, dltD* operon, (E) *ccnB*, and (F) *ccnC*.

## Discussion

General cell wall stress response system CiaRH is highly conserved among Streptococci, underlining its importance for reacting appropriately to a changeable environment (Throup et al., 2000). Indeed, it has so far been associated with virulence, competence, oxidative stress, β-lactam susceptibility, vancomycin tolerance, and biofilm formation (Blanchette-Cain et al., 2013; Guenzi et al., 1994; Ibrahim et al., 2004; Martin et al., 2000; Moscoso et al., 2010). Despite its involvement in many diverse aspects of pneumococcal molecular biology, a specific signal to which CiaH responds has not yet been described. In addition, its regulon is predicted to comprise of 21 operons involved in variable cellular functions, and their respective roles in the CiaRH-mediated stress response are not well understood (Halfmann et al., 2011; Slager et al., 2019) (Table S2).

Previously, point mutations in *ciaH* have been isolated following laboratory selection on CTX and PIP (Guenzi et al., 1994). The resulting substitutions were subsequently shown to result in hyperactivation of the CiaRH system, where CiaH was presumably phosphorylating CiaR at a higher and more constant rate, even in the absence of a stress signal. This could be measured by upregulation of CiaR-dependent promoters (Muller et al., 2011).

Here, we show that point mutations in *ciaH* can also be selected for by AMX, one of the most commonly prescribed antibiotics for upper respiratory tract infections. We confirmed that these CiaH substitutions were responsible for the small decrease in AMX susceptibility (Fig. 1B, Fig. 2), and linked them to upregulation of the CiaRH regulon by using CiaR-dependent promoter $P_{htrA}$-controlled luciferase expression as a reporter (Fig. 3). In addition, we show that $ciaH^{T241P}$ results in significantly higher CiaR-dependent gene expression than $ciaH^{wt}$ in BHI medium, albeit less dramatically than in C + Y.

Mutations in *ciaH* are rare in clinical isolates, but several have been described. These have previously been cloned into laboratory strain backgrounds and compared to laboratory-selected *ciaH* mutations. Interestingly, while mutations from both sources resulted in increased gene expression from CiaR-dependent promoters, the effect was not as strong in the clinical alleles. The effect of these alleles on β-lactam susceptibility was also not as strong, suggesting that the negative effects on fitness of a hyperactive CiaRH system outweigh the benefits in the natural environment (Muller et al., 2011). We isolated one novel *ciaH* allele,

*ciaH*$^{Q437*}$, while the other, *ciaH*$^{T241P}$, had been described following PIP selection before (Guenzi et al., 1994; Muller et al., 2011). While the T241P had the strongest effect on both AMX susceptibility and CiaR-dependent gene expression, the effect of the Q437* CiaH truncation might be more comparable to that of a clinical *ciaH* allele. The effect of an 8 amino acid truncation on CiaH function is not immediately obvious, but may provide some clues to protein function upon further study.

Using CRISPRi-mediated repression of individual operons in the CiaRH regulon, we attempted to identify which pathway was causing the reduced AMX susceptibility in hyperactive CiaH mutants. Under this system, operon expression was essentially unlinked from CiaR activity and could be assessed on its own. In this manner we confirmed the role of *ciaRH*, showing that repression of this operon slightly increased AMX susceptibility when wild-type *ciaH* was present (Fig. 4A). Several other operons in the regulon also demonstrated differential AMX susceptibility when repressed. In the case of three essential operons, where the *dcas9* induction was reduced to mitigate severe growth defects, it was difficult to assess whether the increases in AMX susceptibility were because of a role in antibiotic stress response, or due to an additive effect from operon repression itself. In these cases, an overexpression system may have been more appropriate. This needs to be performed for the *lic1* operon (Fig. 4B), where there is a clear link between its activity and β-lactam-induced autolysis (Howard and Gooder, 1974; Moscoso et al., 2010; Tomasz, 1968).

Another interesting candidate with a close link to the PBP-targeting β-lactams is PsrA. Predicted to be a parvulin-type peptidyl-prolyl isomerase, involved in the correct folding of extracellular proteins such as the PBPs (Slager et al., 2018; Ünal and Steinert, 2014), repression of *prsA* in the *ciaH*$^{wt}$ background resulted in a small decrease in AMX susceptibility. Although this result needs to be validated, it may indicate a novel link between CiaRH and the PBPs, particularly given that a functional CiaRH system was shown to be essential for the pneumococcus to tolerate low-affinity *pbp2x* alleles, and for full penicillin resistance development in combination with *pbp1a* and *pbp2x* in a clinical isolate (Mascher et al., 2006; Peters et al., 2021; Schweizer et al., 2017).

Of the six csRNAs encoded in the CiaRH regulon, two showed large differences in AMX susceptibility when repressed in the *ciaH*$^{T241P}$ background. This correlated with previous

studies showing csRNAs to be involved in *ciaRH* mutant phenotypes, including increased β-lactam susceptibility and decreased natural competence (Schnorpfeil et al., 2013). In addition, repression of single csRNAs did not increase AMX susceptibility to that of the *ciaH*$^{wt}$ background, which was also in agreement with previous work showing that simultaneous deletion of five csRNAs was necessary. These csRNAs are trans-encoded RNAs, affecting translation and stability of their target mRNAs and either increasing or decreasing target translation, depending on the specific interaction (Jabbour and Lartigue, 2021). Their regulons are not known, although at least six putative targets have been described, including competence stimulating peptide (CSP) precursor gene *comC* (Schnorpfeil et al., 2013).

CiaRH is the most well studied TCS in the pneumococcal genome, but much is still unknown about the molecular biology of its signal recognition and response regulation. Here, we discuss at least four different operons in the regulon which may play a role in the response to β-lactam-induced cell wall stress, and co-repression experiments may identify even more. CiaRH is thought to sense general cell wall stress, so it follows that its response would also be broad and multipronged, as opposed to highly specific. Further work is needed to fully untangle the complex regulatory networks of this system, particularly in the different genetic contexts of β-lactam resistant clinical isolates.

## Methods

### *Bacterial strains and growth conditions*

All strains used are derivatives of the *S. pneumoniae* serotype 2 D39V, unless stated otherwise (Slager et al., 2018). Bacteria were cultured in liquid C+Y medium with no shaking at 37°C. C+Y medium was adapted from Adams and Roe (Slager et al., 2018). Strains were stocked at $OD_{595}$ 0.4 in C + Y with 15% glycerol at -80°C. Working stocks (T2) are composed of an $OD_{595}$ 0.3 culture, centrifuged, and resuspended in C + Y and 15% glycerol, stored at -80°C.

*E. coli* strains were grown either in LB broth, at 37°C with shaking, or on LB agar plates containing 100 µg/mL of spectinomycin.

AMX (Sigma Aldrich) was dissolved in 100% DMSO, then diluted working concentrations in 4% DMSO and stored in aliquots at -80.

**Table 2: Genotypes of all strains used in the study.**

| Strain ID | Genotype and relevant characteristics | reference |
|---|---|---|
| D39V | Serotype 2 laboratory strain | (Slager et al., 2018) |
| VL2675 | *D39V; bgaA::PhtrA-luc (tet)* | Laboratory strain collection |
| 28E2 | *VL2675; pbp2b$^{T446A}$* | This study |
| 28F3 | *VL2675; ciaH$^{T241P}$* | This study |
| 28F6 | *VL2675; ciaH$^{Q437*}$* | This study |
| D39V-CiaH$^{28F3}$ | *VL2675; ciaH::ciaH$^{T241P}$-ery* | This study |
| D39V-CiaH$^{28F6}$ | *VL2675; ciaH::ciaH$^{Q437*}$-ery* | This study |
| VL956 | *D39V; CIL::P3-luc (kan)* | (Kjos et al., 2016) |
| PG45 | *D39V; bgaA::Plac-dcas9sp (tet); prsI::F6-lacI-tetR (gen); CEP::PhtrA-luc (chl); ciaH::ciaH$^{wt}$-ery* | This study |
| PG47 | *D39V; bgaA::Plac-dcas9sp (tet); prsI::F6-lacI-tetR (gen); CEP::PhtrA-luc (chl); ciaH::ciaH$^{T241P}$-ery* | This study |
| CRSP1 | *PG45; ZIP::P3-sgRNA$^{ccnC}$* | This study |
| CRSP2 | *PG45; ZIP::P3-sgRNA$^{spv_0098}$* | This study |
| CRSP3 | *PG45; ZIP::P3-sgRNA$^{ccnA}$* | This study |
| CRSP4 | *PG45; ZIP::P3-sgRNA$^{ccnB}$* | This study |
| CRSP5 | *PG45; ZIP::P3-sgRNA$^{ccnD}$* | This study |
| CRSP6 | *PG45; ZIP::P3-sgRNA$^{manN-manM-manL}$* | This study |
| CRSP7 | *PG45; ZIP::P3-sgRNA$^{rimP-nusA-spv_0480-spv_0481-infB-rbfA}$* | This study |
| CRSP8 | *PG45; ZIP::P3-sgRNA$^{ciaR-ciaH}$* | This study |
| CRSP9 | *PG45; ZIP::P3-sgRNA$^{spv_0775}$* | This study |
| CRSP10 | *PG45; ZIP::P3-sgRNA$^{prsA}$* | This study |
| CRSP11 | *PG45; ZIP::P3-sgRNA$^{rlmCD}$* | This study |
| CRSP12 | *PG45; ZIP::P3-sgRNA$^{spv_0913}$* | This study |
| CRSP13 | *PG45; ZIP::P3-sgRNA$^{licC-licB-licA-tarJ-tarI}$* | This study |
| CRSP14 | *PG45; ZIP::P3-sgRNA$^{axe1}$* | This study |
| CRSP15 | *PG45; ZIP::P3-sgRNA$^{srf-21}$* | This study |
| CRSP16 | *PG45; ZIP::P3-sgRNA$^{spv_1769}$* | This study |
| CRSP17 | *PG45; ZIP::P3-sgRNA$^{malP-malQ}$* | This study |
| CRSP18 | *PG45; ZIP::P3-sgRNA$^{dltD-dltC-dltB-dltA-dltX}$* | This study |
| CRSP19 | *PG45; ZIP::P3-sgRNA$^{htrA}$* | This study |

| | | |
|---|---|---|
| CRSP20 | *PG45; ZIP::P3-sgRNA$^{parB}$* | This study |
| CRSP21 | *PG45; ZIP::P3-sgRNA$^{ccnE}$* | This study |
| CRSP22 | *PG47; ZIP::P3-sgRNA$^{ccnC}$* | This study |
| CRSP23 | *PG47; ZIP::P3-sgRNA$^{spv_0098}$* | This study |
| CRSP24 | *PG47; ZIP::P3-sgRNA$^{ccnA}$* | This study |
| CRSP25 | *PG47; ZIP::P3-sgRNA$^{ccnB}$* | This study |
| CRSP26 | *PG47; ZIP::P3-sgRNA$^{ccnD}$* | This study |
| CRSP27 | *PG47; ZIP::P3-sgRNA$^{manN\text{-}manM\text{-}manL}$* | This study |
| CRSP28 | *PG47; ZIP::P3-sgRNA$^{rimP\text{-}nusA\text{-}spv_0480\text{-}spv_0481\text{-}infB\text{-}rbfA}$* | This study |
| CRSP29 | *PG47; ZIP::P3-sgRNA$^{ciaR\text{-}ciaH}$* | This study |
| CRSP30 | *PG47; ZIP::P3-sgRNA$^{spv_0775}$* | This study |
| CRSP31 | *PG47; ZIP::P3-sgRNA$^{prsA}$* | This study |
| CRSP32 | *PG47; ZIP::P3-sgRNA$^{rlmCD}$* | This study |
| CRSP33 | *PG47; ZIP::P3-sgRNA$^{spv_0913}$* | This study |
| CRSP34 | *PG47; ZIP::P3-sgRNA$^{licC\text{-}licB\text{-}licA\text{-}tarJ\text{-}tarI}$* | This study |
| CRSP35 | *PG47; ZIP::P3-sgRNA$^{axe1}$* | This study |
| CRSP36 | *PG47; ZIP::P3-sgRNA$^{srf\text{-}21}$* | This study |
| CRSP37 | *PG47; ZIP::P3-sgRNA$^{spv_1769}$* | This study |
| CRSP38 | *PG47; ZIP::P3-sgRNA$^{malP\text{-}malQ}$* | This study |
| CRSP39 | *PG47; ZIP::P3-sgRNA$^{dltD\text{-}dltC\text{-}dltB\text{-}dltA\text{-}dltX}$* | This study |
| CRSP40 | *PG47; ZIP::P3-sgRNA$^{htrA}$* | This study |
| CRSP41 | *PG47; ZIP::P3-sgRNA$^{parB}$* | This study |
| CRSP42 | *PG47; ZIP::P3-sgRNA$^{ccnE}$* | This study |
| CRSP43 | *PG45; ZIP::P3-sgRNA$^{pbp2b}$* | This study |
| CRSP44 | *PG47; ZIP::P3-sgRNA$^{pbp2b}$* | This study |
| CRSP83 | *PG45; ZIP::P3-sgRNA$^{hlpA}$* | This study |
| CRSP84 | *PG47; ZIP::P3-sgRNA$^{hlpA}$* | This study |

***Transformation of S. pneumoniae***

*S. pneumoniae* was grown in C+Y (pH 6.8) at 37°C to an $OD_{595}$ of 0.1 for transformation. Competence was induced by addition of synthetic CSP-1 and incubation. DNA uptake occurred during 20 min at 37°C, followed by dilution and recovery for 1.5 hr. Transformants were selected by plating inside Columbia agar supplemented with 3% defibrinated sheep blood (CBA; Thermo Scientific) containing the appropriate antibiotic and incubated at 37°C in

5% $CO_2$ overnight. Antibiotics used for selection were; chloramphenicol (4 µg/mL), erythromycin (1 µg/mL), kanamycin (250 µg/mL), spectinomycin (100 µg/mL), and tetracycline (1 µg/mL). Successful transformants were confirmed by PCR and Sanger sequencing (Eurofins Genomics).

### *Cloning*

*ciaH::ciaH$^{allele}$-ery*

Upstream homology, downstream homology, and the *ery* marker were amplified with oligos specified in Table S1. They were assembled in a one-pot Golden Gate reaction with the type II restriction enzyme BsmBI (Engler et al., 2009). This fragment assembly was used for all three ciaH alleles by amplification from the appropriate template strain. To produce the ciaH$^{T241P}$-ery and ciaH$^{wt}$-ery CRISPRi strains, the construct was transformed into VL1998 as above, to produce strains PG45 and PG47.

*CRISPRi strains for CiaRH regulon repression*

The vector pPEPZ-sgRNAclone was digested with BsmBI and purified for gel extraction (Liu et al., 2021). sgRNA for CRISPRi were annealed from two oligos, which contained both the sgRNA sequence, and the overlap necessary for ligation. Oligos used can be found in Table S1 and were taken from the previously described CRISPRi-seq library (Liu et al., 2021), apart from those for *ccnE* (OVL3639 / OVL3640) which were designed in benchling. Oligos were annealed in TEN buffer (10 mM Tris, 1 mM EDTA, 100 mM NaCl, pH 8) at 95°C for 5 minutes, then cooled to room temperature. Annealed oligos were then phosphorylated with T4 polynucleotide kinase. Digested pPEPZ-sgRNAclone and annealed oligos were ligated with T4 ligase, then transformed into E. coli stbl3. Selection was with 100 µg/mL spectinomycin on LB agar. sgRNA plasmids were isolated from the E. coli hosts, confirmed by Sanger sequencing, then transformed into S. pneumoniae PG45 and PG47.

### *Growth curves*

To determine growth curves, $OD_{595}$ 0.1 pre-culture was diluted 100-fold into fresh media and aliquoted in 300 µL volumes in transparent plates. For luminescence measurement, luciferin

was added to 0.045 µg/mL. For growth curves assessing AMX susceptibility, the antibiotic was diluted into the plate prior to inoculation to the appropriate concentration. $OD_{595}$ and relative luminescence (RLU) were measured every 10 minutes in a plate reader at 37°C for up to 24 hours. $OD_{595}$ was normalized by the blank media control. RLUmax was defined as the maximum RLU reached over the time frame of measurement. Significant differences in RLUmax were determined by *t* test with Bonferroni correction for multiple testing. Significance was defined as $p_{adj} < 0.05$.

For induction of $P_{lac}$-*dcas9* in the CRISPRi experiments, all strains were precultured in the absence or presence of IPTG, then diluted 100-fold into fresh C + Y medium with or without IPTG, and in a range of AMX concentrations. 1 mM IPTG was used for most strains, but those containing sgRNA that target essential operons were induced with 0.01 mM ($sgRNA^{spv\_0098\text{-}aatA}$ and $sgRNA^{lic1}$) or 0.04 mM ($sgRNA^{rimP\text{-}nusA\text{-}spv\_0480\text{-}spv\_0481\text{-}infB\text{-}rbfA}$), following optimization.

***Isolation of mutants with reduced AMX susceptibility***

Pre-cultures of VL2675 at $OD_{595}$ 0.1 were diluted 100-fold in 8 mL tubes of C+Y. AMX was pre-diluted into the media in 4 concentrations; 0.006, 0.008, 0.01, 0.012 µg/mL. Tubes were vortexed and then aliquoted in 300 µL volumes into 96-well transparent plates, with 22 replicates for each antibiotic concentration. OD and relative luminescence (RLU) were measured as above. In the WT MIC concentration (0.01 µg/mL) after 15 hr populations would start to grow out. When they reached $OD_{595}$ 0.05 they were collected and concentrated in fresh C+Y. They were streaked for isolation on CBA + 0.01 µg/mL AMX. AMX CBA plates were always poured from the same batch and fresh D39V was streaked as a control for antibiotic concentration variation. Single colonies were grown in AMX 0.01 µg/mL to be stocked as above. *ciaH* and *pbp2b* were amplified and Sanger sequenced.

***Microscopy***

T2 cells were inoculated into C+Y and grown to $OD_{595}$ 0.2. 1 mL was spun down at 7000 g for 3 minutes, the supernatant was removed, and the pellet was resuspended in 20 µL C+Y. 0.4 µL of the cell suspension was dropped onto a PBS agarose pad on a microscope slide. Phase contrast images were acquired with a Leica DMi8. Images were analyzed in ImageJ (Abramoff

et al., 2004), cell segmentation calculated with Oufti (Paintdakhi et al., 2016), and data analyzed using BactMap (Raaphorst et al., 2019).

## Acknowledgements

P.G. was supported by the University of Lausanne Faculty of Biology and Medicine PhD fellowship. Work in the Veening lab is supported by the Swiss National Science Foundation (SNSF) (project grants 192517 and 200792), SNSF JPIAMR grant (40AR40_185533), SNSF NCCR 'AntiResist' (51NF40_180541) and ERC consolidator grant 771534-PneumoCaTChER.

## References


Abramoff MD, Magalhães PJ, Ram SJ. 2004. Image Processing with ImageJ, Biophotonics international. Laurin Pub. Co.

Berg KH, Stamsås GA, Straume D, Håvarstein LS. 2013. Effects of low PBP2b levels on cell morphology and peptidoglycan composition in *Streptococcus pneumoniae* R6. *Journal of Bacteriology* **195**:4342–4354. doi:10.1128/JB.00184-13

Blanchette-Cain K, Hinojosa CA, Akula Suresh Babu R, Lizcano A, Gonzalez-Juarbe N, Munoz-Almagro C, Sanchez CJ, Bergman MA, Orihuela CJ. 2013. *Streptococcus pneumoniae* biofilm formation is strain dependent, multifactorial, and associated with reduced invasiveness and immunoreactivity during colonization. *mBio* **4**. doi:10.1128/mBio.00745-13

Brundish DE, Baddiley J. 1968. Pneumococcal C-substance, a ribitol teichoic acid containing choline phosphate. *Biochem J* **110**:573–582. doi:10.1042/bj1100573

Cassone M, Gagne AL, Spruce LA, Seeholzer SH, Sebert ME. 2012. The HtrA protease from *Streptococcus pneumoniae* digests both denatured proteins and the competence-stimulating peptide. *J Biol Chem* **287**:38449–59. doi:10.1074/jbc.M112.391482

Dagkessamanskaia A, Moscoso M, Hénard V, Guiral S, Overweg K, Reuter M, Martin B, Wells J, Claverys JP. 2004. Interconnection of competence, stress and CiaR regulons in *Streptococcus pneumoniae*: Competence triggers stationary phase autolysis of *ciaR* mutant cells. *Molecular Microbiology* **51**:1071–1086. doi:10.1111/j.1365-2958.2003.03892.x

el Khoury JY, Boucher N, Bergeron MG, Leprohon P, Ouellette M. 2017. Penicillin induces alterations in glutamine metabolism in *Streptococcus pneumoniae*. *Scientific Reports* **7**. doi:10.1038/s41598-017-15035-y

Engler C, Gruetzner R, Kandzia R, Marillonnet S. 2009. Golden gate shuffling: A one-pot DNA shuffling method based on type Ils restriction enzymes. *PLoS ONE* **4**:e5553. doi:10.1371/journal.pone.0005553

Giammarinaro P, Sicard M, Gasc A-M. 1999. Genetic and physiological studies of the CiaH-CiaR two-component signal-transducing system involved in cefotaxime resistance and competence of *Streptococcus pneumoniae*. *Microbiology (N Y)* **145**:1859–1869. doi:10.1099/13500872-145-8-1859

Gibson PS, Bexkens E, Zuber S, Cowley L, Veening J-W. 2021. The acquisition of clinically relevant amoxicillin resistance in *Streptococcus pneumoniae* requires ordered horizontal gene transfer of four loci. *bioRxiv* 2021.12.17.473165. doi:10.1101/2021.12.17.473165

Guenzi E, Gasc A-M, Sicard MA, Hakenbeck R. 1994. A two-component signal-transducing system is involved in competence and penicillin susceptibility in laboratory mutants of *Streptococcus pneumoniae*. *Molecular Microbiology* **12**:505–515. doi:10.1111/j.1365-2958.1994.tb01038.x

Haas W, Kaushal D, Sublett J, Obert C, Tuomanen EI. 2005. Vancomycin stress response in a sensitive and a tolerant strain of *Streptococcus pneumoniae*. *J Bacteriol* **187**:8205–10. doi:10.1128/JB.187.23.8205-8210.2005

Halfmann A, Kovács M, Hakenbeck R, Brückner R. 2007. Identification of the genes directly controlled by the response regulator CiaR in *Streptococcus pneumoniae*: Five out of 15 promoters drive expression of small non-coding RNAs. *Molecular Microbiology* **66**:110–126. doi:10.1111/j.1365-2958.2007.05900.x

Halfmann A, Schnorpfeil A, Müller M, Marx P, Günzler U, Hakenbeck R, Brückner R. 2011. Activity of the two-component regulatory system CiaRH in *Streptococcus pneumoniae* R6. *J Mol Microbiol Biotechnol* **20**:96–104. doi:10.1159/000324893

He LY, Le YJ, Guo Z, Li S, Yang XY. 2021. The Role and Regulatory Network of the CiaRH Two-Component System in Streptococcal Species. *Frontiers in Microbiology*. doi:10.3389/fmicb.2021.693858

Howard L v., Gooder H. 1974. Specificity of the autolysin of *Streptococcus (Diplococcus) pneumoniae*. *Journal of Bacteriology* **117**:796–804. doi:10.1128/jb.117.2.796-804.1974

Ibrahim YM, Kerr AR, McCluskey J, Mitchell TJ. 2004. Control of virulence by the two-component system CiaR/H is mediated via HtrA, a major virulence factor of *Streptococcus pneumoniae*. *Journal of Bacteriology* **186**:5258–5266. doi:10.1128/JB.186.16.5258-5266.2004

Jabbour N, Lartigue MF. 2021. An Inventory of CiaR-Dependent Small Regulatory RNAs in Streptococci. *Frontiers in Microbiology* **12**:925. doi:10.3389/FMICB.2021.669396/BIBTEX

Johnston C, Hauser C, Hermans PWM, Martin B, Polard P, Bootsma HJ, Claverys JP. 2016. Fine-tuning of choline metabolism is important for pneumococcal colonization. *Molecular Microbiology* **100**:972–988. doi:10.1111/mmi.13360

Kaiser S, Hoppstädter LM, Bilici K, Heieck K, Brückner R. 2020. Control of acetyl phosphate-dependent phosphorylation of the response regulator CiaR by acetate kinase in *Streptococcus pneumoniae*. *Microbiology (United Kingdom)* **166**:411–421. doi:10.1099/mic.0.000894

Kjos M, Miller E, Slager J, Lake FB, Gericke O, Roberts IS, Rozen DE, Veening JW. 2016. Expression of *Streptococcus pneumoniae* Bacteriocins Is Induced by Antibiotics via Regulatory Interplay with the Competence System. *PLoS Pathogens* **12**:e1005422. doi:10.1371/journal.ppat.1005422

Kosowska K, Jacobs MR, Bajaksouzian S, Koeth L, Appelbaum PC. 2004. Alterations of Penicillin-Binding Proteins 1A, 2X, and 2B in *Streptococcus pneumoniae* Isolates for Which Amoxicillin MICs Are Higher than Penicillin MICs **48**. doi:10.1128/AAC.48.10.4020-4022.2004

Lalble G, Hakenbeck R. 1987. Penicillin-binding proteins in beta-lactam-resistant laboratory mutants of *Streptococcus pneumoniae*. *Mol Microbiol* **1**:355–363. doi:10.1111/J.1365-2958.1987.TB01942.X

Lange R, Wagner C, de Saizieu A, Flint N, Molnos J, Stieger M, Caspers P, Kamber M, Keck W, Amrein KE. 1999. Domain organization and molecular characterization of 13 two-component systems identified by genome sequencing of *Streptococcus pneumoniae*. *Gene* **237**:223–234. doi:10.1016/S0378-1119(99)00266-8

Liu X, Gallay C, Kjos M, Domenech A, Slager J, Kessel SP, Knoops K, Sorg RA, Zhang J, Veening J, van Kessel SP, Knoops K, Sorg RA, Zhang J, Veening J. 2017. High-throughput CRISPRi phenotyping identifies new essential genes in *Streptococcus pneumoniae*. *Molecular Systems Biology* **13**:931. doi:10.15252/msb.20167449

Liu X, Kimmey JM, Matarazzo L, de Bakker V, van Maele L, Sirard JC, Nizet V, Veening JW. 2021. Exploration of Bacterial Bottlenecks and *Streptococcus pneumoniae* Pathogenesis by CRISPRi-Seq. *Cell Host and Microbe* **29**:107-120.e6. doi:10.1016/j.chom.2020.10.001

Marra A, Asundi J, Bartilson M, Lawson S, Fang F, Christine J, Wiesner C, Brigham D, Schneider WP, Hromockyj AE. 2002. Differential fluorescence induction analysis of *Streptococcus pneumoniae* identifies genes involved in pathogenesis. *Infection and Immunity* **70**:1422–1433. doi:10.1128/IAI.70.3.1422-1433.2002

Martin B, Prudhomme M, Alloing G, Granadel C, Claverys J-P. 2000. Cross-regulation of competence pheromone production and export in the early control of transformation in *Streptococcus pneumoniae*. *Molecular Microbiology* **38**:867–878. doi:10.1046/j.1365-2958.2000.02187.x

Marx P, Meiers M, Bruckner R. 2015. Activity of the response regulator CiaR in mutants of *Streptococcus pneumoniae* R6 altered in acetyl phosphate production. *Frontiers in Microbiology* **5**:772. doi:10.3389/fmicb.2014.00772

Marx P, Nuhn M, Kovács M, Hakenbeck R, Brückner R. 2010. Identification of genes for small non-coding RNAs that belong to the regulon of the two-component regulatory system CiaRH in Streptococcus. *BMC Genomics* **11**. doi:10.1186/1471-2164-11-661

Mascher T, Heintz M, Zähner D, Merai M, Hakenbeck R. 2006. The CiaRH system of *Streptococcus pneumoniae* prevents lysis during stress induced by treatment with cell wall inhibitors and by mutations in pbp2x involved in β-lactam resistance. *Journal of Bacteriology* **188**:1959–1968. doi:10.1128/JB.188.5.1959-1968.2006

Mascher T, Zähner D, Merai M, Balmelle N, de Saizieu AB, Hakenbeck R. 2003. The *Streptococcus pneumoniae* cia regulon: CiaR target sites and transcription profile analysis. *J Bacteriol* **185**:60–70. doi:10.1128/JB.185.1.60-70.2003

Moscoso M, Domenech M, García E. 2010. Vancomycin tolerance in clinical and laboratory *Streptococcus pneumoniae* isolates depends on reduced enzyme activity of the major LytA autolysin or cooperation between CiaH histidine kinase and capsular polysaccharide. *Molecular Microbiology* **77**.

Muller M, Marx P, Hakenbeck R, Bruckner R. 2011. Effect of new alleles of the histidine kinase gene ciaH on the activity of the response regulator CiaR in *Streptococcus pneumoniae* R6. *Microbiology (N Y)* **157**:3104–3112. doi:10.1099/mic.0.053157-0

Paintdakhi A, Parry B, Campos M, Irnov I, Elf J, Surovtsev I, Jacobs-Wagner C. 2016. Oufti: an integrated software package for high-accuracy, high-throughput quantitative microscopy analysis. *Molecular Microbiology* **99**:767–777. doi:10.1111/mmi.13264

Peters K, Schweizer I, Hakenbeck R, Denapaite D. 2021. New insights into beta-lactam resistance of *Streptococcus pneumoniae*: Serine protease HtrA degrades altered penicillin-binding protein 2x. *Microorganisms* **9**. doi:10.3390/microorganisms9081685

Raaphorst R van, Kjos M, Veening J-W. 2019. BactMAP: an R package for integrating, analyzing and visualizing bacterial microscopy data. *bioRxiv* 728782. doi:10.1101/728782

Rane L, Subbarow Y. 1940. Nutritional Requirements of the Pneumococcus. *Journal of Bacteriology* **40**:695–704. doi:10.1128/jb.40.5.695-704.1940

Schnorpfeil A, Kranz M, Kovács M, Kirsch C, Gartmann J, Brunner I, Bittmann S, Brückner R. 2013. Target evaluation of the non-coding csRNAs reveals a link of the two-component regulatory system CiaRH to competence control in *Streptococcus pneumoniae* R6. *Molecular Microbiology* **89**:334–349. doi:10.1111/mmi.12277

Schweizer I, Blättner S, Maurer P, Peters K, Vollmer D, Vollmer W, Hakenbeck R, Denapaite D. 2017. New aspects of the interplay between penicillin binding proteins, murM, and the two-component system CiaRH of penicillin-resistant *Streptococcus pneumoniae* serotype 19A isolates from Hungary. *Antimicrobial Agents and Chemotherapy* **61**. doi:10.1128/AAC.00414-17

Sebert ME, Palmer LM, Rosenberg M, Weiser JN. 2002. Microarray-based identification of htrA, a *Streptococcus pneumoniae* gene that is regulated by the CiaRH two-component system and contributes to nasopharyngeal colonization. *Infection and Immunity* **70**:4059–4067. doi:10.1128/IAI.70.8.4059-4067.2002

Sebert ME, Patel KP, Plotnick M, Weiser JN. 2005. Pneumococcal HtrA protease mediates inhibition of competence by the CiaRH two-component signaling system. *Journal of Bacteriology* **187**:3969–3979. doi:10.1128/JB.187.12.3969-3979.2005

Slager J, Aprianto R, Veening JW. 2019. Refining the pneumococcal competence regulon by RNA sequencing. *Journal of Bacteriology* **201**:e00780-18. doi:10.1128/JB.00780-18

Slager J, Aprianto R, Veening JW. 2018. Deep genome annotation of the opportunistic human pathogen *Streptococcus pneumoniae* D39. *Nucleic Acids Research* **46**:9971–9989. doi:10.1093/nar/gky725

Throup JP, Koretke KK, Bryant AP, Ingraham KA, Chalker AF, Yigong G, Marra A, Wallis NG, Brown JR, Holmes DJ, Rosenberg M, Burnham MKR. 2000. A genomic analysis of two-component signal transduction in *Streptococcus pneumoniae*. *Molecular Microbiology* **35**:566–576. doi:10.1046/j.1365-2958.2000.01725.x

Tomasz A. 1968. Biological consequences of the replacement of choline by ethanolamine in the cell wall of Pneumococcus: chain formation, loss of transformability, and loss of autolysis. *Proc Natl Acad Sci U S A* **59**:86–93. doi:10.1073/pnas.59.1.86

Tomasz A. 1967. Choline in the cell wall of a bacterium: Novel type of polymer-linked choline in pneumococcus. *Science (1979)* **157**:694–697. doi:10.1126/science.157.3789.694

Tsui HCT, Mukherjee D, Ray VA, Sham LT, Feig AL, Winkler ME. 2010. Identification and characterization of noncoding small RNAs in *Streptococcus pneumoniae* serotype 2 strain D39. *Journal of Bacteriology* **192**:264–279. doi:10.1128/JB.01204-09

Ünal CM, Steinert M. 2014. Microbial Peptidyl-Prolyl cis / trans Isomerases (PPIases): Virulence Factors and Potential Alternative Drug Targets. *Microbiology and Molecular Biology Reviews* **78**:544–571. doi:10.1128/mmbr.00015-14

## Supplementary Figures

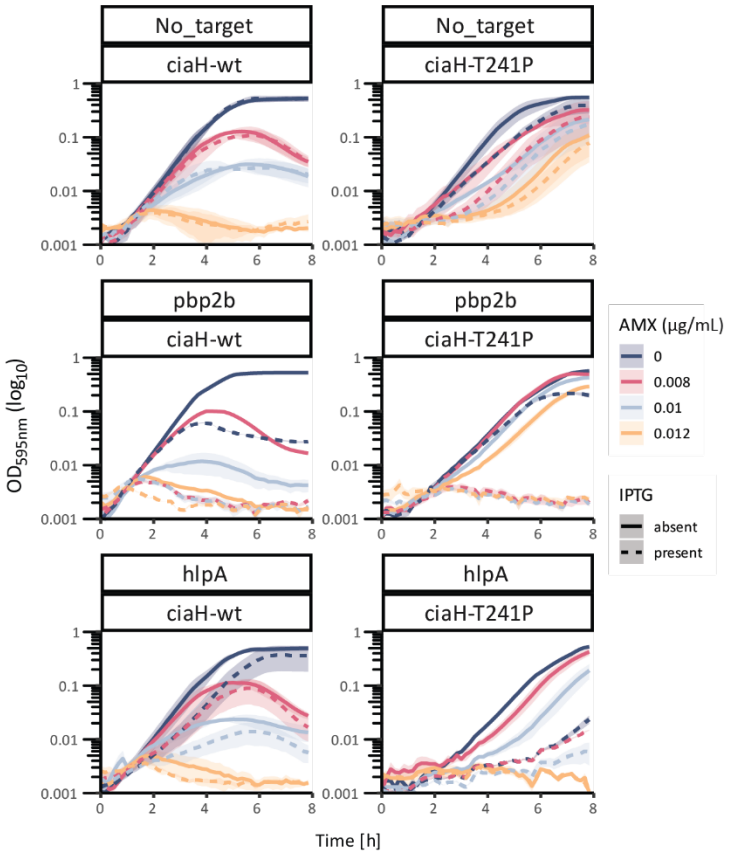


**Figure S1: Growth in absence and presence of IPTG and AMX of CRISPRi control strains.** Plots are labelled with sgRNA target. Control strains were induced with 1 mM IPTG. Color indicates AMX concentration, solid line indicates *dcas9* is not induced, and dashed line indicates presence of inducer IPTG.

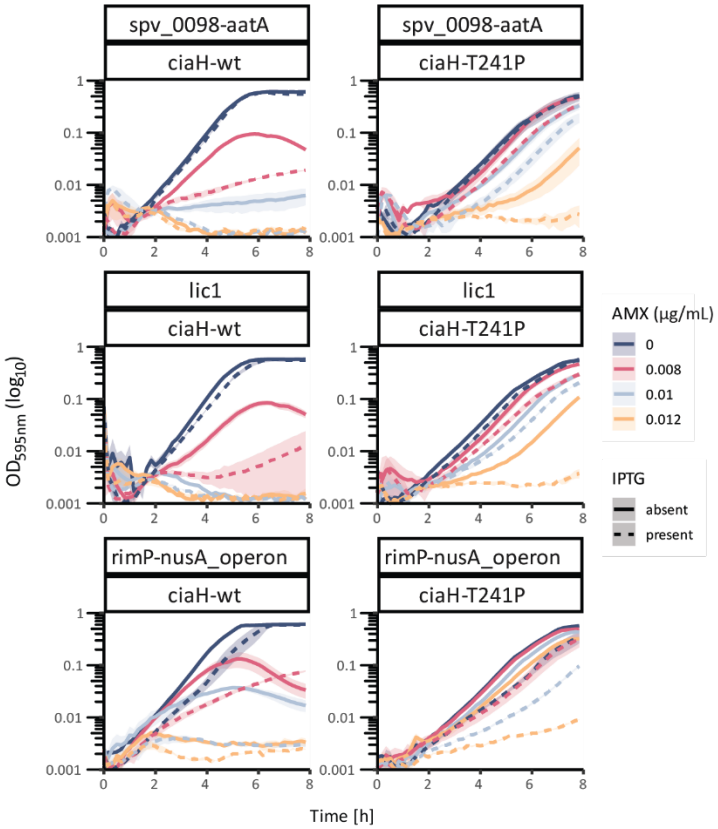


**Figure S2: Growth in absence and presence of IPTG and AMX of CRISPRi strains with sgRNA targeting essential operons.** Plots are labelled with sgRNA target. Operons *lic1* (*tarI, tarJ, licA, licB, licC*) and *spv_0098-aatA* were repressed with 0.01 µM IPTG, and the nusA-rimP operon (*rimP, nusA, spv_0480, spv_0481, infB, rbfA*) with 0.04 µM. Color indicates AMX concentration, solid line indicates *dcas9* is not induced, and dashed line indicates presence of inducer IPTG.

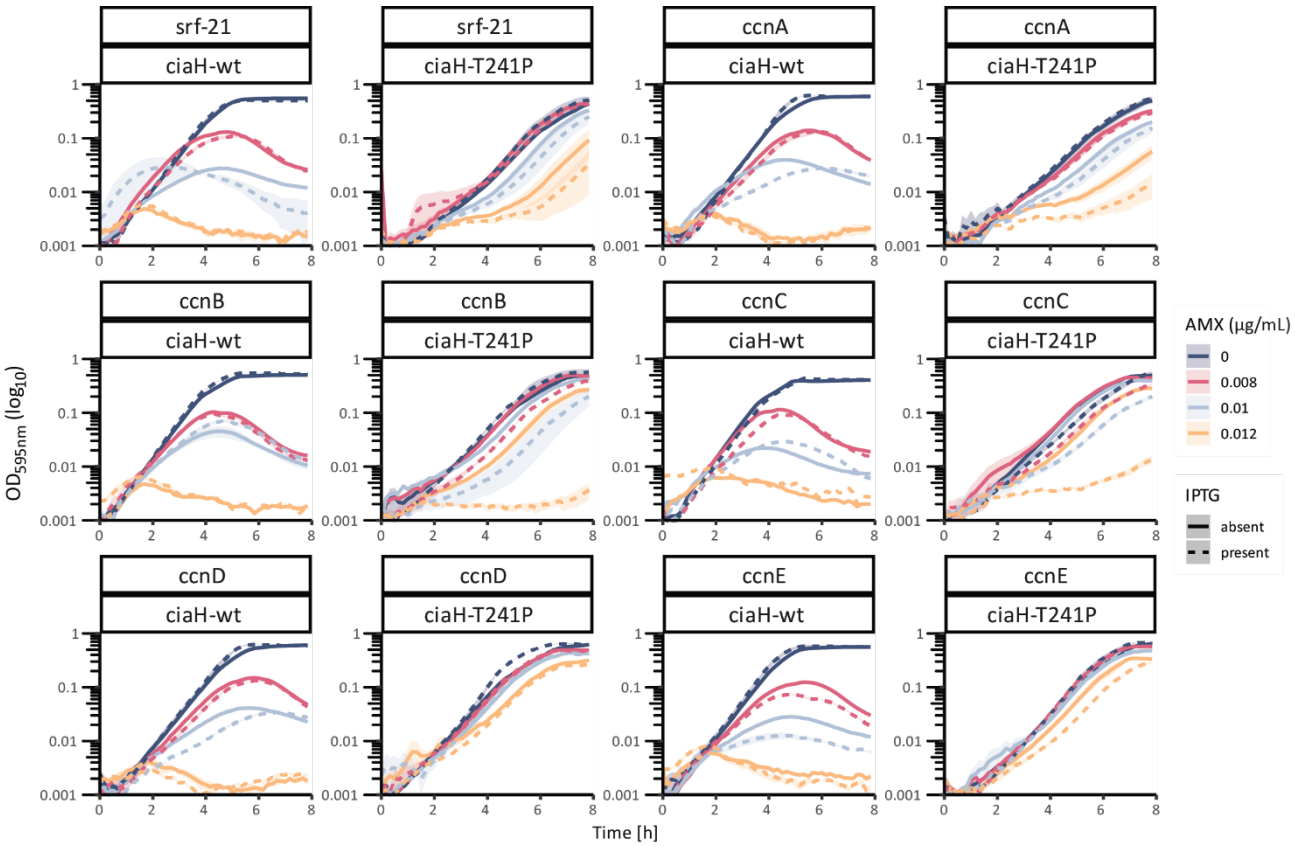


**Figure S3: Growth in absence and presence of IPTG and AMX of strains with CRISPRi-repressed csRNAs.** Plots are labelled with sgRNA target. Color indicates AMX concentration, solid line indicates *dcas9* is not induced, and dashed line indicates presence of inducer IPTG (1 mM).

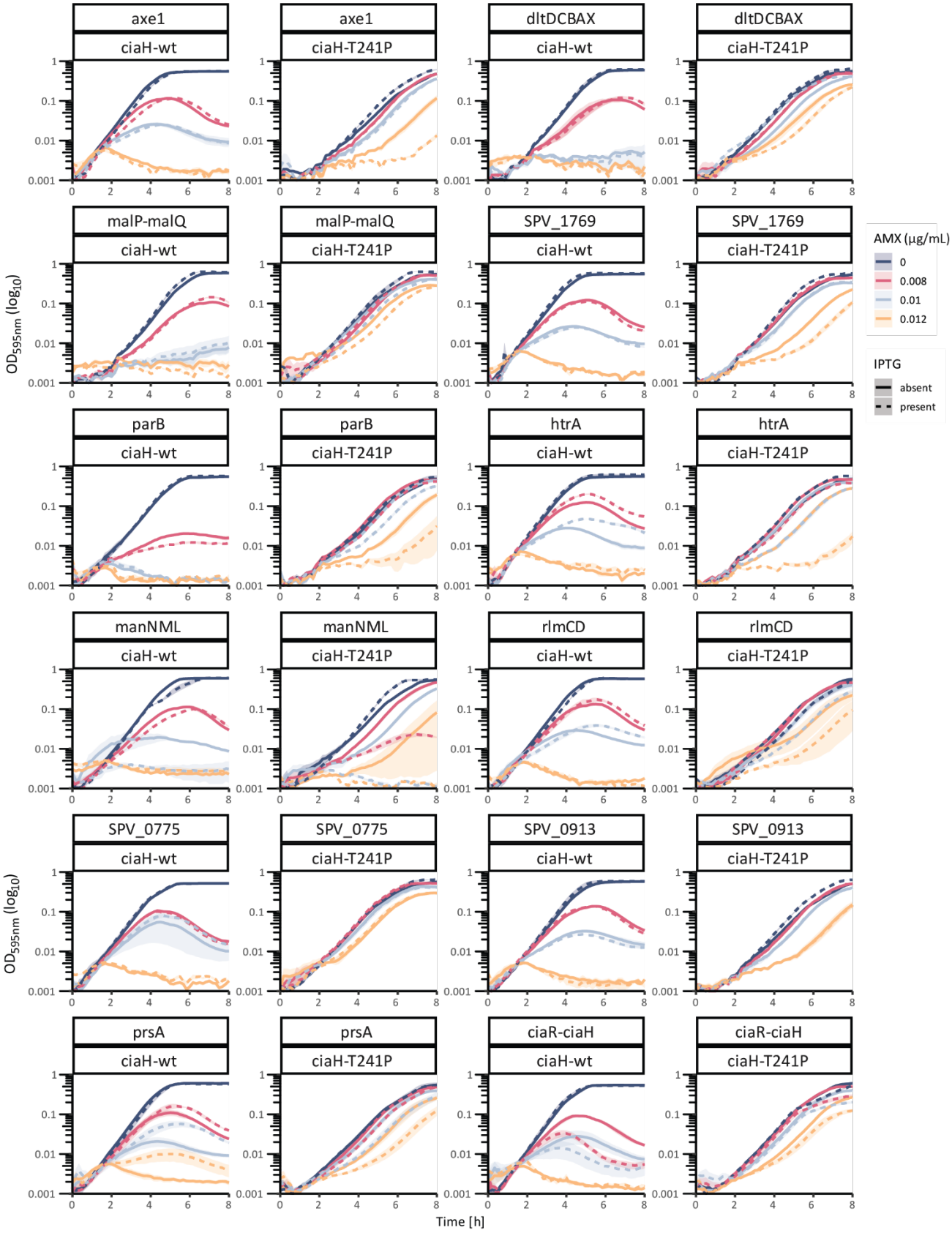


**Figure S4: Growth in absence and presence of IPTG and AMX of CRISPRi control strains.** Plots are labelled with sgRNA target. Strains were induced with 1 mM IPTG. Color indicates AMX concentration, solid line indicates *dcas9* is not induced, and dashed line indicates presence of inducer IPTG.

## Supplementary Tables

**Table S1: Oligos used in the study.**

| **Oligos to clone *ciaH::ciaH$^{allele}$-ery*** | | |
|---|---|---|
| **oligo name** | **5'-3' sequence** | **Description** |
| OVL2166 | CTCAAGCAGTTATTCAGCTGGC | Forward oligo for upstream homology |
| OVL3501 | TCCGTTCGTCTCCCATATTATTTTTT CTTTTTAGATGGTGTCTG | Reverse oligo for upstream homology with BsmBI recognition site |
| OVL844 | TCACACCGTCTCCTATGAACAAAAA TATAAAATATTCTCAAAAC | Forward oligo for ery with BsmBI recognition site |
| OVL845 | TCACACCGTCTCCCTTTATTTCCTCC CGTTAAATAATAGAT | Reverse oligo for ery with BsmBI recognition site |
| OVL3500 | TCCGTTCGTCTCCAAAGAAATATCG CTCCAATTGGGG | Forward oligo for downstream homology with BsmBI recognition site |
| OVL3499 | CCAGGAGTGTAGAGCCCTTCTAG | Reverse oligo for downstream homology |
| **Oligos to amplify ectopic loci** | | |
| **oligo name** | **5'-3' sequence** | **Description** |
| OVL5567 | CCTTCTTAACGCCCCAAGTTCATCACCA | Forward oligo to amplify *bgaA* locus |
| OVL5566 | TAAACCTGCTGCTACTGCTGCTTGGCT | Reverse oligo to amplify *bgaA* locus |
| OVL725 | AGTTAAAGAACTTGGACTGCGCTC | Forward oligo to amplify CEP locus |
| OVL726 | CAATGTGAAAGCGATCAAGAACG | Reverse oligo to amplify CEP locus |
| OVL1005 | GAAACAGATTTTATCTGCTTTATATCG | Forward oligo to amplify ZIP locus / plasmid |
| OVL1004 | ATCAGAAAGCAAACTAGAAAGTTATG | Reverse oligo to amplify ZIP locus / plasmid |
| OVL552 | CTTATTTAGGGCTTGGAAGA | Forward oligo to amplify CIL locus |
| OVL553 | GACTCCGCTTTACGTCAAC | Reverse oligo to amplify CIL locus |
| OVL1809 | CTGGAAGACTAGATCAGGGAATA GTCACAC | Forward oligo to amplify *pbp2b* locus |
| OVL1810 | GTCAATCAACTTGGCAATAGGTGTT GGATAAGC | Reverse oligo to amplify *pbp2b* locus |
| **Oligos which were annealed to form the 20bp sgRNA, which were then inserted into the ZIP locus (Liu et al. 2021)** | | |
| **oligo name** | **5'-3' sequence** | **sgRNA target** |
| sgRNA0005_for | TATACTCTTCCTTTCTCACATACA | *ccnC* |
| sgRNA0005_rev | AAACTGTATGTGAGAAAGGAAGAG | *ccnC* |
| sgRNA0035_for | TATAATTGTATGCACTGATTACAA | *spv_0098* |
| sgRNA0035_rev | AAACTTGTAATCAGTGCATACAAT | *spv_0098* |
| sgRNA0089_for | TATAGATTGTGATGAAAAAAGTTT | *ccnA* |
| sgRNA0089_rev | AAACAAACTTTTTTCATCACAATC | *ccnA* |
| sgRNA1419_for | TATATTTTATTAAATAAAGTTAGG | *ccnB* |
| sgRNA1419_rev | AAACCCTAACTTTATTTAATAAAA | *ccnB* |
| sgRNA1420_for | TATAAGTTTTAGGAGTTTAAGTTA | *ccnD* |
| sgRNA1420_rev | AAACTAACTTAAACTCCTAAAACT | *ccnD* |
| sgRNA0104_for | TATATACCCGCAGCAAATTCGCCG | *manN-manM-manL* |

| | | |
|---|---|---|
| sgRNA0104_rev | AAACCGGCGAATTTGCTGCGGGTA | *manN-manM-manL* |
| sgRNA0184_for | TATATCAAAAGGAGCTTCTATGAC | *rimP-nusA-spv_0480-spv_0481-infB-rbfA* |
| sgRNA0184_rev | AAACGTCATAGAAGCTCCTTTTGA | *rimP-nusA-spv_0480-spv_0481-infB-rbfA* |
| sgRNA0265_for | TATAATACTGAATTTGACAGACCT | *ciaR-ciaH* |
| sgRNA0265_rev | AAACAGGTCTGTCAAATTCAGTAT | *ciaR-ciaH* |
| sgRNA0295_for | TATAGATACTAGCGATTGTAGCAA | *spv_0775* |
| sgRNA0295_rev | AAACTTGCTACAATCGCTAGTATC | *spv_0775* |
| sgRNA0331_for | TATATGCTACTGATAATAGTGTGA | *prsA* |
| sgRNA0331_rev | AAACTCACACTATTATCAGTAGCA | *prsA* |
| sgRNA0381_for | TATAGGCAACTCCTGCCCCTTCAT | *rlmCD* |
| sgRNA0381_rev | AAACATGAAGGGGCAGGAGTTGCC | *rlmCD* |
| sgRNA0382_for | TATAAGAAAGAGTTTCTTTCTCAT | *spv_0913* |
| sgRNA0382_rev | AAACATGAGAAAGAAACTCTTTCT | *spv_0913* |
| sgRNA0431_for | TATACATGCGTGTGCCAGTTCCAC | *licC-licB-licA-tarJ-tarI* |
| sgRNA0431_rev | AAACGTGGAACTGGCACACGCATG | *licC-licB-licA-tarJ-tarI* |
| sgRNA0571_for | TATATTAATTTCTTCTAGCAAAGC | *axe1* |
| sgRNA0571_rev | AAACGCTTTGCTAGAAGAAATTAA | *axe1* |
| sgRNA0572_for | TATACCTTCTTTTGGAAAGTGGTT | *srf-21* |
| sgRNA0572_rev | AAACAACCACTTTCCAAAAGAAGG | *srf-21* |
| sgRNA0655_for | TATAAAAATTGATTGAGACCTGCA | *spv_1769* |
| sgRNA0655_rev | AAACTGCAGGTCTCAATCAATTTT | *spv_1769* |
| sgRNA0716_for | TATAGATCCGATTCCGTAAGCTCC | *malP-malQ* |
| sgRNA0716_rev | AAACGGAGCTTACGGAATCGGATC | *malP-malQ* |
| sgRNA0741_for | TATAAGGCTGTCCGACCAAGAAAG | *dltD-dltC-dltB-dltA-dltX* |
| sgRNA0741_rev | AAACCTTTCTTGGTCGGACAGCCT | *dltD-dltC-dltB-dltA-dltX* |
| sgRNA0767_for | TATAAGTTATTGAAAAACTACCCA | *htrA* |
| sgRNA0767_rev | AAACTGGGTAGTTTTTCAATAACT | *htrA* |
| sgRNA0768_for | TATAAATTCTTTTCGGGGTTGATA | *parB* |
| sgRNA0768_rev | AAACTATCAACCCCGAAAAGAATT | *parB* |
| OVL3639 | TATATCCTTCAAAAGTCGCCTGTA | *ccnE* |
| OVL3640 | AAACTACAGGCGACTTTTGAAGGA | *ccnE* |
| sgRNA0568_for | TATATAAGCCGAATCGGAATCGAA | *pbp2b* |
| sgRNA0568_rev | AAACTTCGATTCCGATTCGGCTTA | *pbp2b* |
| sgRNA0335_for | TATAGACCTCTGCAATCTCACTGA | *hlpA* |
| sgRNA0335_rev | AAACTCAGTGAGATTGCAGAGGTC | *hlpA* |

**Table S2: All operons predicted to be regulated by the CiaRH system** (Slager et al., 2019).

| **sgRNA-targeted operon** | **Product** |
|---|---|
| *ccnC* | csRNA3 |
| *spv_0098; aatA* | Glycosyltransferase, putative UDP-GlcNAc 4,6-dehydratase AatA |

| | |
|---|---|
| *ccnE* | csRNA5 |
| *ccnA* | csRNA1 |
| *ccnB* | csRNA2 |
| *ccnD* | csRNA4 |
| *manN; manM; manL* | Mannose-specific PTS IID, IIC, and IIAB components |
| *rimP; nusA; spv_0480; spv_0481; infB; rbfA* | Bacterial ribsome SSU maturation protein, transcription termintation/antitermination protein, putative transcription termination protein, L7Ae family ribosomal protein, translation initiation factor 2, ribosome-binding factor A |
| *ciaR; ciaH* | Two-component system reponse regulator and histidine kinase |
| *spv_0775* | Acetyltransferase |
| *prsA* | putative parvulin type peptidyl-prolyl isomerase |
| *rimCD* | 23S rRNA (uracil(19390-C(5))-methyltransferase |
| *spv_0913* | Extracellular protein |
| *licC; licB; licA ; tarJ; tarI* | Choline phosphate cytidylyltransferase, choline permease, choline kinase, ribulose-5-phosphate reductase, ribulose-5-phosphate cytidylyltransferase |
| *axe1* | acetyl xylan esterase 1/cephalosporin-C deacetylase |
| *srf-21* | ncRNA of unknown function |
| *spv_1769* | Membrane protein |
| *malP; malQ* | Maltodextrin phosphorylase, 4-alpha-glucanotransferase (amylomaltase) |
| *dltD; dltC; dltB; dltA; dltX* | Poly(glycerophosphate chain) D-alanine transfer protein, D-alanine--poly(phosphoribitol) ligase subunit 2, D-alanyl transfer protein, D-alanine--poly(phosphoribitol) ligase subunit 1, D-alanyl-lipoteichoic acid biosynthesis protein |
| *htrA* | Serine protease |
| *parB* | Chromosome partitioning protein |

# Chapter 5

## General Discussion

Paddy S. Gibson

Department of Fundamental Microbiology, Faculty of Biology and Medicine, University of Lausanne, Biophore Building, CH-1015 Lausanne, Switzerland

This chapter was written by PG with feedback from JWV.

In this thesis we attempted to unravel the many effects that the frontline antibiotic amoxicillin (AMX) has on the molecular biology of *Streptococcus pneumoniae*. We studied how *S. pneumoniae* utilises natural competence and recombination to evolve genetic AMX resistance. We applied AMX-induced lysis in combination with genome-wide synthetic lethal screening to identify a novel protein associated with the regulation of the major pneumococcal autolysin LytA. Finally, we investigated the regulatory mechanism of cell wall stress response two-component system CiaRH. Here, we discuss these results in the broader context, including how all aspects of this thesis are interdependent.

## Amoxicillin resistance evolution through recombination

*S. pneumoniae* is naturally competent and frequently undergoes large-scale recombination events in the natural environment (Croucher et al., 2011; Wyres et al., 2012, 2013). This component of its molecular biology encompasses the potential for enormous genomic plasticity, enabling populations to respond rapidly to environmental change. As for all human pathogens, antibiotic resistance evolution is of great interest, and a significant body of work on recombination at resistance-determining loci has been built up over the last 30 - 50 years. In Chapter 2, we explored the evolution of AMX resistance through recombination using sequential genomic DNA transformation experiments.

β-lactam antibiotics have been critical for the treatment of pneumococcal infections since they were first discovered and the absence of β-lactamase enzymes identified in this and closely related species has made for a tantalizing model of study. Homologous recombination of highly variable donor DNA into loci encoding essential cell wall synthesis proteins (PBPs) seems risky from an individual point of view, yet has enabled the rapid dissemination of low-affinity PBP alleles through pathogenic and commensal Streptococcal populations. This has led to a model of a shared global pool of variable *pbp* alleles, dispersed via frequent lateral transfer among naturally competent species of the upper respiratory tract (Dowson et al., 1997; Hakenbeck et al., 2012; Jensen et al., 2015; Reichmann et al., 1997).

In our system, we synthetically induced competence in a susceptible strain, then transformed with high concentrations of naked genomic DNA from a resistant isolate and selected on AMX. Whole genome sequencing and the high variation between donor and both recipients (>20,000 SNPs) allowed us to identify recombination events down to the nearest SNP. Using

this system, we were able to investigate both non-contiguous recombination, and the optimal order of loci modification for AMX resistance development.

Non-contiguous recombination is the occurrence of fragmented regions of recognisable donor DNA, separated by stretches of recipient genome. This has been observed in both sequenced clinical isolates and laboratory studies previously (Croucher et al., 2012; Gibson et al., 2021; Mell et al., 2011). In Chapter 2, we designed an experiment to compare the frequencies of non-contiguous recombination events with different forms of donor DNA. We observed recombination events both with single long fragments and combinations of shorter fragments. This led to the conclusion that non-contiguous recombination could occur via more than one mechanism, and that the controlling factor could instead be transformation efficiency, dependent on overall length and amount of homology type of donor DNA.

Following the sequential transformation experiment and recombination detection, we observed patterns in modified loci that correlated to strain MIC. This suggested a preferred order of *pbp* and *murM* allele up take. To test this, we performed single and double allele transformation, with AMX selection, to manually build up resistance in naïve D39V. We showed the modified *pbp2x* and *pbp2b* alleles were sufficient to recapitulate the MICs of first generation transformants. We also found that *pbp1a* mutations could not be selected for without the prior acquisition of *pbp2b* and *pbp2x* alleles. Surprisingly, *murM* mutations could be selected for on AMX, suggesting an unknown benefit of increased branched muropeptides in AMX survival. Overall, we showed that early acquisition of low-affinity *pbp2x* was ideal, followed by *pbp2b* and *murM*, and that *pbp1a* mutants could be acquired later for higher level resistance. We also confirmed that a block of 10 substitutions at the C-terminal end of the Pbp2b transpeptidase domain to be a key AMX-specific resistance determinant (du Plessis et al., 2002).

One criticism of this study could be its level of applicability to horizontal gene transfer in the native environment of the pneumococcus. In the nasopharynx the pneumococcus lives in biofilms of mixed species, and any DNA acquired would likely be sourced from low concentrations of free DNA in the environment, or through fratricide-induced lysis of neighbouring cells (Claverys & Håvarstein, 2007; Håvarstein et al., 2006; Veening & Blokesch, 2017). Despite these challenges, significant genome remodelling is observed in pneumococcal clinical isolates, with more than 7% of the genome transferred during co-infection of a

paediatric patient (Hiller et al., 2010). Recombination event length has been shown to increase in the presence of cell-to-cell contact in a biofilm (Cowley et al., 2018), and events as long as 50 Kb have been identified in clinical isolates (Wyres et al., 2012). A well-known example is complete switching of the capsule locus, sometimes including the flanking regions containing the *pbp2x* and *pbp1a* loci (Trzciński et al., 2004; Wyres et al., 2013). Capsule switching was not observed in our model, where transfer of *pbp2x* always occurred in the first round of transformation, and *pbp1a* in the second, displaying a lack of linkage. The cause of this is unknown, although we could hypothesise an effect from lack of close recipient-donor contact. Indeed, the dynamics of DNA uptake and recombination likely differ in our model compared to the natural environment of the pneumococcus, but it remains difficult to predict the effect this might have on recombination.

It is important to note that AMX resistance did not evolve in an entirely naïve population. Penicillin (PEN) had been in use for more than 20 years, and low-affinity *pbp* variants were already being studied by the time AMX resistant strains were isolated (Hansman & Bullen, 1967). When AMX resistant isolates began to appear, they arose from clones already associated with PEN resistance (Pérez-Trallero et al., 2003, 2007; Stanhope et al., 2007). Thus, it appears unlikely that AMX resistance evolved in fully susceptible isolates, but rather in genetic backgrounds already heavily modified for PEN resistance. These backgrounds may have aided in supporting PBP modifications that would otherwise be very costly in terms of fitness. It might be informative to perform similar experiments as in Chapter 2, but using different types of clinical strains with differing PEN and AMX MICs as recipients, to better explore the evolutionary footsteps which may occur during genetic exchange in the natural environment of the pneumococcus.

## Regulating pneumococcal autolysis

The major autolysin and choline binding protein LytA is an important virulence factor for *S. pneumoniae* (Berry et al., 1989; Canvin et al., 1995). It acts by binding to phosphorylcholine residues of wall teichoic acid (WTA), allowing its amidase domain to access and cleave the amide bond between glycan strand and peptide of peptidoglycan (PG). It remains cytoplasmic through exponential phase, does not possess a signal peptide for export, and its activity is

only triggered under certain conditions including β-lactam treatment (Cho et al., 2014; Mellroth et al., 2012; Tomasz, 1968; Tomasz & Waks, 1975). How it gets outside the cell to reach its target, and how the timing of its activity is controlled is not known, although LytA-GFP shows different localization patterns according to the growth phase (Bonnet et al., 2018). In Chapter 3, we used clustered regularly-interspaced short palindromic repeat interference sequencing (CRISPRi-seq) in combination with AMX-induced autolysis to identify novel proteins associated with modified lysis phenotypes. We found BeaU (β-lactam susceptibility and autolysis associated), a small unannotated membrane protein, highly conserved within *S. pneumoniae* strains.

BeaU is predicted to have a transmembrane domain at the N-terminus, with the C-terminus and the bulk of the protein sitting intracellularly. Interestingly, a C-terminal GFP fusion localised in a uniform membrane distribution, but a GFP fusion at the N-terminus resulted in spotty localisations with foci at the poles. The N-terminal tag may interfere with protein folding or membrane insertion. BeaU may exist as a monomer, dimer, or trimer but *in vitro* confirmation is required to confirm these predictions.

Strains mutated for *beaU* showed increased susceptibility to β-lactams, and earlier stationary phase lysis. We demonstrated that the increased lysis was LytA dependent, however a *beaU* deletion mutant was still more susceptible to the addition of purified rLytA than the wild-type. This indicated that the effect of BeaU on LytA activity was likely indirect, and we hypothesise that deleting *beaU* affects the cell wall structure in some way that makes it more susceptible to both LytA and phage lysin activities.

Using a CRISPRi-seq screen for synthetic lethality, we identified 12 operons which were predicted to interact genetically with *beaU*. These included genes encoding for divisome and elongasome proteins CozEa, DivIC, DivIB, FtsE, FtsX, and EzrA, as well as teichoic acid synthesis-related proteins LafB and LytR. Although these interactions remain to be confirmed, they provide further evidence supporting a role for BeaU in cell wall structure formation, correlating nicely with current models for LytA regulation. One hypothesis is that LytA is sequestered on lipoteichoic acids (LTA) during exponential phase, but that degradation of LTA synthase TacL upon entrance to stationary phase shifts synthesis to WTA through reduced substrate competition. This mediates a shift in cell wall composition from LTA to WTA, forcing LytA to move onto the WTA-bound choline instead, where it can access the substrate (Flores-

Kim et al., 2019). Another hypothesis is that LytA is always found in the cell wall to some extent during cell growth, but that mature PG is capped in some way, blocking LytA from accessing the substrate. When cell wall synthesis is stalled near the septum, LytA can then access nascent PG, inducing lysis (Bonnet et al., 2018; Mellroth et al., 2012).

The pneumococcal cell wall is unique in that it is composed of roughly equal amounts of TA and PG. Both of these structures are important to the activity of LytA, and it is conceivable that alterations to either would affect its activity. In addition, the synthesis of both structures is tightly interwoven, particularly as WTA are anchored directly onto the cross-linked PG. Deletion of a protein involved in the synthesis of one, may very well show genetic interactions with proteins in the other pathway. Interestingly, the capsule is also covalently attached to the PG and competes for its attachment site with WTA (Eberhardt et al., 2012). Strikingly, capsule mutants, which thus have relatively more WTA compared to encapsulated strains, are more susceptible to LytA-dependent autolysis (Fernebro et al., 2004 and Chapter 3). It is tempting to speculate that the increases in WTA cause more PG-localised LytA, resulting in the increased lysis phenotype. The next step to elucidate the role of BeaU is to determine which CRISPRi-seq hits, if any, are due to direct protein-protein interactions, allowing us to pinpoint the key pathway for its function. Identifying indirect genetic interactions is also important, they provide observations and novel hypotheses on the complex relationships between cell wall synthesis proteins.

## The pneumococcal response to amoxicillin-induced stress

For bacteria to be able to respond to changes in their environment, they must first be able to sense them. Two-component systems (TCS) are essential for this behavior, and *S. pneumoniae* possesses 13 of them (Throup et al., 2000). CiaRH responds to cell wall stress, such as that induced by β-lactam treatment or competence. The response regulator CiaR is predicted to affect transcription of 21 different operons in the pneumococcal genome upon activation by CiaH (Slager et al., 2018). Mutations in *ciaH* have been associated with both piperacillin and cefotaxime resistance in laboratory mutants (Guenzi et al., 1994; Muller et al., 2011). In Chapter 4, we showed for the first time that AMX exposure also selects for point

mutations in *ciaH*, and confirmed the resulting increase in expression from a CiaR-dependent promoter.

Although CiaH substitutions have been investigated previously, it is challenging to know their downstream effects on the cell as the regulon is large and complex, with several non-coding RNAs (csRNAs) with their own regulons also encoded in the set. A previous study pinpointed five csRNAs to be involved in the decreased β-lactam susceptibility of *ciaH* mutants, although there are several other members of the operons that could conceivably play a role (Schnorpfeil et al., 2013). In Chapter 3, we used targeted CRISPRi repression of CiaR-regulated operons to investigate their individual involvement in the AMX susceptibility phenotype. This approach identified several candidates whose repression affected pneumococcal growth in AMX either in the $ciaH^{wt}$ or $ciaH^{T241P}$ background. Many of these had known links to cell wall synthesis, where alterations in their expression would be expected to impact β-lactam susceptibility. One difficulty of this approach was potential additive effects of repression of essential operons in combination with AMX treatment. Follow up experiments using a system for operon overexpression is required to confirm these results. This is particularly relevant for choline metabolism operon *licD1* given the importance of choline-decorated TAs in LytA-mediated lysis induced by β-lactams.

In addition, two of candidates encode csRNAs, further highlighting the importance of understanding the specificity and extent of non-coding RNA regulatory networks. Although some predictions have been made regarding what mRNAs these particular csRNAs may target, limited experimental confirmations have been performed (Schnorpfeil et al., 2013). These will be essential in fully understanding the interconnected role of CiaRH in cellular stress response.

Although *ciaH* point mutations have been identified in clinical isolates, they are rare and do not cause the same level of CiaH hyperactivity as those isolated in laboratory screenings (Muller et al., 2011). This indicates a loss of fitness in the natural environment too severe to be countered by the increased β-lactam survival benefit. Hyperactive *ciaH* mutants show substantial decreases in natural competence, due to increased competence stimulating peptide (CSP) degradation by protease HtrA (Cassone et al., 2012; Giammarinaro et al., 1999; Sebert et al., 2005). This is thought to be a contributing factor to the rarity of *ciaH* mutants in clinical isolates, as transformation is enormously important to *S. pneumoniae* for the

acquisition of resistance determinants, capsule switching for vaccine escape, and DNA repair (Andam & Hanage, 2015; Johnston et al., 2014; Synefiaridou & Veening, 2021). However, the CiaRH system is also essential for the pneumococcus to tolerate the presence of low-affinity *pbp2x* alleles, required for β-lactam resistance (Mascher et al., 2006). HtrA has been shown to maintain lower levels of Pbp2x in strains with single substitutions in the protein, presumably in response to increased misfolding or altered activity (Peters et al., 2021). This is beneficial at low levels, but hyperactive CiaH results in much higher levels of HtrA in the cell, a condition that led to suppressor mutations in complementation studies (Peters et al., 2021). Interestingly, in the sequential transformation experiments performed in Chapter 2, the *ciaH*$^{D353N}$ mutation present on the donor chromosome was not detected in any of the sequenced recombinants, including those that matched the donor MIC. CiaH$^{D353N}$ has been shown to increase expression from CiaR-dependent promoters, although not to the same extent as T241P (Muller et al., 2011). It would be beneficial assess the role of hyperactive CiaH substitutions in the different AMX-resistance genetic backgrounds generated in Chapter 2 through *ciaH* allele swapping experiments. This may help to elucidate the involvement of hyperactive CiaH substitutions in the development and maintenance of β-lactam resistance in the pneumococcus.

## Outlook

In this thesis we explored three different aspects of the pneumococcal response to AMX treatment. We first investigated the genetic alterations essential for AMX resistance and the horizontal gene transfer mechanisms necessary for their acquisition. We then searched for novel regulatory proteins of autolysis, a phenomenon triggered by β-lactam treatment. Finally, we attempted to unravel the complex regulatory network of CiaRH, to better understand the pneumococcal response to cell wall stress caused by AMX exposure. In every chapter we discussed different factors that reduce AMX susceptibility, all of which are intertwined and interdependent, and all of which require further investigation to fully understand their implications.

In Chapter 2 we investigated one mechanism of AMX resistance development, however higher MICs and other combinations of alleles have been described in resistant isolates.

Comparing horizontal gene transfer between different donor and recipient strains, with different starting MICs, may allow for the exploration of different AMX resistance mechanisms and evolutionary pathways. The identification of BeaU in Chapter 3 provides another clue to the regulation of LytA activity in *S. pneumoniae*. However, this protein is far from being fully characterized, and there are several potential protein-protein interactions still to be explored. Investigating these may allow us to fit this protein into a cellular pathway, and hopefully filling in one of the blanks still present in the cell wall synthesis pathways of *S. pneumoniae*. In Chapter 4, we identified several operons in the CiaRH regulon which could explain the effects of *ciaH* mutations identified in cefotaxime, piperacillin and now AMX selection experiments (Guenzi et al., 1994). These remain to be confirmed, and their downstream effects explored.

Antibiotic resistance is increasing worldwide, sometimes referred to as the “silent pandemic”. Understanding how bacteria respond to antibiotic treatment is critical for elucidating the mechanisms and evolution of antibiotic resistance, necessary for the appropriate implementation of antibiotic stewardship programs. If we wish to continue to rely on antibiotic therapy for life-saving interventions, the activity of current drugs must be conserved for future generations.

## References


Andam, C. P., & Hanage, W. P. (2015). Mechanisms of genome evolution of Streptococcus. *Infection, Genetics and Evolution*, *33*, 334–342. https://doi.org/10.1016/j.meegid.2014.11.007

Berry, A. M., Lock, R. A., Hansman, D., & Paton, J. C. (1989). Contribution of autolysin to virulence of *Streptococcus pneumoniae*. *Infection and Immunity*, *57*(8), 2324–2330. https://doi.org/10.1128/iai.57.8.2324-2330.1989

Bonnet, J., Durmort, C., Mortier-Barrière, I., Campo, N., Jacq, M., Moriscot, C., Straume, D., Berg, K. H., Håvarstein, L., Wong, Y. S., Vernet, T., & di Guilmi, A. M. (2018). Nascent teichoic acids insertion into the cell wall directs the localization and activity of the major pneumococcal autolysin LytA. *Cell Surface*, *2*, 24–37. https://doi.org/10.1016/j.tcsw.2018.05.001

Canvin, J. R., Marvin, A. P., Sivakumaran, M., Paton, J. C., Boulnois, G. J., Andrew, P. W., & Mitchell, T. J. (1995). The Role of Pneumolysin and Autolysin in the Pathology of Pneumonia and Septicemia in Mice Infected with a Type 2 Pneumococcus. *Journal of Infectious Diseases*, *172*(1), 119–123. https://doi.org/10.1093/infdis/172.1.119

Cassone, M., Gagne, A. L., Spruce, L. A., Seeholzer, S. H., & Sebert, M. E. (2012). The HtrA protease from *Streptococcus pneumoniae* digests both denatured proteins and the competence-stimulating peptide. *The Journal of Biological Chemistry*, *287*(46), 38449–38459. https://doi.org/10.1074/jbc.M112.391482

Cho, H., Uehara, T., & Bernhardt, T. G. (2014). Beta-Lactam Antibiotics Induce a Lethal Malfunctioning of the Bacterial Cell Wall Synthesis Machinery. *Cell*, *159*(6), 1300–1311.

Claverys, J. P., & Håvarstein, L. S. (2007). Cannibalism and fratricide: Mechanisms and raisons d'être. In *Nature Reviews Microbiology* (Vol. 5, Issue 3, pp. 219–229). Nat Rev Microbiol. https://doi.org/10.1038/nrmicro1613

Cowley, L. A., Petersen, F. C., Junges, R., Jimson D. Jimenez, M., Morrison, D. A., & Hanage, W. P. (2018). Evolution via recombination: Cell-to-cell contact facilitates larger recombination events in *Streptococcus pneumoniae*. *PLOS Genetics*, *14*(6), e1007410. https://doi.org/10.1371/journal.pgen.1007410

Croucher, N. J., Harris, S. R., Barquist, L., Parkhill, J., & Bentley, S. D. (2012). A high-resolution view of genome-wide pneumococcal transformation. *PLoS Pathogens*, *8*(6), e1002745. https://doi.org/10.1371/journal.ppat.1002745

Croucher, N. J., Harris, S. R., Fraser, C., Quail, M. A., Burton, J., van der Linden, M., McGee, L., von Gottberg, A., Song, J. H., Ko, K. S., Pichon, B., Baker, S., Parry, C. M., Lambertsen, L. M., Shahinas, D., Pillai, D. R., Mitchell, T. J., Dougan, G., Tomasz, A., … Bentley, S. D.

(2011). Rapid pneumococcal evolution in response to clinical interventions. *Science*, *331*(6016), 430–434. https://doi.org/10.1126/SCIENCE.1198545

Dowson, C. G., Barcus, V., King, S., Pickerill, P., Whatmore, A., & Yeo, M. (1997). Horizontal gene transfer and the evolution of resistance and virulence determinants in Streptococcus. *Journal of Applied Microbiology Symposium Supplement*, *83*, 42–51. https://doi.org/10.1046/j.1365-2672.83.s1.5.x

du Plessis, M., Bingen, E., Klugman, K. P., Plessis, M. du, Bingen, E., Klugman, K. P., du Plessis, M., Bingen, E., & Klugman, K. P. (2002). Analysis of Penicillin-Binding Protein Genes of Clinical Isolates of *Streptococcus pneumoniae* with Reduced Susceptibility to Amoxicillin. *Antimicrobial Agents and Chemotherapy*, *46*(8), 2349–2357. https://doi.org/10.1128/AAC.46.8.2349

Eberhardt, A., Hoyland, C. N., Vollmer, D., Bisle, S., Cleverley, R. M., Johnsborg, O., Håvarstein, L. S., Lewis, R. J., & Vollmer, W. (2012). Attachment of capsular polysaccharide to the cell wall in *Streptococcus pneumoniae*. *Microbial Drug Resistance*, *18*(3), 240–255. https://doi.org/10.1089/mdr.2011.0232

Fernebro, J., Andersson, I., Sublett, J., Morfeldt, E., Novak, R., Tuomanen, E., Normark, S., & Normark, B. H. (2004). Capsular Expression in *Streptococcus pneumoniae* Negatively Affects Spontaneous and Antibiotic-Induced Lysis and Contributes to Antibiotic Tolerance. *Journal of Infectious Diseases*, *189*(2), 328–338. https://doi.org/10.1086/380564/2/189-2-328-FIG006.GIF

Flores-Kim, J., Dobihal, G. S., Fenton, A., Rudner, D. Z., & Bernhardt, T. G. (2019). A switch in surface polymer biogenesis triggers growth-phase-dependent and antibiotic-induced bacteriolysis. *ELife*, *8*. https://doi.org/10.7554/eLife.44912

Giammarinaro, P., Sicard, M., & Gasc, A.-M. (1999). Genetic and physiological studies of the CiaH-CiaR two-component signal-transducing system involved in cefotaxime resistance and competence of *Streptococcus pneumoniae*. *Microbiology*, *145*(8), 1859–1869. https://doi.org/10.1099/13500872-145-8-1859

Gibson, P. S., Bexkens, E., Zuber, S., Cowley, L., & Veening, J.-W. (2021). The acquisition of clinically relevant amoxicillin resistance in *Streptococcus pneumoniae* requires ordered horizontal gene transfer of four loci. *BioRxiv*, 2021.12.17.473165. https://doi.org/10.1101/2021.12.17.473165

Guenzi, E., Gasc, A.-M., Sicard, M. A., & Hakenbeck, R. (1994). A two-component signal-transducing system is involved in competence and penicillin susceptibility in laboratory mutants of *Streptococcus pneumoniae*. *Molecular Microbiology*, *12*(3), 505–515. https://doi.org/10.1111/j.1365-2958.1994.tb01038.x

Hakenbeck, R., Brückner, R., Denapaite, D., & Maurer, P. (2012). Molecular mechanisms of β-lactam resistance in *Streptococcus pneumoniae*. In *Future Microbiology* (Vol. 7, Issue 3, pp. 395–410). Future Medicine Ltd London, UK. https://doi.org/10.2217/fmb.12.2

Hansman, D., & Bullen, M. M. (1967). A resistant pneumococcus. *Lancet*, *2*, 264–265.

Håvarstein, L. S., Martin, B., Johnsborg, O., Granadel, C., & Claverys, J. P. (2006). New insights into the pneumococcal fratricide: Relationship to clumping and identification of a novel immunity factor. *Molecular Microbiology*, *59*(4), 1297–1037. https://doi.org/10.1111/j.1365-2958.2005.05021.x

Hiller, N. L., Ahmed, A., Powell, E., Martin, D. P., Eutsey, R., Earl, J., Janto, B., Boissy, R. J., Hogg, J., Barbadora, K., Sampath, R., Lonergan, S., Post, J. C., Hu, F. Z., & Ehrlich, G. D. (2010). Generation of Genic Diversity among *Streptococcus pneumoniae* Strains via Horizontal Gene Transfer during a Chronic Polyclonal Pediatric Infection. *PLOS Pathogens*, *6*(9), e1001108. https://doi.org/10.1371/JOURNAL.PPAT.1001108

Jensen, A., Valdórsson, O., Frimodt-Møller, N., Hollingshead, S., & Kilian, M. (2015). Commensal streptococci serve as a reservoir for β-lactam resistance genes in *Streptococcus pneumoniae*. *Antimicrobial Agents and Chemotherapy*, *59*(6), 3529–3540. https://doi.org/10.1128/AAC.00429-15

Johnston, C., Martin, B., Fichant, G., Polard, P., & Claverys, J. P. (2014). Bacterial transformation: Distribution, shared mechanisms and divergent control. In *Nature Reviews Microbiology* (Vol. 12, Issue 3, pp. 181–196). Nature Publishing Group. https://doi.org/10.1038/nrmicro3199

Mascher, T., Heintz, M., Zähner, D., Merai, M., & Hakenbeck, R. (2006). The CiaRH system of *Streptococcus pneumoniae* prevents lysis during stress induced by treatment with cell wall inhibitors and by mutations in *pbp2x* involved in β-lactam resistance. *Journal of Bacteriology*, *188*(5), 1959–1968. https://doi.org/10.1128/JB.188.5.1959-1968.2006

Mell, J. C., Shumilina, S., Hall, I. M., & Redfield, R. J. (2011). Transformation of natural genetic variation into *haemophilus influenzae* genomes. *PLoS Pathogens*, *7*(7), e1002151. https://doi.org/10.1371/journal.ppat.1002151

Mellroth, P., Daniels, R., Eberhardt, A., Rönnlund, D., Blom, H., Widengren, J., Normark, S., & Henriques-Normark, B. (2012). LytA, major autolysin of *Streptococcus pneumoniae*, requires access to nascent peptidoglycan. *Journal of Biological Chemistry*, *287*(14), 11018–11029.https:// doi.org/10.1074/jbc.M111.318584

Muller, M., Marx, P., Hakenbeck, R., & Bruckner, R. (2011). Effect of new alleles of the histidine kinase gene *ciaH* on the activity of the response regulator CiaR in *Streptococcus pneumoniae* R6. *Microbiology*, *157*(11), 3104–3112. https://doi.org/10.1099/mic.0.053157-0

Pérez-Trallero, E., Marimón, J. M., Ercibengoa, M., Giménez, M. J., Coronel, P., & Aguilar, L. (2007). Antimicrobial susceptibilities of amoxycillin-non-susceptible and susceptible isolates among penicillin-non-susceptible *Streptococcus pneumoniae*. *Clinical Microbiology and Infection*, *13*(9), 937–940. https://doi.org/10.1111/j.1469-0691.2007.01777.x

Pérez-Trallero, E., Marimón, J. M., González, A., García-Rey, C., & Aguilar, L. (2003). Genetic relatedness of recently collected Spanish respiratory tract *Streptococcus pneumoniae* isolates with reduced susceptibility to amoxicillin. *Antimicrobial Agents and Chemotherapy*, *47*(11), 3637–3639. https://doi.org/10.1128/aac.47.11.3637-3639.2003

Peters, K., Schweizer, I., Hakenbeck, R., & Denapaite, D. (2021). New insights into beta-lactam resistance of *Streptococcus pneumoniae*: Serine protease HtrA degrades altered penicillin-binding protein 2x. *Microorganisms*, *9*(8). https://doi.org/10.3390/microorganisms9081685

Reichmann, P., König, A., Liñares, J., Alcaide, F., Tenover, F. C., McDougal, L., Swidsinski, S., & Hakenbeck, R. (1997). A Global Gene Pool for High-Level Cephalosporin Resistance in Commensal *Streptococcus* Species and *Streptococcus pneumoniae*. *The Journal of Infectious Diseases*, *176*(4), 1001–1012. https://doi.org/10.1086/516532

Schnorpfeil, A., Kranz, M., Kovács, M., Kirsch, C., Gartmann, J., Brunner, I., Bittmann, S., & Brückner, R. (2013). Target evaluation of the non-coding csRNAs reveals a link of the two-component regulatory system CiaRH to competence control in *Streptococcus pneumoniae* R6. *Molecular Microbiology*, *89*(2), 334–349. https://doi.org/10.1111/mmi.12277

Sebert, M. E., Patel, K. P., Plotnick, M., & Weiser, J. N. (2005). Pneumococcal HtrA protease mediates inhibition of competence by the CiaRH two-component signaling system. *Journal of Bacteriology*, *187*(12), 3969–3979. https://doi.org/10.1128/JB.187.12.3969-3979.2005

Slager, J., Aprianto, R., & Veening, J. W. (2018). Deep genome annotation of the opportunistic human pathogen *Streptococcus pneumoniae* D39. *Nucleic Acids Research*, *46*(19), 9971–9989. https://doi.org/10.1093/nar/gky725

Stanhope, M. J., Walsh, S. L., Becker, J. A., Miller, L. A., Lefébure, T., Lang, P., Bitar, P. D. P., & Amrine-Madsen, H. (2007). The relative frequency of intraspecific lateral gene transfer of penicillin binding proteins 1a, 2b, and 2x, in amoxicillin resistant *Streptococcus pneumoniae*. *Infection, Genetics and Evolution*, *7*(4), 520–534. https://doi.org/10.1016/J.MEEGID.2007.03.004

Synefiaridou, D., & Veening, J. W. (2021). Harnessing CRISPR-Cas9 for Genome Editing in *Streptococcus pneumoniae* D39V. *Applied and Environmental Microbiology*, *87*(6), 1–15. https://doi.org/10.1128/AEM.02762-20

Throup, J. P., Koretke, K. K., Bryant, A. P., Ingraham, K. A., Chalker, A. F., Yigong, G., Marra, A., Wallis, N. G., Brown, J. R., Holmes, D. J., Rosenberg, M., & Burnham, M. K. R. (2000). A genomic analysis of two-component signal transduction in *Streptococcus pneumoniae*. *Molecular Microbiology*, *35*(3), 566–576. https://doi.org/10.1046/j.1365-2958.2000.01725.x

Tomasz, A. (1968). Biological consequences of the replacement of choline by ethanolamine in the cell wall of Pneumococcus: chain formation, loss of transformability, and loss of autolysis. *Proceedings of the National Academy of Sciences of the United States of America*, *59*(1), 86–93. https://doi.org/10.1073/pnas.59.1.86

Tomasz, A., & Waks, S. (1975). Mechanism of action of penicillin: triggering of the pneumococcal autolytic enzyme by inhibitors of cell wall synthesis. *Proceedings of the National Academy of Sciences of the United States of America*, *72*(10), 4162–4166. https://doi.org/10.1073/pnas.72.10.4162

Trzciński, K., Thompson, C. M., & Lipsitch, M. (2004). Single-step capsular transformation and acquisition of penicillin resistance in *Streptococcus pneumoniae*. *Journal of Bacteriology*, *186*(11), 3447–3452. https://doi.org/10.1128/JB.186.11.3447-3452.2004

Veening, J. W., & Blokesch, M. (2017). Interbacterial predation as a strategy for DNA acquisition in naturally competent bacteria. *Nature Reviews Microbiology 2017 15:10*, *15*(10), 621–629. https://doi.org/10.1038/nrmicro.2017.66

Wyres, K. L., Lambertsen, L. M., Croucher, N. J., McGee, L., von Gottberg, A., Liñares, J., Jacobs, M. R., Kristinsson, K. G., Beall, B. W., Klugman, K. P., Parkhill, J., Hakenbeck, R., Bentley, S. D., & Brueggemann, A. B. (2012). The multidrug-resistant PMEN1 pneumococcus is a paradigm for genetic success. *Genome Biology*, *13*(11), R103. https://doi.org/10.1186/gb-2012-13-11-r103

Wyres, K. L., Lambertsen, L. M., Croucher, N. J., McGee, L., von Gottberg, A., Liñares, J., Jacobs, M. R., Kristinsson, K. G., Beall, B. W., Klugman, K. P., Parkhill, J., Hakenbeck, R., Bentley, S. D., & Brueggemann, A. B. (2013). Pneumococcal capsular switching: A historical perspective. *Journal of Infectious Diseases*, *207*(3), 439–449. https://doi.org/10.1093/infdis/jis703